

TOTAL SYNTHESIS OF MARINE TERPENOIDS

BY

YAROSLAV BOYKO

DISSERTATION

Submitted in partial fulfillment of the requirements
for the degree of Doctor of Philosophy in Chemistry
in the Graduate College of the
University of Illinois Urbana-Champaign, 2021

Urbana, Illinois

Doctoral Committee:

Assistant Professor David Sarlah, Chair
Professor Scott E. Denmark
Professor Paul J. Hergenrother
Professor M. Cristina White

ABSTRACT

Complex architectures of marine terpenoids and vast assortments of their scaffolds have served as a proving ground for synthetic chemists, inspiring them to develop, assess, and test new methodologies and disconnections. Moreover, besides advancing the field of organic synthesis, marine natural products have also had immense influence on medicinal chemistry providing new chemical leads for further development to combat life threatening diseases. Accordingly, several promising families of marine terpenoids were identified to explore their chemistry and biology.

The first chapter of this dissertation describes a full account of our synthetic endeavors towards isomalabaricane triterpenoids, natural products discovered 40 years ago in marine sponges of genera *Stelletta*, *Jaspis*, *Rhabdastrella*, and *Geodia*. Studies showed that these molecules possess valuable biological properties, such as high cytotoxicity, selectivity over non-transformed cells and, hypothetically, a novel mechanism of action. Consequentially, this family of natural products has attracted significant attention from the synthetic community to solve the problem of sustainable supply, and thereby enable further investigation. All attempts however, have failed. Perhaps this is no surprise as the unique structure of isomalabaricanes encompass highly strained *trans-syn-trans* perhydrobenz[*e*]indene core that poses a great challenge. We have been able to develop a series of unconventional transformations to assemble the core architecture in an expedient and enantioselective fashion. To facilitate the development of strategy and completion of the total synthesis, a number of tools at our disposal were utilized, such as computational techniques and a high-throughput screening platform. Enormous strain associated with the core motif manifested itself in various unforeseen reactivities, which could be avoided only upon judicious orchestration of our synthetic manipulations. Finally, our preliminary results reveal a non-intuitive importance of the lipophilic core for the biological activity, and more in-depth studies will be conducted shortly to assess therapeutic potential of the isomalabaricane scaffold.

In the second chapter, we identified the perhydrobenz[*e*]indene core as a highly conserved motif in terpene natural products. This observation allowed us to formulate a concept of a privileged molecular recognition moiety. A two-stage general blueprint was envisioned to access those diverse perhydrobenz[*e*]indene containing natural products under a unified approach. For that, an originally tailored strategy towards isomalabaricanes was expanded upon and rendered divergent with incorporation of several bifurcation points. This design allowed us to rapidly

assemble scaffolds with all the requisite functionalities for further elaboration into natural products and medicinally relevant compounds.

The third chapter describes four generations of strategies towards another marine cytotoxic terpenoid, ineleganolide. This diterpenoid has been recognized as a flagship member of norcembranoid family of natural products. Its highly congested, stereochemically-rich structure inspired us to develop an unparalleled approach to this target based on a late-stage ring-expansion transform. The direct precursor for the natural product was synthesized, employing a novel Ni(0)-catalyzed pentanulation, underutilized Se-B bifunctional reagent and chemoselective aldol cyclization as key steps in the sequence. Additionally, this approach is versatile and can be exploited towards other norcembranoids. Overall, we achieved substantial progress towards the total synthesis of ineleganolide and enabled exploration of the final stage by developing expedient and convergent route to the advanced intermediates.

Dedicated to my wife

ACKNOWLEDGMENTS

Foremost very grateful to my advisor, Professor David Šarlah for the opportunity to come in Illinois and become a part of such a prestigious department, for a stimulating and educational environment, and for all the support in research and beyond. To the rest of my committee, Professor Scott Denmark, Professor Christina White, and Professor Paul Hergenrother, thank you for your feedback and scholarly interactions. It has been a privilege to have you as a part of my experience at UIUC.

To my friends and collaborators with whom I have been working on these projects, Chris, Alex and Lucas, thank you for being close and supportive, for your dedication and hard work, and for the patience and tolerance needed to put up with me.

To all my talented students, Lorenzo, Fedor, Tiffany, Shang, Alek, Cheng, Xuan, Sunyang, whose priceless enthusiasm and tremendous help allowed me to achieve higher goals than I could ever imagine. I wish you best of luck in your future!

To other students from the third generation: graduate school will remain one of the most memorable times not only because of the research that was done, but also because of the people who we were around. Every generation is different and I believe you can relate the most to my experience. I hope to save this bond with you throughout the years. Thank you to the senior students, Dr. Okamura, Dr. Ungarean and Dr. Hernandez for a warm welcoming, your great humor and supportive environment.

To Chris, David, Tanner and Zohaib for countless proof readings of my writing, including this dissertation. I promise, at some point I will use all the articles correctly...but not any time soon.

To my wife, Dina. My vocabulary on either language is futile even to attempt to describe how important you were/are to me during this time, so “Bolshoi Rahmed”!

To the sources of funding that have supported me in my PhD. Thank you to the University of Illinois, and the Bristol-Myers Squibb Fellowship in Organic Chemistry for their generous support.

TABLE OF CONTENT

CHAPTER 1. TOTAL SYNTHESIS OF ISOMALABARICANE TRITERPENOIDS	1
1.1 Introduction.....	1
1.2 Background.....	2
1.3 Results and Discussion	6
1.3.1 Retrosynthetic analysis	6
1.3.2 Synthesis of decalone.....	7
1.3.3 Stereoselective annulation	12
1.3.4 Construction of C-ring via Rautenstrauch cycloisomerization.....	17
1.3.4.1 Background.....	17
1.3.4.2 Synthesis of the 1,4-enyne	20
1.3.4.3 Reactivity validation and optimization	21
1.3.4.4 Scope of the Rautenstrauch cycloisomerization	23
1.3.5 Formation of the <i>trans-syn-trans</i> perhydrobenz[<i>e</i>]indene core	24
1.3.5.1 Direct conjugate reduction.....	24
1.3.5.2 Directed hydrogenation.....	26
1.3.5.3 Intramolecular hydrosilylation.....	30
1.3.5.4 Miscellaneous reductions.....	31
1.3.5.5 Reductive transposition approach	33
1.3.6 Synthesis of the key precursor for late-stage cross-coupling.....	40
1.3.7 Streamlining the synthetic route	46
1.3.8 Synthesis of vinyl electrophile for late-stage cross-coupling	50
1.3.9 Synthesis of side-chain nucleophiles for the cross-coupling	54
1.3.10 Synthesis of isomalabaricane triterpenoids via cross-coupling	56
1.3.11 Structure-activity-relationship study of stelletin A.....	60
1.4 Conclusions and Outlook.....	61
1.5 Experimental Section	63
1.6 Acknowledgment of Contributions.....	88
1.7 References.....	89
CHAPTER 2. GENERAL BLUEPRINT TOWARDS TERPENOID ARCHITECTURES	97
2.1 Introduction.....	97

2.2 Background	100
2.3 Results and Discussion	105
2.3.1 Computational investigation of perhydrobenz[<i>e</i>]indene strain energies	105
2.3.2 Design of the divergent strategy	107
2.3.3 Divergence based on transfer of stereogenicity	108
2.3.4 Stereodivergent catalysis of Rautenstrauch cycloisomerization	111
2.3.5 Efforts towards <i>trans-anti-cis</i> configured dasyscyphin B	114
2.3.6 Efforts towards <i>trans-syn-cis</i> configured polyveoline	118
2.4 Conclusions and Outlook	120
2.5 Experimental Section	120
2.6 Acknowledgment of Contributions	128
2.7 References	129
CHAPTER 3. TOTAL SYNTHESIS OF NORCEMBRANOID DITERPENOIDS	132
3.1 Introduction	132
3.2 Background	134
3.2.1 Biosynthesis	134
3.2.2 Synthetic studies towards ineleganolide and other norcembranoids	137
3.3 Results and Discussion	144
3.3.1 Retrosynthesis	144
3.3.2 Synthesis of the coupling partners for MBH reaction	147
3.3.3 Strategy I: Morita–Baylis–Hillman reaction	152
3.3.4 Strategy II: C12 prefuntionalization	158
3.3.5 Strategy III: use of (<i>S</i>)-norcarvone	163
3.3.6 Strategy IV: acyl-Stille transform	167
3.4 Conclusions and Outlook	169
3.5 Experimental Section	170
3.6 Acknowledgment of Contributions	174
3.7 References	175

CHAPTER 1. TOTAL SYNTHESIS OF ISOMALABARICANE TRITERPENOID[†]

1.1 Introduction

Marine invertebrates have proven to be a rich source of structurally interesting families of terpenes with large potential for medicinal application.³ In search of promising leads a group of unusual sponge-derived triterpenoids, bearing the rare 6-6-5 malabaricane skeleton attracted our attention.⁴⁻⁷ Produced in sponges of the genera *Stelletta*, *Jaspis*, *Rhabdastrella*, and *Geodia*, isomalabaricanes have been the subject of recent studies exploring their noteworthy antiproliferative effects in certain human cancer cell lines.^{4-6,8-12} Interestingly, stelletin A (**1.1**) exhibited a 300-fold increase in cytotoxicity in LNCaP prostate cancer cells when compared to HL-60 human leukemia cells.⁸ Similarly, stelletin E (**1.4**) was found 117 times more potent in p21-deficient HCT-116 cells when compared with the native form (Chart 1.1).⁹ These compounds often have nanomolar and subnanomolar half-maximal inhibitory concentrations (IC₅₀) towards the cell lines in which they are active, but high micromolar activity in others, including a panel of non-transformed cell lines.¹¹ It has been shown that isomalabaricanes like rhabdastrellic acid A (**1.3**)

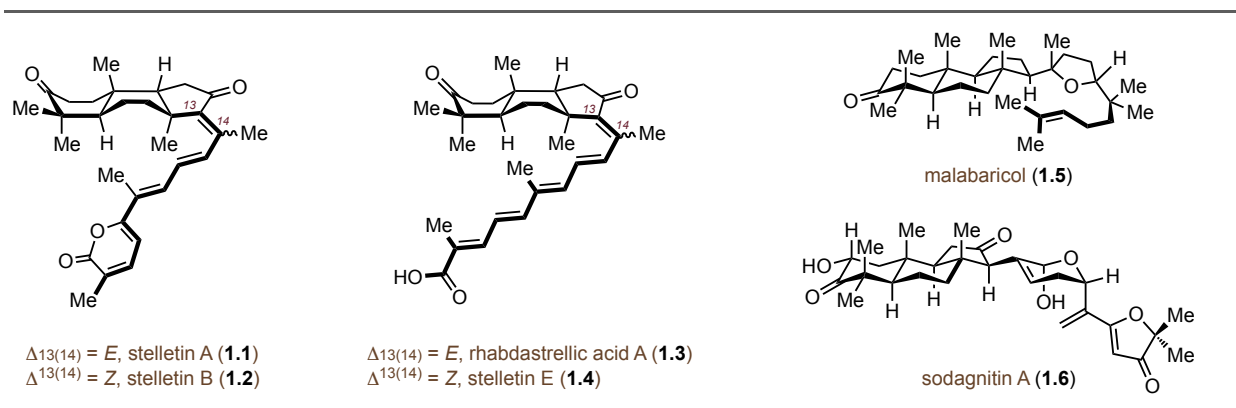


Chart 1.1 Structure of selected isomalabaricane and malabaricane triterpenoids.

and stelletin B (**1.2**) selectively activate apoptosis through the intrinsic pathway, interfere with PI3K/Akt/mTOR growth factor signaling and induce autophagy. However, the initial disruptive event(s) and protein target(s) are unknown. The remarkable profile of these molecules caused a considerable interest from the community as potential new chemical leads in cancer treatment.

[†]Portions of this chapter are reproduced from the key references 1 and 2 with permission from the authors.

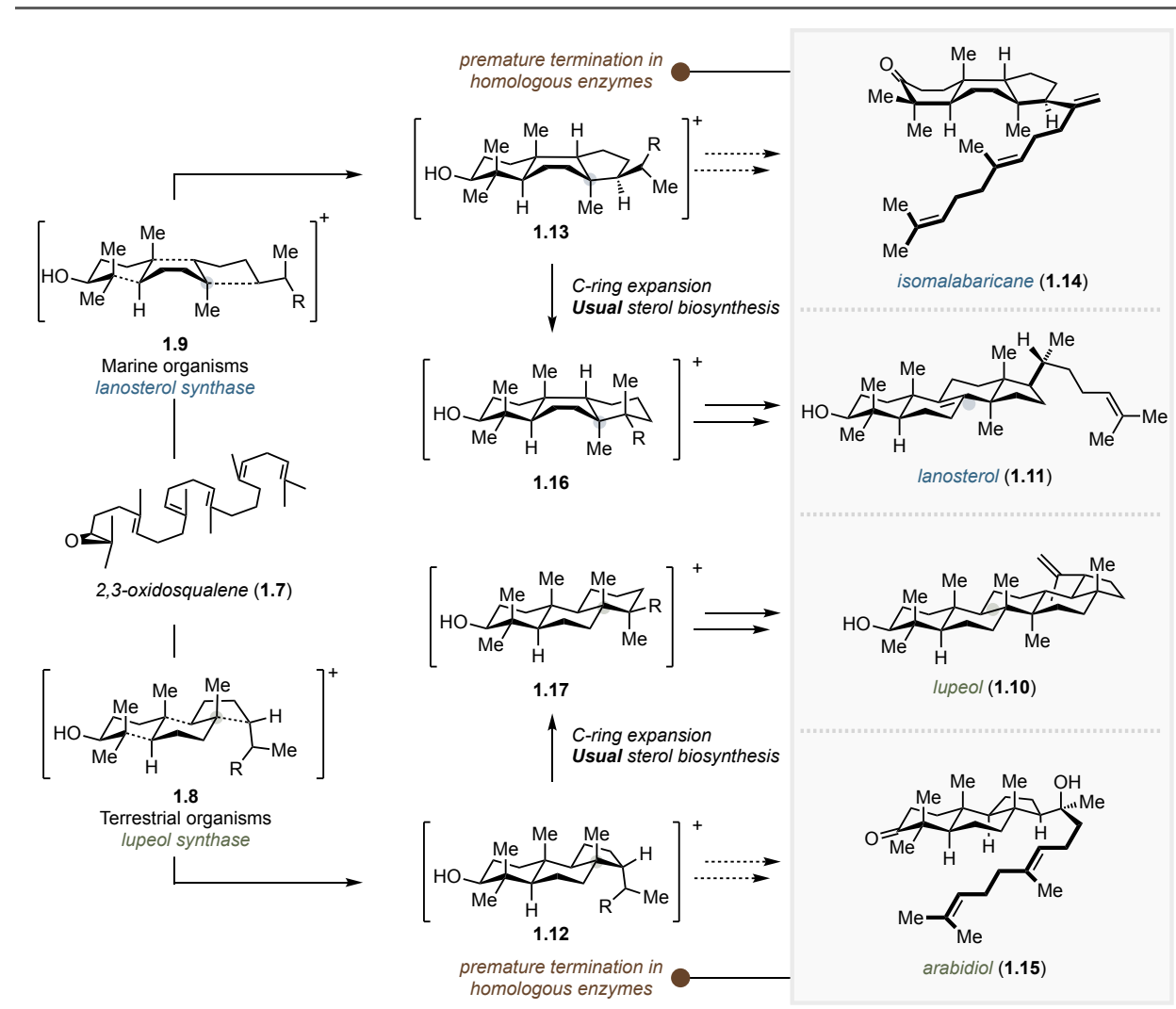
Moreover, the isomalabaricanes unique cytotoxicity pattern (COMPARE analysis) provides a conjecture for a novel mechanism of action, a valuable feature in its own right. Further investigations, however, are significantly limited by the material supply: the isolation yield from natural source is insufficient for more in-depth studies (< 0.012% of sponge wet weight for stelletin A). Finally, despite being characterized nearly 40 years ago, no total synthesis has been completed to date.¹³⁻¹⁶ Aforementioned factors motivated us to initiate a research program devoted to total synthesis of isomalabaricane triterpenoids.

1.2 Background

Besides promising anticancer activity, the isomalabaricane triterpenoids are enticing targets due to their intriguing structures. Seemingly the product of an preemptively terminated cyclization of 2,3-oxidosqualene, the 6-6-5 malabaricane core is quite rare among triterpenoid natural products.⁸ Remarkably, those isolated from terrestrial producing organisms—such as the parent compound malabaricol (**1.5**, Chart 1.1)¹⁷ from the evergreen rainforest tree *Ailanthus malabarica*, and sodagnitin A (**1.6**)¹⁸ from the toadstools *Cortinarius fulvoincarnatus* and *Cortinarius sodagnitus*—possess exclusively *trans-anti-trans* stereochemistry at the ring junctions, while the marine-derived isomalabaricanes are exclusively characterized with the *trans-syn-trans* configuration.

Recent studies of polyene cyclase enzymes and their repertoire in terms of product distributions might offer an insight into this dichotomy (Scheme 1.1). Phylogenetic and chemotaxonomic analyses indicate that the active-site mutations necessary to alter mechanistic features such as the B-ring chair/boat and 17 α / β transitions during oxidosqualene (**1.7**) cyclization are substantial—extremely rare in evolutionary history—and such mechanistic barriers have not been effectively overcome through mutagenesis or directed evolution.¹⁹ In contrast, mutations capable of diverting the termination pathways of the cyclization are relatively common, suggesting that precise cyclase enzymes enforcing either chair-chair-chair (**1.8**) or chair-boat-chair (**1.9**) transition states may have emerged from different ancestors with promiscuity towards various termination mechanisms. Whereas lupeol (**1.10**) and related cyclases demand the former, all-chair transition state, lanosterol cyclase enforces the latter (**1.11**). Homologous cyclase enzymes in either class have been identified that block C-ring expansion of putative malabaricane (**1.12**) and isomalabaricane (**1.13**) cationic precursors into **1.17** and **1.16** respectively.¹⁹ A single-point

lanosterol cyclase mutant has been discovered that produces *trans-syn-trans* tricycle **1.14** in addition to lanosterol *in vitro*.²⁰ In turn, existence of several natural enzymes²¹⁻²⁴ within the *PEN* clade that generates *trans-anti-trans* tricycles like **1.15**



Scheme 1.1 Stereodivergent 2,3-oxidosqualene (7) cyclization pathways and premature termination mechanisms that lead to presumed isomalabaricane and malabaricane precursors **14** and **15**.

either selectively or in a mixture with *trans-anti-trans* tetra- and pentacycles provides compelling evidence for its common biosynthetic origins with **1.14**-like natural products. The taxonomic distribution of malabaricanes and isomalabaricanes suggests that the native enzymes facilitating premature termination of oxidosqualene cyclization in the biosynthesis of these natural products likely evolved independently within terrestrial and marine producing organisms. Chemical defense or some other function for these secondary metabolites could apply selection pressure for this process.

The cyclization event yielding the *trans-syn-trans* products inputs considerable strain in the resulting scaffold. To the best of our knowledge, the only natural product outside of the isomalabaricane family possessing the *trans-syn-trans*-4,4,8,10-tetramethylperhydrobenz[*e*]indene skeleton is the indole diterpenoid 8 α -polyveolinone (**1.18**) and its *N*-acetyl congener (**1.19**).²⁵ The *trans-syn-trans*-perhydrophenanthrene skeleton, in turn, appears to be more common, and is found in such natural products as the notable immunosuppressant brasilicardin A (**1.20**)²⁶ and the topical antibiotic fusidic acid (**1.21**)²⁷ (Chart 1.2). Although not directly indicative of synthetic tractability, the unorthodox conformation

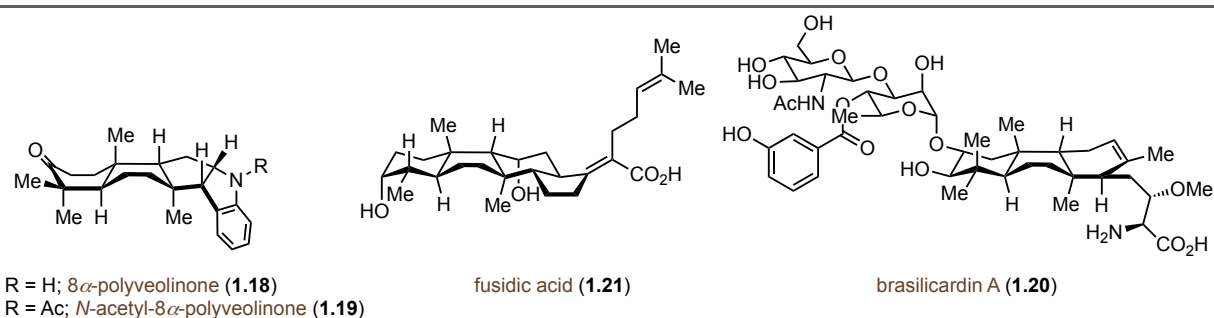
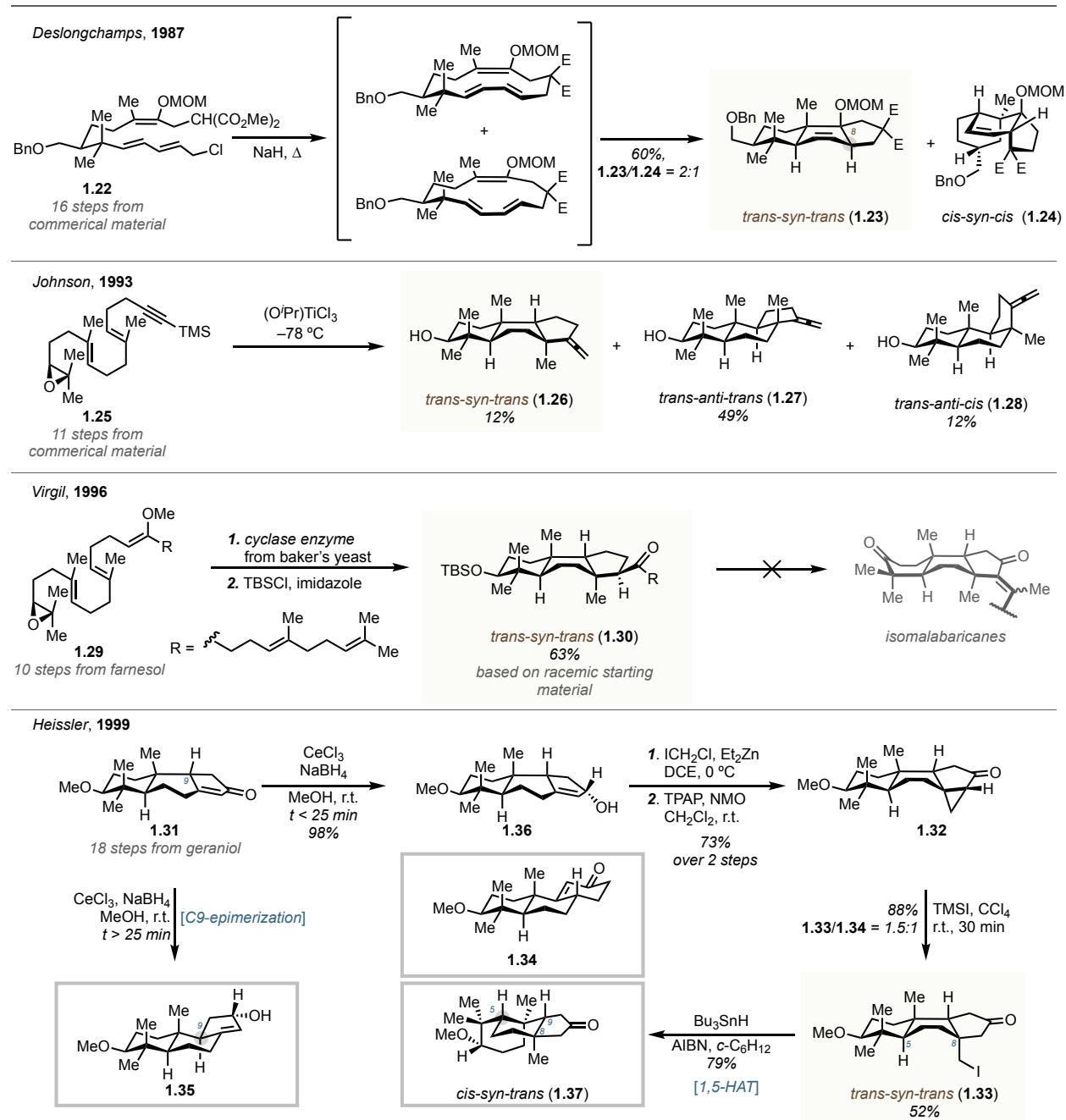


Chart 1.2 Structures of selected *trans-syn-trans* perhydrophenanthrene and perhydrobenz[*e*]indene natural products.

of *trans-syn-trans* fused molecules and associated strain renders them inaccessible through standard methods of terpene synthesis,²⁸ and thus far lengthy sequences have been required to complete the task. Whereas brasilicardin A has recently succumbed to total synthesis with a 28-step sequence to assemble the tricyclic framework,²⁹ fusidic acid has never been accessed through total synthesis (although formal and relay syntheses have been disclosed).³⁰⁻³² Outside of our work, there are no reported total syntheses of any *trans-syn-trans* 6-6-5 natural products. Despite several approaches towards the *trans-syn-trans* 6-6-5 core having been described, this structural motif has never been obtained with high selectivity. Deslongchamps has reported a tandem macrocyclization / transannular Diels–Alder reaction of polyene **1.22**, synthesized in 16 steps, that generates a 2:1 mixture of *trans-syn-trans* and *cis-syn-cis* tricycles **1.23** and **1.24**, conspicuously lacking the C8 methyl substituent (Scheme 1.2).³³ In a single example of Lewis-acid promoted cation-olefin cyclization, Johnson reported that treatment of polyene **1.25**, prepared in 11 steps, with (*i*PrO)TiCl₃ resulted in cyclization to give a mixture of three products **1.26-1.29**, notably obtaining *trans-syn-trans* isomer **1.26** in 12% yield.³⁴⁻³⁷ Such literature precedent suggests that purely chemical cationic-olefin cyclizations in a laboratory setting are unable to overcome the

necessary thermodynamic barriers to construct the *trans-syn-trans* skeleton. Adaptation of the natural process under chemoenzymatic catalysis, however might surmount the obstacle and yield strained the hydrocarbon after the initial cyclization event in a single step. Indeed, pioneering studies from Virgil and co-workers demonstrated the feasibility of this approach using



Scheme 1.2 Prior synthetic efforts towards the *trans-syn-trans* perhydrobenz[e]indene skeleton as well as the isomalabaricane natural products.

the modified oxidosqualene substrate (Scheme 1.2).¹⁵ Synthesized in 10 steps from farnesol, **1.29** was capable of terminating the initial cyclization to build the *trans-syn-trans* oriented perhydrobenz[*e*]indene **1.30**. The authors attempted to apply this powerful transformation towards the total synthesis of the isomalabaricanes; unfortunately, the biocatalytic transformation was not amenable to scale-up attempts, and the studies were halted due to low material throughput. In another synthetic attempt towards the isomalabaricanes, a standard chemical approach to the *trans-syn-trans*-perhydrobenz[*e*]indene framework **1.31** was reported by Heissler and co-workers in 22 steps from geraniol.¹³⁻¹⁴ A key step in this synthesis was the fragmentation of cyclopropane **1.32**, producing *trans-syn-trans* scaffold **1.33** in a 3:2 ratio with the ring expansion product **1.34**. This work revealed much about the instability of strained intermediates *en route* to the isomalabaricanes: enone **1.31** isomerized at the C9 position to **1.35** during a seemingly innocuous Luche reduction (**1.31** → **1.36**). Even more striking was the conversion of the *trans-syn-trans* framework **1.33** to the *cis-syn-trans* **1.37** during radical dehalogenation, proceeding through what is thought to be a 1,5-hydrogen atom transfer from C5 to the C8 methyl group. This intermediate could not be advanced to the natural products due to its propensity for this rearrangement.

1.3 Results and Discussion

1.3.1 Retrosynthetic analysis

Guided by the demonstrated disadvantages of a chemoenzymatic approach along with complete inability to reproduce the naturally occurring polyene cyclization in a flask, we concluded that a biomimetic strategy would not be beneficial for the synthesis of the isomalabaricanes. Furthermore, the challenges described by Heissler displayed the risks associated with the intermediacy of enones of **1.31** type. The activated methine at C9 clearly exhibits a tendency to isomerize, complicating the requisite decoration of the C-ring. With these objections in mind, we developed our retrosynthetic plan (Figure 1.1). Taking into account the sensitivity of the Michael acceptor fragment as well as the divergence among the natural products at the side domain, late stage olefination was recognized as the most versatile and advantageous approach. The corresponding dicarbonyl precursor **1.38** can be rapidly accessed through fragmentation of furan **1.39**. The latter can be traced back to the Wieland–Miescher ketone derivative, decalone **1.40** via annulation transform. The synthesis of the Wieland–Miescher ketone is very well established and robust. Synthetic chemists have relied on this technique for 70 years and still

heavily utilize it to this day. However, we quickly came to the realization that the synthesis of the prerequisite decalone of type **1.40** from commercial 1,3-cyclohexadienone (**1.41**) encompass 9 steps. Thus, the overall effectiveness of this approach would be compromised from an early stage. To obviate these complications, an alternative strategy had to be developed. Therefore, the vital decalone was further traced back to the nitrile **1.42** via radical cyclization transform.

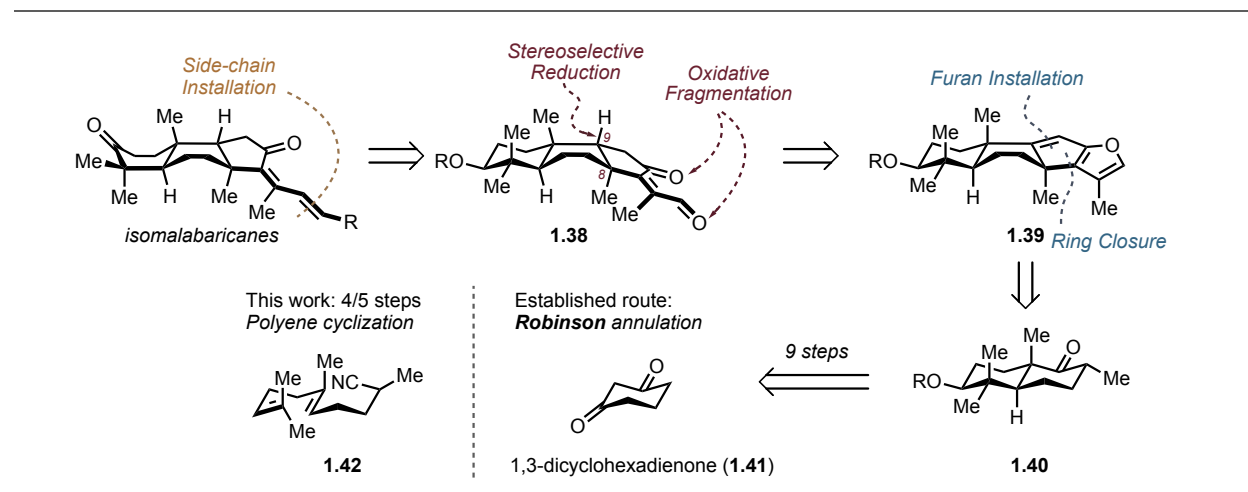


Figure 1.1 Initial retrosynthesis of isomalabaricanes.

1.3.2. Synthesis of decalone

In order to enable rapid assembly of nitrile **1.42**, a challenging sp^3 - sp^3 cross-coupling of easily accessible epoxy-geranyl bromide **1.43** was investigated (Table 1.1). Given literature precedent and the nature of preexisting functional groups, we focused our efforts on the Negishi cross-coupling between **1.43** and organozinc reagent **1.44** derived from 3-iodo-propionitrile.³⁸ Of note, reductive cross-coupling also was explored, however promising results were not achieved, perhaps due to mismatched reactivity of the two electrophiles.

As an outset, several relevant catalytic systems reported by Fu and Knochel were evaluated. Only entry 5 afforded small amounts of the desired product, while other conditions for nickel-, palladium- (entry 3) or cobalt-catalyzed (entry 2) cross-coupling delivered either unreacted starting material or dimer **1.46**.³⁸⁻⁴² Despite discouraging initial results, further screen of commercially available nickel catalysts revealed two promising leads: ligandless Ni(II) conditions and Ni(0) with bulky electron-rich ligands (Table 1.2, entries 5 and 7 respectively). Notably, the use of NMP as a polar additive was required to activate the organozinc reagent for the transmetallation. DMA and HMPA showed analogous effects with similar efficiency. The reaction was carried out at ambient temperature as no reactivity was observed at temperatures below 0 °C. Switching the nature of

Entry	Conditions	Yield ^a	Entry	Conditions	Yield ^a
1	Ni(acac) ₂ (10 mol %), 4-fluorostyrene (20 mol %), Bu ₄ NI (3.0 equiv.), THF/NMP 2:1	n.a.	5	Ni(cod) ₂ (4 mol %), Bn-Pybox (8 mol %), DMA	8%
2	CoBr ₂ (10 mol %), THF	n.a.	6	NiCl ₂ •glyme (5 mol %), <i>i</i> -Pr-Pybox (5.5 mol %), DMA/DMF 1:1	n.a.
3	Pd ₂ (dba) ₃ (2 mol %), PCy ₃ (8 mol %), NMI (1.2 equiv.), THF/NMP 2:1	n.a.	7	NiCl ₂ •glyme (5 mol %), Bn-Pybox (5.5 mol %), DMA/DMF 1:1	n.a.
4	Ni(cod) ₂ (4 mol %), <i>i</i> -Pr-Pybox (8 mol %), DMA	n.a.			

^a NMR yield.

Table 1.1 Survey of reported conditions for Negishi coupling.

electrophile and nucleophile completely suppressed the desired reactivity. Given the versatility of the Ni(0) catalytic system and the wide spectrum of available ligands, the hit from entry 7 was subjected to further optimization.

Entry	Conditions	Yield ^a	Entry	Conditions	Yield ^a
1	Ni(PPh ₃) ₂ Cl ₂	20%	5	NiBr ₂ •glyme	36%
2	Ni(dppf)Cl ₂	n.a.	6	Ni(dmgH) ₂	24%
3	Ni(PCy ₃) ₂ Cl ₂	16%	7	Ni(cod) ₂ + ^t Bu ₃ P•HBF ₄ (10 mol %), KF (1.0 equiv.)	35%
4	Ni(dppe)Cl ₂	8%			

^a NMR yield.

Table 1.2 Screen for Ni-catalyzed Negishi cross-coupling.

After much experimentation, optimal conditions were identified, and the desired product **1.45** was isolated in 60% yield (Table 1.3, entry 1). The reaction proved to be scalable as the product was isolated on 5 mmol scale with negligibly diminished yield (entry 2). 2:1 ligand/metal ratio is critical for high conversion and yield (entry 3) as well as monodentate, bulky, electron-rich phosphine ligand such as ^tBu₃P (entries 4-8). Organic bases outcompete other commonly used options (entries 9-11) and insures homogeneity of the reaction. Of note, under no conditions was complete suppression of electrophile dimerization achieved. Despite good yield of the desired

product there were concerns regarding the economical sustainability of the process considering the early stage of the project and the high cost and required loadings of the catalyst. Therefore, more practical and affordable ligandless conditions (Table 1.2, entry 5) were examined.

$\text{1.43} \xrightarrow[\text{Ni(cod)}_2 \text{ (5 mol \%), } t\text{Bu}_3\text{P}\cdot\text{HBF}_4 \text{ (10 mol \%), DIPEA (1.0 equiv.), NMP (1.3 equiv.), THF, 24 }^\circ\text{C, 16 h}]{\text{IZn-CH}_2\text{CH}_2\text{CN (1.44 (1.2 equiv.))}} \text{1.45}$

standard conditions

Entry	Deviations	Yield ^a	Entry	Deviations	Yield ^a
1	none	60%	7	QPhos instead of $t\text{Bu}_3\text{P}\cdot\text{HBF}_4$	36%
2 ^b	none	58%	8	P(2-furyl) ₃ instead of $t\text{Bu}_3\text{P}\cdot\text{HBF}_4$	0%
3	$t\text{Bu}_3\text{P}\cdot\text{HBF}_4$ (5 mol % instead of 10 mol %)	17%	9	CsF instead of DIPEA	0%
4	PPh ₃ instead of $t\text{Bu}_3\text{P}\cdot\text{HBF}_4$	15%	10	NaOt-Bu instead of DIPEA	40%
5	XPhos instead of $t\text{Bu}_3\text{P}\cdot\text{HBF}_4$	25%	11	Cs ₂ CO ₃ instead of DIPEA	35%
6	DavePhos instead of $t\text{Bu}_3\text{P}\cdot\text{HBF}_4$	24%			

^a isolated yield. ^b 5 mmol scale

Table 1.3 Optimization of Ni(0)-catalyzed Negishi cross-coupling.

Thorough optimization of the reaction parameters was conducted. It was found that pyridine as an additive slightly increased the yield and delivered more reproducible results (entries 1-3). Application of bi- or tridentate ligands either significantly inhibited or completely suppressed desired reactivity (entries 4, 5). THF was identified as an optimal solvent (entry 7). The nature of the electrophilic species is also crucial as only the bromide engaged in the reaction with moderate efficiency (entries 8-10). However, despite further efforts yield greater than 35% could

$\text{1.43} \xrightarrow[\text{NiBr}_2\cdot\text{glyme (5 mol \%), py (0.5 equiv.), THF, 24 }^\circ\text{C, 16 h}]{\text{BrZn-CH}_2\text{CH}_2\text{CN (1.47 (5.0 equiv.))}} \text{1.45}$

standard conditions

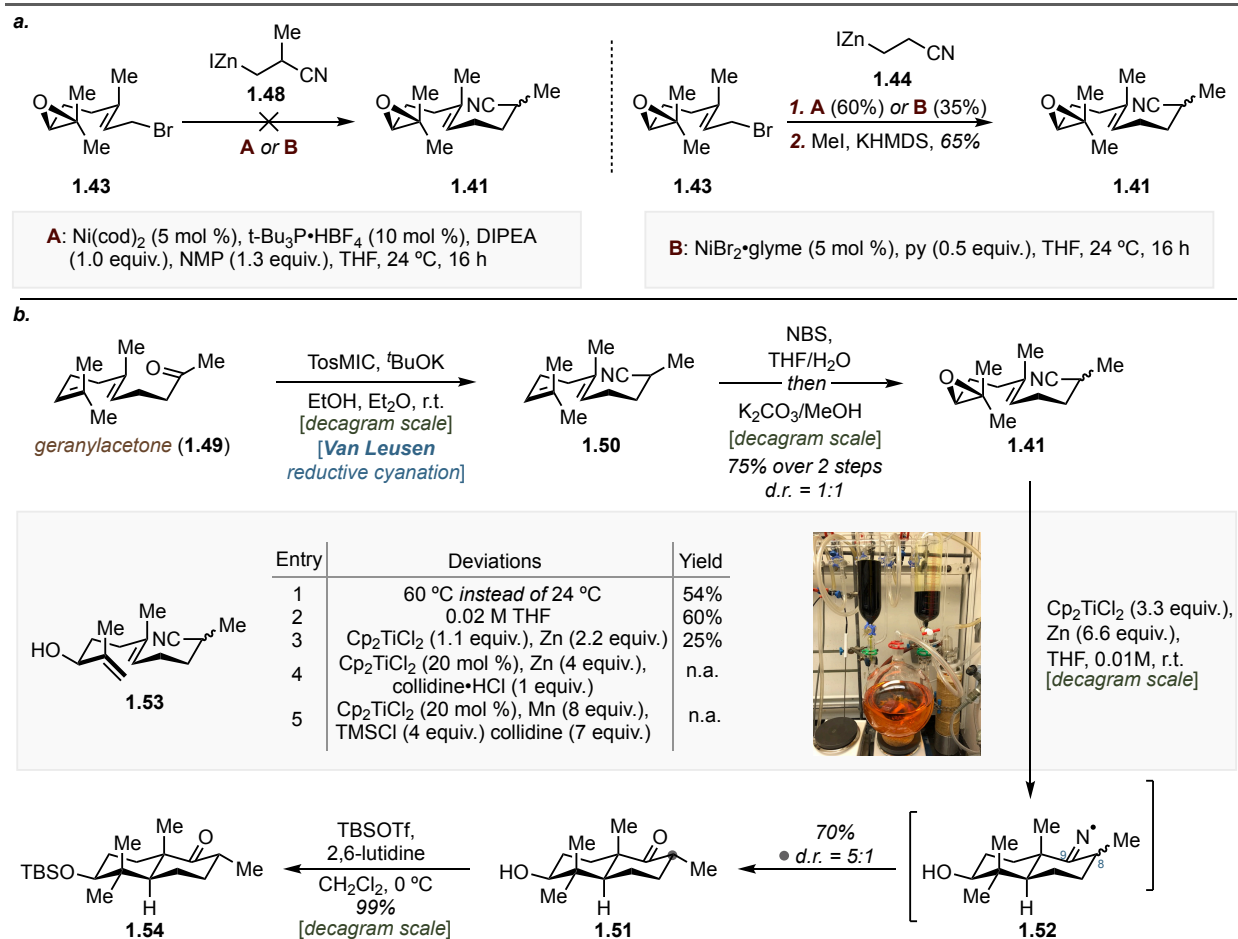
Entry	Deviations	Yield ^a	Entry	Deviations	Yield ^a
1	none	35%	6	NiBr ₂ •glyme (2.5 mol %)	23%
2	no pyridine	30%	7	DMA or NMP instead of THF	0%
3	pyridine (2.0 equiv.)	25%	8	Br → OP(O)(OEt) ₂	8%
4	dtbbpy, 1,10-phen or terpy instead of pyridine	0%	9	Br → OAc	0%
5	bpy instead of pyridine	25%	10	Br → Cl	6%

^a isolated yield.

Table 1.4 Optimization of Ni(II)-catalyzed Negishi cross-coupling.

not be attained. Thus, both developed catalytic systems possess only moderate productivity. Moreover, to our dismay, no cross-coupling product was observed, when organozinc specie **1.48**

was used as a nucleophile under either set of conditions (Scheme 1.3.a). This, in turn, would result in elongation of the linear sequence, since a separate step is required for the introduction of the methyl group at C8. Considering the listed shortcomings, it was decided to reevaluate the synthetic plan towards nitrile **1.41**.

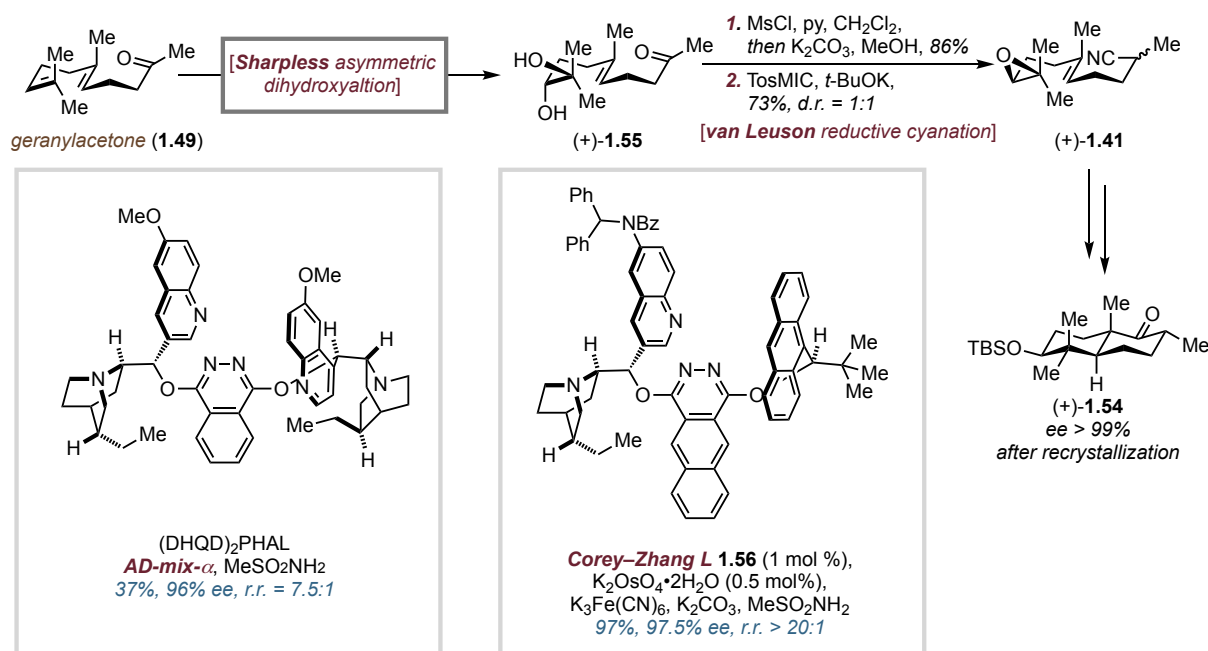


Scheme 1.3.a Unsatisfactory results from Negishi cross-coupling towards **1.41**; **b** Racemic synthesis of decalone **1.54**.

The desired linear precursor for the radical cyclization was traced back to another widely available terpene – geranylacetone (**1.49**). First, the carbonyl motif was subjected to van Leussen reductive cyanation (Scheme 1.3.b). Under reported reaction conditions in THF or DME the transformation proceeded smoothly, furnishing the product in 70% yield. Unfortunately, upon scaling this reaction above 25 grams, we encountered variable results and diminished yields. Switching the reaction solvent to Et₂O resulted in slurry-to-slurry conditions, which in turn led to higher yields and reproducible results. Nitrile **1.50** was regioselectivity epoxidized via a

bromohydrin intermediate, delivering the substrate for the cyclization as a mixture of two diastereomers (*d.r.* = 1:1) in only two steps from the commercial material.

Ti(III)-mediated radical cyclization has been demonstrated as a powerful tool for the rapid generation of complexity.⁴³ Inspired by the nitrile-terminated radical cyclization to access a polycyclic ketone *en route* towards Berkeleyone A disclosed by Maimone and co-workers, reported conditions were tested.⁴⁴ To our delight the desired decalone **1.51** was formed in 70% yield and *d.r.* = 5:1. The reaction displayed unexpected stereoconvergence, which was rationalized through reversible C–C-bond cleavage between C8-C9 of the intermediary iminyl radical **1.52**. The reaction outcome showed strong dependency on concentration and the rate of addition of the reductant (entry 2, Scheme 1.3.b). It is important to maintain the concentration of the active Ti(III)-species at the minimal level to eliminate formation of the allylic alcohol **1.53**. Moreover, a superstoichiometric amount of the Nugent reagent was necessary to achieve full conversion (entry 3). Attempts to employ catalytic conditions were not fruitful as was expected for the *nitrile*-terminated cyclization (entries 4, 5). Silyl-protection of the resulting secondary alcohol afforded decalone **1.54** in only 4 steps and a single chromatographic step from geranylacetone with 50% overall yield. The developed approach is concise, scalable and involves cheap commercial reagents, thus providing a competitive alternative to the Robinson annulation route. To address the final aspect of the approach, enantioselectivity, Sharpless asymmetric dihydroxylation of geranylacetone was performed (Scheme 1.4). Consistent with the literature precedent⁴⁵ diol **1.55** was obtained with high regio- and enantioselectivity, but only moderate conversion. Given the availability of the substrate and the catalyst we believe that this particular shortcoming is insignificant in terms of overall efficiency of the route. With an interest in improving the conversion of the dihydroxylation, our attention turned toward the use of the Corey–Zhang ligand (**1.56**), an underutilized tool finely-tuned to dihydroxylate the terminal olefin in extended polyprenoids such as squalene.^{46,47} We were very pleased to find that, in our hands, application of ligand **1.56** afforded the desired product in 97% yield and 97.5% *ee*. Diol **1.55** was converted into epoxide **1.41** and subsequent radical cyclization, protection and recrystallization delivered optically pure decalone **1.54** (*ee* > 99%).



Scheme 1.4 Enantioselective synthesis of decalone **1.54**.

1.3.3 Stereoselective annulation

Once robust and rapid access to the AB-bicyclic system **1.54** was established, we progressed into next phase of the synthesis, namely, assembly of the C-ring and diastereoselective formation of quaternary center at C8 (Figure 1.2).

First, we opted to exploit a well-established annulative strategy based on an allylation/Wacker

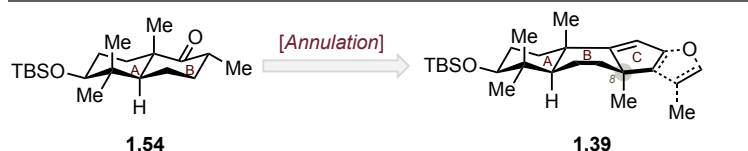
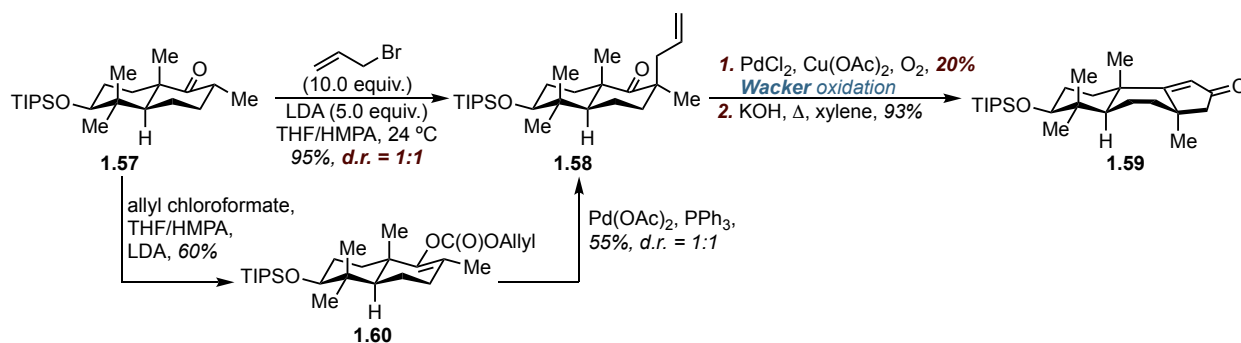


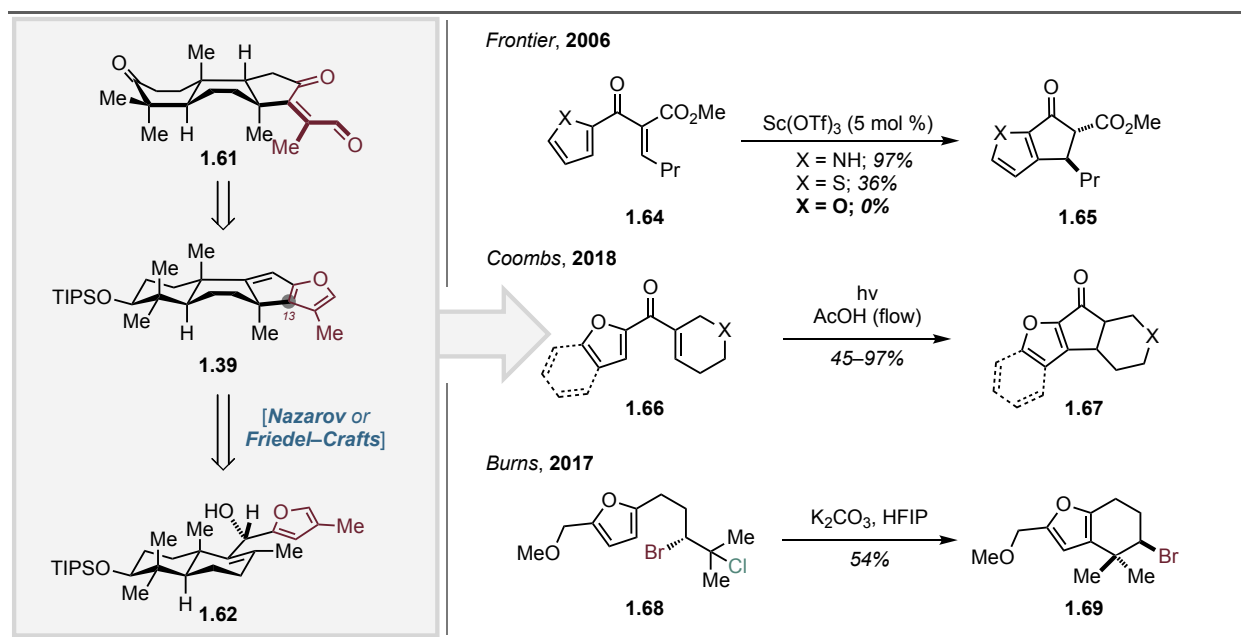
Figure 1.2 Second phase of the synthesis.

oxidation/aldol condensation sequence (Scheme 1.5). Such approaches have been extensively used in the synthesis of various terpenoids such as dichroanone reported by Stoltz group.⁴⁸ Due to the large steric encumbrance of the ketone **1.54** allylation proceeded only under forcing conditions. Surprisingly, poor diastereoselectivity for the transformation was observed. Moreover, we were unable to reproduce the Wacker oxidation of **1.58** reported for a similar substrate.⁴⁸ Regardless of the conditions applied, conversion was stalling at ~20%.⁴⁹ Hence, even though the final condensation to **1.59** proceeded smoothly, the overall strategy was deemed to be unsatisfactory.



Scheme 1.5 Aldol condensation approach towards construction of the C-ring.

Reexamination of the retrosynthesis led to a new approach: tetracyclic compound **1.61** was traced back to the alcohol **1.62** via Nazarov cyclization transform or an intramolecular Friedel–Crafts to construct key C13–C8 bond. Traditionally, enones substituted with 2-furyl rings are considered to be highly challenging substrates for Nazarov cyclization (Scheme 1.6).⁵⁰ Specially tailored substrates are required to promote the desired transformation. Recently, Coombs and co-workers disclosed photochemical conditions applied in flow, which enable formation of the desired fused tricyclic products **1.67** in good yields with broad substrate scope.⁵¹ On the other

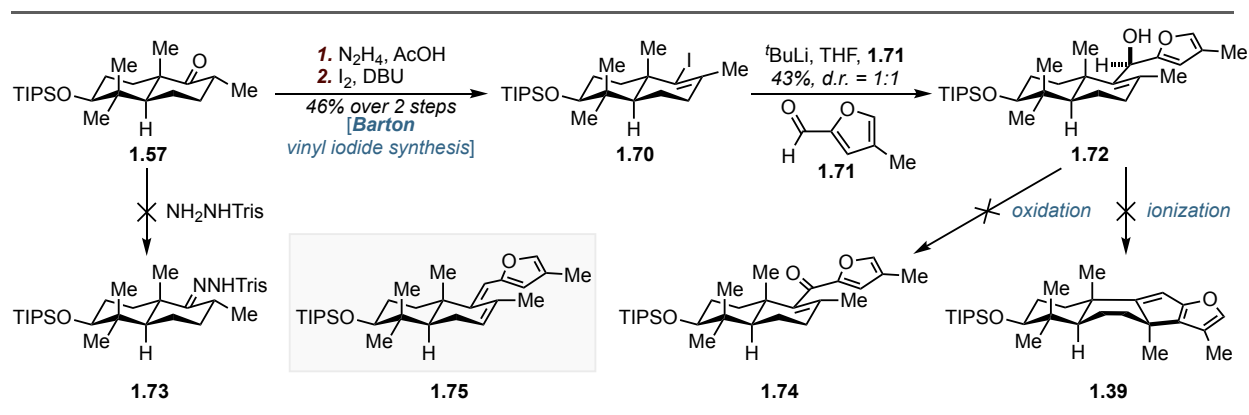


Scheme 1.6 Retrosynthetic plan towards advanced intermediate **1.39** and literature examples supporting proposed disconnections.

hand, a Friedel–Crafts disconnection could also pose a challenge given the lower nucleophilicity of the furan at C13. However, Burns and co-workers have been able to demonstrate the viability of the approach through solvolytic functionalization of bromochloride **1.68**.⁵² Formal Friedel–

Crafts cyclization at the third position of the furan was promoted by formation of the bromonium ion in HFIP furnishing the product **1.69** in 54% yield. With these encouraging examples in mind we have decided to assess our design.

Towards this goal, decalone **1.57** was converted into vinyl iodide **1.70** following Barton's procedure (Scheme 1.7).⁵³ Lithium-halogen exchange and addition into aldehyde **1.71**⁵⁴ afforded alcohol **1.72** in 43% yield and 1:1 diastereoselectivity. Of note, the same disconnection was initially attempted via the Shapiro reaction, however, requisite hydrazone **1.73** could not be formed due to the steric demands of the substrate. Unfortunately, despite our efforts we were unable to isolate ketone **1.74** due to the high sensitivity of the substrate and perhaps the product. Only decomposition was observed for a broad spectrum of mild oxidative conditions. Moreover, attempts to directly ionize the alcohol or activate it via mesylation or tosylation delivered elimination product **1.75** exclusively. For example, exposure of the substrate **1.72** to catalytic amounts of $\text{Sc}(\text{OTf})_3$ cleanly delivered diene **1.75** within 30 seconds.



Scheme 1.7 Attempts towards tetracyclic furan **1.39**.

Given the kinetic incompetence of the substrate for the cationic cyclization, change of polarity for the cyclization event was deemed as a potential solution (Figure 1.3). It is well known that the Giese reaction proceeds through early transition state and thus can forge sterically challenging bonds with high efficiency.⁵⁵ Hence, the addition of a nucleophilic radical derived from an allylic alcohol into a butynolide, oxidized isostere of the furan, was pursued. Corresponding precursor **1.77** was traced back to aldehyde **1.78** via Mukaiyama aldol transform.

To access the aldehyde, several methods for ketone homologation were evaluated (Scheme 1.10.a). First the ketone was converted into vinyl iodide **1.70** as was described previously. Lithium-

halogen exchange followed by addition of DMF delivered product **1.78** in 65% yield. With aldehyde **1.78** in hand, we sought to streamline the process and increase efficiency of the homologation. Adapting previously reported conditions by Taber and Gunn, epoxide **1.79** was isolated in 55% yield.^{56,57} A rearrangement /

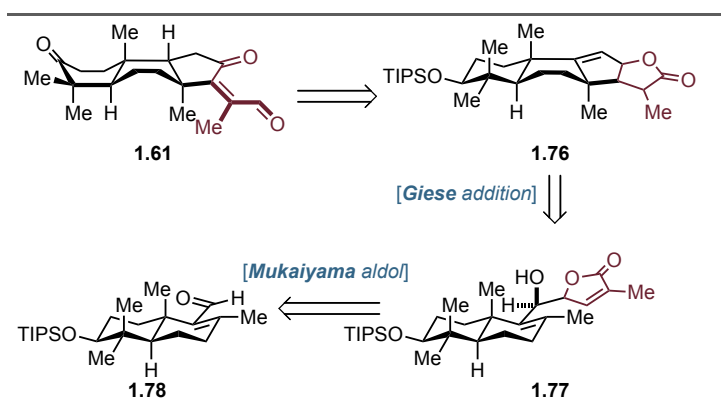
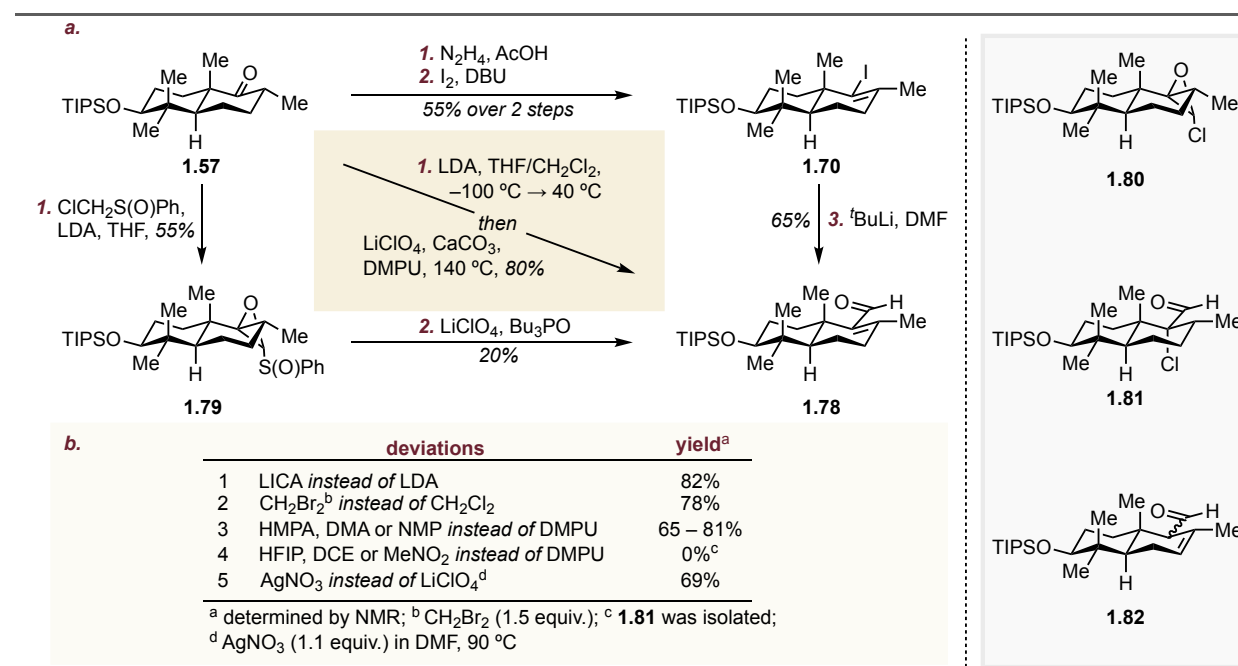


Figure 1.3 Revised retrosynthesis employing Giese addition transform.

elimination cascade, promoted by a Lewis acid, delivered aldehyde **1.78** in only 20% yield, which rendered the method unsuitable for the particular task. Finally, we turned to the one-pot homologation method developed by Nozaki and Yamamoto, where dichloromethane is used as a single-carbon atom source.^{58,59} After minor optimization, the desired product was obtained in 80%

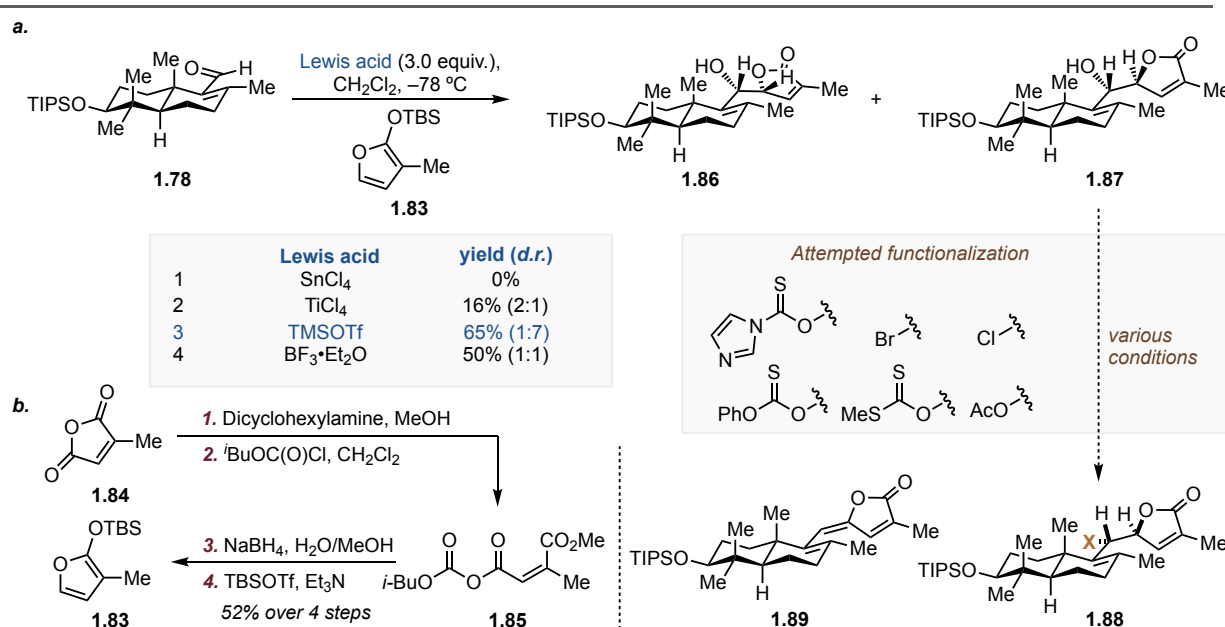


Scheme 1.8.a Synthesis of α,β -unsaturated aldehyde **1.78**; **b** optimization of Nozaki-Yamamoto protocol.

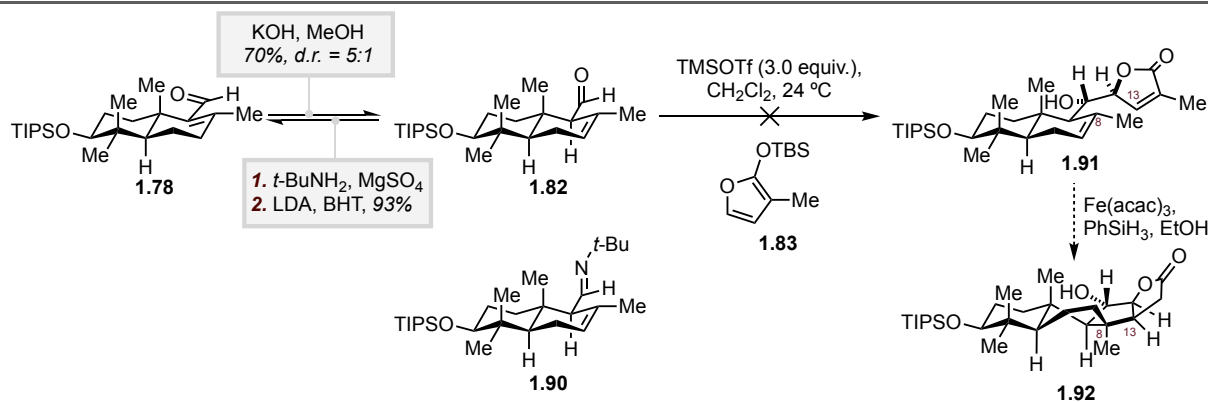
yield directly from the ketone on decagram scale. At the first stage of the process lithiated dichloromethane is added to the carbonyl followed by immediate closure of the epoxide, which could be observed spectroscopically in the crude reaction mixture. Dibromo- and diiodomethane as well as other lithium amide bases also could be used, however it did not increase the isolated

yield, especially on large scale (Scheme 1.8.b). The reaction is then warmed up to 40 °C to facilitate the rearrangement of epoxide **1.80** into α -chloroaldehyde **1.81** (*d.r.* = 3:1), which could be isolated in nearly quantitative yield if needed. The solvent is then swap to DMPU, followed by addition of LiClO₄ and CaCO₃ (acid scavenger). Only very polar aprotic solvents were suitable for the reaction. While other Lewis acids such as AgNO₃ were able to mediate the transformation, stoichiometric amounts were required, rendering LiClO₄ as the most optimal due to its cost and availability. Finally, high temperature is also required as no conversion was observed below 110 °C. Careful timing of the reaction is crucial as the product is not stable under the reaction conditions and readily isomerizes into β,γ -unsaturated aldehyde **1.82**.⁶⁰ Notably, this isomerization is also observed on silica gel and several other absorbents rendering isolation quite challenging.⁶¹

With an ample amount of aldehyde **1.78** in hand, Mukaiyama addition was explored (Scheme 1.9.a). The requisite silyl ketene acetal **1.83** was synthesized from citraconic anhydride (**1.84**) according to know procedure (Scheme 1.9.b).⁶² The reaction was mediated by a wide range of Lewis acids which provided various diastereoselectivities. Trimethylsilyl trifluoromethanesulfonate was chosen for further studies as it provided the adduct **1.87** with higher yield and stereoselectivity. The intent was to convert newly formed secondary alcohol at C11 into a functional group susceptible to homolytic cleavage under single electron reducing conditions. The generated nucleophilic allyl radical would cyclize onto the butenolide and forge the desired



Scheme 1.9.a Mukaiyama aldol and further elaboration of aldehyde **1.78**; **b** Synthesis of silyl ketene acetal **1.83**.



Scheme 1.10 Cyclization via reductive coupling.

scaffold. However, a familiar obstacle was encountered: the doubly activated secondary alcohol was prone to elimination, and only triene **1.89** was isolated from numerous attempts to perform the desired functionalization. The same trend was observed for the minor diastereomer **1.86** as well. To circumvent the undesired reactivity, we decided to leverage the innate propensity of aldehyde **1.78** towards isomerization (Scheme 1.10). First, we identified conditions to interconvert both aldehydes. Thus, β,γ -unsaturated aldehyde can be synthesized under thermodynamic conditions (**1.82**:**1.78** = 5:1), whereas enal **1.78** can be accessed through the formation of aldimine **1.90** / deprotonation / kinetic quench using BHT. The plan was to perform intramolecular olefin reductive coupling⁶³ from the Mukaiyama aldol adduct **1.91** to construct the desired bond and form tetracyclic key intermediate **1.92**. However, to our surprise, no aldol product was isolated even under forcing conditions and only starting material was recovered. Lack of the anticipated reactivity can be rationalized through a change of geometrical orientation of the carbonyl group in the absence of conjugation with the ring. In order to minimize the A-strain the aldehyde is located orthogonally to the bicyclic system such that both sides are shielded from the approaching nucleophile. This unforeseen behavior coupled with previous observations led to the discontinuation of the current approach.

1.3.4 Construction of C-ring via Rautenstrauch cycloisomerization

1.3.4.1 Background

In 1984 Rautenstrauch disclosed a novel method for the construction of cyclopentenones in an orthogonal fashion to the widely used Pauson–Khand and Nazarov reactions (Figure 1.4).⁶⁴ Readily available 1,4-enynes **1.93** undergo cycloisomerization with formation of C–C bond under palladium catalysis (Scheme 1.13). However, unlike its congeners, Rautenstrauch

cycloisomerization remained largely unnoticed in the synthetic community for several decades. Incomplete mechanistic understanding of the reaction and lack of applications in a complex synthetic setting led to its fading comparing to other annulative approaches.

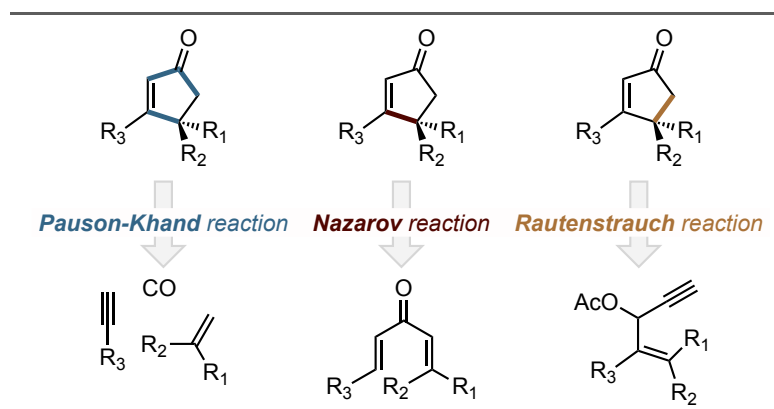
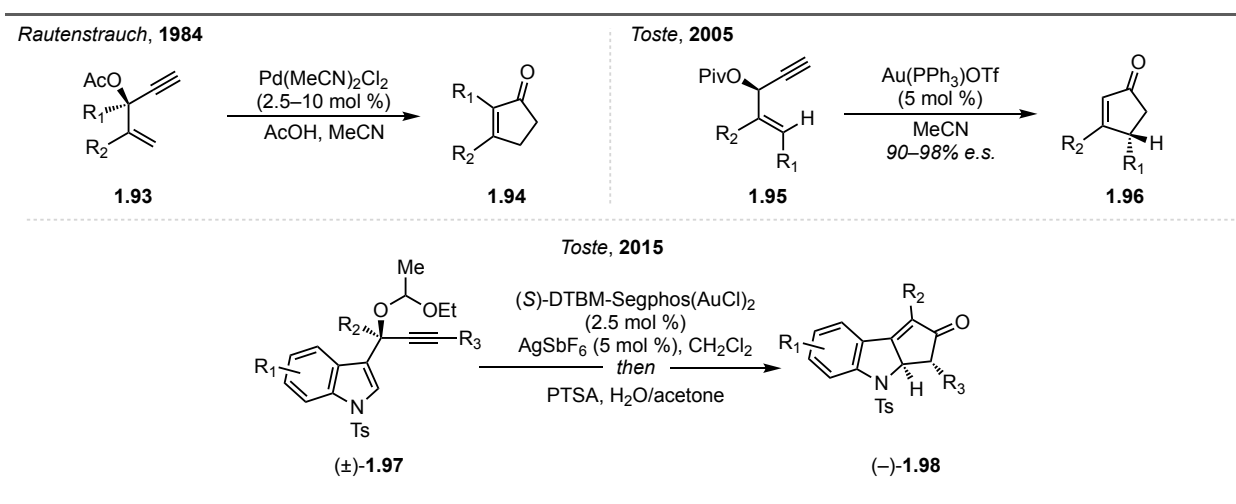


Figure 1.4 Methods for cyclopentenone synthesis.

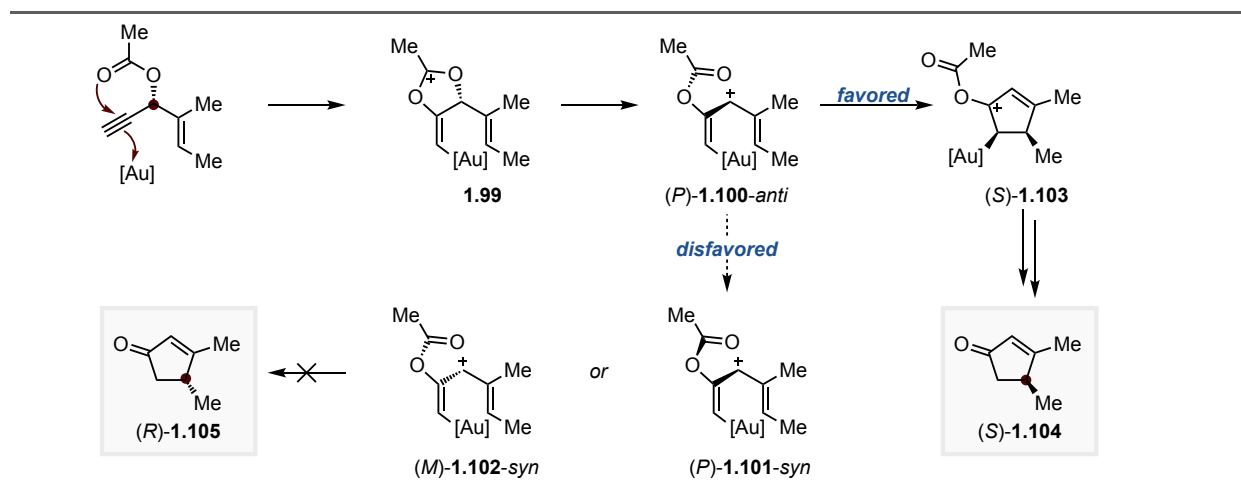
It was not until 2005 when Toste and co-workers reported on a *gold*-catalyzed Rautenstrauch cycloisomerization and revived this powerful transformation (Scheme 1.11).⁶⁵ Shortly after, several procedures using mercury, palladium and platinum catalysis with expanded substrate scope



Scheme 1.11 Development of Rautenstrauch cycloisomerization.

appeared in the literature.^{66,67} Finally, in 2015 an enantioselective Rautenstrauch reaction for the synthesis of cyclopenta[*b*]indoles was reported by Toste and co-workers.⁶⁸ The transformation was also subjected to extensive mechanistic investigations. As was noted in original report by Toste, the reaction possesses remarkable stereospecificity. The stereochemical configuration of the newly formed tertiary stereocenter was seemingly solely dictated by the original configuration of the carbinol. Even though observed empirically these results did not align with mechanistic hypothesis that reaction proceeds through a Nazarov-like intermediate, divinyl carbocation **1.100**. DFT-calculations conducted by de Lera and co-workers in 2006 shed light on this disparity.⁶⁹ Based on the energetic profile of the reaction it was concluded that the reaction proceeds through

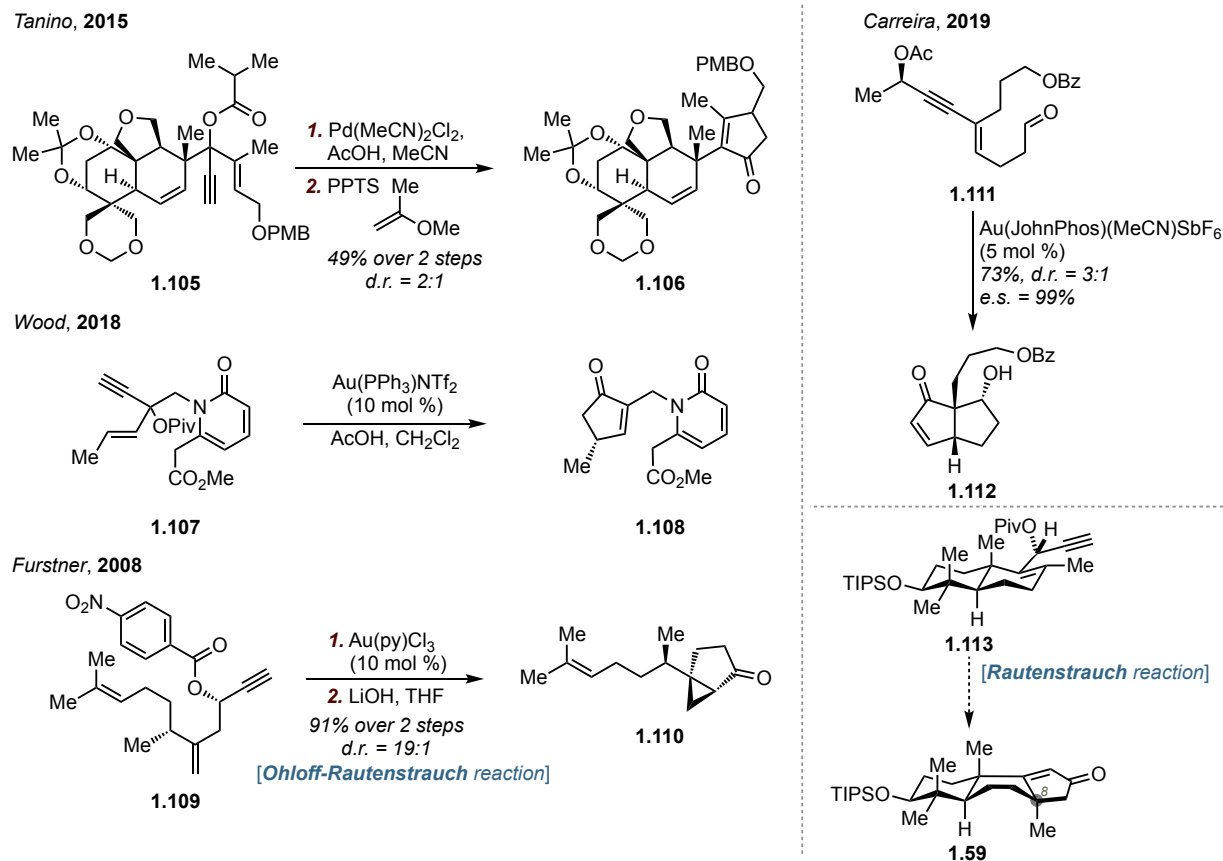
a unique *point-to-helix-to-point* transfer of stereogenicity. Both helix interconversion and the pivaloyl rotation are disfavored relative to the cyclization event leading to the single isomer of the product **1.104** as shown on the Scheme 1.12 (a simplified model for computation studies is provided).



Scheme 1.12 Mechanism of Rautenstrauch reaction and origin of stereospecificity.

Importantly, Rautenstrauch cycloisomerization did not find broad synthetic utility despite the described methodological advances. A single example was reported by Tanino and Sakurai in their synthetic studies towards azadirachtin (Scheme 1.13).⁷⁰ Noteworthy, another application of the Rautenstrauch reaction was disclosed by Wood and co-workers in an elegant synthesis of hosieline A during our own synthetic studies.⁷¹ Meanwhile a few other related gold-catalyzed transformations were successfully employed in total synthesis of natural products. Ohloff–Rautenstrauch cycloisomerization of 1,5-enyne **1.109** was employed to assemble the [3.1.0]-bicycle **1.110** in a single step and achieve the total synthesis of epoxysesquithujene.⁷² Analogously, enynyl acetate **1.111** underwent gold-catalyzed cycloisomerization to furnish intermediate **1.112** *en route* towards meroterpenoid merochlorin A reported by Carriera and co-workers.⁷³

Encouraged by the documented power of the Rautenstrauch reaction towards the stereoselective assembly of densely substituted cyclopentenone fragments, we have decided to put this transformation to the test. In particular, we envisioned the cycloisomerization of 1,4-enyne **1.113**. If successful, the new C–C bond along with a quaternary stereocenter at C8 will be formed delivering the desired, but so far elusive, ABC-tricyclic core of the isomalabaricane triterpenoids. However, we anticipated a significant complication: there were no reported examples of the use of



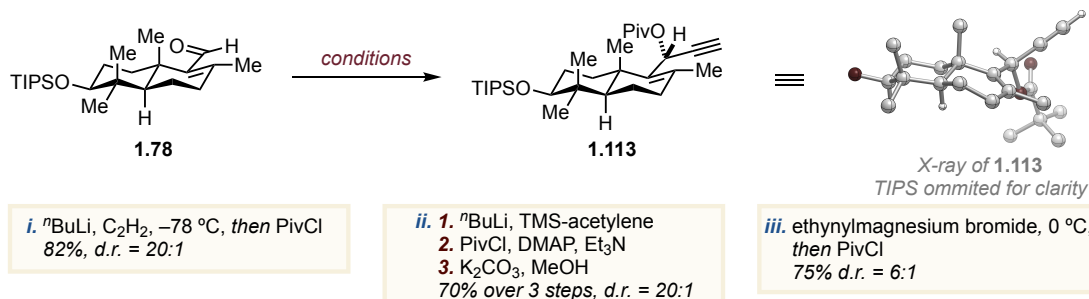
Scheme 1.13 Synthetic utility of gold-catalyzed cycloisomerizations.

tetrasubstituted alkenes in a Rautenstrauch reaction. Consequentially, formation of quaternary stereocenters remained out of reach for this approach. Nevertheless, we embarked on this synthetic challenge.

1.3.4.2 Synthesis of the 1,4-enyne

Aldehyde **1.78** was considered an ideal precursor for the requisite 1,4-enyne **1.113** (Scheme 1.14). The desired product was obtained either through a three-step sequence or the addition of freshly prepared lithium acetylide followed by *in situ* quench with pivaloyl chloride. Regardless, the product was isolated in high yields and excellent diastereoselectivity that was dictated by the strong substrate bias. The *S-trans* configuration of the α,β -unsaturated aldehyde is more favorable due to additional orbital overlap. Thus, approach from the *Si*-face for the incoming nucleophile is blocked by the axial methyl substituent, resulting in a strong bias towards attack from the *Re*-face. The configuration of C11 was confirmed by X-ray analysis. Remarkably, the use of the commercial Grignard reagent provided less satisfactory yields as well as diminished diastereoselectivity (*d.r.* = 6:1). Highly sensitive 1,4-enyne **1.113** could be purified by

chromatography using C₁₈-modified silica gel. Purification proved to be critically important as the next step gives irreproducible results otherwise. This observation was attributed to the inhibition of the catalyst by polyacetylenic by-products.



Scheme 1.14 Synthesis of 1,4-enyne **1.113**.

1.3.4.3 Reactivity validation and optimization

With necessary precursor **1.113** in hand we tested several reported catalytic systems based on Au(I), Cu(I), Pt(II) and Pd(II). To our delight the desired product was obtained under gold-catalyzed conditions in excellent yield and good diastereoselectivity (Table 1.5). Every parameter of the reaction was analyzed and optimized in order to render the transformation scalable, robust

Entry	Deviations	Yield ^a	Entry	Deviations	Yield ^a
<i>Catalyst instead of Au(PPh₃)Cl</i>			<i>Counterions instead of OTf</i>		
2	PtCl ₂	n.r.	12	AgNTf ₂	75%
3	Cu(MeCN) ₄ BF ₄	n.r.	13	AgPF ₆	74%
4 ^b	Pd(MeCN) ₂ Cl ₂	82%	14	AgBF ₄	77%
5 ^c	Au(PPh ₃)Cl	28%	15	AgSbF ₆	80%
<i>Solvents instead of CH₂Cl₂</i>			<i>Additives instead of H₂O</i>		
6	PhMe	n.r.	16	TFA	64%
7	THF	n.r.	17	AcOH	60%
8	DCE	75%	18	TFE	58%
9	EtOH	14%	<i>Control experiments</i>		
10	MeCN	71%	19	without AgOTf	n.r.
<i>Carboxylate instead of Piv</i>					52%
11	Ac	n.r.	20	without H ₂ O	16%
					(1.114)
			21	at 0 °C	4%

^a NMR yield. ^b d.r. = 1:1; ^c 1.0 mol %;

Table 1.5 Optimization of Rautenstrauch cycloisomerization.

and efficient. First, only gold and palladium catalysts showed catalytic activity. Catalyst loading for the former can be as low as 2.5%, while use of 1.0% of the catalyst lead to only poor conversion due to catalyst leaching (entry 5). Chlorinated solvents along with acetonitrile can be used with nearly identical results among multiple runs. Use of a gold complex with a non-coordinating anion obtained via salt metathesis with the corresponding silver salt proved to be critical for the transformation (entry 19). While numerous silver salts offered superior yields (entries 12-15) we decided to use silver triflate as the most affordable option. A protic additive is required to insure the hydrolysis of enol ester **1.114**.⁷⁴ Water is an optimal additive, while more acidic substituents attenuated the efficiency of the reaction. Notably, even under strictly anhydrous conditions hydrolysis of **1.114** was inevitable. Ease of this process is ascribed to the presence of a gold catalyst: isolated **1.114** could be hydrolyzed only under forcing conditions (KOH, reflux). Finally, use of a pivaloyl ester over an acetate is obligatory (acetate maintained reactivity under Pd(II)-catalysis, for more detailed discussion see p. 113). With optimized conditions, we proceeded to the robustness tests. The reaction was found to be highly reliable and reproducible, affording the product on decagram scale with identical yields and reaction time. The outcome was not sensitive towards air, concentration effects nor the use of unpurified commercial solvents (Table 1.5).

The diastereoselectivity of the process deserves a separate discussion. We were very pleased to observe 88% selectivity towards the desired isomer with the Me-group on the α -face as was established by single crystal X-ray analysis (Figure 1.5). The sense of selectivity matches with what one can predict using a *center-to-helix-to-center* chirality transfer model. As can be seen from a three-dimensional structure, the obtained isomer features a twist-boat conformation of the B-ring. Thus, compound **1.59** is associated with a higher strain energy relative to its diastereomer **1.115** with the Me-group on the β -face. Nevertheless, product **1.59** still prevails due to the stereospecific mechanism of the transformation. Thus, exclusive substrate control of the alkyne addition was leveraged to enable formation of the demanding quaternary stereocenter with high selectivity. The level of diastereoselectivity remained nearly identical regardless of the specific conditions that were applied in the course of

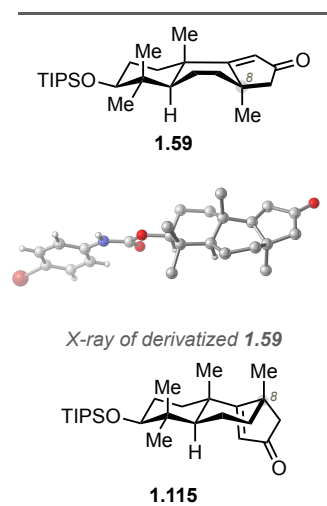


Figure 1.5 Products from Rautenstrauch reaction.

optimization, however it is unique to gold catalysis as *d.r.* = 1:1 was observed using Pd(MeCN)₂Cl₂ (Table 1.5, entry 4).⁷⁵

1.3.4.4 Scope of the Rautenstrauch cycloisomerization

Next, we decided to investigate the scope of the transformation with respect to alkyne component (Chart 1.3). The use of an internal alkyne might enable synthesis of the ABC-core with a substituent at C13. Appropriate functionality at that position, in turn, could facilitate further stages of the synthesis and elaboration of the synthetic intermediate. Firstly, we determined

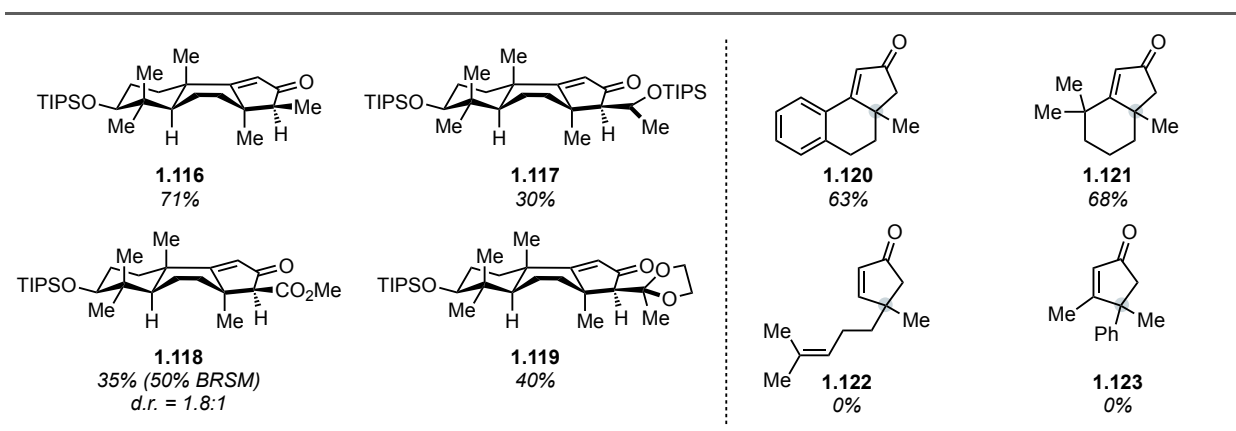


Chart 1.3 Scope of the Rautenstrauch cycloisomerization.

that reaction is generally compatible with internal alkynes. Indeed, enone **1.116** with a methyl substituent at C13 was obtained in 71% yield. Notably, the overall process sets two contiguous stereocenters (quaternary and tertiary) with great stereoselectivity and retained efficiency. The use of an internal alkyne probably enhances the rigidity of the helical transition state, which reflects in the improved diastereoselectivity of C8-stereocenter formation. Then, functional group tolerance was explored. Substrates **1.117**, **1.118**, **1.119** that correspond to the formal aldol or Claisen reaction of the enone **1.59** with various carbonyl compounds could be furnished in a single step. Only modest yields were observed, however, no special attempts to optimize these transformations were made either. Although, the accessed substrates turned out not to be viable intermediates towards the isomalabaricanes, they showcased the ability of the Rautenstrauch cycloisomerization to produce highly substituted and functionalized cyclopentenones in good yield from readily available precursors. Interestingly, no substrates with tetrasubstituted olefins were displayed within the reported scope. Originally, we ascribed the success of our transformation to the inherent destabilizing A-strain of enyne **1.113**. However, it turned out not to be the case as the reaction successfully proceeded for other monocyclic compounds delivering products **1.120** and

1.121 in synthetically useful yields. At the moment, we attribute the observed reactivity to the Thorpe–Ingold effect, since no product formation was observed for the linear substrates.

Overall, we have been able to develop a new strategy towards synthetically useful fused cyclopentenones with a quaternary stereocenter at the ring junction through an orthogonal disconnection

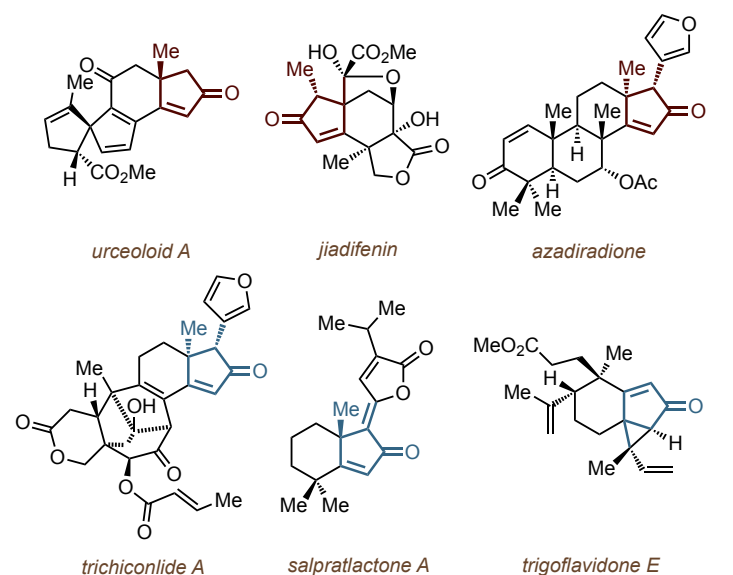


Chart 1.4 Natural products containing fused cyclopentenones.

with respect to other well-established annulative methods (*e.g.* Nazarov or Pauson–Khand reactions). Given the widespread nature of such structural motifs in terpenoids and limonoids specifically (Chart 1.4), we believe that the developed approach could be easily applied to total syntheses of numerous natural products.

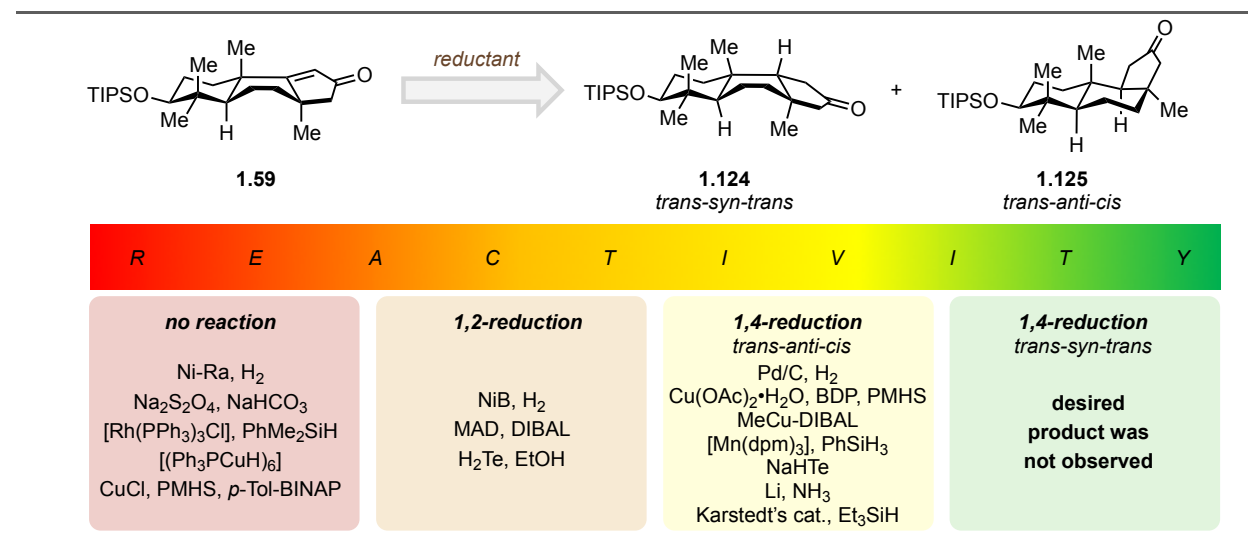
1.3.5 Formation of the *trans-syn-trans* perhydrobenz[*e*]indene core

1.3.5.1 Direct conjugate reduction

Once the carbon skeleton of the key tricyclic intermediate was assembled, the project entered its next phase – installation of the final stereocenter and completion of the *trans-syn-trans* perhydrobenz[*e*]indene core. This goal ultimately amounted to a stereoselective reduction of the α,β -unsaturated enone portion of the molecule. Careful examination of the X-ray structure of enone **1.59** provided valuable information (Figure 1.5). In fact, due to the twist-boat conformation of the B-ring, successful formation of the *trans-syn-trans* fusion required reduction from the concave face of the BC-bicyclic system. Notably, the reacting carbon center at C9 is a part of an *electron-deficient trisubstituted olefin positioned at a bisneopentyl site*. Therefore, general low reactivity is anticipated. Moreover, it was expected that the *trans-syn-trans* isomer is the highest in energy and therefore the undesired *trans-anti-cis* fused tricycle represented the thermodynamic product of the reaction. In essence, the reluctant nature of the substrate in conjunction with the

kinetic and thermodynamic penalties strongly disfavored the formation of the desired product during the course of the reaction.

A plethora of methods for conjugate reduction of enones has been reported to date. We surveyed a broad spectrum of reductive conditions in order to interrogate the system and reveal general trends and patterns of reactivity (Scheme 1.15). Hydrogenation, radical, and ionic manifolds were examined. To summarize, many conventional methods for conjugated reduction, such as hydrosilylation under rhodium and copper catalysis, failed to deliver the product. Stryker's reagent also did not show any reactivity towards the enone. Even though 1,2-reduction was not usually observed, several reaction conditions afforded the corresponding allylic alcohol as the major product. Some of the most powerful methods known for conjugate reduction, such as platinum-catalyzed hydrosilylation,⁷⁶ "Hot Stryker's" reagent developed by Lipshutz,⁷⁷ copper(I)-mediated hydride delivery,⁷⁸ radical-based methods, and heterogeneous hydrogenation effected the transformation. These reactions proceeded across a spectrum of efficiency but with stubbornly similar stereoselectivity profiles. Only *trans-anti-cis* isomer **1.125** was observed in every case. None of the reaction conditions provided even a trace of the desired diastereomer **1.124**.



Scheme 1.15 Examined conditions for enone **1.59** reduction.

In order to investigate what we suspected would be profound substrate bias for hydrogenation from the α -face, we turned to computational methods and performed an accurate thermochemistry evaluation (Figure 1.6). Geometries and thermochemistry corrections, obtained at RIJCOSX- ω B97X-D3 / def2-TZVP(-f) level of theory, revealed that the hydrogenation of

enone **1.59** to either diastereomer **1.124** or **1.125** is an exothermic and exergonic reaction. To ensure that the electronic energy evaluation was done with the highest precision affordable, we used single point DLPNO-CCSD(T) / def2-TZVPP calculations for electronic energy evaluations.^{79,80} While $\Delta_r S^\circ_{298}$ in both reactions seem to be the same, enthalpy changes $\Delta_r H^\circ_{298}$ are considerably different. We attribute this significant difference in hydrogenation enthalpies to a large relative total strain, which was estimated to be 32.9 kJ mol^{-1} . Distortion of the B-ring of

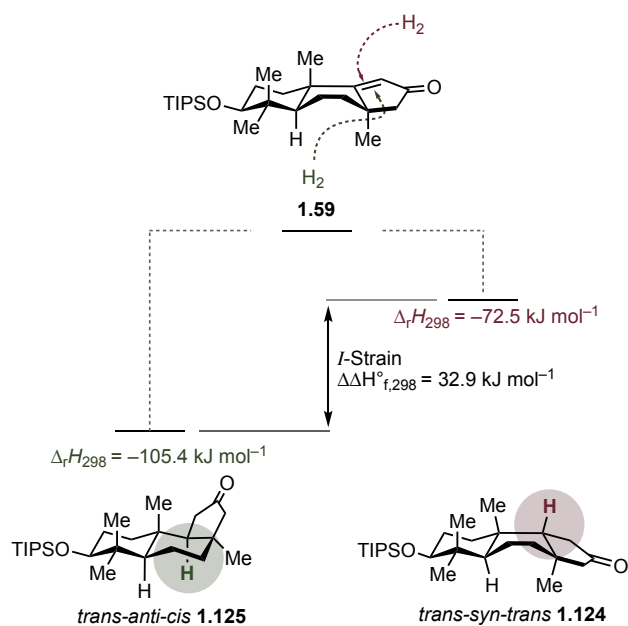


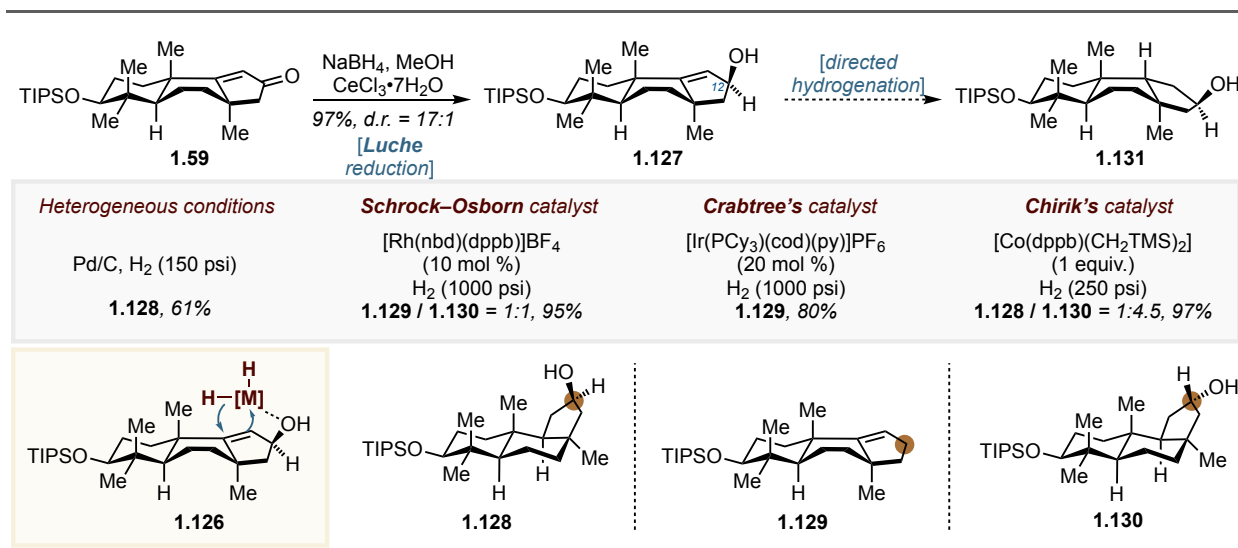
Figure 1.6 DLPNO-CCSD(T) / def2-TZVPP // RIJCOSX-B97X-D3 / def2-TZVP(-f) computed thermochemistry parameters for hydrogenation of enone **1.59**

the perhydrobenz[*e*]indene core in the *trans-syn-trans* isomer **1.124** to a twist-boat conformer resulted in a significant strain buildup, as compared to the *trans-anti-cis* isomer **1.125**. It is worthy of note that while the B-ring in the starting enone **1.59** also adopts a twist-boat conformation, both in solid phase (experimental X-ray) and in gas phase (calculated), it does not cause a strain buildup. The computed hydrogenation enthalpy of enone **1.59** is close that of cyclopentenone⁸¹ ($-97.1 \pm 2.1 \text{ kJ mol}^{-1}$), which suggests that despite having an unusual B-ring conformation, enone **1.59** does not suffer from a significant destabilization.

1.3.5.2 Directed hydrogenation

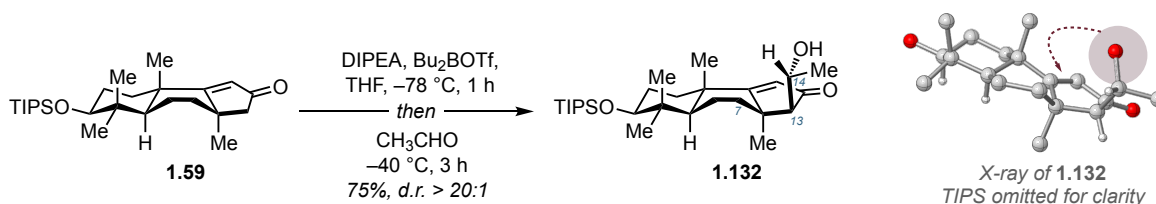
Realizing that reagent-controlled reduction is not a viable strategy for the synthesis of the *trans-syn-trans* perhydrobenz[*e*]indene core, we turned our attention to a directed approach. Allylic alcohols are known to be suitable substrates for directed hydrogenation (**1.126**, Scheme 1.16).^{82,83} Our requisite substrate was prepared through Luche reduction of enone **1.59** and afforded the desired isomer, **1.127**, in 97% yield. The relative configuration at C12 was confirmed by 2D NMR analysis. As expected, an elevated pressure of hydrogen was required. The product of heterogeneous hydrogenation, **1.128**, was used as a control experiment. To our surprise,

Crabtree's catalyst afforded exclusively **1.129**, the product of deoxygenation. The process, perhaps, proceeds via formation of Ir- π -allyl complex. Use of the Schrock–Osborn catalyst also provided



Scheme 1.16 Directed reduction of the allylic alcohol **1.127**.

an unexpected outcome: along with deoxygenation, epimerization of the stereocenter at C12 occurred followed by a presumably directed hydrogenation (**1.130**). Finally, a cobalt catalyst developed by Chirik group for directed hydrogenation⁸⁴ resulted in partial epimerization at C12 and reduction of the alkene from the convex face of each diastereomer. Extensive screening of catalysts, solvents, and additives did not lead to any improvements. These studies illustrated the resilience of the system towards the desired reactivity and demonstrated that an allylic alcohol is unsuitable substrate for directed hydrogenation.



Scheme 1.17 Synthesis of β -hydroxyketone **1.132**

The undesired reactivity observed in the latter approach was attributed to the close proximity of the reacting olefin to the directing group. We premised that positioning the directing group at a more distal region of the molecule could be advantageous. To this end, β -hydroxyketone **1.132** was synthesized (Scheme 1.17). Based on a three-dimensional model, it appeared that different

diastereomers could have substantially different reactivity profiles. Therefore, to gain reliable results and to simplify the analysis, a single isomer was desired, despite ablation of the stereogenic centers in the following steps according to the synthetic plan. This task was accomplished utilizing the reaction of boron-enolate of **1.59** and acetaldehyde.^{85,86} Due to the closed transition state of the transformation and pronounced substrate-control, only one isomer out of the four possible was obtained. The relative configuration was proven by single-crystal X-ray diffraction data. The hydroxyl group or a derivative thereof on the side fragment was intended to be used as a directing group.

In recognition of the rotational freedom of the hydroxyethyl adduct, we endeavored to validate the feasibility of utilizing this moiety as a directing group. This was done by employing a relaxed surface scan (RSS). This procedure allowed us to incrementally change one internal coordinate (dihedral angle θ , Figure 1.7) and perform geometry optimization of the molecule, while keeping the changed coordinate constrained. The resulting potential energy landscape should most closely correspond to the rotational motion of the hydroxyethyl side-chain. Inspired by the outstanding performance of ω B97X-D3 in hydrogenation thermochemistry calculations, we decided to use this function for energy evaluations in this task. RSS constrained optimizations were performed using the PBEh-3c method.^{xx} We then performed 60 energy evaluations with ω B97X-D3 / def2-TZVP around the full circle of rotational motion and identified three minima and three transition states. From the plot on Figure 1.9, it is evident that the minimal energy conformer (approx. 80% equilibrium population) places the hydroxyl group above the C-ring ($\theta = 16^\circ$) and over the double bond. The second lowest energy conformer (+3.4 kJ mol⁻¹, approx. 20% equilibrium population) can be reached through a small interconversion barrier of approximately 19 kJ mol⁻¹, which positions the hydroxyl group over the carbonyl fragment. These data suggested that we could reasonably

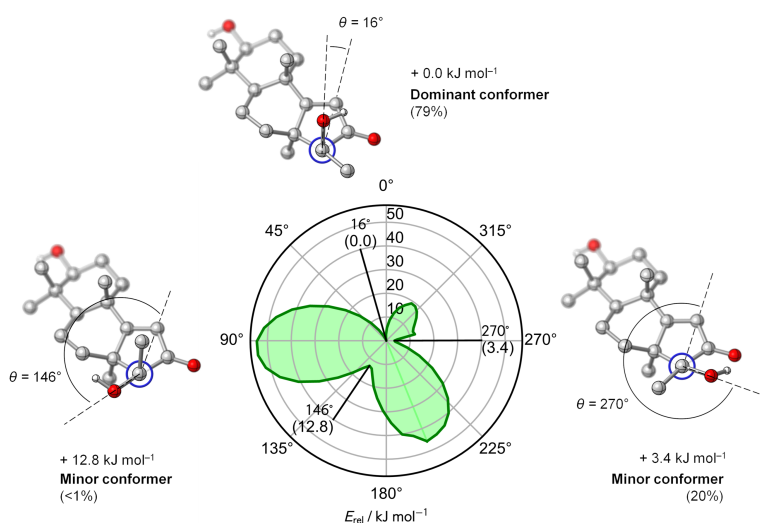
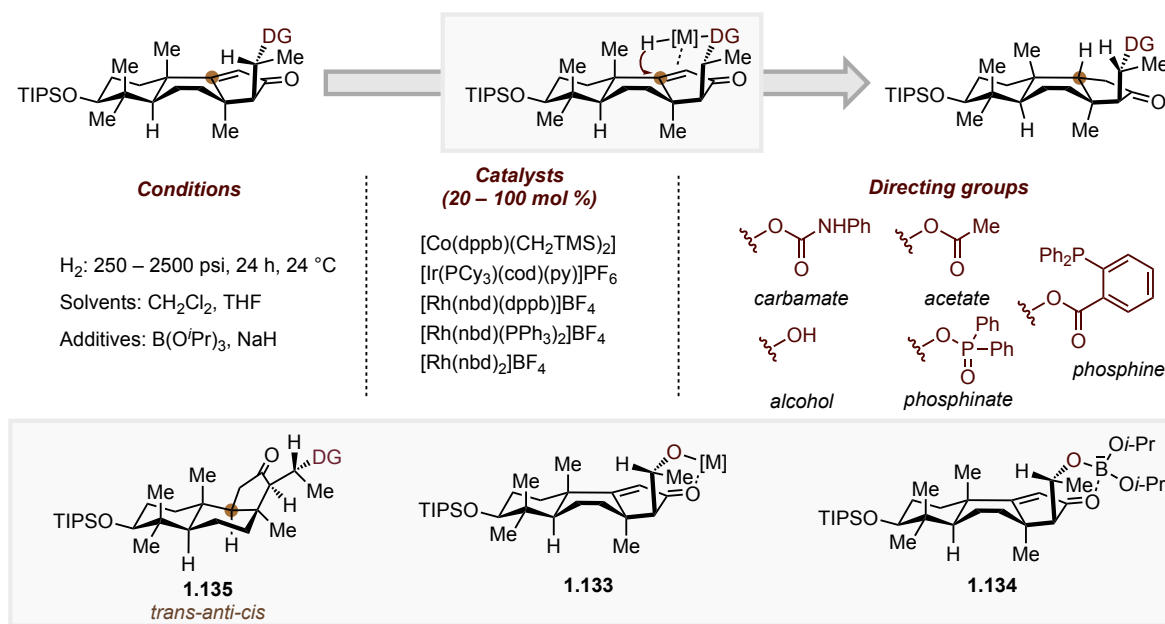


Figure 1.7 Relaxed surface energy at ω B97X-D3 / def2-TZVP // PBEh-3c level and minimal energy structures of **1.132**.

expect the hydroxyethyl moiety to be positioned in a favorable arrangement in order to direct the enone hydrogenation.

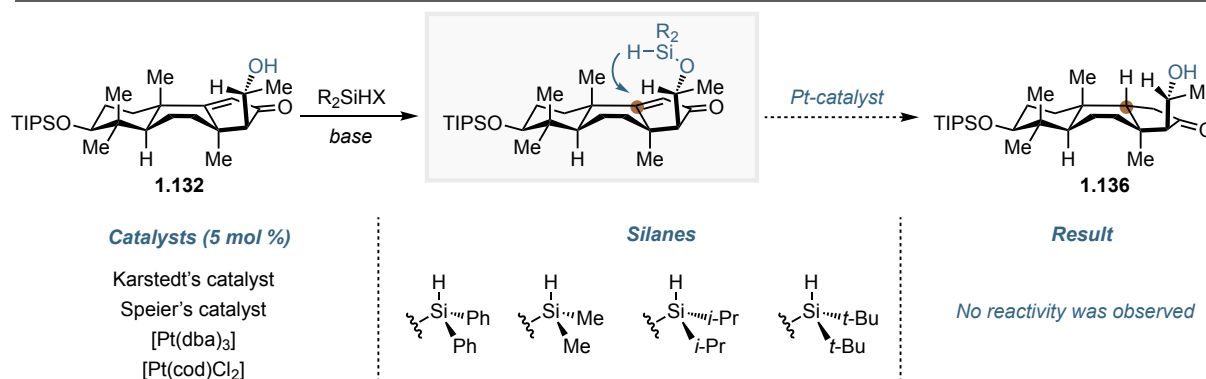
Despite the sensible theoretical validation of the proposed maneuver and numerous relevant literature examples, the substrate was found to be exceptionally resistant towards reduction under the conditions examined (Scheme 1.18).⁸⁸ We rationalized that the Lewis basic carbonyl motif coordinates to the metal center along with a directing group and lead to the formation of strong chelate **1.133**. Once formed, hydrogenation cannot proceed, since the π -system was not geometrically accessible. An alternative explanation is that formation of the chelate saturates the ligand environment of the metal center disabling oxidative addition into H₂. Lewis acidic additives have been widely used to circumvent this issue and to quench the most basic site of the substrate.⁸⁹ Implementation of this technique was not beneficial. Presumably, upon addition of a Lewis acid, a similar chelate between the β -hydroxyketone moiety and Lewis acid **1.134** is formed, which is not a competent substrate for directed hydrogenation. Analogous observations were made while varying the catalyst, solvent, pressure and other variables of the reaction. Alternative directing groups, such as carbamate, acetate, phosphine, phosphinate, *etc.* led to negligible improvements. Hydrogenation proceeded in rare cases at high pressure of hydrogen using stoichiometric amounts of precious metal complexes. In addition to challenges associated with reactivity, to our dismay, the *trans-anti-cis* isomer **1.135** was obtained as the sole product in all cases. This remarkably attenuated reactivity could be ascribed to either the absence of catalytic turnover in the case of phosphine or phosphinate directing groups or to preferential coordination to the ketone motif rather than carbamate or acetate. Only the combination of acetate as a directing group in the presence of one equivalent of triisopropyl borate was amenable to catalytic hydrogenation under forcing conditions. Specifically, 90% conversion was observed using only 20 mol % of the catalyst at 2000 psi after 36 hours. The unique behavior of this system is ascribed to high affinity of the catalyst to acetate as a directing group, while borate preferentially interacts with the ketone. Thus, both Lewis acids possess orthogonal selectivity and do not interfere with one another. Nevertheless, even in this case the undesired isomer was formed exclusively. Overall, the need for high pressure and long reaction time can be attributed to the necessity of unlocking intermolecular hydrogen delivery, which is manifested in the observed selectivity.



Scheme 1.18 Directed hydrogenation of **1.132** and derivatives thereof.

1.3.5.3 Intramolecular hydrosilylation

After the failed directed hydrogenation approach, we sought a process which exhibited a higher degree of stereocontrol over the course of the reaction. Intramolecular delivery of a hydride possesses this feature and should not leave any ambiguity regarding the stereoselectivity of the transformation. Therefore, intramolecular silylation of the enone became the reaction of focus (Scheme 1.19).^{90,91} Various silanes were installed using reported procedures. Substrates with small



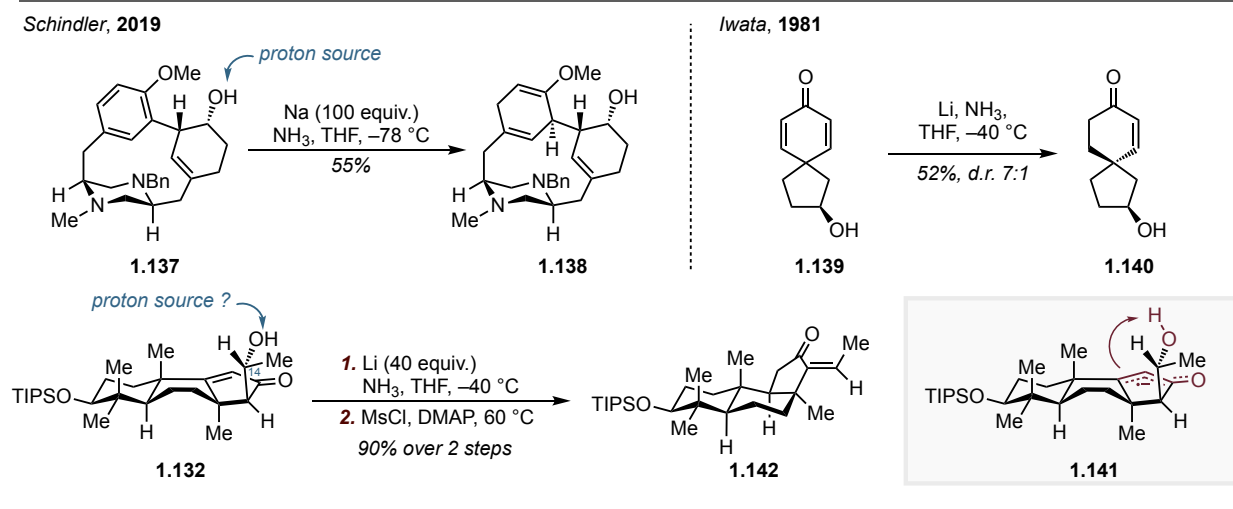
Scheme 1.19 Intramolecular hydrosilylation.

substituents on silicon were obtained in quantitative yields and used without purifications. Ones bearing large alkyl groups were stable towards purification using flash chromatography. Hydrosilylation typically proceeds employing platinum catalysis with high turnover numbers and

overall efficiency. Numerous platinum sources in combination with different silanes were tested. However, no satisfactory result was achieved: reduction was not observed and after acidic workup only starting alcohol **1.132** was recovered. The observed lack of reactivity was in agreement with the intense steric bulk of the reacting center and the restrictively congested transition state for the desired reaction.

1.3.5.4 Miscellaneous reductions

Several rather unconventional approaches for directed or intramolecular reduction were evaluated as well. First, we sought to assess the potential of directed Birch reduction (Scheme 1.20).⁹² The underlying concept of this methodology is that the hydroxyl group acts as an intramolecular proton donor after first reduction event. This cooperative effect enables not only a regio- and stereoselective reduction, but also reduction of otherwise unreactive functional groups (*e.g.* non-activated olefins). Despite being discovered several decades ago, such an unusual approach has only been exploited or observed a few times in total synthesis endeavors.⁹³ One of the most recent examples is the total synthesis of herquelines reported by Schindler and coworkers.⁹⁴ There, the presence of a homobenzylic hydroxyl group enables the reduction of arene

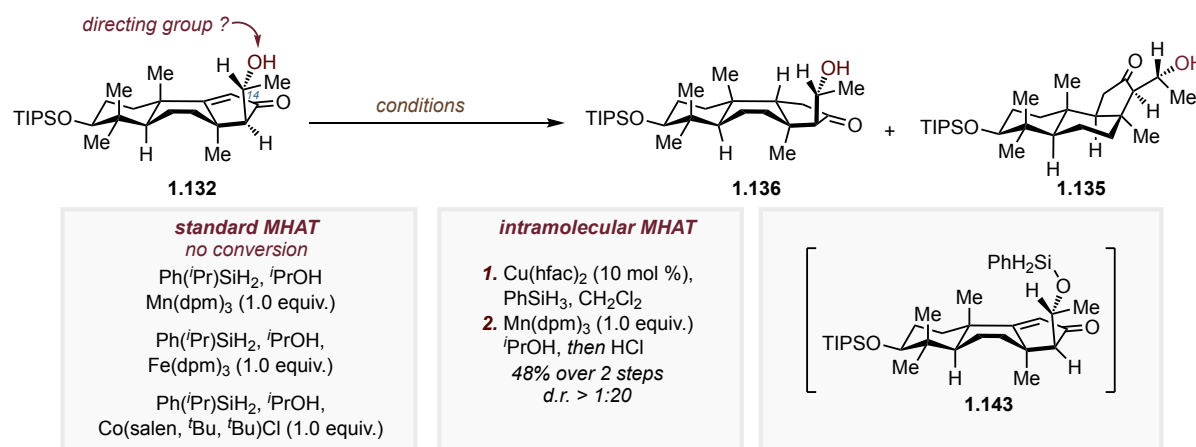


Scheme 1.20 Directed Birch reduction.

1.137, which was unreactive in the absence of this intramolecular proton shuttle. Along these lines we hypothesized that the secondary alcohol at C14 could be used in similar fashion (**1.141**). In order facilitate the analysis of the stereochemical outcome (reduce number of stereogenic centers and avoid issues with potential epimerization at C13) immediate dehydration was carried out. A

single product **1.142** was isolated with routinely observed *trans-anti-cis* configuration (determined by 2D-NMR, configuration of the olefin remains ambiguous).

Then we turned to a HAT-type reduction manifold (Scheme 1.21). Even though directed HAT processes are extremely rare,⁹⁵ we decided to examine this possibility. The standard set of conditions did not provide any conversion of the starting material. We then decided to explore a so far unprecedented strategy and use existing the secondary alcohol of the substrate as a silane carrier (similar to hydrosilylation). Shenvi and co-workers established that isopropoxy(phenyl)silane is the most kinetically competent reductant for MHAT.⁹⁶ We hypothesized that the secondary alcohol at C14 can act as a surrogate of isopropanol, which would bring the two reacting species (enone and silane) in close spatial proximity (**1.143**). This in turn might

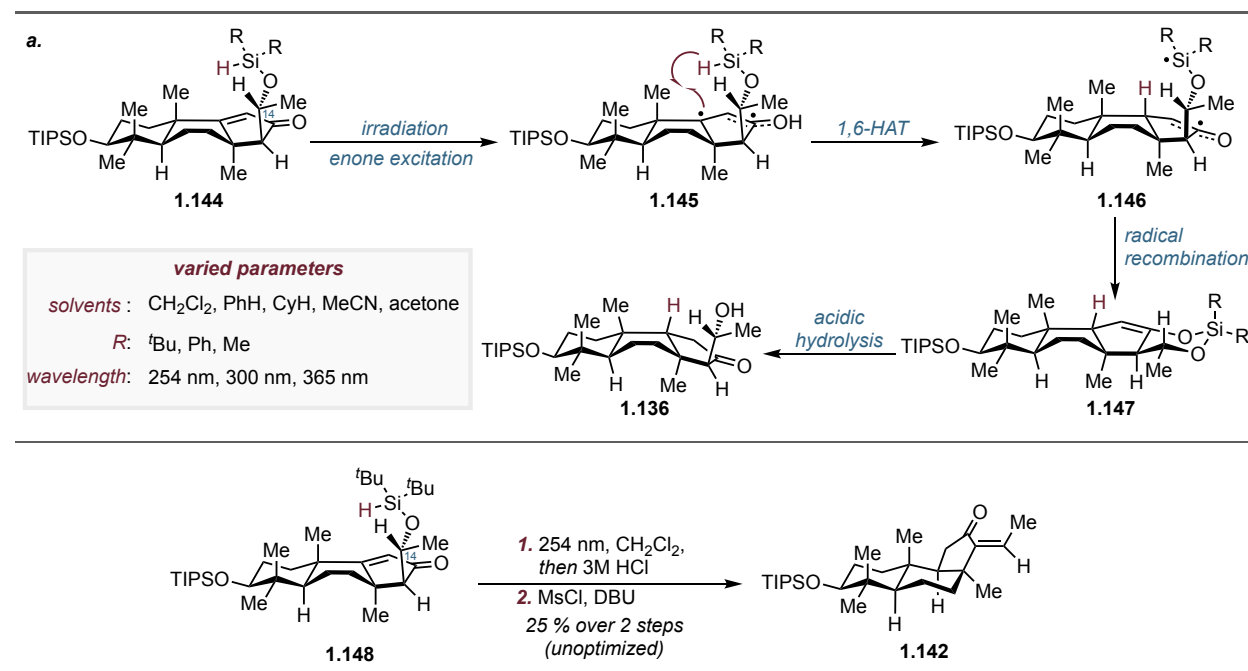


Scheme 1.21 MHAT reduction.

facilitate MHAT reduction and potentially be stereospecific if atom transfer occurs at an appropriate rate. Indeed, our hypothesis turned out to be partially valid. Cu-catalyzed alcohol silylation followed by rapid extraction and addition of the Mn(dpm)₃ under oxygen free conditions afforded a reduced product in moderate yield. Unfortunately, and maybe at this point of discussion anticipated, the product, **1.135**, possessed *trans-anti-cis* configuration of the core.

These intriguing results from our attempts to perform intramolecular MHAT made us question the necessity of a transition metal catalyst to perform the desired atom transfer (Scheme 1.22). The following mechanism could be envisioned: irradiation of substrate **1.144** with UV-light brings the enone to its excited state (**1.145**). Then 1,6-HAT from the silane to the carbon-centered radical is anticipated as it would generate the more stable silyl-radical **1.146**. Simple

recombination would, in turn, furnish cyclic silyl enol ether **1.147**, which will be hydrolyzed upon acidic workup. Notably, while the overall concept is elegant and rather simple, we failed to find any similar precedent in the literature. Encouraged by an opportunity to explore new reactivity and enable the so far elusive transformation, the array of silanes **1.144** was synthesized. Various solvents, photosensitizers and wavelengths of irradiation were examined. In most of the cases, intractable mixtures were formed with full consumption of a starting material. However, one set of



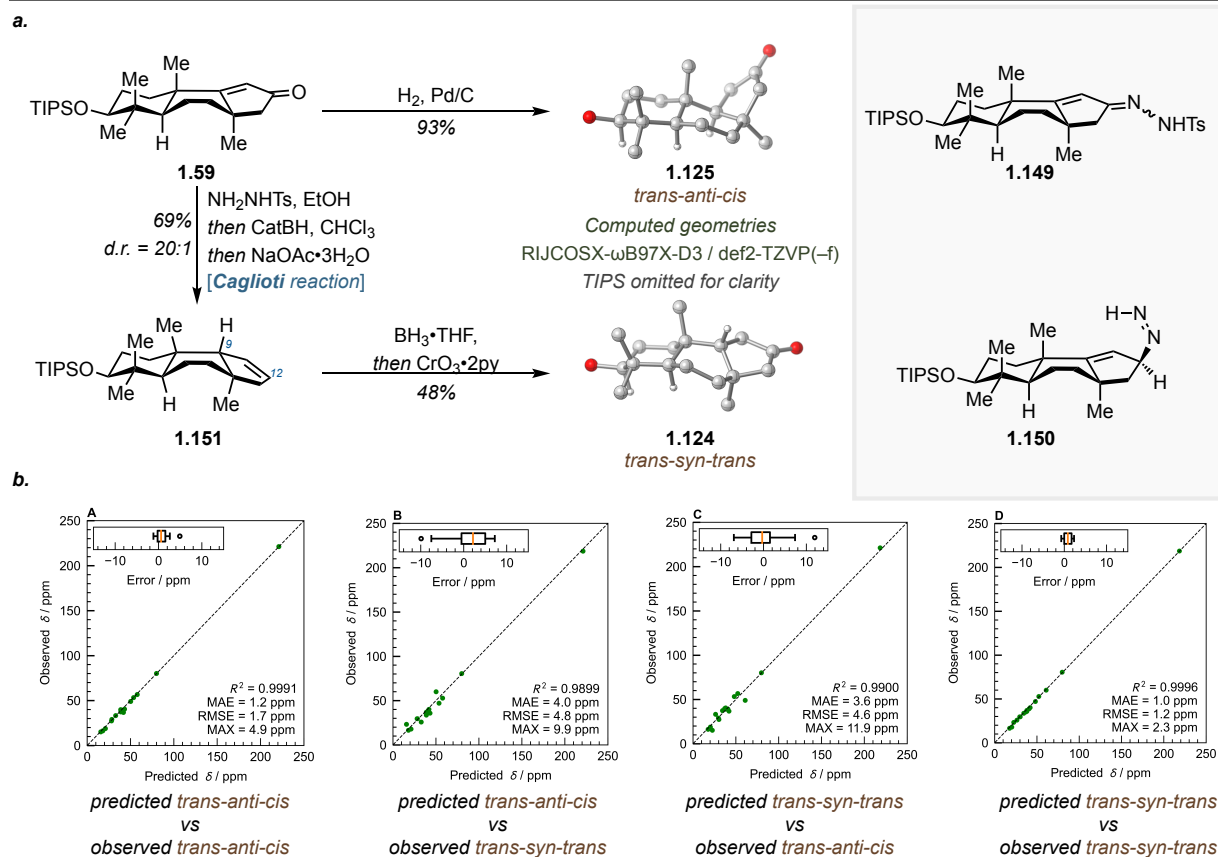
Scheme 1.22 Reduction via 1,6-HAT. **a** Mechanistic hypothesis; **b** Initial hit.

conditions afforded a promising result: bis(*tert*-butyl)silane **1.148** in dichloromethane upon irradiation with 254 nm delivered a product, which after dehydration matched by NMR the previously obtained enone, **1.142**. Since the stereoselectivity of the reaction was undesired, the transformation was not subjected to further investigation and optimization. However, we believe that the described process has a potential to become a valuable tool for stereospecific reduction of aldol products.

1.3.5.5 Reductive transposition approach

After all the tested approaches had failed, we recognized that only one final manifold for stereocontrol remained unprobed that holds a great promise to overcome kinetic and thermodynamic barriers. Due to the enormous substrate bias and steric hindrance of the desired reactive site, the *stereoselective* transformations were found to be unproductive. We envisioned

that the only reliable way of relaying stereochemical information would be a *stereospecific* transformation, such as a Caglioti reaction.⁹⁷ Application of this principle to the synthesis of *trans-syn-trans* perhydrobenz[*e*]indene is shown on the Scheme 1.23.a. We hypothesized that ketone **1.59** could be converted into the corresponding tosylhydrazone, **1.149**, which upon treatment with catecholborane, according to a protocol developed by Kabalka, furnished allylic diazene **1.150**.⁹⁸



Scheme 1.23.a Reductive transposition of enone **1.59**; **b** and scatter plots of predicted/observed ^{13}C NMR shifts. Insets correspond to error distributions. Diagonal dashed line: $y = x$.

Based on previous observations, reduction of the hydrazone is expected to be stereoselective, where the incoming nucleophile should approach from the β -face of the molecule. Finally, the allylic diazene should spontaneously undergo a retro-ene reaction to liberate nitrogen and deliver olefin **1.151** with the desired configuration at C9. Overall, reductive transposition should occur with exclusive stereospecificity due to the pericyclic nature of the process. Previously, it was documented for simple systems that this transformation is generally extremely exothermic ($-224.3 \text{ kJ mol}^{-1}$) with a remarkably low kinetic barrier (24.3 kJ mol^{-1}).⁹⁹ Moreover, the activation enthalpy for an alternative diradical pathway has been shown to be prohibitively high

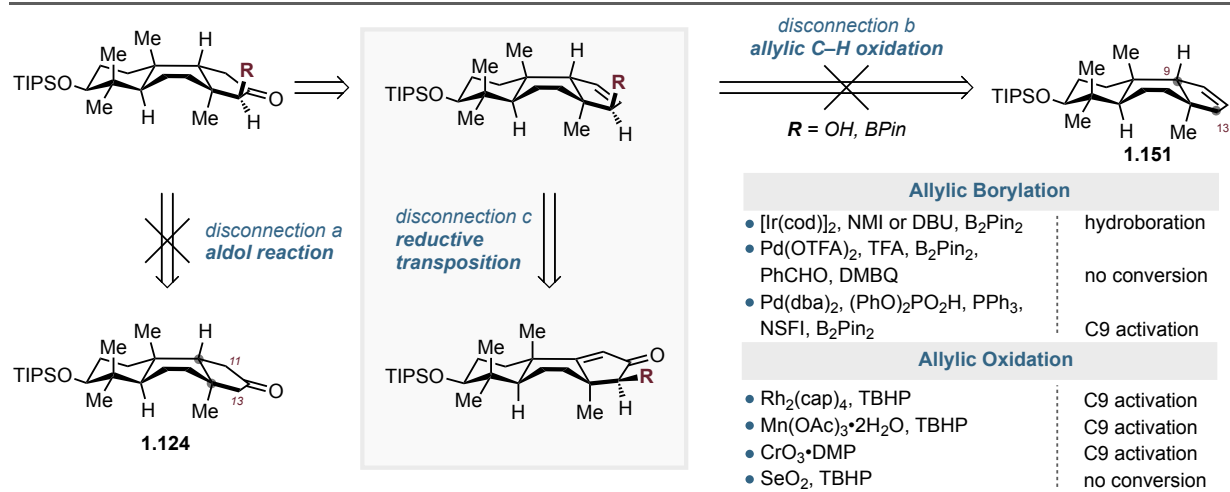
(211.3 kJ mol⁻¹) and should not be considered as a possible mechanism regardless of the substrate. In practice, product **1.151** was obtained in high yield as a single isomer. Its relative configuration was tentatively assigned as *trans-syn-trans*. Compound **1.151** was subsequently subjected to a hydroboration / oxidation sequence. Encouragingly, newly formed ketone **1.124** did not spectroscopically match with the previously obtained *trans-anti-cis* ketone, **1.125**.

However, being aware of the propensity of the core towards various rearrangements, more convincing proof of stereochemistry was sought. Due to a congested core with multiple contiguous stereocenters 2D NMR was not sufficient for this purpose. Moreover, the low crystallinity of the material hampered X-ray analysis. A substantial difference between the experimental ¹³C NMR spectra of the newly obtained compound and that of the *trans-anti-cis* isomer **1.125** (mean absolute error, MAE = 3.7 ppm, maximum absolute deviation, MAX = 11.1 ppm) was sufficient to attempt a computational study. Since modern density functional theory calculations can be used for the prediction of NMR properties with deviations lower than those observed between the two spectra, we decided to corroborate our stereochemical assignment by finding the closest matches between the predicted and observed NMR data (Scheme 1.23.b).^{100,101} We computed isotropic shielding values by means of GIAO-PBE0 / pcSseg-2 calculation.^{102,103} The conversion from isotropic shielding to chemical shifts was performed with a linear scaling calibration on a set of small molecules. We found that resolution of identity and chain-of-spheres (RIJCOSX) approximation, as implemented in ORCA 4.2.1,^{104,105} significantly decreased the typical calculation times without any noticeable effect on the accuracy of the method.¹⁰⁶ When applied to the calibration set, the method resulted in excellent correlation ($R^2 = 0.9995$), small errors (mean absolute error, MAE = 1.2 ppm, maximum absolute error, MAX = 3.4 ppm), and few outliers. To our delight, similarly low errors (MAE ≤ 1.2 ppm, MAX ≤ 4.9 ppm) were found for matching pairs of model and experimental spectra. Moreover, the deviation statistics bear high resemblance to those of the experimental NMR datasets. We were confident in our assignment of models to the corresponding experimental spectra, as the errors were several times higher (MAE ≤ 4.0 ppm, MAX ≤ 11.9 ppm), and the correlation was poorer for those models that were compared with the mismatched experimental data (Scheme 1.23.b **B, C**). This provided strong evidence that, for the first time, the correct isomer of the product was obtained. Eventually, through moderate derivatization, a suitable crystal for X-ray diffraction was obtained, with a geometry very similar to that calculated, and the structure of this compound could be confirmed unequivocally to indeed be the long sought after

trans-syn-trans perhydrobenz[*e*]indene **1.124**.

With the tricyclic core in hand focus was shifted to the adjustment of oxidation states in the carbon framework and the attachment of the corresponding side fragment. In order to complete the total synthesis of the isomalabaricane triterpenoids, one crucial C–C bond needed to be built at the C13 position. Two possible solutions were examined. C13 could be functionalized using an aldol reaction on ketone **1.124** or allylic oxidation of the methylene group on alkene **1.151** (Scheme 1.24). The prospects of the carbonyl substrate for further elaboration were evaluated first (disconnection a). A challenge of selective formation of an enolate towards the quaternary stereocenter (C13) rather than tertiary (C11) was anticipated. Only a single relevant example was reported in which unique sets of conditions were able to provide moderate selectivity in favor of the desired constitutional isomers.¹⁰⁷ A general solution to this problem remains elusive and, in most cases, the strategy of blocking the more activated site prior to the desired functionalization is the commonly used bypass. The reaction between ketone **1.124** and benzaldehyde was used as a model to evaluate the feasibility of the intended strategy. Enolization under kinetic conditions only furnished functionalization at C11, whereas thermodynamic enolization did not provide product altogether. In a desire to avoid excessive protecting-group manipulations, the aldol disconnection was disregarded. On the other hand, neither of the methods examined for allylic C–H oxidation or borylation of **1.151** were effective either (disconnection b). For instance, Ir-catalyzed C–H borylation developed by the Szabo group furnished the hydroboration product instead, whereas Pd-catalysis was completely inactive.^{108,109} Interestingly, the protocol reported by Gong and co-workers indeed afforded allylic C–H borylation.¹¹⁰ However, the C9-methine was activated instead of the more sterically accessible C13-methylene group resulting in formation of the allylic alcohol after oxidative work-up (NaOH, H₂O₂). A similar tendency was observed for radical-based oxidation conditions.^{111–113} Enone **1.59** was observed as a sole product of strain-releasing oxidation of the C9-methine over the C13-methylene. Other conditions failed to trigger any reactivity (*e.g.* Sharpless oxidation).¹¹⁴ These endeavors prompted us to conclude that functionalization of the C13 position prior to reductive transposition (disconnection c) would be required for further elaboration of the respective synthetic intermediate into the natural product.

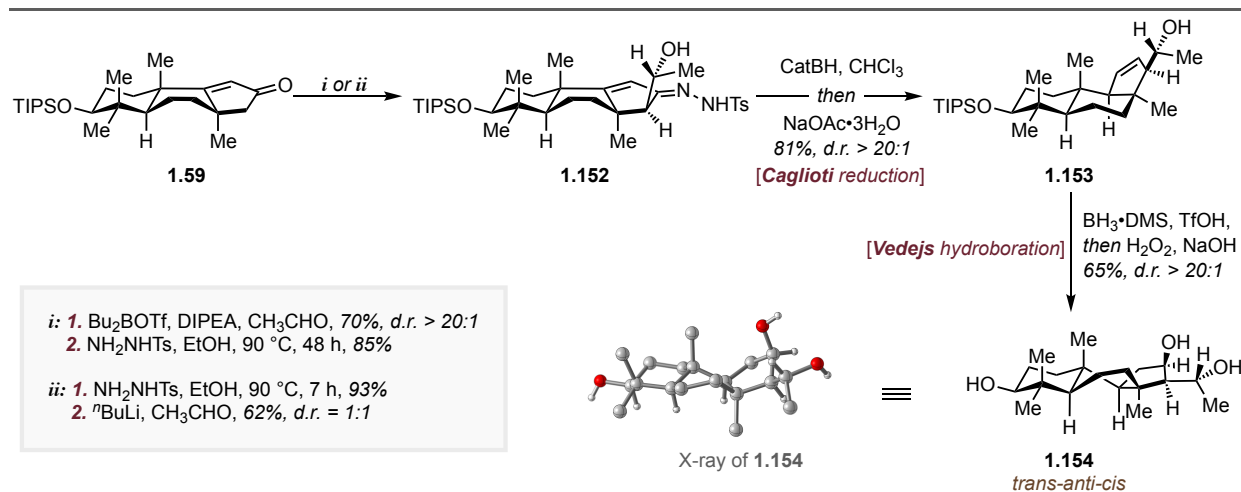
The choice of β -hydroxyketone **1.132** (Scheme 1.17) as a functionalized substrate for reductive transposition was apparent (Scheme 1.25). It already possesses the necessary connectivity for rapid elaboration to the natural product (see Figure 1.1). However, use of the more



Scheme 1.24 Attempted elaboration of the synthetic intermediates **1.124** and **1.151**.

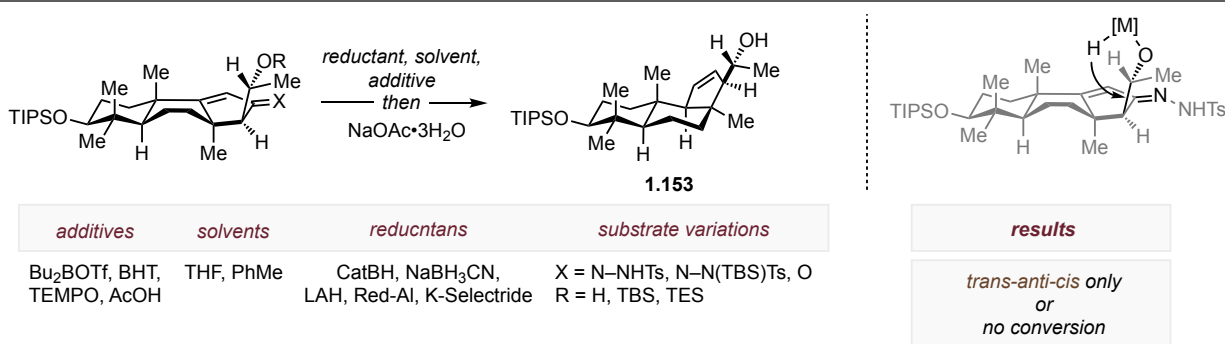
sterically congested substrate resulted in sluggish formation of the requisite tosylhydrazone **1.152**. Use of dehydrating additives (Na_2SO_4 , $MgSO_4$, mol. sieves) or an acid catalyst (AcOH) did not improve conversion. Alcoholic solvents and high temperatures were crucial for success. Notably, toluene led to clean conversion of the starting material into another unidentified product, whereas no reaction was observed in refluxing DCE, MeCN or PhH. The same precursor for transposition, **1.152**, can be synthesized via double deprotonation of the intermediary hydrazone (conditions *ii*) followed by addition to the C2-synthone, acetaldehyde.¹¹⁵ A low ratio of diastereomers at C14, however, was obtained in stark contrast to the boron-aldol reaction. Formation of the transposed olefin, **1.153**, occurred smoothly in good yield and with exclusive stereoselectivity. To restore the oxidation state at C12, an underutilized hydroxyl-directed hydroboration developed by Vedejs was employed.¹¹⁶ Unforeseen deprotection of the silyl-group occurred, and after oxidative workup triol **1.154** was isolated as a single isomer in 65% yield. X-ray analysis confirmed the expected configuration of the introduced secondary alcohol. Astonishingly, the crystal structure of triol **1.154** also displayed *trans-anti-cis* fusion of the tricyclic core instead of expected *trans-syn-trans*! Of note, despite being able to adopt a chair conformation, the B-ring retains its twist-boat structure to avert severe diaxial interactions.

Due to the stereospecificity of the retro-ene reaction, the altered selectivity of the process can be traced back to the reduction of the hydrazone. Despite being more sterically congested, hydride delivery presumably occurred from the α -face. The most sensible explanation for the observed outcome is that neighboring hydroxyl group directs the approach of hydride. Several control experiments were run to test this hypothesis (Scheme 1.26). Sodium cyanoborohydride as



Scheme 1.25 Reductive transposition of the aldol adduct.

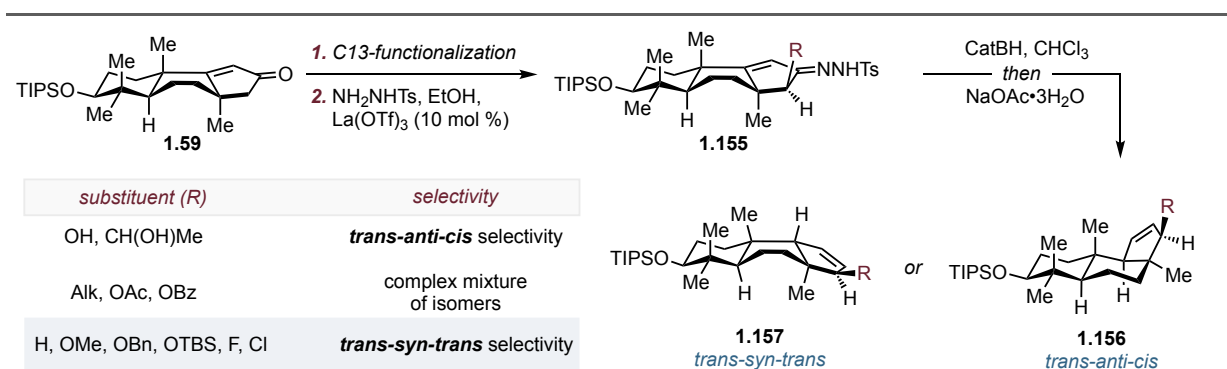
a reductant offered similar a result as well as use of a coordinating solvent (THF) or an additional equivalent of Lewis acid to insure precomplexation of the substrate prior reduction. A wide array of reductants was examined, but most of them failed to react due to the high basicity of the tosylhydrazone. Finally, the silyl protected hydrazone or alcohol failed to react altogether.¹¹⁷ Most importantly, reduction of the parent ketone with CatBH delivered the expected stereoisomer in accordance with the literature,¹¹⁸ although with significantly lower rate. This experiment suggests (but does not rule out) that directional effects are not responsible for the selectivity change. To rule out any radical pathways, the reaction was carried out under strictly deoxygenated conditions in the presence of radical scavengers (TEMPO, BHT). The course of the reaction remained invariable as was expected.



Scheme 1.26 Interrogation of the reductive transposition.

Recognizing that the retro-ene reaction is, perhaps, the only viable way to access the desired *trans-syn-trans* carbon framework within the current strategy, all efforts were focused on resolving this unexpected challenge. An important observation was made, when substrates with

various substituents at C13 were evaluated in terms of their reactivity and selectivity profile for reductive transposition (Scheme 1.27). The requisite substrates were synthesized via functionalization of enone **1.59** followed by hydrazone formation. In line with previous observations, condensation of derivatized enones were hampered relative to their parent compound due to steric factors. Necessary prolonged heating led to substantial decomposition of the substrates. $\text{La}(\text{OTf})_3$ was found to be an excellent catalyst for the process allowing for the reduction of temperature and time. Finally, rather bizarre results were obtained when prepared substrates **1.155** were subjected to the standard transpositive conditions. α -hydroxy enone delivered *trans-anti-cis* product **1.156** which is consistent with the previously observed inversed stereoselectivity for the β -hydroxy substrate. In contrast, alkyl and silyl ethers afforded the *trans-syn-trans* isomer as a sole product of the reaction. Use of a better nucleofuge such as acetate or benzoate led to a complex mixture of unidentified products. Finally, use of alkyl substituents led to the mixture of presumable isomers, where the compound with desired *trans-syn-trans* junction, **1.157**, was the major product. Thus, precise control over selectivity of the reductive transposition was attained based on the substituent at C13 position. That in turn enabled access to allylic ethers of type **1.157**, the missing link between unfunctionalized *trans-syn-trans* carbon framework and isomalabaricane triterpenoids.



Scheme 1.27 C13-functionalized enones in reductive transposition. Controllable stereoselectivity.

Ultimately, after myriad failed attempts we were able to identify a successful strategy for the stereoselective formation of *trans-syn-trans* perhydrobenz[e]indene core with appropriate functional handles for the first time. With these encouraging results, we aimed to complete the synthesis of the planned electrophile for cross-coupling and streamline the synthetic route if needed.

1.3.6. Synthesis of the key precursor for late-stage cross-coupling

At this stage, we set out to establish a link between the product of reductive transposition and the precursor of the natural product, triketone **1.158** (Figure 1.8). To accomplish the task a sequence comprising an allylic coupling of the transposed olefin with a C2-synthon, followed by selective oxidation at C12 needed

to be developed.

Retrosynthetically, cross-

electrophile coupling (XEC) via

umpolung of an allylic partner,

1.157, was envisioned as a key

transform. The established way to

enable the crucial C–C bond

forming event is the formation of

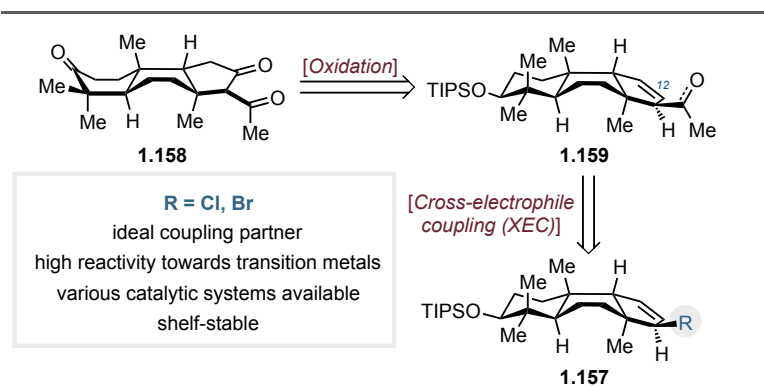
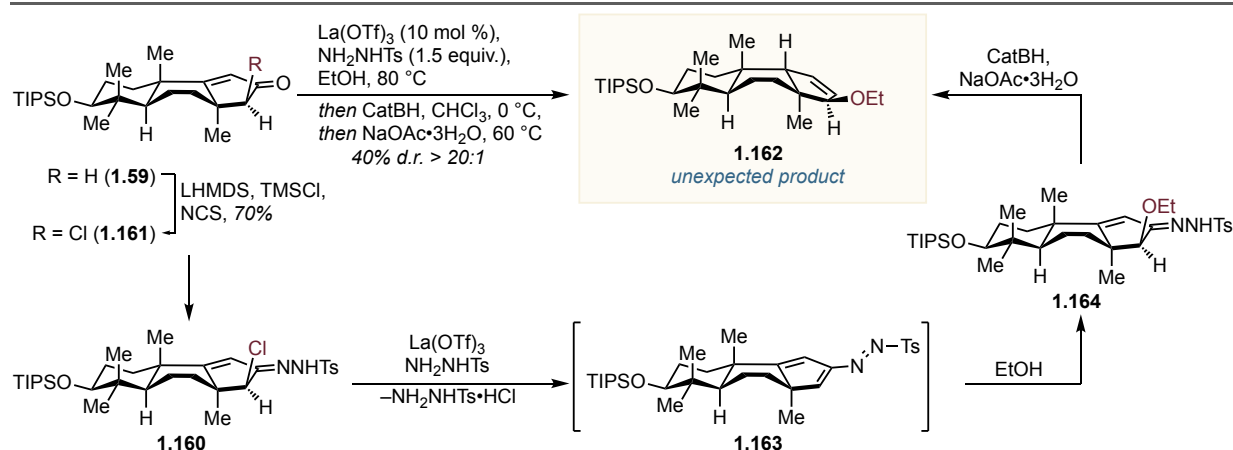


Figure 1.8 Revised retrosynthetic plan towards key precursor **1.158**.

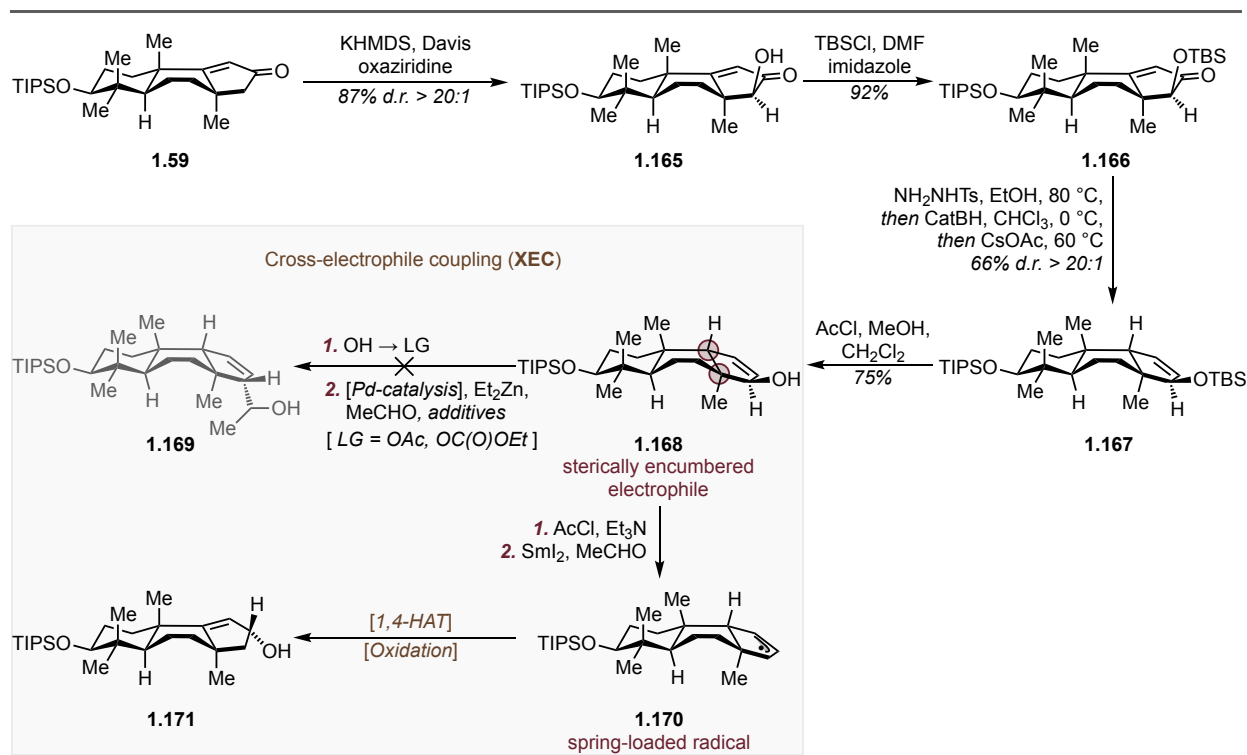
π -allyl species from an allylic electrophile. At the outset, we pursued a halide as the preferred coupling partner based on literature precedent. To synthesize the aimed substrate, reductive transposition of α -halohydrazone **1.160** was sought (Scheme 1.28). Towards this goal, chlorination of enone **1.59** was conducted uneventfully. However, after subjection of **1.161** to the standard conditions for the transposition, to our surprise, only allyl ethyl ether **1.162** was isolated from the reaction mixture in 40% yield. Literature survey of the reactivity of α -substituted hydrazones shed some light on the possible reaction pathway. The employed conditions for the hydrazone formation permits soft deprotonation. The following chloride expulsion generates aza-alkene **1.163**. Due to the high reactivity of the latter as a Michael acceptor, it gets trapped by ethanol present in solvent quantities. The resulting α -ethoxyhydrazone **1.164** undergoes routine reductive transposition delivering the observed product **1.162**. These results are also in line with poor representation of α -acetoxy and benzyloxy-enones as substrates for the transposition due to their high nucleofugality. Consequentially, peculiar features of the reductive transposition restrict the scope of possible substituents at C13. In turn, the inevitable poor leaving group ability of the substituent will jeopardize its activation for XEC. Nevertheless, we opted to surmount this obstacle invoking so far underutilized transformations.



Scheme 1.28 Unexpected result for reductive transposition of α -chlorohydrazone.

Allyl acetate was pursued first, since it could possess sufficient reactivity for the desired XEC and could be obtained in an indirect manner despite the discussed constraints. Thus, α -hydroxylation of enone **1.59** with Davis oxaziridine afforded product in 87% yield (Scheme 1.29). The resulting alcohol, **1.165**, was silyl-protected and subjected to the transposition conditions furnishing the expected product in 66% yield, **1.167**. The TBS-group was swapped to the leaving group of choice (acetate, carbonate). The synthesized electrophiles were examined as substrates for the generation of allylzinc species via a π -allyl palladium complex and subsequent *in situ* trapping with acetaldehyde. In the prior literature, this transformation was extensively studied, a remarkable substrate scope was demonstrated and therefore it held great promise to achieve our goal.^{119,120} Sadly, despite numerous attempts only starting material was fully recovered. The same outcome was observed when unprotected alcohol **1.168** was used instead under conditions reported by Tamaru and co-workers.¹²¹ The reluctance of the system can be ascribed to two factors: the electrophile was not engaging in the reaction due to high steric hindrance and the high propensity of acetaldehyde towards oligomerization at elevated temperatures rendering it as an unsuitable coupling partner. During attempts to attain the desired reactivity, a rather unusual process was documented that shows the ramification of high inherent strain associated with a *trans-syn-trans* configured core. In particular, we were attracted to the report from the Fiaud group on Sm(II)-mediated coupling of allylic acetates with carbonyl compounds.¹²² Mechanistic studies led the authors to conclude that cyclic five-membered allylic acetates undergo SET-reduction, producing an allylic radical, which can then add to an exogenous carbonyl compound. It was surmised that alternation of the transition metal catalysis to a radical

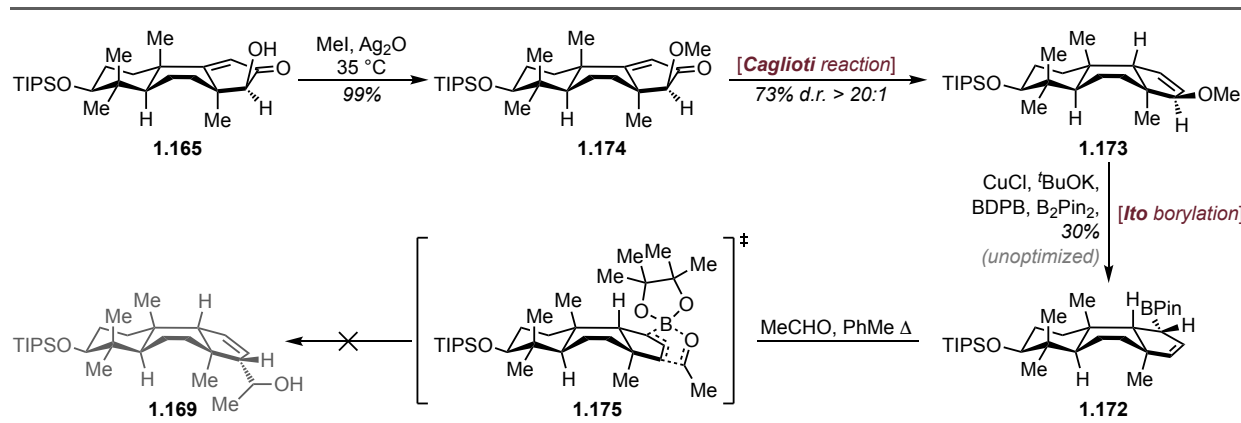
regime might provide a better chance for success. Towards this aim, allylic alcohol **1.168** was acetylated and exposed to excess of SmI_2 in the presence of acetaldehyde. Encouragingly, full consumption of starting material was achieved. Upon isolation, to our wonder, allylic alcohol **1.171** was identified as a single product of the reaction (spectroscopically matching with the previously obtained compound). The result can be explained by invoking a rather unusual 1,4-HAT in **1.170** followed by oxidation of the ensuing radical upon quenching with ambient oxygen. The displayed reactivity is most likely driven by the release of accumulated strain energy within *trans-syn-trans* core.



Scheme 1.29 Attempted cross-electrophile coupling.

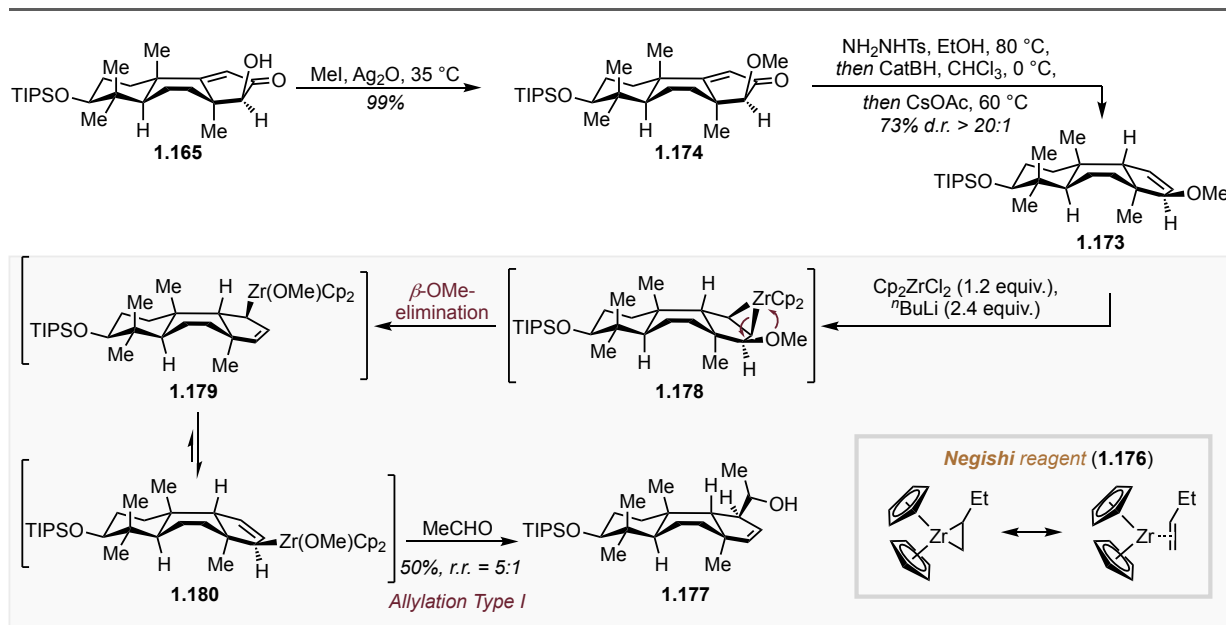
The observed incompatibility of surveyed substrates for the desired XEC led to reevaluation of the proposed disconnection and incorporation of an intermediary allyl boronate, **1.172**, which could be isolated if needed (Scheme 1.30). Switching from an umpolung mode to a well-established coupling processes was thought to be beneficial for the desired net reductive transformation. With this objective in mind, allyl methyl ether **1.173** was synthesized accordingly using standard protocols. Following conditions for Cu-catalyzed *anti*- $\text{S}_{\text{N}}2'$ -type borylation reported by Ito and co-workers, we were pleased to isolate the desired compound, **1.172**, in 30% yield.^{123,124} With a sufficient amount of substrate in hand, we proceeded to the next step before

optimization of the borylation. Allylation, employing nucleophilic boronates, is a robust method for C–C bond formation. This reaction proceeds via a six-membered transition state with mutual activation of coupling partners. Thus, catalysts/promoters are typically not required. In order to facilitate the transformation for the challenging substrates thermal conditions are applied (refluxing toluene). The reaction of interest is regarded as challenging based on steric demands and required boat-like transition state **1.175**, dictated by the substrate. Use of a volatile electrophile such as acetaldehyde again was detrimental for the reaction outcome. $\text{Sc}(\text{OTf})_3$ as a catalyst did not improve the performance either.¹²⁵



Scheme 1.30 Borylative approach.

Given the reported low reactivity of allyl ethers as electrophiles, the available toolbox for their activation is constrained. Thorough literature search revealed the unique, but underutilized ability of the Negishi reagent (**1.176**) to perform the desired activation even in favor of seemingly more reactive allylic halides (Scheme 1.31).^{126,127} Such an outstanding reactivity is attributed to the high oxophilicity of zirconium. First, zirconium complexes to the substrate (**1.178**) via irreversible ligand exchange, liberating butene. Subsequent intramolecular migration of the alkoxide to zirconium produces an allyl zirconium species **1.179** amenable to coupling with an appropriate electrophile. Generation of the Negishi reagent (**1.176**) from zirconocene and $n\text{BuLi}$, forms an organozirconium species which then couples with acetaldehyde in a single pot allowed for isolation of homoallylic alcohol **1.177** in 50% yield ($r.r.$ = 5:1). We were delighted to observe the desired reactivity, even though with the wrong regioselectivity. This result suggests that zirconium mainly resides on C13 (**1.180**) as the reaction with acetaldehyde proceeds through a closed six-membered transition state. Therefore, we hypothesized, that if the mechanism of the coupling is switched to one that proceeds through an open transition state, the



Scheme 1.31 Zr-mediated reductive coupling.

desired regioselectivity may be obtained. Addition to acetyl chloride as the C2-synthon was envisioned in particular. It has been documented in the literature that the presence of another metal-catalyst is required as the intrinsic nucleophilicity of the substrate is insufficient for the reaction to proceed. Ni(0) and Pd(0) catalysts for Negishi cross-coupling in the presence of zinc salts did not display any reactivity (entries 2-3, Table 1.6).^{128,129} Cu-catalysts, on the contrary, afforded the desired product in 21% yield along with starting material and the protodezirconation product (entry 1).¹³⁰ Notably, β,γ -unsaturated ketone was isolated as a mixture of constitutional isomers in 5:1 ratio favoring **1.159** as a single diastereomer, confirming our hypothesis. The high diastereoselectivity could be explained either by a steric argument and larger accessibility of β -face or the presumed stereospecificity of the transformation.

Since the reaction constitutes two separate processes, the optimization was carried out in two phases. First, a more effective formation of organozirconium species was investigated. Two parameters were found to be crucial: time and concentration. A concentrated solution as well as prolonged reaction times (~ 36 hours) are required to achieve full conversion. More consistent results were obtained under an argon atmosphere. The necessity of long reaction times is the major limitation of the developed process: larger scale requires even longer reaction times (> 48 hours) rendering the transformation impractical. Moreover, the intermediary allyl zirconium was found to be unstable for $t > 36$ hours, leading to diminished results. The use of cyclopentyl magnesium

bromide as a reductant was found to be less effective (entry 4). An increase in the equivalence of the Negishi reagent and temperature also led to lower yields. Finally, TMSCl as an additive to facilitate migration of methoxide had a negligible effect (entry 5). Based on the gained understanding of the transformation the following conclusion was made: rearrangement of zirconium complex **1.178** into allyl metallic species **1.180** is kinetically gating. Due to the unimolecular nature of the process there are fewer available tools to affect the rate. Thus, this aspect remains to be addressed for the reaction to become truly practical and scalable.

Entry	Deviations	Yield ^a	Entry	Deviations	Yield ^a
1	CuBr•Me ₂ S	21%	<i>Deviations in the second stage</i>		
2	Ni(PPh ₃) ₄	0%	6	CuI	55%
3	Pd(PPh ₃) ₄	0%	7	none	64%
<i>Deviations in the first stage</i>			8	[Cu(MeCN) ₄]BF ₄	41
4	^t PentylMgBr instead of ⁿ BuLi	0%	9	HMPA	0%
5	TMSCl as an additive	23%	10	BF ₃ •Et ₂ O	0%
			11	55 °C → 40 °C	45%

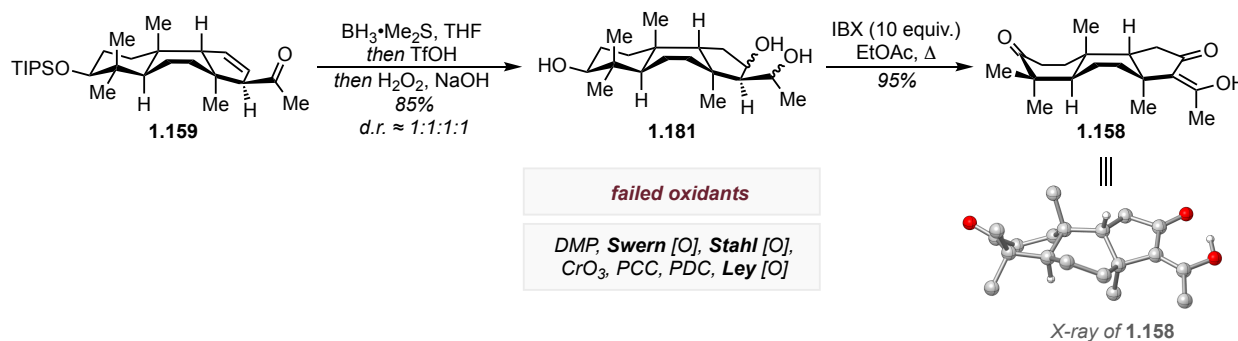
^a isolated yield.

Table 1.6 Optimization of the Zr-mediated reductive coupling.

Next, coupling of an allyl zirconium specie with acetyl chloride was investigated. A broad screen of various metals revealed Cu(I) salts as the most potent catalysts with CuOAc being the most productive (entry 7). The catalysis remained efficient at loadings as low as 5 mol %, albeit 20 mol % was typically used for operational ease. Addition of a second solvent was not found to be beneficial. Use of typical additives for copper-catalysis only had a negative impact (entries 9, 10). Importantly, the thermal regime was crucial for this step. 55 °C was determined to be optimal to balance regioselectivity and overall efficiency (entry 11). The reaction did not proceed at ambient temperatures. In total, optimization led to reproducible 64% isolated yield on 100 mg scale. To the best of our knowledge this is the first use of a Zr-mediated coupling of allylic ethers in synthesis. Successful application of such a unique transformation in a complex setting underscores its utility and calls for further development of the reactive manifold.

With the final C–C bond towards key triketone **1.158** installed, the requisite redox adjustments were explored (Scheme 1.32). Following our previous results for the *trans-anti-cis* isomer, the ketone was subjected to hydroboration. Use of 1.5 equivalents of borane ensured

complete conversion of the starting material. We speculate that the reaction proceeds in a relay fashion by first reducing the carbonyl¹³¹ followed by an intramolecular hydroboration of the olefin. Thus, no undesired constitutional isomer should be observed. However, contradictory to this hypothesis, all four potential isomers of the product **1.181** were formed in nearly equimolar quantities (inconsequential). *In situ* deprotection of the TIPS-group was achieved by addition of trifluoromethanesulfonic acid. Finally, oxidative workup delivers isomeric triols¹³² **1.181** from **1.159** in one-pot manner and 85% isolated yield. Use of stronger oxidants to directly access triketone **1.158** from an alkylborane species, such as high-valent chromium, TPAP, *etc.* have failed. Moreover, even oxidation of triol **1.181** turned out be a more challenging task than was originally anticipated. Most of the standard oxidation protocols failed (PCC, DMP, Swern, Parikh–Doering, Stahl, Ley). 1,3-diols were reported in the literature as notorious substrates for oxidation since many side-reactions typically occur throughout the process. Remarkably, use of 7–10 equiv. of IBX (~3 equiv. per alcohol) in refluxing ethylacetate delivered spectroscopically clean product in nearly quantitative yield.¹³³ The structure of the product and configuration of the carefully orchestrated stereocenters was unambiguously confirmed by single crystal X-ray diffraction. A salient feature of the obtained crystal structure is the geometry of the core: both A and B-rings adopt twist-boat conformations (which is also observed in the crystal structure of stelletin A).



Scheme 1.32 Synthesis of triketone **1.158**.

1.3.7 Streamlining the synthetic route

Having established viable disconnections and identified the required transformation towards the core fragment of the isomalabaricane triterpenoids, we set out to streamline the synthetic route. In particular, we envisioned that the synthetic sequence **1.113** → **1.173** could be facilitated if redox manipulations are more judiciously orchestrated (Figure 1.9).

As was discussed in the earlier chapters, Rautenstrauch cycloisomerization proceeds through the formation of pivaloyl enol ester **1.114** (Scheme 1.33.a). Use of a protic additive insures hydrolysis of that intermediate to furnish the expected cyclopentenone product. However, the nucleophilic nature of **1.114** could be harvested instead to our favor and enable α -functionalization of the enone in the same pot, increasing redox- and step-economy by omitting the hydroxylation step. With this concept in mind, an array of suitable electrophiles was tested. Early on it was recognized that stepwise protocol of additions is not necessary and simultaneous addition of electrophile with the catalyst is even more

advantageous. Notably, the use of strong oxidants in presence of Au(I)-catalyst does not intervene in the catalytic cycle, moreover it improves the rate. Full conversion of the 1,4-enyne **1.114** was typically observed within 1 min. Meta-chloroperbenzoic acid was identified as the most efficient source of electrophilic oxygen. The major product of the reaction, meta-chlorobenzoate **1.182** can be hydrolyzed *in situ* by virtue of K_2CO_3 and methanol. Desired alcohol **1.165** was isolated in 52% yield as a single diastereomer from the 1,4-enyne in just one operation. Initial formation of ester **1.182** is rationalized by the intermolecular opening of epoxide **1.183** with the exogenous acid (Scheme 1.33.b). This mechanism was supported by a cross-over experiment. The presence of benzoic acid affords a mixture of respective esters in a 1.5:1 ratio, validating the intermolecular nature of the process. The residual mass-balance of the transformation corresponds to regular Rautenstrauch product **1.59** (~10%) and pivaloyl ester **1.185** (~20%), which can also be hydrolyzed into α -hydroxyl enone **1.165** under more forcing conditions (refluxing KOH).

Encouraged by these results, other electrophiles were examined. The reactive paradigm turned out to be quite general and various α -functionalized products **1.186** were isolated in good to excellent yields (Scheme 1.34).¹³⁴ In related fashion fluorination, chlorination, bromination and iodinations could be performed using abundant electrophiles. A single diastereomer was isolated in each case. The executed transformation represents a powerful tool for complexity generation: vicinal tertiary and quaternary stereocenters are installed with perfect stereocontrol delivering densely substituted cyclopentenones in a single step from a readily available precursor.

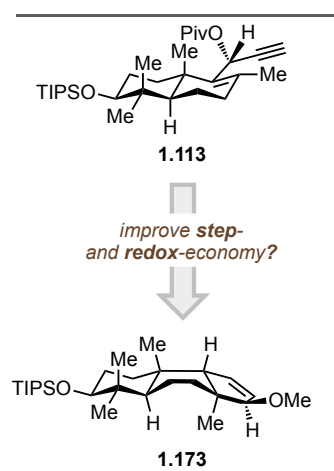
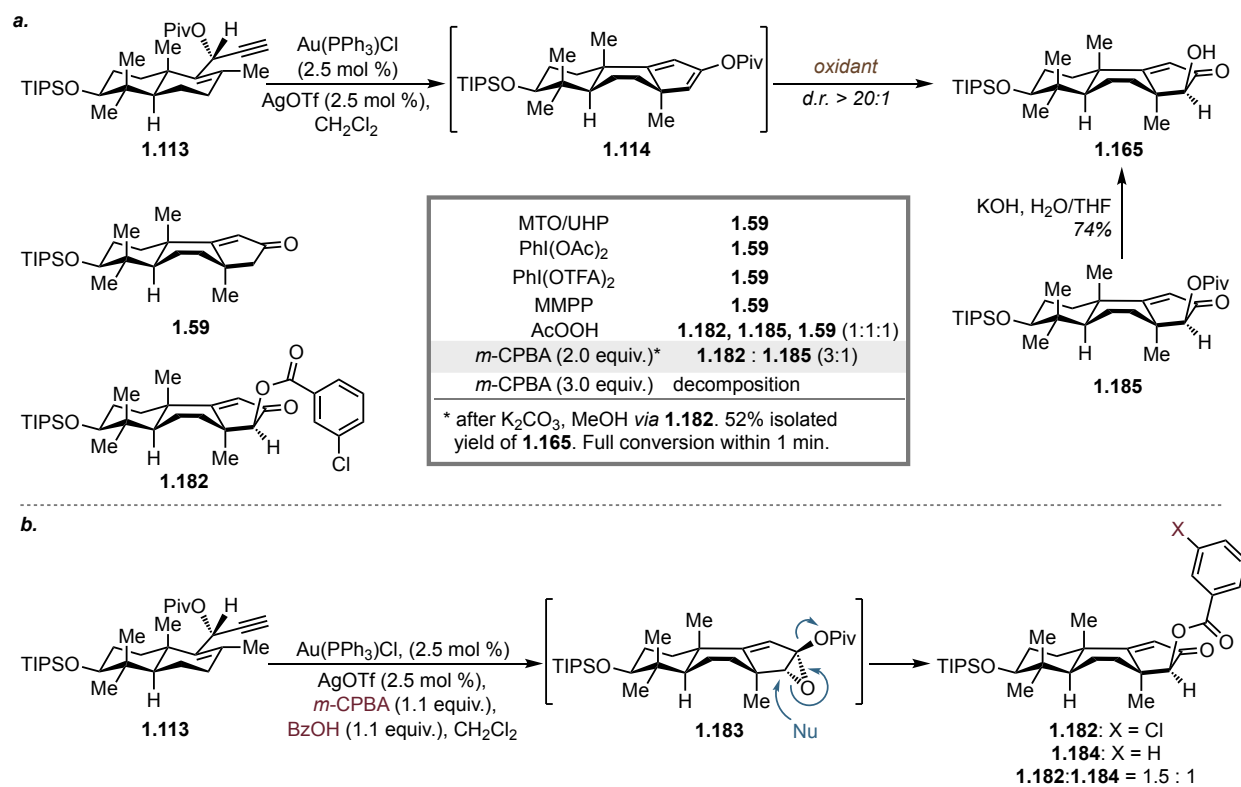
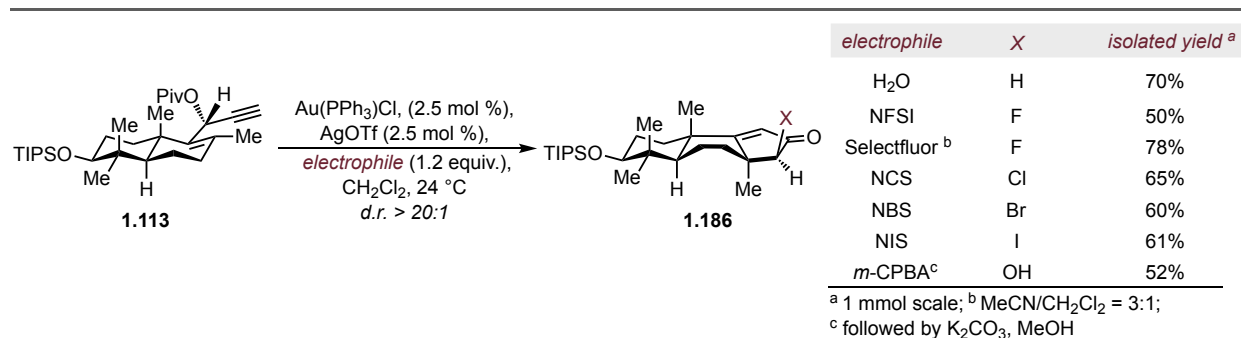


Figure 1.9 Goal to increase efficiency of the synthetic sequence.



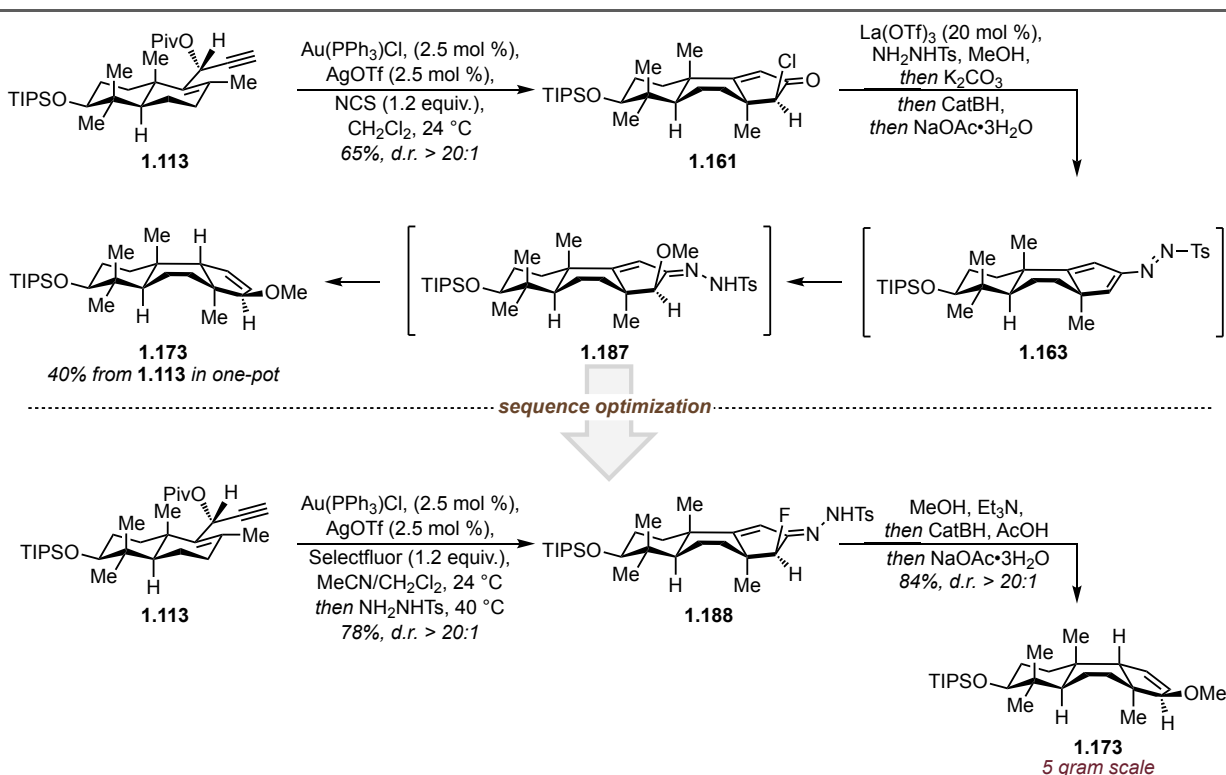
Scheme 1.33.a One-pot Rautenstrauch reaction / oxidation cascade; **b** cross-over experiment.

Bearing in mind the necessity of the methoxy-substituent at C13, we opted to install that group directly, omitting the methylation step and further increasing step-economy. The lack of readily available and safe source of “OMe⁺” renders our interrupted Rautenstrauch approach inadequate for this purpose. Recalling the previously observed undesired reactivity of α -functionalized hydrazones, we surmised that its combination with the modified Rautenstrauch cycloisomerization protocol might achieve the desired transformation. In practice, first we performed the chlorinative



Scheme 1.34 Interrupted Rautenstrauch cycloisomerization; scope of electrophiles.

cyclization (Scheme 1.35). Resulting enone **1.161** was then subjected to hydrazone formation followed by an *in situ* substitution via aza-alkene intermediate **1.163** and finally *one-pot* reductive transposition. This operation stereoselectively furnished the allyl ether **1.173** in 40% yield. Reassured by this outcome we performed an optimization of the protocol. Use of a fluoride substituent instead of a chloride was highly beneficial and dramatically improved the yields and scalability.¹³⁵ The trend was ascribed to (a) smaller size and larger inductive effect of fluorine that enables expedient condensation with hydrazide at lower temperatures, (b) lower nucleofugality of fluorine that stabilizes the intermediary hydrazone, but does not affect downstream reactivity. Finally, the optimal performance of the sequence was achieved, when hydrazone formation was conducted during the cyclization step. For that purpose, tosylhydrazide was employed as a quenching reagent instead of ammonia. Aging the reaction at 40 °C furnished hydrazone in 78% yield. Sequential one-pot substitution/reduction/transposition in turn delivered desired product in 84% yield reproducibly on gram scale.



Scheme 1.35 Final optimization of the synthetic sequence.

In summary, a new route to allylic ether **1.173** was developed, shortening the overall synthetic sequence. This was enabled by novel methods for harvesting chemical reactivity of rather unusual and underutilized intermediates such as an aza-alkene and an alkyl fluoride (Figure 1.10).

In total, for the first time, gram scale access to the *trans-syn-trans* perhydrobenz[*e*]indene scaffold and the direct precursor to isomalabaricane triterpenoids from commercial materials was established in 8 and 11 steps respectively.

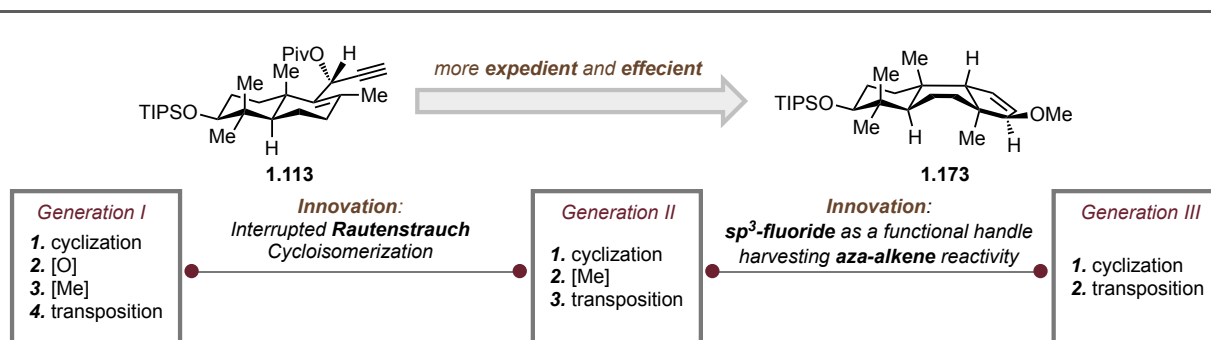


Figure 1.10 Three generations of the synthetic design.

1.3.8 Synthesis of vinyl electrophile for late-stage cross-coupling

To successfully complete the total of the isomalabaricane triterpenoids we had to surmount one final challenge: late-stage cross-coupling between the triketone-derived coupling partner and the requisite polyene (Figure 1.11). The foundation of our synthetic attempts lies in work directed towards accessing retinoic acid derivatives. The highly conjugated nature of the corresponding products and its sensitivity imposes limitations on the synthetic toolbox applicable for such a system. As was established in prior literature, the use of a sterically congested vinyl electrophile in combination with a polyenyl nucleophile often leads to superior results compared to the reversed scenario.¹³⁶ Accordingly, we aimed to convert the triketone into appropriate electrophile **1.188**. The 1,3-dicarbonyl motif in **1.158** is unsymmetrical, posing the issue of regiocontrol. A solution to this problem has yet to be established and selectivity can be attained only in *a priori* biased systems.¹³⁷ In a more general sense, researches have to rely on intrinsic substrate bias or avoid such intermediates altogether.

Only a single cautionary example has been reported for 2-acylsubstituted cyclic ketones. Trauner and co-workers have reported the synthesis of vinyl triflate **1.191a** with exclusive selectivity opposite to the one desired in our case (Figure 1.11).¹³⁸ Nevertheless, we have pursued a regioselective functionalization approach. The decision was made based on an observable intrinsic bias of triketone **1.158**: both in solid state (according to X-ray) and in solution (according to 2D NMR) the desired tautomer prevails. If successfully leveraged, the bias will provide access to electrophilic coupling partner **1.188** with high fidelity.

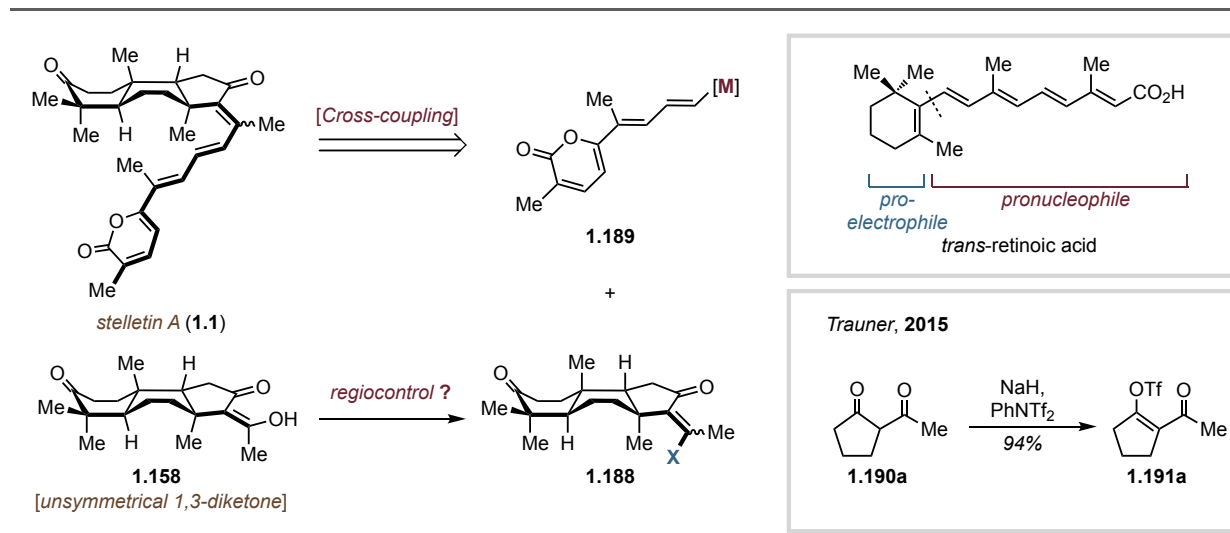
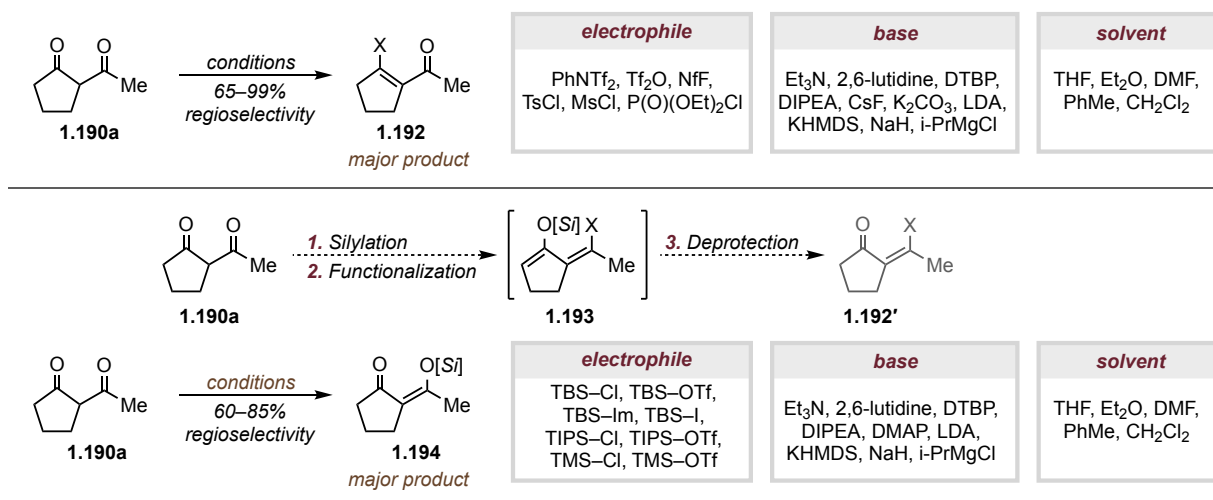


Figure 1.11 Retrosynthesis of the final stage and concerns of regiocontrol.

First, direct functionalization was explored on the model 2-acetylcyclopentanone (**1.190a**) (Scheme 1.36). The relevance of this model system was validated by several cross-experiments with triketone **1.158**, where similar selectivities were observed for both substrates. In agreement with previously reported data, the reaction uniformly occurred on the endocyclic ketone despite the nature of the employed electrophile, solvent, base and temperature. While various conditions were translated into various levels of selectivity, its sense remained constant. Even conditions previously reported for the similar system in synthetic studies towards isomalabaricanes delivered undesired constitutional isomer **1.192** exclusively.¹⁶

Next, we sought to incorporate a strategy of transient protection (Scheme 1.42). Namely, protection of the more reactive carbonyl as a silyl enol ether, followed by a second deprotonation/functionalization (**1.193**). *In situ* deprotection would reveal desired electrophile **1.192'**. Surprisingly, implementation of this strategy afforded endocyclic isomer **1.192** as the major product again. After thorough analysis of the reaction mixture, an interesting observation was made. Depending on the conditions utilized either exocyclic silyl enol ether **1.194** with modest selectivity was obtained or a nearly equimolar mixture of both constitutional isomers. An alternative set of electrophiles profoundly affected the outcome. Thus, the envisaged transient protection or exchange of a silyl group to triflate or nonaflate,^{139,140} were deemed as nonviable due to the inherent low selectivity of silylation for either site.

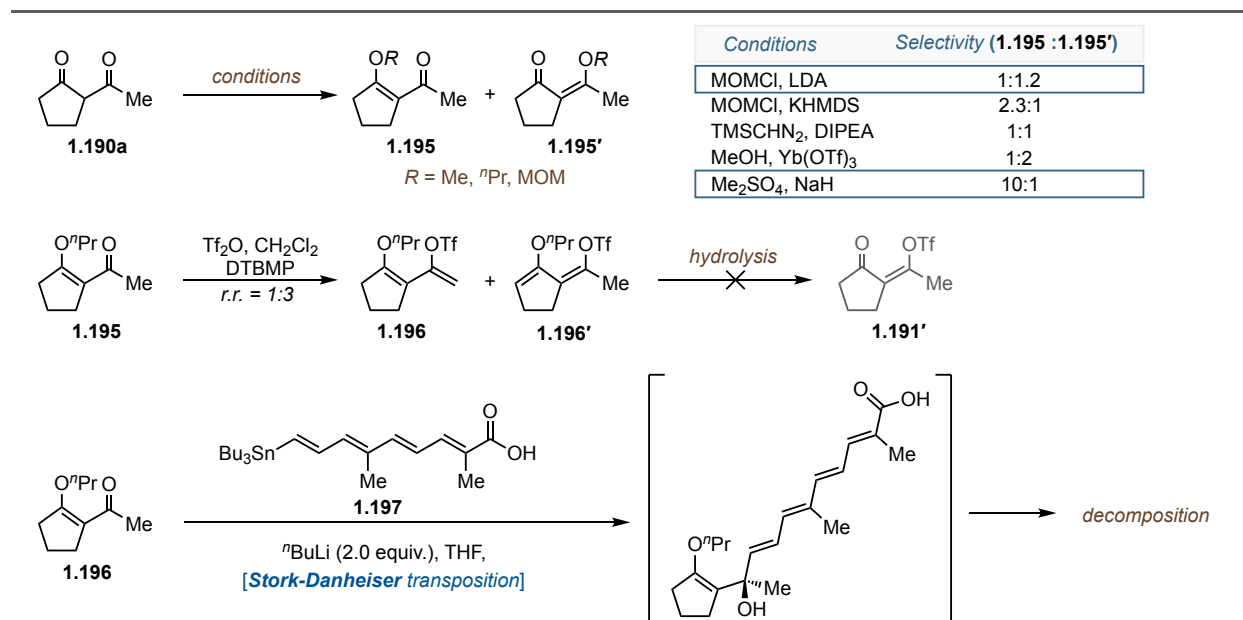
Alkylation of the dicarbonyl compound was investigated as well (Scheme 1.37). Similar to previous systems, the selectivity behaved as a complex function of the



Scheme 1.36 Attempts towards regioselective functionalization of the model system **1.190a**.

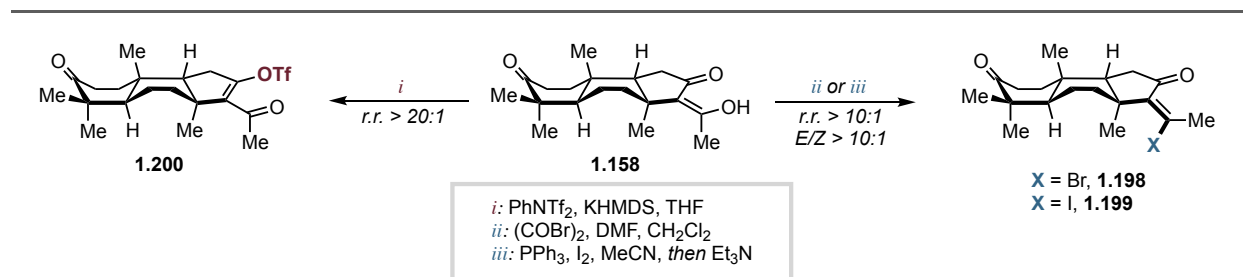
employed reaction parameters. After screening conditions that operate under various mechanistic manifolds, endocyclic alkyl ether **1.195** could be obtained as a sole product. With **1.195** in hand, several approaches were explored. Regular triflation delivered a mixture of anticipated products (**1.196**:**1.196'** = 1:3). However, the obtained vinyl ethers were remarkably reluctant towards hydrolysis and were recovered even after treatment with perchloric acid. The Stork–Danheiser method for the synthesis of β -substituted enones was evaluated as well. While 1,2-addition of the nucleophile derived from acid **1.197** (for its synthesis see p. 55) was observed spectroscopically, the subsequent hydrolysis / elimination cascade yielded only an intractable mixture of decomposed products.

We presume that design of a tailored alkyl ether and optimization of the sequence would eventually lead to success of the strategy depicted on Scheme 1.37. However, accumulated data from described attempts prompted us to reassess our original approach. The occasional switch of regioselectivity hinted on the possibility of identifying conditions for direct functionalization, which would be an ideal solution. After additional rounds of screening conditions reported by Mewshaw, to our delight, favored formation of the **1.192'** type exocyclic vinyl bromide (*r.r* = 3.3:1).¹⁴¹ Moreover, when this set of conditions was probed on triketone **1.158**, exclusive regioselectivity and diastereoselectivity were observed (Scheme 1.38). This unusual outcome is ascribed to non-basic conditions, which allows for leveraging the innate tautomeric form of the substrate. The hypothesis is supported by identical results obtained for the model system using a triphenylphosphine / iodine combination.¹⁴² Overall, we achieved regio- and stereoselective access



Scheme 1.37 Regioselective alkylation of the model system and further manipulations.

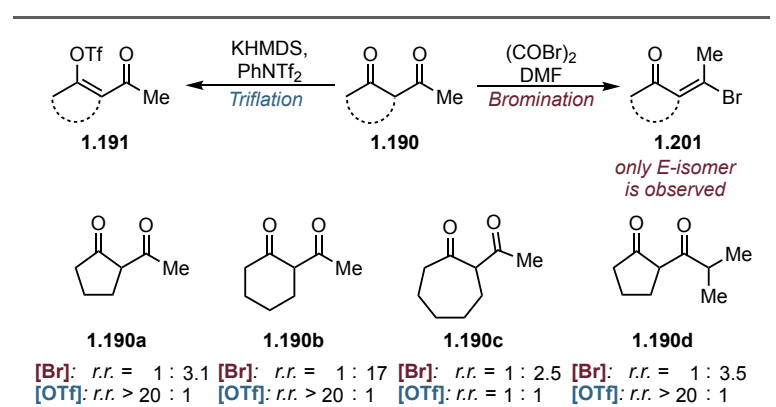
to the versatile electrophiles for cross-coupling from unsymmetrical 1,3-diketone **1.158**. Isomeric triflate **1.200** can be easily obtained in a divergent manner from the same precursor **1.158** enabling the synthesis of structural analogues of the isomalabaricane triterpenoids.



Scheme 1.38 Regioselective functionalization of the triketone **1.158**.

Recognizing that regioselective functionalization of nonsymmetric and electronically unbiased 1,3-diketones is an unsolved problem in organic synthesis, we have decided to explore the scope for this transformation (Scheme 1.39). A small set of substrates with various substitution patterns and ring sizes was synthesized. To our delight the reactivity pattern observed for triketone **1.158** was translated into simpler systems. 1,3-diketones containing five- and six-membered rings (**1.190a**, **1.190b**) exhibit exceptional endo-selectivity for triflation and orthogonal exo-selectivity for bromination, albeit to a moderate degree. Substrate **1.190d** and triketone **1.158** showcase the toleration of substitution at various positions. The only exception found is seven-membered system

1.190c, which gives a somewhat synthetically useful ratio of 1:2.5 for bromination but complete ablation of selectivity for triflation. Thus, the major constitutional isomers of the activated electrophile for cross-coupling can be obtained in each case in a controllable fashion by the choice of reaction conditions. Even



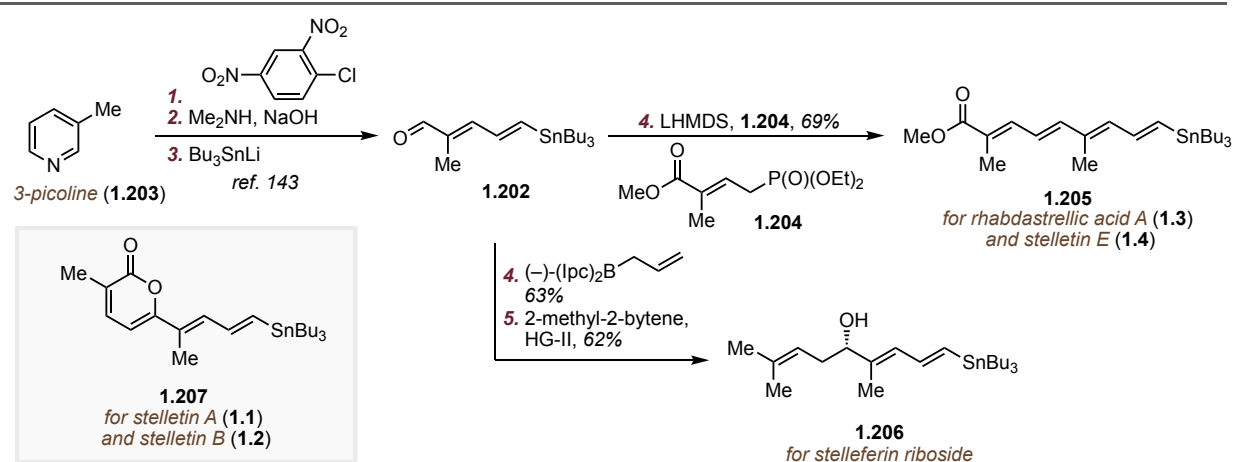
Scheme 1.39 Scope of divergent functionalization of 1,3-diketones.

though the selectivities for bromination are fairly modest, we believe this divergent activation of electronically unbiased 1,3-diketones is a useful method for synthetic applications. The remarkable *E/Z* selectivity of the bromination deserves a separate notion. Initial attempts to provide a rational with DFT techniques were fruitless. However, preliminary results suggest that the outcome is dictated by post-transition state bifurcation and delicate dynamic effects.

1.3.9 Synthesis of side-chain nucleophiles for the cross-coupling

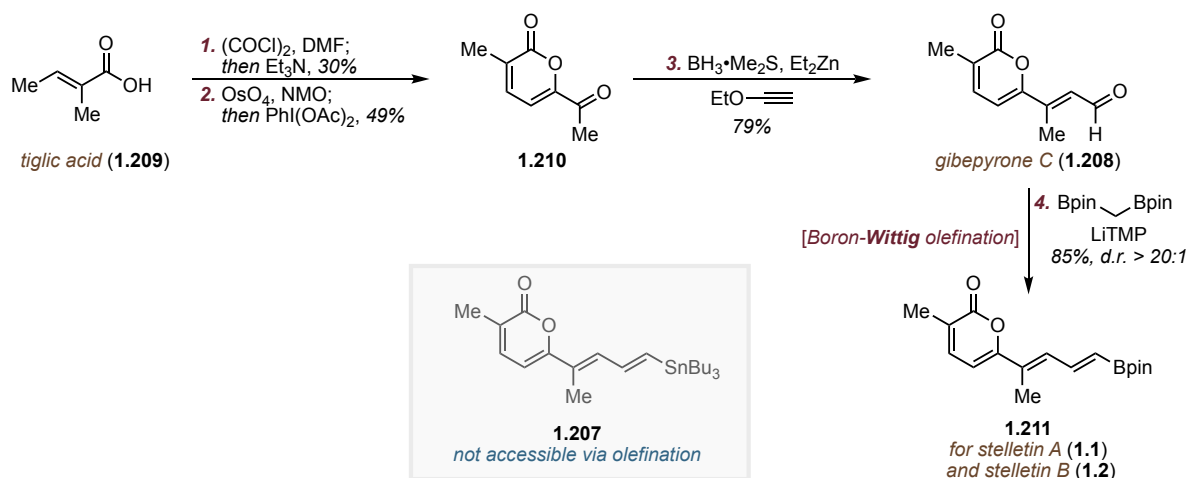
Having arrived at a vinyl electrophile for the last key coupling event we turned our attention towards assembly of the appropriate coupling partner. As was noted earlier, the variability of natural products within the family is derived mostly from the different side-chain fragments. We were keen to identify a simple precursor, which would allow for divergent access to them in an expedient manner. Major concerns that had to be considered as well were the expected instability of the highly unsaturated product under reaction conditions and the presence of the various functional groups such as carboxylic acids, alcohols, *etc.* Initial efforts were concentrated on the synthesis of the polyenyl stannane suitable for the Stille coupling, known for its mildness and robustness. Ultimately, aldehyde **1.202** was identified as an attractive common intermediate (Scheme 1.40). **1.202** was synthesized according to the sequence previously reported by Vanderwal and co-workers in three steps from 3-picoline (**1.203**), employing the Zincke reaction.¹⁴³ Notably, the use of a widely available substituted heterocycle as a starting material highlights the adaptiveness of the approach towards analogue synthesis. A straightforward Horner–Wadsworth–Emmons olefination with phosphonate **1.204** was conducted in order to attain coupling partner **1.205** for rhabdastrellic acid A (**1.3**) and stelletin E (**1.4**).¹⁴⁴ The common intermediate **1.202** was also transformed into the side-chain for the stelleferin riboside (**1.206**).

First, enantioselective Brown allylation was carried out followed by cross-metathesis to install geminal substitution at the alkene terminus.



Scheme 1.40 Synthesis of the side-chains for Stille cross-coupling.

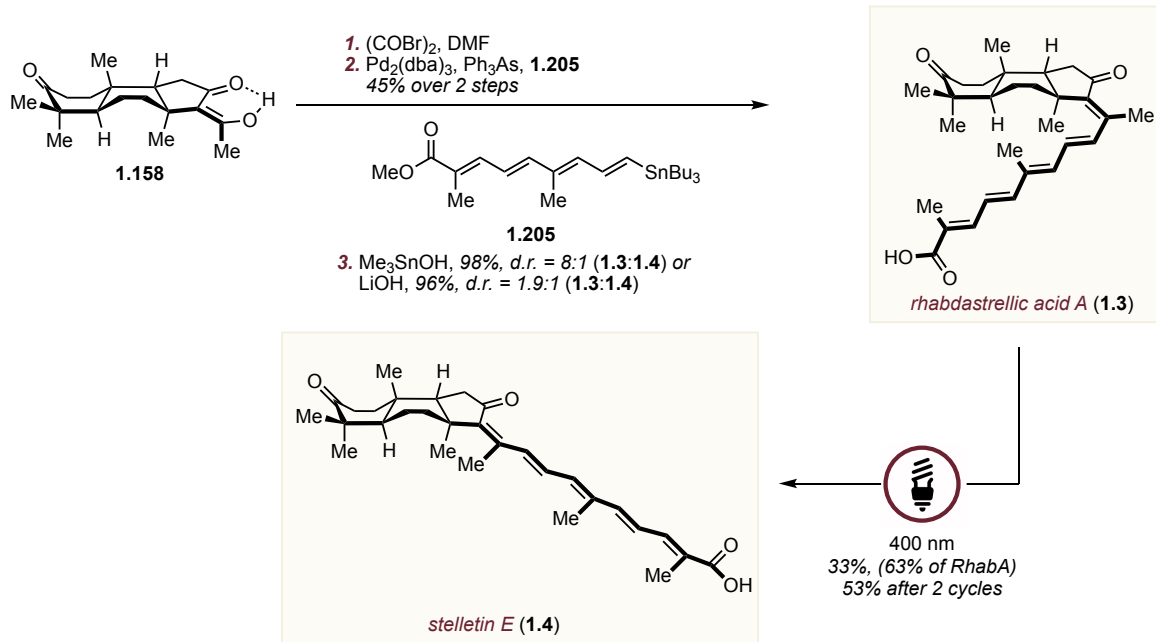
Stelletin A (**1.1**) and stelletin B (**1.2**) have been studied the most in the prior literature and demonstrated very promising results. Interested in their proapoptotic properties and potential for further development as a new chemical lead, we have decided to target these terpenoids as well. To achieve this aim, the pyrone-containing building block **1.207** was required (Scheme 1.40). While aldehyde **1.202** could serve as precursor for **1.207**, certain challenges were anticipated, including the sensitivity of the organotin moiety towards projected steps. Thus, an alternative route incorporating olefination of the natural product gibepyrone C (**1.208**) was conceived (Scheme 1.41).¹⁴⁵ Gibepyrone C is not readily available and so a brief forward synthesis was pursued. Dimerization of tiglic acid (**1.209**) proceeded according to literature protocol,¹⁵ followed by Johnson–Lemieux oxidation to furnish a ketone **1.210**. The homologation was complicated by high acidity of the substrate, and standard ethoxyvinyl lithium reagent would act as a base rather than a nucleophile. In contrast, use of a less basic zinc reagent, following a protocol disclosed by Walsh, was a suitable solution, delivering the product in 79% yield.¹⁴⁶ Finally, Takai olefination, which is well-established for similar systems, was exploited.¹⁴⁷ Unfortunately, no product was obtained, seemingly due to its instability under reaction conditions. Several alternative strategies towards vinyl tin coupling partner **1.207** were explored to no avail. This failure prompted us to pursue vinylboronic ester **1.211** instead as an alternative coupling partner for a Suzuki reaction. The synthesis was carried out through a boron–Wittig reaction^{148–151} on gibepyrone C, proceeding in high yield and with excellent diastereoselectivity.



Scheme 1.41 Synthesis of the side-chain for Suzuki cross-coupling.

1.3.10 Synthesis of isomalabaricane triterpenoids via cross-coupling

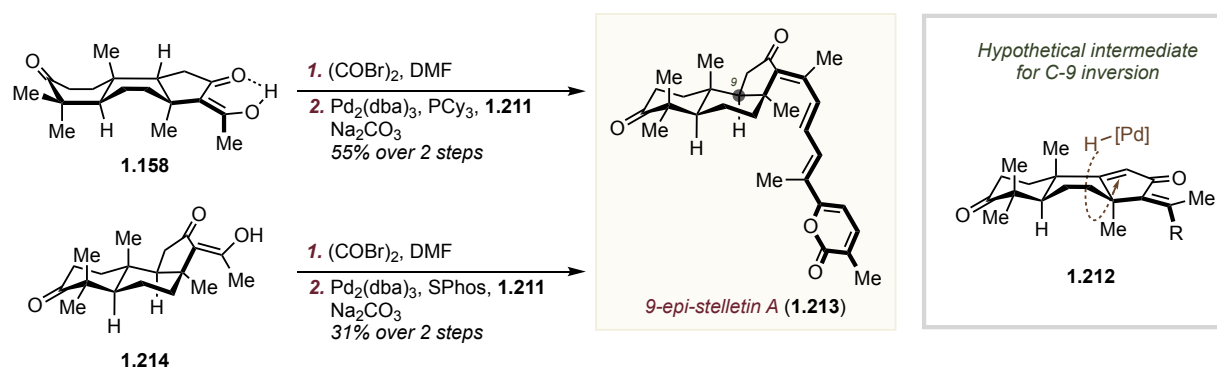
With secured access to both coupling partners the stage was set for the final C–C bond forming reaction. Stille cross-coupling was investigated first (Scheme 1.42). Slow reactivity and moderate yield was anticipated, given the steric encumbrance of the electrophilic species (tetrasubstituted olefin with quaternary stereocenter in close proximity). Indeed, initial attempts were unproductive. **1.205** was susceptible to homocoupling as a result of the high degree of unsaturation.¹⁵² This process overwhelmingly dominated in presence of copper, a known additive for the Stille reaction to facilitate transmetalation. Moreover, traces of oxygen would also mediate the homocoupling process, hence all the solvents had to be thoroughly degassed. Several established conditions were examined and only the use of the more kinetically labile ligand triphenylarsine and high catalyst loading enabled the bond formation.¹⁵³ After additional optimization of the reaction parameters, the desired product was obtained in 45% yield over 2 steps from diketone **1.158**. Hydrolysis of the methyl ester under mild conditions delivered rhabdastrellic acid (**1.3**) in quantitative yield.¹⁵⁴ In order to access stelletin E (**1.4**) the well-known facile C13-C14 photoisomerization⁷ of the isomalabaricanes was exploited. Brief exposure (< 5 minutes) to violet light promoted equilibration of the natural products to a photostationary state (**1.3**:**1.4** = 1.9:1), which could be separated by preparative HPLC. In this manner, stelletin E could be obtained in 53% isolated yield from rhabdastrellic acid A methyl ester after aqueous hydrolysis and two cycles of photoisomerization, with almost full recovery of rhabdastrellic acid A. Notably, isomerization can be induced not only by light exposure, but also through an enolization



Scheme 1.42 Synthesis of rhabdastrellic acid and stelletin E.

mechanism. Using harsher hydrolysis conditions (LiOH), mixture **1.3**:**1.4** = 1.9:1 can be obtained directly.

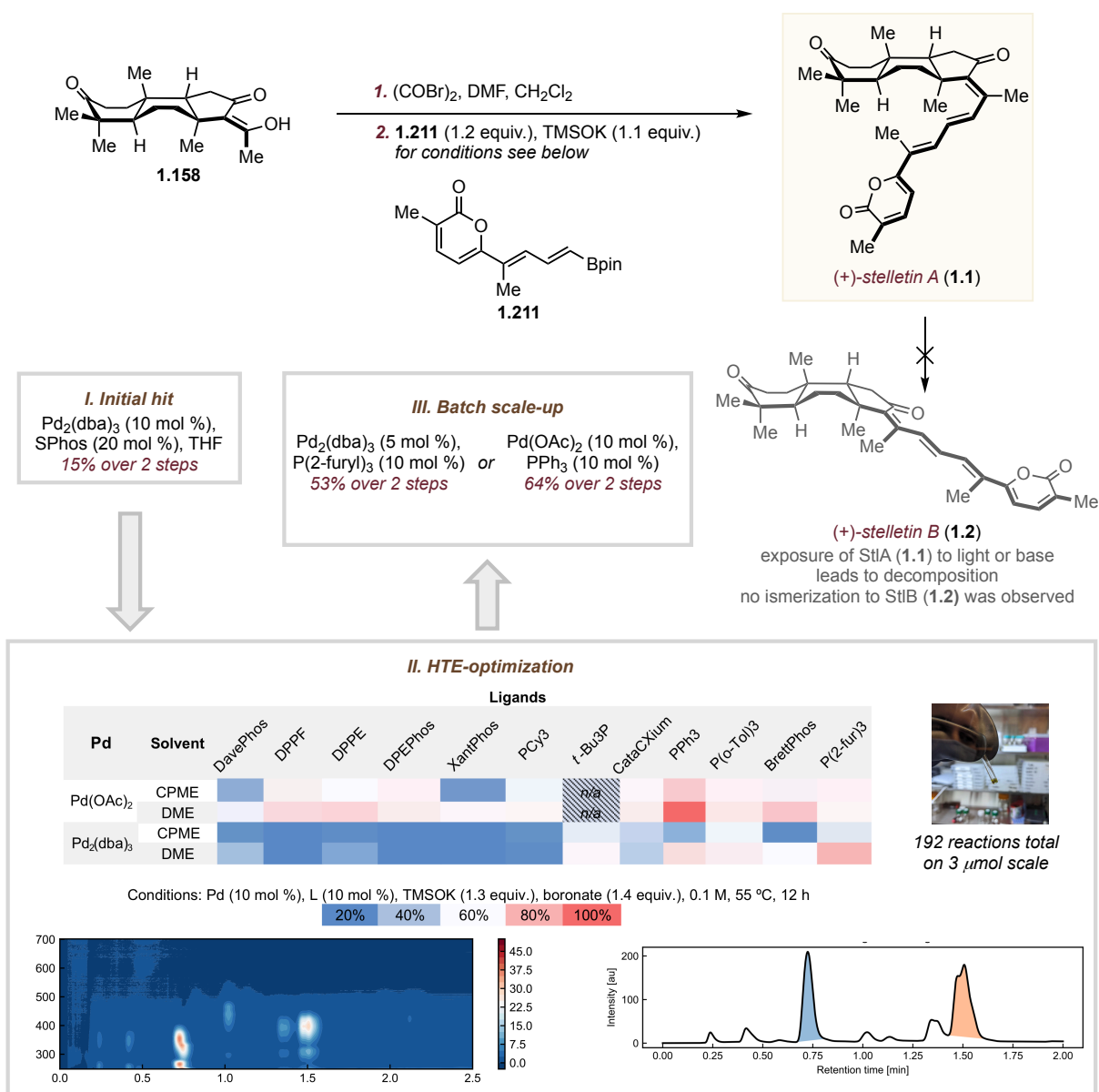
Next, the Suzuki reaction towards stelletin A (**1.1**) was investigated (Scheme 1.43). Given the success of Stille coupling, no issues were expected with a seemingly similar transformation. After small optimization of the ligand structure a coupling product was obtained in appreciable yield under otherwise standard conditions. Surprisingly, after purification we realized that the isolated product did not correspond to stelletin A (**1.1**)¹⁵⁵ nor its olefin isomer stelletin B (**1.2**),¹⁵⁶ although the same mass and degree of unsaturation was confirmed by LCMS and UV spectra respectively. Being completely assured of the structural identity of **1.158** and **1.211**, we surmised that the product is a constitutional or stereochemical isomer of the natural product. The former was ruled out by examination of its HMBC spectrum, and the latter was suspected based on observed NOE correlations and our familiarity with subtle details of the ¹³C NMR chemical shifts in these systems. Given the previously reported tendency of the *trans-syn-trans* system to undergo skeletal rearrangements, as well as our own struggle to construct this scaffold, we wondered if the molecule might have epimerized to the *trans-anti-cis* framework under the reaction conditions. Perhaps, the basic conditions of the Suzuki cross-coupling could induce enolization and Saegusa-type oxidation on the far side of the ketone, followed by reinsertion into **1.212** from the opposite face. In order to



Scheme 1.43 Suzuki cross-coupling under standard conditions.

put our hypothesis into test *9-epi*-stelletin A (**1.213**) was targeted for the direct spectroscopic comparison. The requisite epimeric triketone **1.214** was easily synthesized from the triol (**1.154**, see Scheme 1.25 for its synthesis). Importantly, the Suzuki reaction delivered a compound spectroscopically matching with the previously obtained product, validating our speculation. Consequentially, we postulated that the undesired isomerization can be avoided if base is removed from the reaction conditions. While the role of base for a successful transmetalation is critical, a recent report from the Denmark laboratory drew our attention.¹⁵⁷ The ability of potassium trimethylsilanolate under anhydrous conditions to promote Suzuki cross-coupling with an extraordinary rate was disclosed. While potassium trimethylsilanolate still can act as a base, anhydrous conditions and excess of the boronic ester insures its complete recruiting to form the boronate species. Following this literature precedent, we were very pleased to find that the cross-coupling proceeded without any isomerization to furnish stelletin A in 15% yield (Scheme 1.44). Unfortunately, numerous attempts to isomerize stelletin A into stelletin B have failed. Irradiation with various wavelengths led only to degradation of the substrate, while basic conditions were incompatible with the sensitive pyrone functionality.

While the ¹H NMR spectrum of **1.1** matched with literature data, there was no reported ¹³C NMR spectrum. To corroborate our assignment, we decided to repeat our previous NMR calculations at the GIAO CPCM(CHCl₃) RIJCOSX-PBE0 / pcSseg-2 // RIJCOSX-ωB97X-D3 / def2-TZVP(-f) on a full natural product structure (Figure 1.12). Analogously to the aforementioned studies, the predicted NMR of the natural product displayed small errors (MAE = 1.4 ppm, MAX = 5.6 ppm), which were consistent with those observed in the calibration set. Maximum absolute deviation, unfortunately, was quite high. The corresponding carbon atom



Scheme 1.44 Synthesis of stelletin A and HTE optimization.

belonged to the carbonyl group of the pyrone, while no significant deviation of signals within the *trans-syn-trans* core or polyene fragment was observed. We were confident in the assignment since the offending carbon resides on an unambiguous part of the molecule, and since similar outliers were not detected in any other regions of the full structure. Still curious about the outcome of the initial Suzuki coupling, we performed an identical analysis on the computed geometry of 9 *epi* stelletin A (**1.213**) and obtained a close correlation as well, offering additional prove of an isomerization at C9.

Although the anhydrous Suzuki coupling conditions from the original report were sufficient to obtain enough material for characterization, we desired a higher-yielding protocol for the attachment of the side chain specifically in our system. Optimization of cross-coupling reactions is certainly a routine process in organic synthesis, but considering the unique steric environment of the isomalabaricane core and already established rather unique side-reactivity, it was evident that reaction screening would best be performed on the natural product itself. Other than the use of TMSOK in ethereal solvent, we had little understanding of what parameters were most vital in the cross-coupling such as ligand structure, palladium source, stoichiometry, *etc.* To interrogate the system, as diverse conditions as possible were needed to be examined on the assumption that a few hits might inform superior choices. Given the limited access to the advanced intermediate and enormous number of possible variations, we turned to high-throughput experimentation (HTE) (Scheme 1.44). An initial model screen was performed on model bromide **1.201a** in order to test the robustness of the system and narrow down the most critical factors of the transformation. Running plates of 48 reactions simultaneously, the parameters of solvent, ligand type, palladium source, catalyst loading (5% and 20%), and vinyl bromide loading (1.2 and 1.8 equiv.) were evaluated, indicating that solvent effects, catalyst loading, and substrate loading were statistically insignificant (one-factor ANOVA test, $p > 0.05$). The essential variables of palladium source and ligand were then screened on the natural product itself, and optimized conditions were identified for both Pd(0) and Pd(II) sources. From 192 reactions on 3 μmol scale we found that the combination of 10 mol % $\text{Pd}_2(\text{dba})_3$ and $\text{P}(2\text{-fur})_3$ or 10 mol % $\text{Pd}(\text{OAc})_2$ and PPh_3 in DME could increase the yield of the cross-coupling from 15% over two steps from triketone **1.158** to 53% and 64% respectively.

1.3.11 Structure-activity-relationship study of stelletin A

With the synthetic material in hand we were excited to test its anticancer activity in house. A growing body of evidence has shown that the isomalabaricanes activate apoptosis through the intrinsic pathway at very low concentrations in select cancer cell lines in a rather selective manner.¹⁵⁸⁻¹⁶¹ The vivid structural feature of stelletin A, a Michael acceptor, is most likely responsible for the effect. In order to account for the reported selectivity, we reasoned that the unusual *trans-syn-trans*-perhydrobenz[*e*]indene skeleton might function as a recognition site for the native target. Having synthesized several useful analogues of stelletin A,

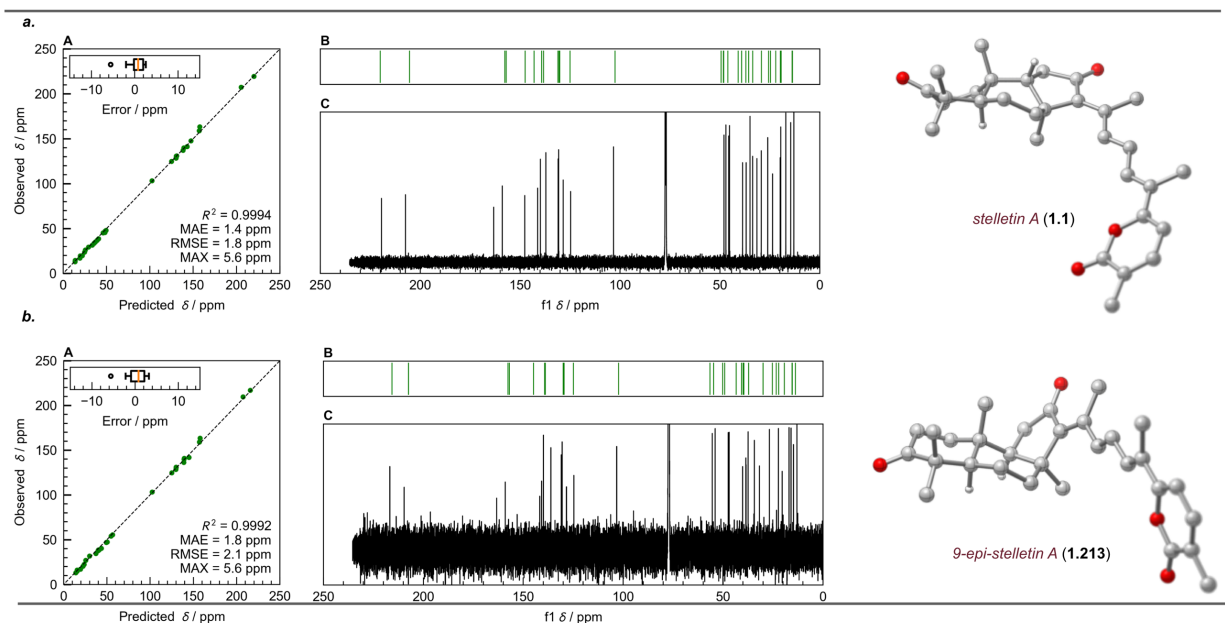


Figure 1.12. **a** Optimized geometry of **1.1** and scatter plot of predicted (B) / observed (C) ^{13}C NMR shifts. Inset corresponds to error distribution. Diagonal dashed line: $y = x$; **b** Optimized geometry of **1.213** and comparison of predicted (B) and observed (C) ^{13}C NMR shifts.

albeit unintentionally, we were well situated to investigate this hypothesis. In addition to stelletin A (**1.1**), three compounds—9-*epi*-stelletin A (**1.213**), a constitutional isomer (**1.215**, obtained as a minor product during Suzuki coupling), and a truncated analogue (**1.216**, from the HTE model system)—were tested for cytotoxicity against the U251 glioblastoma and A549 non-small cell lung cancer cell lines (Chart 1.5). **1.216** was regarded as the putative “warhead” in isolation, whereas 9-*epi*-stelletin A (**1.213**) was seen as a valuable analogue with a single-point stereochemical mutation that induces a significant conformational change in the core. Remarkably, all three tested analogues **1.213**, **1.215** and **1.216** exhibited no activity at high micromolar concentrations in the U251 and A549 cell lines, whereas stelletin A (**1.1**) was very potent, with measured IC_{50} values of 118 nM and 125 nM respectively. These results emphasize the crucial role of the highly strained tricyclic core and perhaps dismisses the commonsense notion that these molecules function as promiscuous Michael acceptors. Further studies of isomalabaricanes as a new lead in anticancer treatment are currently underway in our laboratory.

1.4 Conclusions and Outlook

To conclude, a general strategy for the enantioselective total synthesis of the isomalabaricane triterpenoids was developed. The strategy was successfully realized towards

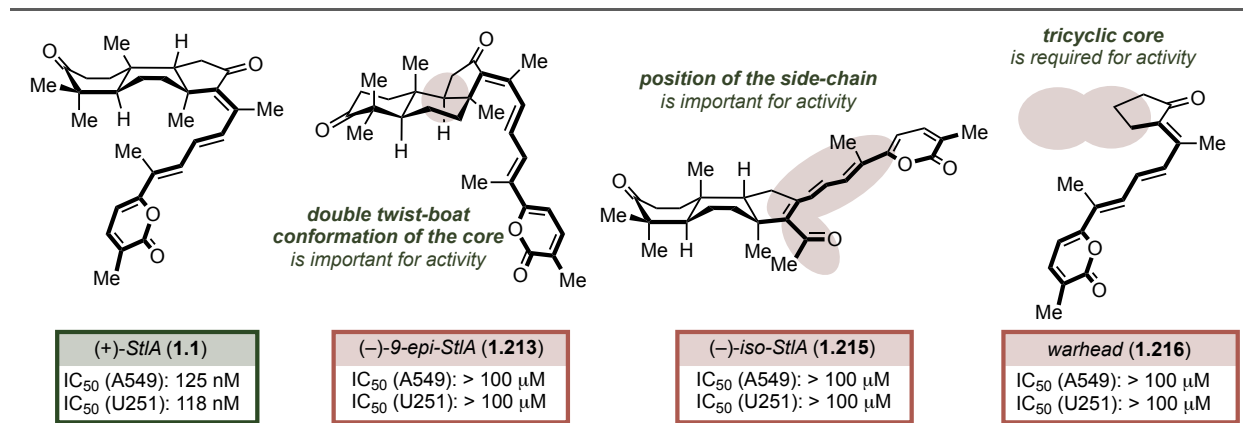


Chart 1.5 Preliminary structure-activity-relationship study on stelletin A. IC₅₀ values were obtained after 72-hour incubation of cells with compound and quantification of cell viability by Alamar Blue staining with Raptinal used for the 100% dead control.

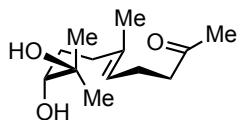
the syntheses of stelletin A (**1.1**), rhabdastrellic acid A (**1.3**), stelletin E (**1.4**). These natural products are not susceptible to traditional ring-forming methods used in terpene synthesis due to the unusual stereochemistry of their tricyclic core, and thus provided an opportunity to explore and implement some unconventional chemistry in a complex setting. The high strain energy of the *trans-syn-trans* core thwarted many efforts for its construction and led to a number of unexpected behaviors from synthetic intermediates with related structures. One of these, the epimerization of a distal stereocenter in the core during a routine Suzuki coupling, was resolved through the use of state-of-the-art anhydrous conditions. Other highlights from the route include a Rautenstrauch cycloisomerization with concomitant fluorination, a Caglioti reductive transposition with *in situ* umpolung substitution, and cross-coupling of an allylic ether via an organozirconium species. An improved scalable, asymmetric route to a common Wieland–Miescher synthetic building block was reported as well. The synthetic sequence comprises only 12 or 13 steps for racemic or enantioselective synthesis respectively with 4% overall yield for latter.

Several techniques outside of the common toolbox of synthetic chemistry proved quite valuable in this endeavor. Geometry optimization and ¹³C NMR facilitated structural assignment of diastereomers. Conformational analyses and thermochemical calculations were employed to rationalize obtained results and, thus guide further efforts. The high-throughput experimentation allowed for a large screen of cross-coupling conditions to be carried out on precious material in a quite effective fashion. A preliminary structure-activity-relationship study conducted on stelletin A revealed the vital role of the tricyclic core, and gives credence to reports suggesting the isomalabaricanes show promise as potential lead scaffolds for the development of targeted

anticancer therapies. Further investigation of the isomalabaricanes' efficacy, selectivity and pharmacokinetic profile is ongoing in our laboratory.

1.5 Experimental Section

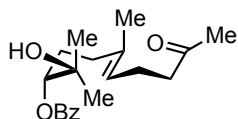
Synthesis of compound **1.55**:



Reaction was carried out according to modified literature procedure. A mixture of ligand **1.56** (6.31 mg, 6.18 μ mol, 1 mol %), $\text{K}_2\text{OsO}_4 \cdot 2\text{H}_2\text{O}$ (2.3 mg, 6.18 μ mol, 1 mol %), $\text{K}_3\text{Fe}(\text{CN})_6$ (610 mg, 1.85 mmol, 3.0 equiv.), K_2CO_3 (256 mg, 1.85 mmol, 3.0 equiv.), $\text{CH}_3\text{SO}_2\text{NH}_2$ (59 mg, 618 μ mol, 1.0 equiv.) were dissolved in DI water / *t*-BuOH (6.2 mL, 0.1 M, 1:1) and stirred vigorously at ambient temperature for 30 min. Orange solution was cooled down in ice-bath. Geranylacetone **1.49** (120 mg, 618 μ mol, 1.0 equiv.) was added in a single portion. Temperature was slowly increased to 24 °C. Conversion was monitored by TLC (hexanes : EtOAc = 1:1). After 10 h the reaction was quenched with Na_2SO_3 (aq., 1.0 mL, 10 w/w %) and $\text{Na}_2\text{S}_2\text{O}_3$ (aq., 1.0 mL, 10 w/w %) and stirred for 45 min. After removal of *t*-BuOH under reduced pressure, the reaction mixture was extracted with EtOAc (3 \times 10 mL). The combined extracts were washed with NaOH (aq., 10 mL, 10 w/w %), followed by brine (10 mL), dried over Na_2SO_4 , and concentrated *in vacuo*. Spectroscopically clean material **1.55** was obtained (135 mg, 596 μ mol) as a colorless oil in 97% yield and 97.5% ee as determined by HPLC after benzylation.

R_f : 0.22 (SiO_2 , Hexanes : EtOAc = 1:1); ^1H NMR: (500 MHz, CDCl_3): δ 5.11 (tt, J = 5.8, 1.4 Hz, 1H), 3.30 (dd, J = 10.5, 2.0 Hz, 1H), 2.45 (t, J = 7.3 Hz, 2H), 2.36 (br, 1H), 2.24 (q, J = 7.0 Hz, 2H), 2.19 (dd, J = 8.9, 5.4 Hz, 1H), 2.11 (s, 3H), 2.03 (m, 1H), 1.60 (s, 3H), 1.55 (dddd, J = 13.7, 9.0, 7.0, 2.0 Hz, 1H), 1.37 (dddd, J = 13.9, 10.5, 8.8, 5.4 Hz, 1H), 1.17 (s, 3H), 1.13 (s, 3H).; ^{13}C NMR: (126 MHz, CDCl_3): δ 209.2, 136.3, 123.3, 78.2, 73.1, 43.7, 36.8, 30.0, 29.7, 26.5, 23.3, 22.5, 16.0; $[\alpha]_D$: +19.2 ° (c = 0.78, CHCl_3 , 21.5 °C)

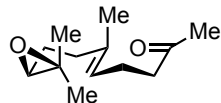
Synthesis of compound **S1.1**:



To a solution of the diol **1.55** (337 mg, 1.48 mmol, 1.0 equiv.) in CH_2Cl_2 (4 mL, 0.3 M) DMAP (72.1 mg, 590 μ mol, 0.4 equiv.) and Et_3N (299 mg, 0.41 mL, 2.95 mmol, 2.0 equiv.) were added. The flask was purged by nitrogen. Benzoyl chloride (311 mg, 257 μ L, 2.21 mmol, 1.5 equiv.) was added dropwise. The reaction was

left at ambient temperature overnight. Once TLC showed complete conversion, the reaction was quenched by the addition of saturated NH_4Cl (4 mL), Organic layer was separated and washed with water (5 mL), 10% KHCO_3 (10 mL), water (10 mL) and brine (10 mL). Solution was dried over MgSO_4 , concentrated under *vacuo* and purification by liquid chromatography (SiO_2 , hexanes : EtOAc = 5:1). Desired benzoate **S1.1** (378 mg, 1.14 mmol) was isolated as a pale yellow viscous oil in 77% yield. Enantiomeric excess was determined with HPLC analysis using Diacel Chiracel[®] OJ-3 column, 7.5% *i*-PrOH in *n*-Hexane, 1.0 mL/min, $t_R(\text{major}) = 14.9$ min, $t_R(\text{minor}) = 17.8$ min. **R_f**: 0.27 (SiO_2 , hexanes : EtOAc = 5:2); **¹H NMR** (500 MHz, CDCl_3): δ 8.05 (dd, $J = 8.3$, 1.4 Hz, 2H), 7.56 (m, 1H), 7.45 (t, $J = 7.8$ Hz, 2H), 5.03 (m, 2H), 2.39 (m, 2H), 2.26–2.13 (m, 2H), 2.10 (s, 3H), 2.07–1.97 (m, 3H), 1.89–1.75 (m, 2H), 1.59 (s, 3H), 1.25 (m, 6H); **¹³C NMR**: (126 MHz, CDCl_3): δ 208.9, 166.6, 135.2, 133.1, 130.2, 129.7, 128.4, 123.5, 80.0, 72.6, 43.5, 36.1, 29.9, 27.8, 26.4, 25.3, 22.3, 15.9; **HRMS**: (ES+, m/z) $[\text{M}+\text{H}]^+$ calcd. for $\text{C}_{20}\text{H}_{29}\text{O}_4$, 333.2066; found, 333.2067; **IR**: (ATR, neat, cm^{-1}): 3480 (br), 2974 (m), 1712 (s), 1601 (w), 1584 (w), 1271 (s), 1113 (s), 710 (s).; **[α]_D**: +12.2 ° ($c = 1.0$, CHCl_3 , 21 °C)

Synthesis of compound S1.2:

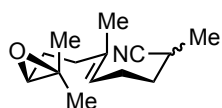


To a stirred solution of the diol **1.55** (3.45 g, 15.1 mmol, 1.0 equiv.) in CH_2Cl_2 (65 mL, 0.2 M) and pyridine (12.0 g, 151 mmol, 12.0 mL, 10.0 equiv.) was added MsCl (2.6 g, 22.7 mmol, 1.77 mL, 1.5 equiv.) dropwise at 5 °C. The reaction was completed after stirring overnight at ambient temperature. Then, the mixture was diluted with methanol (190 mL), and solid K_2CO_3 (20.9 g, 151 mmol, 10.0 equiv.) was added. The resulting suspension was stirred for 6 h at ambient temperature. Upon reaction was completed as judged by TLC, water (190 mL) was added. The product was extracted with ether (4×190 mL). The combined organic layer was washed with a saturated aqueous CuSO_4 solution (150 mL), dried over MgSO_4 , and concentrated under reduced pressure on rotary evaporator (20 °C, 200 mTorr). The epoxide was purified by column chromatography (SiO_2 , pentane : $\text{Et}_2\text{O} = 94:6$). Product **S1.2** (2.73 g, 13.0 mmol) was isolated as a colorless oil in 86% yield.

R_f: 0.31 (SiO_2 , hexanes : EtOAc = 5:1); **¹H NMR**: (500 MHz, CDCl_3): δ 5.15 (tq, $J = 7.0$, 1.3 Hz, 1H), 2.70 (t, $J = 6.2$ Hz, 1H), 2.48 (t, $J = 7.4$ Hz, 2H), 2.30 (q, $J = 7.1$ Hz, 2H), 2.20–2.06 (m, 2H), 2.16 (s, 3H), 1.65 (s, 3H), 1.65–1.61 (m, 2H), 1.32 (s, 3H), 1.28 (s, 3H).; **¹³C NMR**: (126 MHz,

CDCl₃): δ 208.8, 135.6, 123.3, 64.2, 58.4, 43.8, 36.4, 30.1, 27.5, 25.0, 22.5, 18.9, 16.1; [a]_D: +4.4 ° (c = 1.0, CHCl₃, 21.5 °C)

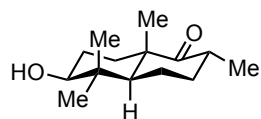
Synthesis of compound 1.41:



The ketone **S1.2** (2.50 g, 11.9 mmol, 1.0 equiv.) was dissolved in THF (120 mL, 1.0 M), solution was treated with EtOH (1.2 mL, 1.8 equiv.) followed by TosMIC (3.02 g, 15.5 mmol, 1.3 equiv.). Mixture was cooled down to 5 °C in ice-bath and *t*-BuOK (3.20 g, 28.5 mmol, 2.4 equiv.) was added as solid in a single portion. Ice-bath was removed. In 10 min orange, clear solution turned into gel. TLC after 30 min displayed full conversion of starting material. Reaction was partitioned between water (180 mL) and ether (80 mL). Layers were separated. Aqueous phase was backwashed twice with ether (80 mL). Combined organic phase was washed with brine (80 mL) and dried over MgSO₄. Solution was concentrated on rotary evaporator (20 °C, 250 mTorr). Residual oil was purified by liquid chromatography (SiO₂, pentane : Et₂O = 5:1).

R_f: 0.18 (SiO₂, hexanes : EtOAc = 10:1); ¹H NMR: (500 MHz, CDCl₃): δ 5.13 (t, *J* = 7.0 Hz, 1H), 2.69 (t, *J* = 6.2 Hz, 1H), 2.61 (dq, *J* = 9.2, 7.1, 5.6 Hz, 1H), 2.22 – 2.07 (m, 4H), 1.73 – 1.53 (m, 4H), 1.66 (s, 3H), 1.31 (d, *J* = 7.1, 3H), 1.30 (s, 3H), 1.26 (s, 3H); ¹³C NMR: *Since product consists of two diastereomers in ratio 1:1 and peaks could not be ascribed to any particular isomer, all peaks are listed.* (126 MHz, CDCl₃): δ 136.5, 123.2, 122.83, 122.81, 64.22, 64.21, 58.4, 36.54, 36.52, 34.27, 34.23, 27.54, 27.51, 25.59, 25.55, 25.09, 25.06, 25.04, 18.9, 18.17, 18.15, 16.2; HRMS: (ES⁺, *m/z*) [M+H]⁺ calcd. for C₁₄H₂₄NO, 222.1858; found, 222.1863; IR: (ATR, neat, cm⁻¹): 2925 (s), 2239 (w), 1667 (w), 1455 (s), 1378 (s), 1250 (m), 899 (w), 796 (w)

Synthesis of compound 1.51:

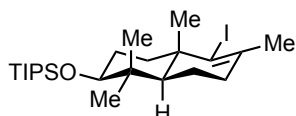


In an oven-dried 5 L round-bottom flask, titanocene dichloride (37.9 g, 152 mmol, 3.3 equiv.) and activated zinc (19.9 g, 304 mmol, 6.6 equiv.) were vigorously stirred in degassed THF (1.0 L) under nitrogen for 20 minutes. The appearance of a dark-green color indicates the formation of Cp₂TiCl, which was transferred dropwise to a solution of epoxynitrile **1.41** (10.2 g, 46.1 mmol) in degassed THF (3.5 L) over the course of 8 hours *via* cannula under an atmosphere of nitrogen. Alternatively, a dropping funnel under nitrogen can be used for this process (see Picture 1), but the slow, dropwise rate of addition

is critical. Once the addition is done, the reaction was quenched with NaH_2PO_4 (sat. aq. 500 mL) and left to stir overnight at ambient temperature. The resulting mixture was filtered, concentrated to remove THF, and partitioned between EtOAc (2.0 L) and water (1.5 L). The organic phase was separated and the aqueous portion was extracted with EtOAc (2×500 mL). The combined organic extracts were washed with brine (1.0 L), dried over MgSO_4 , filtered and concentrated *in vacuo*. The residue was purified by flash chromatography (SiO_2 , 12:1 \rightarrow 10:1 hexanes : EtOAc) to give the title compound (**1.51**) (7.20 g, 32.1 mmol, 70%, *d.r.* = 5:1) as a colorless oil that solidifies upon storage. The major isomer (β) was further purified by recrystallization from cold MeOH for characterization.

R_f: 0.23 (SiO_2 , hexanes/EtOAc = 3:1) ; **T_{melt.}** : 79.7 – 80.9 °C; **¹H NMR**: (500 MHz, CDCl_3): δ 3.20 (dt, J = 10.1, 4.5 Hz, 1H), 2.67 (dp, J = 12.8, 6.4 Hz, 1H), 2.12 (ddt, J = 13.2, 6.5, 3.2 Hz, 1H), 1.80 – 1.73 (m, 3H), 1.69 (dd, J = 14.2, 3.7 Hz, 1H), 1.62 – 1.57 (m, 2H), 1.35 (d, J = 5.3 Hz, 1H), 1.21 (ddt, J = 15.1, 8.3, 5.3 Hz, 1H), 1.14 (s, 3H), 1.10 (dd, J = 8.5, 6.9 Hz, 1H), 1.00 (s, 3H), 0.98 (d, J = 6.4 Hz, 3H), 0.90 (s, 3H); **¹³C NMR**: (126 MHz, CDCl_3): δ 216.2, 78.3, 53.4, 48.5, 40.0, 39.9, 35.7, 31.5, 28.1, 27.2, 21.2, 19.0, 15.9, 15.0; **HRMS**: (EI+, m/z) [M]⁺ calcd. for $\text{C}_{14}\text{H}_{24}\text{O}_2$, 224.1776; found, 224.1780.; **IR**: (ATR, neat, cm^{-1}): 3452 (br), 2968 (s), 2933(s), 1702 (s), 1141 (m); **[α]_D**: +12.8 ° (c = 0.5, CHCl_3 , 25 °C)

Synthesis of compound 1.70:

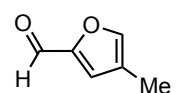


A solution of ketone **1.57** (421 mg, 1.10 mmol, 1.0 equiv.) in ethanol (2.2 mL, 0.5 M) was sequentially treated with hydrazine (1.73 mL, 55.8 mmol, 50 equiv.) and acetic acid (0.31 mL, 5.58 mmol, 5 equiv.) under inert atmosphere. Resulting mixture was brought to refluxing temperature and aged for 18 h. Then the reaction was then cooled to ambient temperature and concentrated *in vacuo*. The residue was redissolved in EtOAc (5 mL) and transferred to a separatory funnel with NaHCO_3 (aq. sat., 10 mL). The mixture was vigorously shaken, layers were separated and aqueous phase was backwashed with EtOAc (2×5 mL). The combined organic layers were washed with brine (30 mL) and dried over MgSO_4 . Solution was filtered and concentrated *in vacuo* to afford crude hydrazone in quantitative yield as a white solid, which was used for the next step without purification.

To a stirring solution of hydrazone, and DBU (3.18 mL, 21.1 mmol, 20 equiv.) in Et₂O (7 mL) at room temp was added dropwise a solution of iodine (590 mg, 2.32 mmol, 2.2 equiv.) in Et₂O (4 mL). The solution was allowed to stir for 30 min before being quenched with NaHCO₃ (aq. sat., 10 mL) and extracted with Et₂O (3 × 5 mL). The combined organic layer was washed with brine (10 mL), dried over MgSO₄, filtered and concentrated. The residue was dissolved in PhH (11 mL) and treated with DBU (0.8 mL, 5.28 mmol, 5 equiv.). The solution was then brought to reflux and aged for 5 h. Reaction mixture was cooled to ambient temperature and concentrated *in vacuo*. The residue was redissolved in Et₂O, washed with Na₂S₂O₃ (aq. 10 w/w %, 5 mL), brine (10 mL) and dried over MgSO₄. The solution was concentrated and the crude material was purified liquid chromatography (SiO₂, hexanes) to yield light-sensitive vinyl iodide **1.70** (241 mg, 0.49 mmol) in 46% yield.

R_f: 0.80 (SiO₂, hexanes); **¹H NMR**: (500 MHz, CDCl₃): δ 3.41 (dd, *J* = 11.1, 4.9 Hz, 1H), 2.28-2.18 (m, 2H), 1.86-1.82 (m, 1H), 1.84 (s, 3H), 1.74-1.59 (m, 3H), 1.65-1.46 (m, 1H), 1.31 (dd, *J* = 12.5, 1.9 Hz, 1H), 1.19 (td, *J* = 13.1, 4.4 Hz, 1H), 1.06 (m, 21H), 1.02 (s, 3H), 1.01 (s, 3H), 0.79 (s, 3H); **¹³C NMR**: (126 MHz, CDCl₃): δ 136.9, 120.8, 80.0, 51.6, 42.9, 42.3, 40.1, 35.3, 30.7, 28.8, 28.6, 20.0, 19.0, 18.52, 18.45, 16.0, 13.2; **HRMS**: (EI+, *m/z*) [*M*]⁺ calcd. for C₂₃H₄₃OSi, 490.2128; found, 490.2138; **IR**: (ATR, neat, cm⁻¹): 2941 (s), 2864 (s), 1110 (s), 1066 (s), 1055 (m), 823 (m).

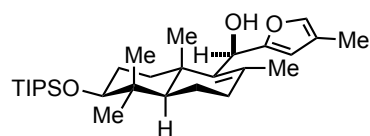
Synthesis of compound 1.71:



A mixture of the known alcohol (900 mg, 8.03 mmol, 1.0 equiv.), BaMnO₄ (2.67 g, 10.4 mmol, 1.3 equiv.), and dry benzene (40 mL, 0.2 M) was heated at 70 °C for 6 h. The cooled reaction mixture was filtered through a pad of celite by the aid of pentane and ether, and the filtrate was concentrated under reduced pressure on rotary evaporator (20 °C, 150 mTorr). Purification of the residue by fractional distillation (70 °C, 15 mbar) furnished 623 mg (70%) of the furaldehyde **1.71** as a colorless oil.

R_f: 0.50 (SiO₂, Penatne:Et₂O = 5:1); **¹H NMR**: (500 MHz, CDCl₃): δ 9.63 (s, 1H), 7.50 (s, 1H), 7.14 (s, 1H), 2.15 (s, 3H); **¹³C NMR**: (126 MHz, CDCl₃): δ 176.9, 151.9, 144.5, 144.5, 122.1, 8.5; **HRMS**: (ES+, *m/z*) [*M*+H]⁺ calcd. for C₆H₇O₂, 111.0446; found, 111.0441; **IR**: (ATR, neat, cm⁻¹): 2929 (m), 2856 (w), 1711 (m), 1678 (s), 769 (s)

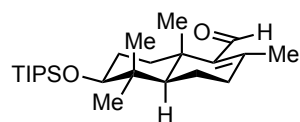
Synthesis of compound 1.72:



To an oven dried 8-ml vial, a solution of vinyl iodide **1.70** (188 mg, 383 μ mol, 1.0 equiv.) in THF (2 mL) was added *t*-BuLi (0.56 mL, 1.7 M in toluene, 958 μ mol, 2.5 equiv.) dropwise at -78 °C under inert atmosphere. After 1.5 h at this temperature, 4-methylfuran-2-carbaldehyde **1.71** (127 mg, 1.15 mmol, 3.0 equiv.) in THF (2 mL) was added via cannulation. The reaction mixture was warmed to 0 °C over 3 h and stirred at this temperature for an additional hour. Finally, the reaction mixture was quenched with NH_4Cl (aq. sat., 5 mL) and transferred into separatory funnel. The organic layer was separated, and the aqueous layer was backwashed with EtOAc (3×10 mL). The combined organic layer was washed with brine (15 mL), dried over Na_2SO_4 , filtered and concentrated. The crude oil was purified by liquid chromatography (SiO_2 , hexanes : EtOAc = 14:1) to provide the desired alcohol **1.72** (78 mg, 165 μ mol, 43%, *d.r.* = 1.3:1) as a pale-yellow oil. The major isomer was characterized.

R_f: 0.30 (SiO_2 , hexanes : EtOAc = 14:1); **¹H NMR**: (500 MHz, CDCl_3): δ 7.11 (d, J = 0.8 Hz, 1H), 5.92 (s, 1H), 5.35 (d, J = 3.8 Hz, 1H), 3.47 – 3.39 (m, 1H), 2.16 – 2.05 (m, 2H), 2.03 (d, J = 4.2 Hz, 1H), 1.99 (d, J = 1.2 Hz, 3H), 1.71 (ddd, J = 12.0, 9.0, 4.9 Hz, 3H), 1.55 (s, 3H), 1.54 – 1.39 (m, 2H), 1.15 (dd, J = 12.4, 1.8 Hz, 1H), 1.07 (s, 21H), 1.02 (s, 3H), 1.00 (s, 3H), 0.81 (s, 3H).; **¹³C NMR**: (126 MHz, CDCl_3): δ 157.35, 140.41, 138.03, 134.72, 120.76, 108.64, 79.84, 65.55, 51.63, 40.01, 38.55, 35.38, 35.16, 28.71, 28.38, 21.15, 20.63, 18.91, 18.52, 18.46, 16.09, 13.19, 9.98.; **HRMS**: (ES^+ , m/z) [$\text{M}+\text{H}$] $^+$ calcd. for $\text{C}_{29}\text{H}_{51}\text{O}_3\text{Si}$, 475.3607; found, 475.3620; **IR**: (ATR, neat, cm^{-1}): 3420 (br), 2942 (s), 2865 (s), 1462 (m), 1110 (s)

Synthesis of compound 1.78:

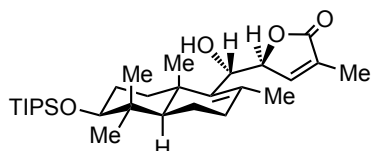


Caution! Product isomerizes on SiO_2 to the β,γ -unsaturated aldehyde. In an oven-dried round-bottom flask, a solution of LDA (7.0 mL, 0.7 M in THF, 4.68 mmol, 1.8 equiv.) was prepared *in situ* and cooled down to -100 °C under nitrogen atmosphere. After 20 minutes, a solution of decalone **1.57** (1.00 g, 2.63 mmol, 1.0 equiv.) in CH_2Cl_2 (2.6 mL) was added dropwise, over the course of 10 minutes, with careful monitoring of the low temperature in an EtOH/liq. N_2 bath. The mixture was allowed to warm up to -20 °C over 2 hours and then followed by a gentle reflux at 60 °C for an additional 1 hour. The resulting black solution was cooled down to room temperature, concentrated under

reduced pressure, and redissolved in DMPU (4.5 mL). LiClO₄ (280 mg, 2.63 mmol, 1.0 equiv.) and CaCO₃ (263 mg, 2.63 mmol, 1.0 equiv.) were added sequentially with vigorous stirring, and the suspension was heated up to 140 °C for 1.5 hours. Finally, the reaction was cooled down to room temperature, carefully quenched with aqueous HCl (3 M, 5 mL), and partitioned between Et₂O (30 mL) and water (30 mL). The organic phase was separated and the aqueous layer was washed with Et₂O (3 × 20 mL). The combined organic fractions were washed with brine (30 mL), dried over MgSO₄, filtered, and concentrated. Flash chromatography (basic Al₂O₃, 0% → 5% Et₂O in hexanes) furnished **1.78** (820 mg, 2.63 mmol, 80%).

R_f: 0.30 (SiO₂, hexanes : EtOAc = 25:1); **T_{melt.}** : 75.7 – 76.8 °C; **¹H NMR**: (500 MHz, CDCl₃) δ 10.03 (s, 1H), 3.41 (dd, *J* = 11.0, 5.1 Hz, 1H), 2.59 (dt, 13.4, 3.6 Hz, 1H), 2.28 (m, 2H), 2.03 (s, 3H), 1.75 – 1.64 (m, 3H), 1.50 (tdd, *J* = 13.1, 10.1, 7.2 Hz, 1H), 1.17 (s, 3H), 1.09 – 1.03 (m, 23H), 1.02 (s, 3H), 0.82 (s, 3H); **¹³C NMR**: (126 MHz, CDCl₃): δ 192.4, 154.4, 143.5, 79.9, 51.3, 40.2, 37.4, 37.0, 34.5, 28.8, 28.3, 20.2, 19.1, 18.52, 18.45, 18.41, 16.2, 13.2; **HRMS**: (ES⁺, *m/z*) calcd. for C₂₄H₄₅O₂Si [M+H]⁺ calcd.: 393.3189; found: 393.3208.; **IR**: (ATR, neat, cm⁻¹): 2939 (m), 2864 (s), 1669 (s), 1612 (w), 1111 (s), 882 (m), 679(s)

Synthesis of compound **1.87**:

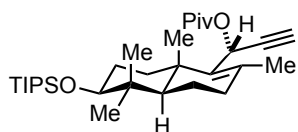


To a solution of aldehyde **1.78** (460 mg, 1.17 mmol, 1.0 equiv.) CH₂Cl₂ (5 mL) was added *tert*-butyldimethyl((3-methylfuran-2-yl)oxy)silane **1.83** (344 mg, 1.52 mmol, 1.3 equiv.) dropwise at –78 °C. After 20 min, a solution of trimethylsilyl trifluoromethanesulfonate (104 mg, 85 μL, 470 μmol, 40 mol %) in CH₂Cl₂ (6.7 mL) was added dropwise over a course of 5 min via syringe pump. The reaction mixture was stirred for additional 2 h at –78 °C and then quenched with NaHCO₃ (aq. sat., 5 mL). The organic layer was separated, and the aqueous layer was extracted with CH₂Cl₂ (3 × 10 mL). The combined organic layer was washed with brine, dried over Na₂SO₄, filtered and concentrated. The crude oil was purified by flash chromatography (SiO₂, hexanes : EtOAc = 10:1–5:1) affording the desired allylic alcohol **1.87** (319 mg, 650 μmol, 57%), minor diastereomers (42 mg, 94 μmol, 8%) and unreacted starting material.

R_f: 0.16 (SiO₂, hexanes : EtOAc = 7:1); **¹H NMR**: (500 MHz, CDCl₃): δ 6.82 (t, *J* = 1.7 Hz, 1H), 5.47 (d, *J* = 8.7 Hz, 1H), 4.00 (br, 1H), 3.41 (dd, *J* = 10.9, 5.1 Hz, 1H), 2.39 (s, 1H), 2.17–2.03 (m, 2H), 1.91 (t, *J* = 1.8 Hz, 3H), 1.82 (s, 3H), 1.73–1.64 (m, 3H), 1.48–1.22 (m, 3H), 1.10 (s, 1H),

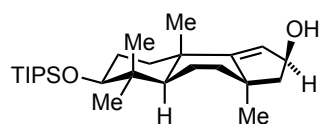
1.05 (s, 21H), 1.01 (s, 3H), 0.89 (s, 3H), 0.79 (s, 3H).; ^{13}C NMR: (126 MHz, CDCl_3): δ 174.0, 146.6, 137.6, 135.2, 131.2, 85.1, 79.7, 73.7, 51.7, 40.0, 38.9, 35.8, 34.7, 28.8, 28.1, 21.3, 20.7, 18.9, 18.5, 18.4, 16.3, 13.2, 10.8.; HRMS: (ES+, m/z) $[\text{M}+\text{H}]^+$ calcd. for $\text{C}_{29}\text{H}_{51}\text{O}_4\text{Si}$, 491.3557; found, 491.3575.; IR: (ATR, neat, cm^{-1}): 3462 (br), 2942 (m), 2865 (m), 1760 (s), 1657 (w). 1110 (s), 1058 (s).

Synthesis of compound 1.113:



To a solution of freshly prepared lithium acetylide in THF (200 mL, 0.1 M, 20.6 mmol, 1.8 equiv.) at $-78\text{ }^{\circ}\text{C}$, a solution of the aldehyde **1.78** (4.50 g, 11.5 mmol, 1.0 equiv.)⁶ in THF (30 mL) was added dropwise over the course of 5 min. The reaction was maintained at $-78\text{ }^{\circ}\text{C}$ for 3 h. Upon completion (TLC monitoring), pivaloyl chloride (2.8 mL, 22.9 mmol, 2.0 equiv.) was added and the resulting solution was slowly warmed up to ambient temperature and stirred for additional 4 h at room temperature. The reaction was quenched with NH_4OH (aq. 2.0 M, 200 mL), THF was removed under reduced pressure and resulting solution was partitioned between Et_2O (300 mL) and water (100 mL). The organic layer was separated and the aqueous phase was washed with Et_2O ($2 \times 100\text{ mL}$). The combined organic fractions were vigorously washed with NH_4OH (aq. 2 M, $2 \times 200\text{ mL}$) and brine (200 mL), dried over MgSO_4 , filtered and concentrated. This crude residue was purified by flash chromatography (C_{18} reverse phase SiO_2 , gradient 90% \rightarrow 100% MeCN in H_2O), which afforded **1.113** as a white crystalline material (4.70 g, 9.35 mmol, 82%, *d.r.* $> 20:1$). R_f : 0.68 (SiO_2 , hexanes : $\text{EtOAc} = 20:1$); $T_{\text{melt.}}$: $97.4 - 98.9\text{ }^{\circ}\text{C}$; ^1H NMR: (500 MHz, CDCl_3): δ 6.01 (d, $J = 2.4\text{ Hz}$, 1H), 3.38 (m, 1H), 2.44 (d, $J = 2.4\text{ Hz}$, 1H), 2.12–2.09 (m, 2H), 1.89 (s, 3H), 1.83 (dt, $J = 13.0, 3.6\text{ Hz}$, 1H), 1.71–1.64 (m, 3H), 1.46 (tdd, $J = 13.0, 10.2, 7.7\text{ Hz}$, 1H), 1.21 (s, 9H), 1.15 (dd, $J = 11.2, 5.2\text{ Hz}$, 1H), 1.08–1.04 (m, 1H), 1.06 (s, 21H), 1.03 (s, 3H), 1.00 (s, 3H), 0.79 (s, 3H); ^{13}C NMR: (126 MHz, CDCl_3): δ 177.3, 136.7, 136.4, 82.5, 79.8, 72.7, 60.1, 51.4, 40.0, 38.9, 38.8, 35.2, 34.4, 28.7, 28.2, 27.2, 21.1, 20.7, 18.8, 18.52, 18.46, 16.2, 13.2; HRMS: (EI+, m/z) $[\text{M}]^+$ calcd. for $\text{C}_{31}\text{H}_{54}\text{O}_3\text{Si}$, 502.3842; found, 502.3855.; IR: (ATR, neat, cm^{-1}): 3311 (w), 2942 (m), 2866 (m), 1736 (s), 1141 (s), 1113 (s), 1067 (w), 882 (m).

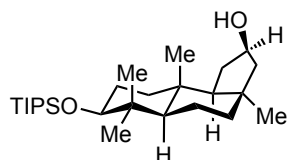
Synthesis of compound **1.127**:



Enone **1.59** (61 mg, 147 μmol , 1.0 equiv.) in MeOH (1.5 mL, 0.1 M) was treated with cerium(III) chloride heptahydrate (66 mg, 176 μmol , 1.2 equiv.) under inert atmosphere. After 10 min resulting suspension was cooled 5 $^{\circ}\text{C}$ and sodium borohydride (14 mg, 367 μmol , 2.6 equiv.) was added. The reaction progress was monitored by TLC. Upon completion, the resulting white cloudy solution was quenched by NH_4Cl (aq. sat., 3 mL). EtOAc was added and the mixture was transferred to a separatory funnel. Layers were separated and the aqueous layer was washed thrice with CH_2Cl_2 (5 mL). The combined organic layer was dried over MgSO_4 and concentrated to yield allylic alcohol **1.127** (60 mg, 147 μmol , 97 %, *d.r.* = 17:1) as a colorless oil.

R_f: 0.13 (SiO_2 , hexanes : EtOAc = 10:1); **^1H NMR**: (500 MHz, CDCl_3): δ 5.31 (s, 1H), 4.95 (q, J = 6.7 Hz, 1H), 3.38 (dd, J = 11.0, 4.6 Hz, 1H), 2.20 (ddd, J = 11.3, 5.8, 1.1 Hz, 1H), 1.85 (dt, J = 13.3, 3.1 Hz, 1H), 1.78–1.59 (m, 5H), 1.55–1.48 (m, 2H), 1.35–1.28 (m, 2H), 1.14 (s, 3H), 1.10 (s, 3H), 1.07 (s, 21H), 0.97 (s, 3H), 0.88 (s, 3H).; **^{13}C NMR**: (126 MHz, CDCl_3): δ 166.7, 123.1, 80.5, 76.3, 56.4, 46.3, 43.4, 40.3, 38.0, 37.0, 33.4, 28.7, 28.6, 28.0, 26.3, 18.53, 18.47, 17.7, 15.9, 13.2.; **HRMS**: (ES⁺, *m/z*) [$\text{M}+\text{Na}$]⁺ calcd. for $\text{C}_{26}\text{H}_{48}\text{O}_2\text{NaSi}$, 443.3321; found, 443.3335.; **IR**: (ATR, neat, cm^{-1}): 3312 (br), 2942 (br), 2865 (s), 1631 (w), 1461 (m), 1113 (s), 882 (m).

Synthesis of compound **1.128**:

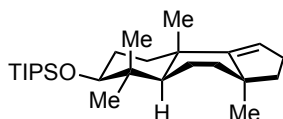


To the allylic alcohol **1.127** (60 mg, 140 μmol , 1.0 equiv.) in MeOH (0.5 mL, 0.3 M) was added Pd/C (15 mg, 10 w/w %) and the suspension was subjected hydrogenation (150 psi, 24 $^{\circ}\text{C}$, 5 h) in stainless steel autoclave. The resulting mixture was filtered through celite and directly dry-loaded onto celite. Alcohol **1.128** (37 mg, 88 μmol , 61%) was isolated via liquid chromatography (SiO_2 , hexanes : EtOAc = 10:1) as a white foam along with isomerized ketone (18.5 mg, 44 μmol , 31%).

R_f: 0.13 (SiO_2 , hexanes : EtOAc = 10:1); **^1H NMR**: (500 MHz, CDCl_3): δ 4.39 (ddt, J = 9.2, 7.8, 6.7 Hz, 1H), 3.37 (dd, J = 11.4, 3.9 Hz, 1H), 2.13 (dt, J = 13.7, 8.1 Hz, 1H), 1.69 (td, J = 13.4, 12.8, 6.8 Hz, 2H), 1.65–1.41 (m, 8H + H_2O), 1.36 (dt, J = 13.5, 6.8 Hz, 1H), 1.18 (dd, J = 8.3, 6.5 Hz, 1H), 1.06 (s, 21H), 0.97 (s, 3H), 0.95 (s, 3H), 0.92 (s, 3H), 0.92–0.89 (m, 2H), 0.85 (s, 3H).; **^{13}C NMR**: (126 MHz, CDCl_3): δ 80.6, 72.3, 59.8, 50.4, 49.9, 40.7, 40.5, 40.3, 36.2, 36.1, 35.6,

32.8, 28.6, 27.8, 18.8, 18.53, 18.47, 17.0, 15.8, 13.2.; **HRMS**: (ES⁺, m/z) [M+H]⁺ calcd. for C₂₆H₅₁O₂Si, 423.3658; found, 423.3676.; **IR**: (ATR, neat, cm⁻¹): 3337 (br), 2941 (s), 2865 (m), 1712 (w), 1461 (w), 1110 (s), 882 (m).

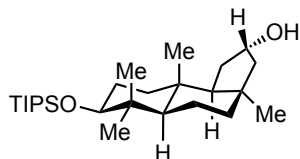
Synthesis of compound **1.129**:



Allylic alcohol **1.127** (14 mg, 33 μ mol, 1.0 equiv.) was dissolved in dry CH₂Cl₂ (1 mL, 0.03 M) and transferred to a sealed vial with the Crabtree's catalyst (5.4 mg, 6.7 μ mol, 20 mol %). The vial was pressurized to 1000 psi of H₂. The reaction was aged for 24 h. Reaction mixture was directly dry-loaded onto celite. Purification by liquid chromatography (SiO₂, hexanes) afforded titled compound **1.129** (10.8 mg, 27 μ mol, 80%) as a colorless oil.

R_f: 0.82 (SiO₂, 100% hexanes); **¹H NMR**: (500 MHz, CDCl₃): δ 5.28 (dd, J = 3.5, 1.6 Hz, 1H), 3.38 (dd, J = 11.1, 4.6 Hz, 1H), 2.35 (dddd, J = 15.6, 10.8, 6.0, 1.6 Hz, 1H), 2.03 (ddd, J = 15.7, 8.5, 3.5 Hz, 1H), 1.87 (dt, J = 13.4, 3.5 Hz, 1H), 1.77–1.70 (m, 2H), 1.69–1.61 (m, 4H), 1.54–1.42 (m, 3H), 1.33 (td, J = 13.4, 4.1 Hz, 1H), 1.09 (s, 3H), 1.07 (s, 21H), 1.04 (s, 3H), 0.97 (s, 3H), 0.87 (s, 3H).; **¹³C NMR**: (126 MHz, CDCl₃): δ 164.3, 118.6, 80.9, 45.9, 45.4, 44.0, 38.5, 37.4, 33.9, 29.7, 29.01, 29.00, 26.8, 25.8, 18.8, 18.7, 18.3, 16.1, 13.5.; **HRMS**: (EI⁺, m/z) [M]⁺ calcd. for C₂₆H₄₈OSi, 404.3474; found, 404.3478.; **IR**: (ATR, neat, cm⁻¹): 2942 (s), 2865 (m), 1462 (w), 1109 (s), 882 (m).

Synthesis of compound **1.130**:

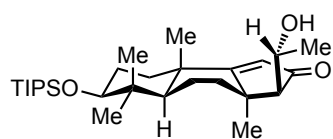


Allylic alcohol **1.127** (19 mg, 45 μ mol, 1.0 equiv.) was dissolved in dry CH₂Cl₂ (0.9 mL, 0.05 M) and transferred to a sealed vial with the Schrock-Osborn catalyst (3.2 mg, 64.5 μ mol, 10 mol %). The vial was pressurized to 1000 psi of H₂. The reaction was aged for 24 h. Reaction mixture was directly dry-loaded onto celite. Purification by liquid chromatography (SiO₂, hexanes : EtOAc = 10:1) afforded alcohol **42** (8.6 mg, 20 μ mol, 45%) as a white solid along with deoxygenated product **1.130** (9.6 mg, 24 μ mol, 53%).

R_f: 0.15 (SiO₂, hexanes : EtOAc = 10:1); **T_{melt.}**: 103.5 – 104.4 °C; **¹H NMR**: (500 MHz, CDCl₃): δ 4.37 (tdd, J = 7.7, 5.6, 2.4 Hz, 1H), 3.38 (dd, J = 10.6, 4.6 Hz, 1H), 2.01 (ddd, J = 14.3, 7.3, 2.1 Hz, 1H), 1.95 (dd, J = 13.9, 7.7 Hz, 1H), 1.78 (ddd, J = 14.2, 8.4, 5.6 Hz, 1H), 1.71 – 1.66 (m,

1H), 1.60–1.55 (m, 2H), 1.54–1.49 (m, 2H), 1.39–1.23 (m, 5H), 1.12 (s, 3H), 1.06 (s, 21H), 0.98 (s, 3H), 0.95–0.81 (m, 2H), 0.80 (s, 3H), 0.75 (s, 3H).; ¹³C NMR: (126 MHz, CDCl₃): δ 80.5, 73.8, 61.6, 51.6, 48.6, 41.2, 40.1, 40.0, 37.6, 36.7, 36.2, 33.6, 28.8, 27.8, 18.7, 18.53, 18.47, 16.3, 16.2, 13.2.; **HRMS**: (ES⁺, *m/z*) [M+H]⁺ calcd. for C₂₆H₅₁O₂Si, 423.3658; found, 423.3672.; **IR**: (ATR, neat, cm⁻¹): 3460 (br), 2947 (s), 2876 (m), 1713 (w), 1461 (w), 1117 (s), 887 (m).

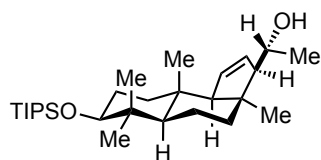
Synthesis of compound **1.132**:



To the solution of enone **1.59** (570 mg, 1.36 mmol, 1.0 equiv.) in THF (9.5 mL) at –78 °C DIPEA (440 mg, 593 μL, 3.40 mmol, 2.5 equiv.) and solution of Bu₂BOTf (3.27 mL, 1.0 M in PhMe, 2.4 equiv.) were added sequentially. Reaction became more viscous and change its color to yellow. The temperature was slowly raised up to –30 °C over 1.5 h and cold, freshly distilled acetaldehyde (300 mg, 380 μL, 6.81 mmol, 5.0 equiv.) was added in a single portion. The reaction mixture was aged at –30 °C for 2 h. Disappearance of color was observed. Finally, reaction was quenched with H₂O₂ (aq. 30%, 1.4 mL), warmed up to room temperature and kept stirring for 6 h. Product was extracted with ether (2 × 20 mL). Organic layer was washed with brine (10 mL), dried over MgSO₄, filtered and concentrated in *vacuo*. Purification was accomplished by liquid chromatography (SiO₂, hexanes : EtOAc = 10:1 – 5:1) affording desired product **1.132** (475 mg, 1.03 mmol, 75%) as white solid.

R_f: 0.36 (SiO₂, hexanes : EtOAc = 3:1); **T_{melt.}**: 127.5 – 129.1 °C; ¹H NMR: (500 MHz, CDCl₃): δ 5.80 (s, 1H), 3.94 (dt, *J* = 6.4, 4.8 Hz, 1H), 3.42 (dd, *J* = 10.8, 4.9 Hz, 1H), 2.10 (m, 2H), 2.04 (dt, *J* = 12.8, 9.1 Hz, 1H), 1.93 (dt, *J* = 13.3, 3.4 Hz, 1H), 1.88 (m, 1H), 1.83–1.71 (m, 5H), 1.44 (td, *J* = 13.0, 4.4 Hz, 1H), 1.38 (d, *J* = 6.2 Hz, 3H), 1.36 (s, 3H), 1.18 (s, 3H), 1.08 (s, 21H), 1.01 (s, 3H), 0.92 (s, 3H).; ¹³C NMR: (126 MHz, CDCl₃): δ 210.8, 201.7, 124.0, 80.0, 67.6, 67.2, 46.7, 42.4, 40.5, 39.7, 36.5, 32.4, 28.6, 28.2, 25.4, 25.2, 22.8, 18.52, 18.45, 17.2, 16.0, 13.2.; **HRMS**: (ES⁺, *m/z*) [M+H]⁺ calcd. for C₂₈H₅₁O₃Si, 463.3607; found, 463.3611.; **IR**: (ATR, neat, cm⁻¹): 3418 (br), 2941 (s), 2866 (m), 1681 (s), 1600 (w), 1461 (w), 1113 (s), 1094 (m), 882 (m).

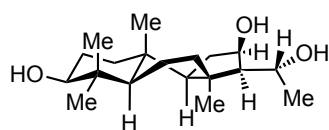
Synthesis of compound 1.153:



Enone **1.132** (28 mg, 61 μ mol, 1.0 equiv.) was mixed with *p*-toluenesulfonyl hydrazide (23 mg, 120 μ mol, 2.0 equiv.) in EtOH (0.5 mL, 0.1 M). The solution was heated to 80 °C for 8 h. Once full conversion was achieved, as judged by TLC, the solution was cooled down, all volatiles were removed *in vacuo*, and the residue was azeotropically distilled with toluene (2 \times 0.5 mL). The white foam was redissolved in degassed CHCl₃ (0.3 mL, 0.2 M) under inert atmosphere. The solution was cooled to 0 °C and treated with catecholborane (19 μ L, 180 μ mol, 3.0 equiv.). The ice-bath was removed and the reaction was stirred for 1.5 h. Then degassed CHCl₃ (0.3 mL) and NaOAc \cdot 3H₂O (33 mg, 240 μ mol, 4.0 equiv.) was added in one portion. The pale-yellow suspension was heated to 65 °C for an additional 1.5 h. The resulting thick suspension was cooled down and filtered through celite, and the residual oil was purified by flash chromatography (SiO₂, hexanes : EtOAc = 99:1). The product **1.153** (22 mg, 49 μ mol, 81%, *d.r.* > 20:1) was isolated as a white foam.

R_f: 0.26 (SiO₂, hexanes : EtOAc = 10:1); **¹H NMR**: (500 MHz, CDCl₃): δ 5.74 (m, 2H), 3.85 (pd, *J* = 6.4, 3.2 Hz, 1H), 3.41 (dd, *J* = 11.1, 4.3 Hz, 1H), 2.34 (m, 1H), 1.97 (m, 1H), 1.92 (s, 1H), 1.72–1.63 (m, 3H), 1.61–1.50 (m, 2H), 1.32 (dd, *J* = 13.5, 8.0 Hz, 1H), 1.26 (d, *J* = 6.3 Hz, 3H), 1.20 (d, *J* = 6.8 Hz, 1H), 1.11 (m, 4H), 1.07 (s, 21H), 0.94 (s, 3H), 0.87 (s, 3H), 0.79 (s, 3H).; **¹³C NMR**: (126 MHz, CDCl₃): δ 134.2, 127.3, 80.5, 70.7, 66.6, 65.8, 46.4, 41.24, 41.22, 40.5, 36.0, 32.8, 27.9, 27.8, 25.6, 24.7, 18.4, 18.3, 18.0, 17.9, 15.1, 13.1.; **HRMS**: (EI+, *m/z*) [*M*]⁺ calcd. for C₂₈H₅₁O₂Si, 447.36584; found, 447.36609.; **IR**: (ATR, neat, cm⁻¹): 3371 (br), 2942 (s), 2865 (s), 1462 (m), 1388 (m), 1110 (s), 677 (m)

Synthesis of compound 1.154:

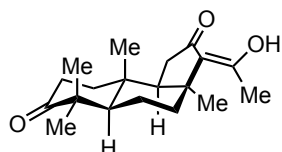


The following protocol was adopted from literature.¹⁰ CH₂Cl₂ (0.5 mL) was cooled to -78 °C. Neat Me₂S \cdot BH₃ (47 μ L, 0.49 mmol, 5.0 equiv.) was added followed by TfOH (44 μ L, 0.49 mmol) dropwise. Each drop of TfOH initially froze on the surface, forming a white solid that dissipated after a few seconds of stirring. Gas evolution was observed. This solution was stirred for 35 min before dropwise addition of a solution of **1.153** (44 mg, 98 μ mol) in CH₂Cl₂ (0.5 mL). The clear solution

was stirred at $-20\text{ }^{\circ}\text{C}$ for 36 h and was then treated slowly with a solution of 20% NaOH (4.8 mL) in MeOH (5.2 mL). The mixture was stirred 30 min at $-20\text{ }^{\circ}\text{C}$ before being stirred vigorously at $0\text{ }^{\circ}\text{C}$ for slow dropwise addition of 35% H_2O_2 (0.40 mL) in MeOH (0.43 mL). This mixture was warmed to $24\text{ }^{\circ}\text{C}$ and stirred for 6 h before transferring to a separatory funnel with 10 mL of Et_2O . Brine (4 mL) was then added, and the aqueous layer was extracted with Et_2O ($3 \times 5\text{ mL}$). The combined organic layers were dried (MgSO_4), concentrated and purified by flash chromatography (SiO_2 , hexanes : $\text{EtOAc} = 5:1 - 3:1 - 1:1$). Triol **1.154** (20 mg, 64 μmol , 65%, *d.r.* $> 20:1$) was isolated as a white solid along with deprotected starting material (6 mg, 21 μmol , 20%). Suitable crystals for X-ray analysis were obtained for boronate intermediate (prior oxidative work-up).

R_f: 0.45 (SiO_2 , hexanes : $\text{EtOAc} = 1:1$); **T_{melt.}**: $196.0 - 196.5\text{ }^{\circ}\text{C}$; **$^1\text{H NMR}$** : (500 MHz, CDCl_3): δ 4.57 (t, $J = 4.5\text{ Hz}$, 1H), 4.17 (p, $J = 6.1\text{ Hz}$, 1H), 3.23 (dd, $J = 9.9, 5.8\text{ Hz}$, 1H), 2.06 (m, 4H), 1.83 (ddd, $J = 15.1, 11.2, 4.9\text{ Hz}$, 1H), 1.76 (dd, $J = 15.0, 3.0\text{ Hz}$, 1H), 1.67 (m, 1H), 1.64–1.55 (m, 4H), 1.52 (dd, $J = 11.4, 2.8\text{ Hz}$, 1H), 1.40–1.36 (m, 5H), 1.20 (dd, $J = 11.0, 8.4\text{ Hz}$, 1H), 1.10 (s, 3H), 1.05 (ddd, $J = 12.4, 11.6, 4.9\text{ Hz}$, 1H), 0.99 (s, 3H), 0.96 (s, 3H), 0.91 (s, 3H).; **$^{13}\text{C NMR}$** : (126 MHz, CDCl_3): δ 79.9, 75.6, 67.1, 62.7, 62.2, 46.1, 43.5, 42.4, 39.5, 36.7, 34.1, 32.2, 27.7, 27.5, 27.4, 24.8, 18.1, 16.9, 15.1.; **HRMS**: (ES^+ , m/z) $[\text{M}+\text{H}]^+$ calcd. for $\text{C}_{19}\text{H}_{35}\text{O}_3$, 311.2586; found, 311.2586.; **IR**: (ATR, neat, cm^{-1}): 3359 (br, s), 2927 (s), 2869 (m), 1465 (w), 1400 (w), 1037 (m).

Synthesis of compound **1.214**:

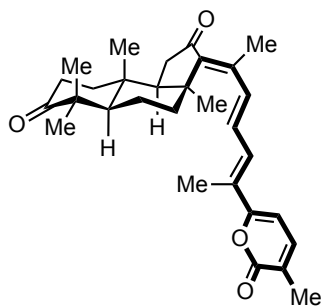


The triol **1.154** (90 mg, 0.29 mmol, 1.0 equiv.) was dissolved in EtOAc (3.0 mL, 0.1 M). IBX (812 mg, 2.90 mmol, 10 equiv.) was added and the suspension was brought to reflux for 5 h until conversion was observed as judged by TLC. Then the solution was cooled to room temperature, filtered through a short pad of celite, and concentrated. The resulting pale-yellow product **1.214** (84 mg, 0.28 mmol, 95%) was sufficiently clean for the next step and was not further purified. However, if necessary, purity of product **56** can be readily enhanced via recrystallization from MeOH.

R_f: 0.33 (SiO_2 , hexanes : $\text{EtOAc} = 5:1$); **T_{melt.}**: $168.1 - 168.5\text{ }^{\circ}\text{C}$; **$^1\text{H NMR}$** : (500 MHz, CDCl_3) δ 14.27 (s, 1H), 2.66 (ddd, $J = 18.3, 8.1, 3.0\text{ Hz}$, 1H), 2.59 (ddd, $J = 16.0, 13.3, 6.3\text{ Hz}$, 1H), 2.41 (dt, $J = 15.3, 4.3\text{ Hz}$, 1H), 2.33 (ddd, $J = 16.1, 8.4, 3.1\text{ Hz}$, 1H), 2.29 (d, $J = 18.6\text{ Hz}$, 1H), 2.08 (s, 3H), 1.87 (ddd, $J = 13.4, 6.3, 3.1\text{ Hz}$, 1H), 1.59–1.35 (m, 6H), 1.18 (s, 3H), 1.10 (s, 3H), 1.04 (s,

3H), 0.91 (s, 3H).; ^{13}C NMR: (126 MHz, CDCl_3): δ 216.5, 208.9, 172.8, 117.0, 56.3, 53.6, 47.6, 42.9, 39.0, 38.0, 37.1, 36.1, 34.3, 31.9, 26.4, 22.3, 20.3, 20.1, 14.6.; HRMS: (ES+, m/z) $[\text{M}+\text{H}]^+$ calcd. for $\text{C}_{19}\text{H}_{29}\text{O}_3$, 305.2117; found, 305.2119.; IR: (ATR, neat, cm^{-1}): 3389 (br, w), 2934 (s), 1706 (s), 1649 (s), 1611 (m), 1385 (w), 1231 (w).

Synthesis of compound 1.213:



A mixture of triketone **1.214** (19.7 mg, 65 μmol , 1.0 equiv.), DMF (6.5 μL , 84 μmol , 1.30 equiv.), and CH_2Cl_2 (310 μL) was cooled to 0 $^\circ\text{C}$, and oxalyl bromide (7.3 μL , 78 μmol , 1.20 equiv.) was added dropwise, with concurrent gas evolution. After 10 min ice-bath was removed and the reaction was stirred for 3 h. The brown reaction mixture was poured into Et_2O (3 mL) and an ice-cold solution of NaHCO_3 (3 mL). The

organic layer was separated, washed with brine (5 mL), dried over Na_2SO_4 and filtered. Quantitative conversion to a single isomer of vinyl bromide (24 mg, 65 μmol) was observed, and this material was used immediately in the next stage directly without additional purification due to instability of the compound on silica gel.

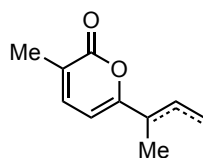
Caution! Product is light-sensitive. All workup and purification procedures were performed with rigorous protection from light, working in a dark room with foil-wrapped, amber glassware.

A 4-mL drum-vial was charged with $\text{Pd}_2(\text{dba})_3 \cdot \text{CHCl}_3$ (2.7 mg, 2.6 μmol , 5 mol%), and SPhos (2.1 mg, 5.2 μmol , 10 mol %). The vial was placed under an atmosphere of argon, and THF (0.2 mL) was added. The solution was stirred for 5 minutes at room temperature. A solution of crude vinyl bromide (1.0 equiv.) and boronic ester **1.211** (23 mg, 78 μmol , 1.5 equiv. in THF (0.3 mL) was added at room temperature, and resulting solution was degassed by passing Ar through the solution with sonication. At this point, lights were turned off and degassed aqueous solution of Na_2CO_3 (0.1 mL, 1.0 M, 2.0 equiv.). Temperature was raised to 65 $^\circ\text{C}$ and reaction was aged for 6 h. Upon completion mixture was cooled to ambient temperature and then partitioned between water and Et_2O (10 mL, 1:1). Organic layer was separated and washed with brine. Combined aqueous phase was backwashed with Et_2O (3×5 mL). Organic phase was dried over Na_2SO_4 , filtered and concentrated *in vacuo*. The red residue was dry-loaded onto celite and purified by liquid chromatography (SiO_2 , hexanes : EtOAc = 5:1 – 3:1 – 1:1). Coupling product (7.5 mg, 16 μmol) was obtained in 31% yield with minor impurities (constitutional and stereoisomer).

Spectroscopically clean **1.213** was obtained by reverse phase preparative HPLC (Kinetex® 5 μ m Biphenyl 100 Å LC Column 250 \times 10 mm, 5.2 mL/min, MeCN : H₂O = 1:1, detection at λ = 374 nm, t_R = 30.1 min).

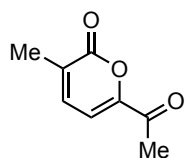
R_f: 0.13 (SiO₂, hexanes : EtOAc = 2:1); **¹H NMR**: (500 MHz, C₆D₆): δ 7.47 (d, J = 11.4 Hz, 1H), 7.10 (d, J = 15.0 Hz, 1H), 6.90 (dd, J = 15.0, 11.5 Hz, 1H), 6.24 (dq, J = 6.9, 1.3 Hz, 1H), 5.46 (d, J = 6.9 Hz, 1H), 2.60 (s, 3H), 2.49 (m, 1H), 2.26 (dd, J = 18.2, 8.2 Hz, 1H), 2.12–2.10 (m, 2H), 2.08 (d, J = 18.2 Hz, 1H), 1.86 (s, 3H), 1.55 (d, J = 1.1 Hz, 3H), 1.28 (ddd, J = 13.3, 6.3, 3.5 Hz, 2H), 1.15–1.07 (m, 2H), 1.07 (s, 3H), 1.05–1.00 (m, 2H), 0.96 (s, 3H), 0.86 (ddd, J = 13.0, 12.9, 6.1 Hz, 1H), 0.79 (s, 3H), 0.66 (s, 3H); **¹³C NMR**: (126 MHz, C₆D₆): δ 213.7, 208.1, 161.8, 158.7, 141.2, 140.5, 138.5, 136.4, 130.7, 130.1, 128.7, 124.9, 102.6, 55.3, 54.0, 47.2, 46.7, 39.9, 38.6, 38.3, 37.4, 34.2, 31.7, 26.7, 22.2, 20.3, 16.9, 15.9, 14.4, 12.5; **HRMS**: (ES⁺, m/z) [M+H]⁺ calcd. for C₃₀H₃₉O₄, 463.2848; found, 463.2842.; **IR**: (ATR, neat, cm⁻¹): 2925 (m), 2861 (w), 1711 (s), 1544 (m), 1128 (m).

Synthesis of compound S1.3:



To tiglic acid (16.0 g, 160 mmol, 1.0 equiv.) in CH₂Cl₂ (266 mL, 0.6 M) at 0 °C in a round bottom flask attached to an oil bubbler was added dimethylformamide (2 drops) and freshly distilled oxalyl chloride (14.0 mL, 160 mmol, 1.0 equiv.). After 30 min at 0 °C the reaction mixture was warmed to 24 °C for 3 h. The crude acid chloride was re-cooled to 0 °C and Et₃N (44 mL, 320 mmol, 2.0 equiv.) was slowly added. A white precipitate formed immediately. The reaction mixture was warmed to 24 °C and stirred for 2.5 h. It was poured into water (400 mL) and extracted with CH₂Cl₂ (3 \times 100 mL). The combined organic layers were dried over MgSO₄, concentrated and purified by liquid chromatography (SiO₂, hexanes : Et₂O = 10:1 – 5:1 – 4:1) to yield inseparable mixture of pyrones **S1.3** and **S1.3'** (7.78 g, 47.5 mmol, 30%) as red oil. *All spectral data matched with reported.*

Synthesis of compound 1.210:

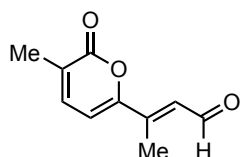


To a 250-ml flask, mixture of pyrones **S1.3/S1.3'** (2.0 g, 12.2 mmol, 1.0 equiv.) was dissolved in THF/water (10:1, 99 mL, 0.12 M). 2,6-Lutidine (2.82 mL, 24.4 mmol, 2.0 equiv.) and NMO (2.14 g, 18.3 mmol, 1.5 equiv.) was added followed

by OsO₄ (1.22 mL, 244 μmol, 0.2 M in MeCN, 2 mol %). The reaction progress was monitored by TLC. Full conversion was observed within 3 h. PIDA (5.88 g, 18.3 mmol, 1.5 equiv.) was added in a single portion, and the reaction was stirred overnight. Reaction mixture was quenched with sodium thiosulfate (aq. 10 w/w %, 30 mL). EtOAc (100 mL) was added. The organic layer was separated. Aqueous phase was backwashed with EtOAc (2 × 50 mL). Combined organic phase was washed with CuSO₄ (aq. 10 w/w %, 100 mL), dried over MgSO₄, filtered and concentrated. The residue was directly recrystallized from PhMe yielding the pale-yellow crystals. The mother liquor was purified by liquid chromatography (SiO₂, hexanes : Et₂O = 3:1). Thus, the ketone **1.210** (910 mg, 5.98 mmol) was isolated in 49 % yield.

R_f: 0.212 (SiO₂, hexanes : Et₂O = 3:1); **T_{melt}**: 177.3 – 178.6 °C; **¹H NMR**: (500 MHz, CDCl₃) δ 7.25 (d, *J* = 6.7 Hz, 1H), 6.95 (d, *J* = 6.7 Hz, 1H), 2.51 (s, 3H), 1.19 (s, 3H); **¹³C NMR**: (126 MHz, CDCl₃): δ 191.5, 161.4, 153.5, 138.1, 132.1, 107.3, 26.0, 17.7; **HRMS**: (EI⁺, *m/z*) [*M*]⁺ calcd. for C₈H₈O₃, 152.0473; found, 152.0475.; **IR**: (ATR, neat, cm⁻¹): 3084 (w), 1703 (s), 1694 (m), 1688 (s), 1088 (w).

Synthesis of compound 1.208:



Reaction was carried out in accordance with literature protocol with minor modifications.¹²

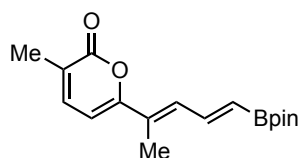
50 w/w % solution of ethoxyacetylene (0.65 mL, 3.29 mmol, 2.5 equiv.) in hexanes was transferred to a flamed dried 25-mL flask, followed by addition of THF (4 mL). The flask was then purged with N₂ for 1 min before cooling to 0 °C. With stirring, borane dimethyl sulfide complex (0.1 mL, 1.05 mmol, 0.8 equiv.) in THF (4 mL) was added dropwise over a course of 4 min. The reaction mixture warmed to 24 °C and stirred for 12 h before heated for 1 h at 60 °C. Then the oil bath was replaced with a water bath, volatile material was removed *in vacuo* delivering red residue, which was further dissolved in PhMe (3.75 mL) to yield ~0.28 M solution.

The 0.28 M vinylborane solution was cooled to –78 °C, Et₂Zn (3.15 mL, 3.15 mmol, 1.0 M in hexanes, 2.4 equiv.) was added slowly over a course of 3 min by submerging the needle into the solution and stirred for 1 hour. The mixture was quickly transferred via cannula to the 25-mL flask with ketone **1.210** (200 mg, 1.31 mmol, 1.0 equiv.) at –78 °C. The yellow mixture was stirred at this temperature for an additional 3 h, and then warmed to ambient temperature. The color of the mixture gradually became red and the mixture was stirred for additional 40 min until the mixture

became completely homogeneous. At this point the reaction was cooled again to 0 °C, and brine (3 mL) was cautiously added. The mixture was allowed to stir for five minutes as the zinc salts precipitates, then HCl (1.0 M, 9 mL) was slowly added. The mixture was vigorously stirred for 10 min. Most of the desired aldehyde **1.208** was crashed out as elimination occurred. After 10 min, some EtOAc (20 mL) was added and the mixture was transferred to a separatory funnel. The organic layer was separated, and the aqueous layer was washed with EtOAc (3 × 10 mL). The combined organic phase was washed with water (40 mL), brine (40 mL), filtered and concentrated. The crude material was purified by liquid chromatography (SiO₂, hexanes : Et₂O = 3:1 – 1:1) to afford the product **1.208** (187 mg, 1.05 mmol) as pale yellow solid in 80 % yield.

R_f: 0.22 (SiO₂, hexanes : EtOAc = 1:1); **T_{melt.}** : 128.0 – 128.8 °C; **¹H NMR**: (500 MHz, CDCl₃) δ 10.18 (d, *J* = 7.3 Hz, 1H), 7.19 (dq, *J* = 6.8, 1.3 Hz, 1H), 6.79 (dd, *J* = 7.3, 1.4 Hz, 1H), 6.53 (d, *J* = 6.8 Hz, 1H), 2.37 (d, *J* = 1.3 Hz, 3H), 2.16 (d, *J* = 1.3 Hz, 3H).; **¹³C NMR**: (126 MHz, CDCl₃): δ 191.0, 161.9, 157.0, 144.3, 138.5, 128.6, 127.2, 106.2, 17.2, 12.8.; **HRMS**: (ES+, *m/z*) [M+H]⁺ calcd. for C₁₀H₁₁O₃, 179.0708; found, 179.0703.; **IR**: (ATR, neat, cm⁻¹): 3069 (w), 2888 (w), 1723 (s), 1663 (s), 1595 (m), 1146 (m), 838 (m).;

Synthesis of compound **1.211**:

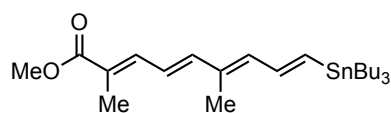


Solution of [bis(pinacolato)boryl]methane (256 mg, 0.95 mmol, 1.2 equiv.) in dry THF (2.1 mL) was added to the solution of freshly prepared LiTMP (0.95 mmol, 1.2 equiv.) in THF (2.7 mL) at 0 °C. After 5 min white suspension was cooled down to –78 °C and treated with solution of the gibepyrone C **1.208** (142 mg, 0.80 mmol, 1.0 equiv.) in THF (2.8 mL). Color turned into dark-red; stirring was continued for 3 h at above temperature followed by quench with CuSO₄ (5 mL, 10 w/w %). Product was extracted with Et₂O (20 mL), aqueous layer was backwashed with Et₂O (2 × 10 mL). Combined organic layers were washed with CuSO₄ (2 × 5 mL, 10 w/w %), brine (20 mL), dried over Na₂SO₄, filtered and concentrated *in vacuo*. The residue was passed through short plug of SiO₂ with eluent hexanes : EtOAc = 5:1. Prone to hydrolysis vinyl boronate **1.211** (230 mg, 0.76 mmol, 96%) was isolated as a pale yellow solid and was used for the next step without additional purification.

R_f: 0.17 (SiO₂, hexanes/EtOAc = 5:1); **T_{melt.}** : 133.7 – 135.6 °C; **¹H NMR**: (500 MHz, CDCl₃) δ 7.33 (dd, *J* = 17.5, 10.4 Hz, 1H), 7.13-7.07 (m, 2H), 6.20 (d, *J* = 6.3 Hz, 1H), 5.85 (d, *J* = 17.3 Hz,

1H), 2.09 (s, 3H), 2.02 (s, 3H), 1.27 (s, 12H).; ^{13}C NMR: (126 MHz, CDCl_3): δ 163.1, 159.1, 144.1, 139.6, 131.7, 129.2, 124.6, 103.1, 83.5, 24.9, 16.9, 12.9.; HRMS: (ES+, m/z) $[\text{M}+\text{H}]^+$ calcd. for $\text{C}_{17}\text{H}_{24}\text{BO}_4$, 303.1768; found, 303.1760.; IR: (ATR, neat, cm^{-1}): 2478 (w), 1714 (s), 1608 (m), 1552 (w), 1380 (m), 1370 (m), 1346 (s), 1324 (s), 1264 (m), 1142 (s), 1116 (w).

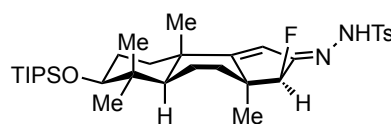
Synthesis of compound 1.205:



To a solution of phosphonate **1.204** (195 mg, 0.779 mmol, 1.5 equiv.) in THF (24 mL, 0.033M) under nitrogen was added a 1.0 M THF solution of LHMDs (143 mg, 0.857 mmol, 0.860 mL, 1.65 equiv.) dropwise at $-10\text{ }^\circ\text{C}$. After ten minutes, the reaction was cooled to $-60\text{ }^\circ\text{C}$ and HMPA (0.271 mL, 1.56 mmol, 3.0 equiv.) was added dropwise. After ten minutes, the reaction was cooled to $-78\text{ }^\circ\text{C}$, and a solution of stannanedienal **1.202** in THF (200 mg, 0.519 mmol, 0.55mL, 0.95 M, 1.0 equiv.) was added dropwise. The reaction was held at $-78\text{ }^\circ\text{C}$ for 1.5 hours and then warmed to room temperature. After stirring for 30 minutes at room temperature, the reaction was quenched with NH_4Cl (aq.sat. 30 mL), and extracted with Et_2O ($3 \times 15\text{ mL}$), washed with brine (40 mL), and dried over MgSO_4 . The solvent was removed *in vacuo*. The material was quickly purified with short plug of silica gel with 10% of EtOAc in hexanes to remove the excess phosphonate. Stannane **1.205** was obtained as a bright yellow oil (173 mg, 0.519 mmol, 68% yield) that was used for the next step without additional purification. For characterization, this material was purified using Biotage[®] Isolera[™] One (Cartridge Biotage[®] SNAP Ultra, HP-Sphere C18; 25 μm ; 12g, 100% MeCN; detection at $\lambda = 353\text{ nm}$)

R_f: 0.24 (SiO_2 , hexanes : EtOAc = 99:1); ^1H NMR: (500 MHz, CDCl_3) δ 7.28 (d, $J = 11.0\text{ Hz}$, 1H), 6.92 (dd, $J = 18.5, 10.6\text{ Hz}$, 1H), 6.53 (m, 3H), 6.19 (d, $J = 10.7\text{ Hz}$, 1H), 3.76 (s, 3H), 1.99 (s, 3H), 1.97 (s, 3H), 1.52 (p, $J = 8.1, 8.1, 7.6, 7.6\text{ Hz}$, 6H), 1.32 (h, $J = 7.3\text{ Hz}$, 6H), 0.93 (m, 6H), 0.90 (t, $J = 7.5, 7.5\text{ Hz}$, 9H); ^{13}C NMR: (126 MHz, CDCl_3): δ 169.1, 144.6, 142.8, 139.7, 139.1, 137.6, 133.7, 126.0, 123.6, 51.9, 29.3, 27.4, 13.9, 13.0, 12.8, 9.8; HRMS: (ES+, m/z) $[\text{M}+\text{Na}]^+$ calcd. for $\text{C}_{24}\text{H}_{42}\text{NaO}_2^{120}\text{Sn}$, 505.2104; found, 505.2125.; IR: (ATR, neat, cm^{-1}): 2923 (br), 1705 (s), 1618 (w), 1582 (m), 1284 (m), 1227 (s)

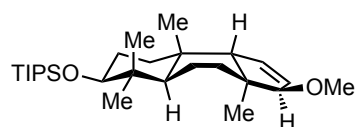
Synthesis of compound 1.188:



Enyne **1.113** (920 mg, 1.83 mmol, 1.0 equiv.) was dissolved in the mixture MeCN : CH₂Cl₂ = 2.5:1 (9.1 mL, 0.20 M). SelectFluor[®] (843 mg, 2.92 mmol, 1.3 equiv.) was added. A separate 4-mL vial was charged with [Au(PPh₃)Cl] (23 mg, 0.046 mmol, 2.5 mol %) and AgOTf (12 mg, 0.046 mmol, 2.5 mol%) inside of a nitrogen-filled glovebox. Dry CH₂Cl₂ (0.5 mL) was added under inert atmosphere and stirred at room temperature with protection from light. After 10 minutes, precipitated AgCl was visible and the suspension was transferred into the reaction mixture. Conversion was monitored by TLC. Once full conversion was achieved (about 1-2 hours), *p*-toluenesulfonyl hydrazide (511 mg, 2.74 mmol, 1.4 equiv.) was added and the reaction was heated to 40 °C for 10 h. The resulting suspension was partitioned between CH₂Cl₂ (40 mL) and water (80 mL). The organic layer was separated and the aqueous layer was washed with CH₂Cl₂ (3 × 20 mL). The combined organic phases were dried over MgSO₄, filtered, and concentrated *in vacuo*. Hydrazone **1.188** (900 mg, 1.49 mmol, 81%, *d.r.* > 20:1) was isolated as a white solid using the Biotage[®] Isolera[™] One (AQ C18 column Spherical; 20 – 35 μm; 100A; 20g, 75% → 100% MeCN in H₂O, detection at λ = 275 nm).

R_f: 0.41 (SiO₂, hexanes : EtOAc = 5:1); **T_{melt.}**: 169.3 – 171.2 °C; **¹H NMR**: (500 MHz, CDCl₃): δ 7.86 (d, *J* = 8.4 Hz, 2H), 7.66 (s, 1H), 7.31 (d, *J* = 8.4 Hz, 2H), 5.95 (s, 1H), 4.65 (d, *J* = 55.7 Hz, 1H), 3.37 (dd, *J* = 10.3, 5.3 Hz, 1H), 2.42 (s, 3H), 1.95 (dt, *J* = 13.6, 9.5 Hz, 1H), 1.88 – 1.80 (m, 2H), 1.78 – 1.67 (m, 3H), 1.59 – 1.52 (m, 2H), 1.36 (m, 1H), 1.12 (d, *J* = 2.2 Hz, 3H), 1.09 (s, 3H), 1.07 (s, 21H), 0.99 (s, 3H), 0.88 (s, 3H); **¹³C NMR**: (126 MHz, CDCl₃): δ 184.5 (d, *J* = 3.3 Hz), 159.5 (d, *J* = 14.6 Hz), 144.3, 135.4, 129.8, 128.1, 110.3, 99.2 (d, *J* = 189.4 Hz), 80.0, 48.2 (d, *J* = 19.4 Hz), 43.2, 40.5, 38.7, 36.8, 28.6, 28.2, 26.8 (d, *J* = 4.8 Hz), 25.1, 22.6 (d, *J* = 9.3 Hz), 21.8, 18.52, 18.45, 16.7, 15.9, 13.2; **¹⁹F NMR**: (470 MHz, CDCl₃): δ -178.0 (d, *J* = 55.7 Hz); **HRMS**: (ES⁺, *m/z*) [M+H]⁺ calcd. for C₃₃H₅₄N₂O₃SiSF, 605.3608; found, 605.3587.; **IR**: (ATR, neat, cm⁻¹): 3216 (br), 2942 (s), 2866 (s), 1597 (w), 1462 (m), 1345 (s), 1165 (s)

Synthesis of compound 1.173:

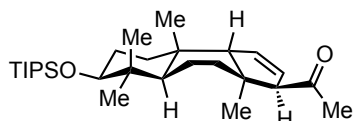


The α-fluorohydrazone **1.188** (960 mg, 1.56 mmol, 1.0 equiv.) was dissolved in the mixture CHCl₃/MeOH (2:1, 16 mL, 0.1 M). The solution was treated with Et₃N (0.28 mL, 2.03 mmol, 1.3 equiv.) and

stirred for 2 h. The solvent and excess of Et₃N were removed *in vacuo*. The remaining yellow foam was redissolved in *dry and degassed* CHCl₃ (16 mL, 0.1 M) under a nitrogen atmosphere, cooled down to 0 °C. Catecholborane (250 µL, 2.33 mmol, 1.5 equiv.) was added in dropwise. After 5 min, the yellow suspension was warmed up to room temperature and stirred for additional 3 h. CsOAc (747 mg, 3.89 mmol, 2.5 equiv.) was added in one portion as a solid and the mixture was heated to 65 °C for another 4 h. The thick white suspension was cooled down to ambient temperature and filtered through celite. This filtrate was concentrated and purified by flash chromatography (SiO₂, 1% of Et₂O in hexanes). Allyl ether **1.173** (395 mg, 0.909 mmol, 58%, *d.r.* > 20:1) was isolated as a clear pale-yellow oil (see Picture 2).

R_f : 0.42 (SiO₂, hexanes : EtOAc = 20:1); **¹H NMR**: (500 MHz, CDCl₃): δ 6.14 (dd, *J* = 6.0, 1.8 Hz, 1H), 6.05 (ddd, *J* = 6.0, 3.6, 2.4 Hz, 1H), 3.42 (dd, *J* = 10.6, 5.8 Hz, 1H), 3.36 (d, *J* = 2.4 Hz, 1H), 3.29 (s, 3H), 2.76 (dd, *J* = 3.6, 1.8 Hz, 1H), 2.19 (dd, *J* = 12.9, 8.7 Hz, 1H), 1.76 – 1.70 (m, 3H), 1.67 (dd, *J* = 13.5, 9.0 Hz, 1H), 1.48 (dt, *J* = 13.0, 3.7 Hz, 1H), 1.42 (dt, *J* = 12.3, 9.0 Hz, 1H), 1.37 – 1.29 (m, 2H), 1.14 (s, 3H), 1.07 (s, 21H), 1.02 (s, 3H), 1.00 (s, 3H), 0.79 (s, 3H); **¹³C NMR**: (126 MHz, CDCl₃): δ 136.9, 131.5, 91.2, 80.8, 57.7, 57.5, 47.1, 46.5, 40.4, 35.1, 33.7, 29.9, 29.8, 28.4, 27.0, 23.9, 18.8, 18.6, 18.5, 16.6, 13.2; **HRMS**: (ES⁺, *m/z*) [M–OCH₃]⁺ calcd. for C₂₆H₄₇OSi, 403.3396; found, 403.3403.; **IR**: (ATR, neat, cm^{−1}): 2940 (br), 2866 (s), 1463 (w), 1106 (m), 1057 (w)

Synthesis of compound 1.159:

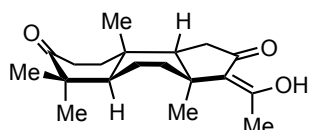


To a solution of **1.173** (80 mg, 0.18 mmol, 1.0 equiv.) and Cp₂ZrCl₂ (70 mg, 0.24 mmol, 1.3 equiv.) in THF (0.32 mL, 0.6 M) was added dropwise a solution of *n*-BuLi (0.28 mL, 1.6 M, 0.44 mmol, 2.4 equiv.) under a nitrogen atmosphere at 0 °C. The yellow reaction mixture underwent a color change to brown. The ice bath was removed after 10 minutes and the mixture was stirred at ambient temperature for 36 hours. A separate 4-mL vial was charged with CuOAc (4.5 mg, 0.037 mmol, 0.20 equiv.) inside of a glovebox, and a suspension was prepared in THF (0.9 mL). This suspension was heated to 55 °C and treated with acetyl chloride (0.053 mL, 0.74 mmol, 4.0 equiv.). The orange allylzirconium in the first flask was transferred *via* cannula to the copper catalyst and acetyl chloride in the second vessel. An additional portion of THF (0.3 mL) was used for washing the initial flask and then transferred to the second vessel by cannulation as well. After stirring for

3 hours at 55 °C the reaction was quenched with 1 M HCl (1 mL) and partitioned between EtOAc (7 mL) and water (5 mL). The organic layer was separated and the aqueous phase was washed with EtOAc (2 × 5 mL). The combined organic fractions were washed with brine (10 mL), dried over MgSO₄, filtered and concentrated. This material was purified by flash chromatography (1% EtOAc in hexanes) to give skipped enone **1.159** (53 mg, 0.12 mmol, 64%) and its constitutional isomer (13 mg, 0.029 mmol, 16%) as crystalline solids in a ratio of 4:1.

R_f: 0.48 (SiO₂, hexanes : EtOAc = 40:1); **T_{melt.}** : 76.5 – 77.3 °C; **¹H NMR**: (500 MHz, CDCl₃): δ 6.11 (d, *J* = 5.7 Hz, 1H), 5.76 (dt, *J* = 6.1, 3.2 Hz, 1H), 3.42 (dd, *J* = 9.7, 6.8 Hz, 1H), 3.06 (d, *J* = 2.7 Hz, 1H), 2.77 (d, *J* = 3.6 Hz, 1H), 2.11 (s, 3H), 1.83 (dd, *J* = 13.4, 8.9 Hz, 1H), 1.77 – 1.71 (m, 2H), 1.68 (m, 1H), 1.64 (dd, *J* = 13.1, 8.9 Hz, 1H), 1.56 – 1.50 (m, 2H), 1.44 – 1.35 (m, 2H), 1.32 (s, 3H), 1.08 (s, 21H), 1.03 (s, 3H), 0.98 (s, 3H), 0.78 (s, 3H); **¹³C NMR**: (126 MHz, CDCl₃): δ 209.6, 134.6, 130.6, 80.7, 70.3, 58.7, 49.3, 45.7, 40.4, 35.6, 33.6, 32.1, 31.1, 30.3, 29.9, 29.8, 24.1, 18.8, 18.6, 18.5, 16.6, 13.2; **HRMS**: (ES⁺, *m/z*) [M+H]⁺ calcd. for C₂₈H₅₁O₂Si, 447.3658; found, 447.3662.; **IR**: (ATR, neat, cm⁻¹): 2942 (br), 2865 (s), 1708 (m), 1463 (w), 1111 (m)

Synthesis of compound **1.158**:



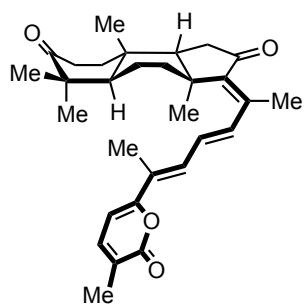
The enone **1.159** (36 mg, 0.081 mmol, 1.0 equiv.) was dissolved in dry THF (0.8 mL, 0.1 M) under a nitrogen atmosphere and cooled to –20 °C. The substrate was treated with BH₃•Me₂S (9.2 μl, 0.097 mmol, 1.2 equiv.) and slowly warmed up to room temperature. After stirring for 8 hours, the solution was cooled down to 0 °C, trifluoromethanesulfonic acid (14 μl, 0.16 mmol, 2.0 equiv.) was added, and the reaction was allowed to warm to room temperature again. After 2 hours at ambient temperature, the reaction mixture was cooled to 0 °C again and treated with NaOH (0.32 mL, 10% in MeOH, 10 equiv.) followed by H₂O₂ (0.08 mL, 30%_{aq}, 10 equiv.). The resulting solution was aged for an additional 6 hours and then partitioned between EtOAc and water (20 mL, 1:1). The aqueous layer was separated and extracted with EtOAc (2 × 5 mL). The combined organic portions were washed with brine (20 mL), dried over MgSO₄, filtered, and concentrated.

The resultant material from the first stage was redissolved in EtOAc (0.8 mL, 0.1 M). IBX (225 mg, 0.81 mmol, 10 equiv.) was added and the suspension was refluxed for 3 hours until conversion was observed (monitoring by TLC). Then the solution was cooled to room temperature, filtered through a short pad of SiO₂, and concentrated. The residue was purified by flash chromatography

(SiO₂, hexanes : EtOAc = 10:1) and desired triketone **1.158** (19 mg, 0.062 mmol, 80%) was isolated as a white crystalline solid.

R_f: 0.33 (SiO₂, hexanes : EtOAc = 3:1); **T_{melt.}**: 134.1 – 134.8 °C; **¹H NMR**: (500 MHz, CDCl₃) δ 13.66 (s, 1H), 2.72 (ddd, J = 16.1, 12.0, 5.8 Hz, 1H), 2.43 (dd, J = 13.1, 2.6 Hz, 1H), 2.37 (ddd, J = 16.1, 9.8, 3.1 Hz, 1H), 2.31 – 2.22 (m, 2H), 2.16 (ddd, J = 12.5, 12.3, 3.1 Hz, 1H), 2.04 (dd, J = 13.3, 8.7 Hz, 1H), 1.99 (s, 3H), 1.93 (t, J = 9.3 Hz, 1H), 1.89 (ddd, J = 14.1, 13.4, 8.7 Hz, 1H), 1.63 – 1.57 (m, 1H), 1.55 – 1.48 (m, 2H), 1.34 (s, 3H), 1.11 (s, 3H), 1.05 (s, 3H), 0.85 (s, 3H); **¹³C NMR**: (126 MHz, CDCl₃, *Major enol form 26*): δ 219.2, 207.3, 172.5, 123.7, 50.7, 47.1, 45.3, 41.3, 35.9, 34.7, 34.6, 33.6, 31.3, 29.3, 26.4, 23.7, 19.5, 19.4, 19.0; (126 MHz, CDCl₃, *Minor ketone form 26'*, only distinguishable peaks are listed): δ 218.7, 210.7, 48.9, 45.7, 42.9, 36.0, 35.7, 34.7, 33.3, 32.0, 31.5, 24.2, 21.4, 19.4, 18.9; **HRMS**: (ES⁺, m/z) [M+H]⁺ calcd. for C₁₉H₂₉O₃, 305.2117; found, 305.2118; **IR**: (ATR, neat, cm⁻¹): 2935 (br), 1704 (s), 1650 (m), 1615 (m), 1382 (w), 1230 (w)

Synthesis of stelletin A (1.1):



A mixture of triketone **1.158** (1.0 equiv.), DMF (1.30 equiv.), and CH₂Cl₂ (0.2 M) was cooled to 0 °C, and oxalyl bromide (1.20 equiv.) was added dropwise, with concurrent gas evolution. After 10 min ice-bath was removed and the reaction was stirred for 3 h. The brown reaction mixture was poured into Et₂O and an ice-cold solution of NaHCO₃. The organic layer was separated, washed with brine, dried over

Na₂SO₄ and filtered. Quantitative conversion to a single isomer of vinyl bromide **1.198** was observed, and this material was used immediately in the next stage directly without additional purification due to instability of the compound on silica gel.

Caution! Product is light-sensitive. All workup and purification procedures were performed with rigorous protection from light, working in a dark room with foil-wrapped, amber glassware.

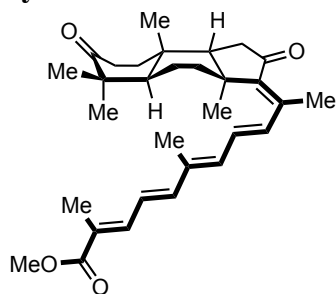
A 4-mL drum-vial was charged with catalyst (10 mol %), and ligand (10 mol %). The vial was placed under an atmosphere of argon, and solvent was added. The solution was stirred for 5 min at room temperature. A solution of crude vinyl bromide **1.198** (1.0 equiv.) and boronic ester **1.211** (1.5 equiv.) in respective solvent was added at room temperature. The dark-red 0.1 M solution was treated with solution of TMSOK (1.0 M, 1.3 equiv.) dropwise via syringe with filter. Temperature

was raised to 55 °C and reaction was aged for 12 h. Upon completion mixture was cooled to ambient temperature and then partitioned between water and Et₂O (1:1). Organic layer was separated and washed with brine. Combined aqueous phase was backwashed thrice with Et₂O. Organic phase was dried over Na₂SO₄, filtered and concentrated *in vacuo*. The red residue was dry-loaded onto celite and purified by liquid chromatography (SiO₂, hexanes : EtOAc = 3:1 – 1:1) furnishing mixture of constitutional isomers **1.1** : **1.215** in *ca.* 7:1 ratio. Isomers were separated by reverse phase preparative HPLC (Kinetex[®] 5 µm Biphenyl 100 Å LC Column 250 × 10 mm, 5.5 mL/min, MeCN : H₂O = 55:45, detection at λ = 374 nm, *t_R* = 21.1 min).

Compound readily decomposes under ambient light and was stored in foil-covered vessel at – 20 °C. Notably, only minor isomerization of the double-bound into stelletin B (1.2) was observed.

R_f: 0.40 (SiO₂, hexanes : EtOAc = 1:1); **¹H NMR**: (500 MHz, CDCl₃): δ 7.27 (d, *J* = 11.0 Hz, 1H), 7.17 (d, *J* = 6.8 Hz, 1H), 7.01 (dd, *J* = 14.9, 11.0 Hz, 1H), 6.94 (d, *J* = 14.9 Hz, 1H), 6.24 (d, *J* = 6.8 Hz, 1H), 2.76 (ddd, *J* = 16.2, 12.0, 5.8 Hz, 1H), 2.45 (dd, *J* = 13.2, 2.2 Hz, 1H), 2.40–2.32 (m, 2H), 2.35 (s, 3H), 2.25–2.17 (m, 4H), 2.14 (s, 3H), 2.05 (s, 3H), 1.88 (t, *J* = 11.1 Hz, 1H), 1.67 (dd, *J* = 12.8, 8.9 Hz, 1H), 1.54–1.48 (m, 2H), 1.46 (s, 3H), 1.15 (s, 3H), 1.06 (s, 3H), 0.86 (s, 3H); **¹³C NMR**: (126 MHz, CDCl₃, *not previously reported*): δ 219.4, 207.4, 163.2, 158.9, 147.7, 141.2, 139.9, 137.1, 131.0, 130.7, 128.5, 124.7, 103.3, 48.0, 47.0, 45.6, 45.2, 38.7, 36.9, 34.9, 33.6, 31.5, 29.3, 26.1, 23.7, 19.8, 19.5, 17.0, 14.5, 13.0; **HRMS**: (ES⁺, *m/z*) [M+H]⁺ calcd. for C₃₀H₃₉O₄, 463.2848; found, 463.2845; **IR**: (ATR, neat, cm^{–1}): 2957 (m), 1703 (s), 1543 (m), 1118 (m); **[α]_D**: +44.2 ° (c = 0.16, CHCl₃, 22 °C) / *reported*: +28.8 ° (c = 0.16, CHCl₃, 20 °C)

Synthesis of rhabdastrellic acid A methyl ester (**S1.4**):



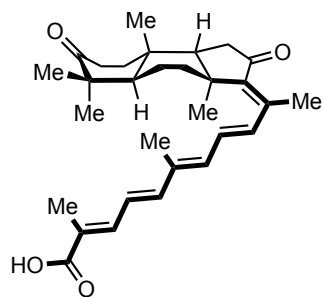
A mixture of triketone **1.158** (5.80 mg, 19.1 µmol, 1.0 equiv.), DMF (1.9 µL, 24.8 µmol, 1.30 equiv.), and CH₂Cl₂ (100 µL) was cooled to 0 °C, and oxalyl bromide (2.15 µL, 22.9 µmol, 1.20 equiv.) was added dropwise, with concurrent gas evolution. The reaction was allowed to warm to ambient temperature while stirring for approximately 2 hours, and then poured into ether and a cold solution of NaHCO₃. The organic layer was separated, dried over anhydrous sodium sulfate and

filtered. Quantitative conversion to a single isomer of vinyl bromide **29** was observed, and this material was used in the next stage directly without additional purification due to instability of the compound on silica gel.

Caution! Product is light-sensitive. All workup and purification procedures were performed with rigorous protection from light, working in a dark room with foil-wrapped, amber glassware.

In a nitrogen-filled glovebox, an amber glass vial was charged with $\text{Pd}_2(\text{dba})_3$ (1.7 mg, 1.9 μmol , 10 mol%), and Ph_3As (1.8 mg, 5.7 μmol , 30 mol%). The vial was placed under an atmosphere of argon, and 100 μL of NMP (degassed under nitrogen by 5 freeze-pump-thaw cycles) was added, and the solution was stirred for 5 minutes at room temperature. A solution of crude vinyl bromide (7.0 mg, 19 μmol , 1.0 equiv.) in 100 μL of NMP was added at room temperature, and stirred for ten minutes. At this time, the vessel was shielded from all possible sources of light, and a solution of stannane **1.205** (14 mg, 29 μmol , 1.5 equiv.) in 100 μL of NMP was added, and the reaction was heated to 70 $^\circ\text{C}$. After two hours, the reaction was cooled to room temperature, 300 μL of saturated KF solution was added. The reaction was stirred at room temperature for 30 minutes, after which it was extracted with Et_2O ($3 \times 5 \text{ mL}$). The combined organic extracts were washed with water (10 mL), washed with KF (aq. sat. 10 mL), dried with MgSO_4 , and concentrated *in vacuo*. The methyl ester **S7** was purified by preparative TLC, with two developments in a hexanes : $\text{EtOAc} = 2:1$, the desired compound eluting as the bottom bright yellow bands easily visible to the eye. This band was scraped off of the silica, stirred in EtOAc for 40 minutes, filtered, rinsed again with EtOAc , and concentrated *in vacuo*. Methyl ester **S1.4** was obtained as a bright yellow oil (4.0 mg, 45%), in an 8:1 mixture with stelletin E methyl ester. These diastereomers were separated for characterization by reverse phase preparative HPLC (Kinetex[®] 5 μm Biphenyl 100 Å LC Column 250 x 10 mm, 5 mL/min, $\text{MeCN} : \text{H}_2\text{O} = 4:3$, detection at $\lambda=374 \text{ nm}$, $t_R = 30.3 \text{ min}$).

R_f: 0.40 (SiO_2 , hexanes : $\text{EtOAc} = 2:1$); **¹H NMR**: (500 MHz, CDCl_3): δ 7.29 (m, 1H), 7.05 (dd, $J = 15.0, 11.3 \text{ Hz}$, 1H), 6.62 (m, 2H), 6.39 (d, $J = 11.4 \text{ Hz}$, 1H), 3.78 (s, 3H), 2.74 (m, 1H), 2.42 (m, 1H), 2.35 (s, 3H), 2.23 (m, 2H), 2.21-2.14 (m, 2H), 2.04 (s, 3H), 2.02 (s, 3H), 1.88 (m, 1H), 1.71-1.61 (m, 3H), 1.57-1.49 (m, 2H), 1.44 (s, 3H), 1.13 (s, 3H), 1.06 (s, 3H), 0.86 (s, 3H); **¹³C NMR**: (126 MHz, CDCl_3): δ 219.3, 207.2, 169.0, 146.7, 143.4, 141.9, 138.8, 138.7, 135.1, 134.4, 132.1, 127.5, 125.0, 52.1, 48.0, 47.0, 45.6, 45.2, 38.6, 36.9, 34.9, 33.6, 31.5, 29.4, 26.1, 23.6, 19.9, 19.5, 14.7, 13.2, 13.1; **HRMS**: (ES^+ , m/z) $[\text{M}+\text{H}]^+$ calcd. for $\text{C}_{31}\text{H}_{43}\text{O}_4$, 479.3161; found, 479.3159.; **IR**: (ATR, neat, cm^{-1}): 2948 (br), 1702 (s), 1616 (w), 1576 (m), 1266 (m), 1231 (s), 1126 (m)

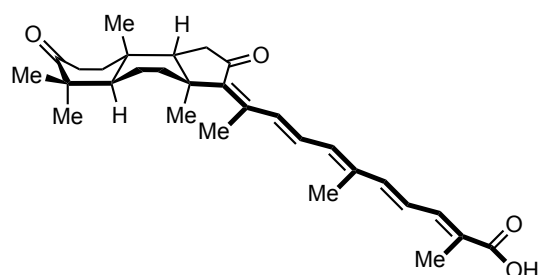


Synthesis of rhabdastrellic acid A (**1.3**):

Caution! Product is light-sensitive. Isomerization into thermodynamic mixture of isomers (**1.3**:**1.4** = 1.9:1) occurs within several hours upon exposure to ambient light, decomposition observed within 24 h. All workup and purification procedures were performed with rigorous protection from light, working in a dark room with foil-wrapped, amber glassware. Product is thermally stable.

A mixture of methyl ester **S1.4** (13.0 mg, 27.2 μmol , 1.0 equiv.), trimethyltin hydroxide (24.6 mg, 136.0 μmol , 5.0 equiv.), in DCE (0.4 mL) was heated to 75 $^{\circ}\text{C}$. Two additional portions of trimethyltin hydroxide (24.6 mg, 136.0 μmol , 5.0 equiv.) were added with 12 hours interval. After 36 hours, full conversion was observed by TLC. The resulting suspension was cooled to ambient temperature, partitioned between CH_2Cl_2 (8 mL) and 1 M HCl (8 mL). Organic layer was separated, washed with 1 M HCl (3×5 mL), dried over Na_2SO_4 and concentrated *in vacuo*. Resulting mixture was purified by flash chromatography (SiO_2 , hexanes : EtOAc = 3:1) that allowed for isolation of rhabdastrellic acid A (**1.3**) (12.3 mg, 26.5 μmol , 98%) as yellow solid. Material was further purified by reverse phase preparative HPLC (Kinetex[®] 5 μm Biphenyl 100 \AA LC Column 250 x 10 mm, 4.02 mL/min, MeCN : H_2O = 1.15:1, detection at $\lambda=374$ nm, $t_R = 22.0$ min).

R_f: 0.27 (SiO_2 , hexanes : EtOAc = 1:1); **¹H NMR**: (500 MHz, CDCl_3): δ 7.39 (dt, $J = 9.0, 1.6$ Hz, 1H), 7.05 (dd, $J = 15.0, 11.5$ Hz, 1H), 6.75 (d, $J = 15.0$ Hz, 1H), 6.64 (m, 2H), 6.42 (d, $J = 11.5$ Hz, 1H), 2.74 (ddd, $J = 16.0, 11.9, 5.8$ Hz, 1H), 2.42 (dd, $J = 9.8, 3.0$ Hz, 1H), 2.39 (m, 1H), 2.35 (s, 3H), 2.24 (m, 2H), 2.20 (m, 2H), 2.16 (m, 1H), 2.05 (s, 3H), 2.03 (s, 3H), 1.88 (dd, $J = 12.0, 10.2$ Hz, 1H), 1.63 (m, 1H), 1.53 (m, 2H), 1.44 (s, 3H), 1.13 (s, 3H), 1.06 (s, 3H), 0.86 (s, 3H); **¹³C NMR**: (126 MHz, CDCl_3): δ 219.3, 207.2, 171.8, 146.9, 144.4, 141.8, 140.6, 138.6, 135.7, 134.8, 132.0, 126.3, 124.8, 48.0, 47.0, 45.6, 45.2, 38.7, 36.8, 34.9, 33.6, 31.5, 29.4, 26.1, 23.6, 19.9, 19.5, 14.7, 13.2, 12.9; **HRMS**: (ES⁺, m/z) [$\text{M}+\text{H}$]⁺ calcd. for $\text{C}_{30}\text{H}_{41}\text{O}_4$, 465.3005; found, 465.3012.; **IR**: (ATR, neat, cm^{-1}): 2950 (m), 1690 (s), 1167 (w)



Synthesis of stelletin E (1.4):

Rhabdastrellic acid A (**1.3**) (8.6 mg, 19.0 μmol , 1.0 equiv.) was dissolved in MeCN (7.5 mL, 0.025 M). Resulting yellow solution was irradiated with ultra violet LED (395–405 nm range) for 3 min and isomers were separated by reverse phase preparative HPLC as above to yield stelletin E (**1.4**) (2.8 mg, 6.0 μmol ,

33%) The recovered rhabdastrellic acid A (**1.3**) (5.4 mg, 12.0 μmol , 63%) was recycled. Overall, stelletin E (**1.4**) can be obtained from **S1.4** after hydrolysis and two cycles of photoisomerization in 53% isolated yield.

R_f: 0.27 (SiO₂, hexanes : EtOAc = 1:1); **¹H NMR**: (750 MHz, CDCl₃): δ 8.15 (d, J = 15.2 Hz, 1H), 7.39 (dd, J = 11.3, 1.8 Hz, 1H), 6.99 (dd, J = 15.2, 11.3 Hz, 1H), 6.68 (d, J = 15.0 Hz, 1H), 6.57 (dd, J = 15.0, 11.5 Hz, 1H), 6.48 (d, J = 11.5 Hz, 1H), 2.73 (ddd, J = 16.8, 12.0, 5.9 Hz, 1H), 2.38 (d, J = 13.4 Hz, 1H), 2.37 (m, 1H), 2.24 (m, 2H), 2.18 (dd, J = 13.6, 8.4 Hz, 1H), 2.16 (dd, J = 13.2, 12.4 Hz, 1H), 2.09 (m, 1H), 2.05 (s, 3H), 2.01 (s, 3H), 2.00 (s, 3H), 1.88 (dd, J = 12.5, 9.7 Hz, 1H), 1.61 (dd, J = 13.7, 8.4 Hz, 1H), 1.52 (m, 1H), 1.50 (ddd, J = 13.2, 9.9, 5.9 Hz, 1H), 1.40 (s, 3H), 1.11 (s, 3H), 1.05 (s, 3H), 0.85 (s, 3H); **¹³C NMR**: (126 MHz, CDCl₃): δ 219.2, 206.2, 171.4, 146.3, 144.9, 142.6, 140.9, 138.0, 136.5, 135.0, 130.6, 125.6, 124.1, 48.1, 47.0, 45.5, 45.1, 37.3, 37.0, 34.9, 33.6, 31.5, 29.4, 24.8, 23.6, 19.8, 19.5, 16.1, 13.1, 12.8; **HRMS**: (ES⁺, m/z) [M+H]⁺ calcd. for C₃₀H₄₁O₄, 465.3005; found, 465.3005.; **IR**: (ATR, neat, cm⁻¹): 2957 (m), 1688 (s), 1244 (w), 1174 (m)

1.6 Acknowledgment of Contributions

S. A. Shved performed computational studies (*i.e.* conformational analysis, thermochemistry calculations, ¹³C NMR prediction, optimization of geometries, *etc.*). S. A. Shved and Y. D. Boyko performed HTE optimization of Suzuki coupling. S. A. Shved wrote the code to extract the data and facilitate analysis of HTE. C. J. Huck explored the Nazarov transform for the annulation strategy, implemented aza-alkene chemistry into the synthetic route, completed the synthesis of the side-chain for rhabdasterlic acid A and optimized the Stille cross-coupling. C. Yang carried out initial experiments with anhydrous Suzuki conditions and completed the synthesis of the side-chain for stelleferin riboside. S. Ning optimized synthesis of the side-chain for stelletin A and assessed the substrate scope for divergent functionalization of 1,3-diketones. T.

Chu and Y. D. Boyko explored scope of interrupted Rautenstrauch cycloisomerization with formation of quaternary stereocenters. The design of retrosynthesis, project planning, the rest of synthetic work and analysis of the results described herein was conducted by Y. D. Boyko.

1.7 References

1. Y. D. Boyko, C. J. Huck, D. Sarlah, *J. Am. Chem. Soc.* **2019**, *141*, 14131–14135.
2. Y. D. Boyko, C. J. Huck, S. Ning, A. S. Shved, C. Yang, T. Chu, E. J. Tonogai, P. J. Hergenrother, D. Sarlah, *J. Am. Chem. Soc.* **2021**, *accepted*.
3. A. R. Carroll, B. R. Copp, R. A. Davis, R. A. Keyzers, M. R. Prinsep, *Nat. Prod. Rep.*, **2020**, *37*, 175–223.
4. S. S. Ebada, W. Lin, P. Proksch, *Mar. Drugs* **2010**, *8*, 313–346.
5. N. G. M. Gomes, R. Dasari, S. Chandra, R. Kiss, A. Kornienko, *Mar. Drugs* **2016**, *14*, 98–136.
6. M. Essack, V. B. Bajic, J. C. Archer, *Mar. Drugs* **2011**, *9*, 1580–1606.
7. V. Domingo, J. F. Arteaga, J. F. del Moral, A. F. Barrero, *Nat. Prod. Rep.* **2009**, *26*, 115–134.
8. W. K. Liu, F. W. K. Cheung, C.-T. Che, *J. Nat. Prod.* **2006**, *69*, 934–937.
9. D. Tasdemir, G. C. Mangalindan, G. P. Concepcion, S. M. Verbitski, S. Rabindran, M. Miranda, M. Greenstein, J. N. A. Hooper, M. K. Harper, C. M. Ireland, *J. Nat. Prod.* **2002**, *65*, 210–214.
10. J. Guo, J. Zhou, Y. Zhang, R. Deng, J. Liu, G. Feng, Z. Liu, D. Xiao, S. Deng, X. Zhu, *Cell Biol. Int.* **2008**, *32*, 48–54.
11. S.-A. Tang, Q. Zhou, W.-Z. Guo, Y. Qiu, R. Wang, M. Jin, W. Zhang, K. Li, T. Yamori, S. Dan, D. Kong, *Mar. Drugs* **2014**, *12*, 4200–4213.
12. R. Wang, Q. Zhang, X. Peng, C. Zhou, Y. Zhong, X. Chen, Y. Qiu, M. Jin, M. Gong, D. Kong, *Sci. Rep.* **2016**, *6*, 27071.
13. F. Raeppe, J.-M. Weibel, D. Heissler, *D. Tetrahedron Lett.* **1999**, *40*, 6377–6381.
14. F. Raeppe, D. Heissler, *D. Tetrahedron Lett.* **2003**, *44*, 3487–3488.
15. K. E. Rosner, Approaches to the Synthesis of Stelliferin, a Marine Isomalabaricane Triterpene. PhD Dissertation, MIT, 1996.
16. M. H. Fisher, Efforts towards the Synthesis of Stelliferin Natural Products. MS

Dissertation, MIT, 1997.

17. A. Chawla, S. Dev, *Tetrahedron Lett.* **1967**, 8, 4837–4843.
18. B. Sontag, R. Fröde, M. Bross, W. Steglich, *Eur. J. Org. Chem.* **1999**, 1999, 255–260.
19. Q. Xiong, F. Rocco, W. K. Wilson, R. Xu, M. Ceruti, S. P. T. Matsuda, *J. Org. Chem.* **2005**, 70, 5362–5375.
20. S. Lodeiro, W. K. Wilson, H. Shan, S. P. T. Matsuda, *Org. Lett.* **2006**, 8, 439–442.
21. T. Xiang, M. Shibuya, Y. Katsube, T. Tsutsumi, M. Otsuka, H. Zhang, K. Masuda, Y. Ebizuka, *Org. Lett.* **2006**, 8, 2835–2838.
22. M. D. Kolesnikova, A. C. Obermeyer, W. K. Wilson, D. A. Lynch, Q. Xiong, S. P. T. Matsuda, *Org. Lett.* **2007**, 9, 2183–2186.
23. G. C. Fazio, R. Xu, S. P. T. Matsuda, *J. Am. Chem. Soc.* **2004**, 126, 5678–5679.
24. S. Lodeiro, Q. Xiong, W. K. Wilson, M. D. Kolesnikova, C. S. Onak, S. P. T. Matsuda, *J. Am. Chem. Soc.* **2007**, 129, 11213–11222.
25. S. F. Kouam, A. W. Ngouonpe M. Lamshöft, F. M. Talontsi J. O. Bauer, C. Strohmann, B. T. Ngadjui, H. Laatsch, M. Spiteller, *Phytochemistry* **2014**, 105, 52–59.
26. H. Shigemori, H. Komaki, K. Yazawa, Y. Mikami, A. Nemoto, Y. Tanaka, T. Sasaki, Y. In, T. Ishida, J. Kobayashi, *J. Org. Chem.* **1998**, 63, 6900–6904.
27. W. O. Godtfredsen, W. Daehne, S. Angedal, A. Marquet, D. Arigoni, A. Melera, *Tetrahedron* **1965**, 12, 3505–3530.
28. R. E. Ireland, P. Beslin, R. Giger, U. Hengartner, H. A. Kirst, H. Maag, *J. Org. Chem.* **1977**, 42, 1267–1276.
29. F. Yoshimura, R. Itoh, Torizuka, K. Tanino, *Angew. Chem. Int. Ed.* **2018**, 57, 17161–17167.
30. R. E. Ireland, R. Giger, S. Kamata, *S. J. Org. Chem.* **1977**, 42, 1276–1282.
31. W. G. Dauben, C. R. Kessel, M. Kishi, M. Somei, M. Tada, D. Guillermin, *J. Am. Chem. Soc.* **1982**, 104, 303–305.
32. R. H. Peters, D. M. Yasuda, M. Tanabe, *Tetrahedron Lett.* **1977**, 18, 1481–1484.
33. G. Berube, P. Deslongchamps, *Tetrahedron Lett.* **1987**, 28, 5255–5258.
34. V. P. Fish, A. R. Sudhakar, W. S. Johnson, *Tetrahedron Lett.* **1993**, 34, 7849–7852.
35. M. Taton, P. Benveniste, A. Rahier, W. S. Johnson, H. T. Liu, A. R. Sudhakar,

- Biochemistry* **1992**, *31*, 7892–7898.
36. D. Guay, W. S. Johnson, U. Schubert, *J. Org. Chem.* **1989**, *54*, 4731–4732.
 37. R. Schmid, P. L. Huesmann, W. S. Johnson, *J. Am. Chem. Soc.* **1980**, *102*, 5122–5123.
 38. A. E. Jense, P. Knochel, Nickel-Catalyzed Cross-Coupling between Functionalized Primary or Secondary Alkylzinc Halides and Primary Alkyl Halides *J. Org. Chem.* **2002**, *67*, 79–85.
 39. C. K. Reddy, P. Knochel New Cobalt- and Iron-Catalyzed Reactions of Organozinc compounds *Angew. Chem. Int. Ed.* **1996**, *35*, 1700–1701.
 40. J. Zhou, G. C. Fu Palladium-Catalyzed Negishi Cross-Coupling Reactions of Unactivated Alkyl Iodides, Bromides, Chlorides, and Tosylates *J. Am. Chem. Soc.* **2003**, *125*, 12527–12530.
 41. J. Zhou, G. C. Fu Cross-Couplings of Unactivated Secondary Alkyl Halides: Room-Temperature Nickel-Catalyzed Negishi Reactions of Alkyl Bromides and Iodides *J. Am. Chem. Soc.* **2003**, *125*, 14726–14727.
 42. S. Son, G. C. Fu Nickel-Catalyzed Asymmetric Negishi Cross-Couplings of Secondary Allylic Chlorides with Alkylzincs *J. Am. Chem. Soc.* **2008**, *130*, 2756–2757.
 43. A. Fernández-Mateos, H. P. Teijón, R. R. Clemente, R. R. González, F. S. González Stereoselective Radical Cascade Cyclizations of Unsaturated Epoxynitriles: Quadruple Radical Cyclization Terminated by a 4-exo Process onto Nitrile *Synlett* **2007**, *17*, 2718–2722
 44. C. P. Ting, G. Xu, X. Zeng, T. J. Maimone Annulative Methods Enable a Total Synthesis of the Complex Meroterpene Berkeleyone A *J. Am. Chem. Soc.* **2016**, *138*, 14868–14871.
 45. J. F. Arteaga, V. Domingo, J. F. Quílez, A. F. Barrero, *Org. Lett.* **2008**, *10*, 1723–1726.
 46. E. J. Corey, M. C. Noe, S. Lin *Tetrahedron Lett.* **1995**, *36*, 8741–8744.
 47. E. J. Corey, J. Zhang, *Org. Lett.* **2001**, *3*, 3211–3214
 48. R. M. McFadden, B. M. Stoltz *J. Am. Chem. Soc.* **2006**, *128*, 7738–7739.
 49. Various solvents, palladium and copper sources were screened. While satisfactory results most likely could be obtained at oxygen pressure above 1 bar, such experiment was not conducted.
 50. J. A. Malona, J. M. Colbourne, A. J. Frontier, *Org. Lett.* **2006**, *8*, 5661–5664.
 51. W. L. Ashley, E. L. Timpy, T. C. Coombs, *J. Org. Chem.* **2018**, *83*, 2516–2529.

52. A. J. Burckle, B. Gál, F. J. Seidl, V. H. Vasilev, N. Z. Burns, *J. Am. Chem. Soc.* **2017**, *139*, 13562–13569.
53. M. E. Jung, B. A. Duclos, *Tetrahedron* **2006**, *62*, 9321–9334.
54. Aldehyde **1.71** was obtained from the known alcohol by oxidation using BaMnO₄. See details in the experimental section.
55. C. C. Nawrat, C. R. Jamison, Yu. Slutskyy, D. W. C. MacMillan, L. E. Overman, *J. Am. Chem. Soc.* **2015**, *137*, 11270–11273.
56. D. F. Taber, B. P. Gunn, *J. Org. Chem.* **1979**, *44*, 450–452. (b)
57. M. L. Trudell, D. Soerens, R. W. Weber, L. Hutchins, D. Grubisha, D. Bennett, J. M. Cook, *Tetrahedron* **1992**, *48*, 1805–1822.
58. H. Taguchi, S. Tanaka, H. Yamamoto, H. Nozaki, *Tetrahedron Lett.* **1973**, *14*, 2465–2468
59. D. H. Dethe, S. K. Sau, S. Mahapatra, *Org. Lett.* **2016**, *18*, 6392–6395.
60. V. K. Aggarwal, P. A. Bethel, R. Giles, *J. Chem. Soc., Perkin Trans. 1*, **1999**, 3315–3321.
61. Basic Al₂O₃ was identified as the most optimal absorbent. However, no more than 1 gram should be purified at a time in order to achieve high isolation yields and avoid isomerization/decomposition.
62. G. H. L. Nefkens, J. W. J. F. Thuring, B. Zwanenburg, *Synthesis* **1997**, *3*, 290–292.
63. J. C. Lo, Y. Yabe, P. S. Baran, *J. Am. Chem. Soc.* **2014**, *136*, 1304–1307
64. V. Rautenstrauch, *J. Org. Chem.* **1984**, *49*, 950–952.
65. X. Shi, D. J. Gorin, F. D. Toste, *J. Am. Chem. Soc.* **2005**, *127*, 5802–5803.
66. P. A. Caruana, A. J. Frontier, *Tetrahedron* **2007**, *63*, 10646–10656.
67. B. A. B. Prasad, F. K. Yoshimoto, R. Sarpong, *J. Am. Chem. Soc.* **2005**, *127*, 12468–12469.
68. W. Zi, H. Wu, F. D. Toste, *J. Am. Chem. Soc.* **2015**, *137*, 3225–3228.
69. O. N. Faza, C. S. Lopez, R. Alvarez, A. R. de Lera, *J. Am. Chem. Soc.* **2006**, *128*, 2434–2437.
70. K. Sakurai, K. Tanino, *Tetrahedron Lett.* **2015**, *56*, 496–499.
71. Y.-W. Huang, K. Kong, J. L. Wood, *Angew. Chem. Int. Ed.* **2018**, *57*, 7664–7667.
72. A. Furstner, A. Schlecker, *Chem. Eur. J.* **2008**, *14*, 9181–9191.
73. M. Brandstätter, M. Freis, N. Huwyler, E.M. Carreira, *Angew. Chem. Int. Ed.* **2019**, *58*, 2490–2494.
74. C. Bürki, A. Whyte, S. Arndt, A. S. K. Hashmi, M. Lautens, *Org. Lett.* **2016**, *18*, 5058–

- 5061.
75. For more data regarding effect of catalyst structure on diastereoselectivity see section 2.3.4.
 76. C. R. Johnson, R. K. Raheja, *J. Org. Chem.* **1994**, *59*, 2287–2288.
 77. B. A. Baker, Ž. V. Bošković, B. H. Lupshutz, *Org. Lett.* **2008**, *10*, 289–292.
 78. T. Tsuda, T. Hayashi, H. Satomi, T. Kawamoto, T. Saegusa, *J. Org. Chem.* **1986**, *51*, 537–540.
 79. C. Riplinger, B. Sandhoefer, A. Hansen, F. Neese, *J. Chem. Phys.* **2013**, *139*, 134101.
 80. D. G. Liakos, F. Neese, *J. Chem. Theory Comput.* **2015**, *11*, 4054–4063.
 81. D. W. Rogers, Y. Zhao, M. Traetteberg, M. Hulce, J. Liebman, *J. Chem. Thermodyn.* **1998**, *30*, 1393–1400.
 82. D. A. Evans, M. M. Morrissey, *J. Am. Chem. Soc.* **1984**, *106*, 3866–3868.
 83. R. H. Crabtree, M. W. Davis, *J. Org. Chem.* **1986**, *51*, 2655–2661.
 84. M. R. Friedfeld, G. W. Margulieux, B. A. Schaefer, P. J. Chirik, *J. Am. Chem. Soc.* **2014**, *136*, 13178–13181.
 85. T. Inoue, T. Mukaiyama *Bull. Chem. Soc. Jpn.* **1980**, *53*, 174–178.
 86. D. A. Evans, J. V. Nelson, E. Vogel, T. R. Taber, *J. Am. Chem. Soc.* **1981**, *103*, 3099–3111.
 87. S. Grimme, J. G. Brandenburg, C. Bannwarth, A. Hansen, *J. Chem. Phys.* **2015**, *143*, 054107.
 88. B. M. Trost, M. T. Rudd, *Org. Lett.* **2003**, *5*, 1467–1470.
 89. T. J. Maimone, J. Shi, S. Ashida, P. S. Baran, *J. Am. Chem. Soc.* **2009** *131*, 17066–17067.
 90. S. E. Denmark, D. C. Forbes, *Tetrahedron Lett.* **1992**, *33*, 5037–5040.
 91. M. P. Sibi, J. W. Christensen, *Tetrahedron Lett.* **1995**, *36*, 6213–6216.
 92. C. Iwata, K. Miyashita, Y. Ida, M. Yamada *J. Chem. Soc., Chem. Commun.* **1981**, 461–463.
 93. C. Iwata, K. Murakami, O. Okuda, T. Morie, N. Maezaki, H. Yamashita, T. Kuroda, T. Imanishi, T. Tanaka, *Chem. Pharm. Bull.* **1993**, *41*, 1900–1905.
 94. X. Zhu, C. C. McAtee, C. S. Schindler, *J. Am. Chem. Soc.* **2019**, *141*, 3409–3413.
 95. To the best of our knowledge there was only one example of presumably directed HAT reported: C. S. Schindler, C. R. J. Stephenson, E. M. Carreira, *Angew. Chem. Int. Ed.* **2008**,

- 47, 8852–8855.
96. C. Obradors, R. M. Martinez, R. A. Shenvi, *J. Am. Chem. Soc.* **2016**, *138*, 4962–4971.
 97. R. O. Hutchins, C. A. Milewski, B. E. Maryanoff, *J. Am. Chem. Soc.* **1973**, *95*, 3662–3668.
 98. G. W. Kabalka, D. T. C. Yang, J. D. Baker, Jr., *J. Org. Chem.* **1976**, *41*, 574–575.
 99. A. Jabbari, E. J. Sorensen, K. N. Houk, *Org. Lett.*, **2006**, *8*, 3105–3107.
 100. G. Saielli, K. C. Nicolaou, A. Ortiz, H. Zhang, A. Bagno, *J. Am. Chem. Soc.* **2011**, *133*, 6072–6077
 101. M. W. Lodewyk, M. R. Siebert, D. J. Tantillo, *Chem. Rev.* **2012**, *112*, 1839–1862.
 102. F. Jensen, *J. Chem. Theory Comput.* **2015**, *11*, 132–138.
 103. V. A. Semenov, L. B. Krivdin, *Magn. Reson. Chem.* **2020**, *58*, 56–64.
 104. F. Neese, Software Update: The ORCA Program System, Version 4.0. *Wiley Interdiscip. Rev. Comput. Mol. Sci.* **2018**, *8*, e1327.
 105. F. Neese, The ORCA Program System. *Wiley Interdiscip. Rev. Comput. Mol. Sci.* **2012**, *2*, 73–78.
 106. G. L. Stoychev, A. A. Auer, F. Neese, *J. Chem. Theory Comput.* **2018**, *14*, 4756–4771.
 107. D. F. Taber, Q. Jiang, B. Chen, W. Zhang, C. L. Campbell, *J. Org. Chem.* **2002**, *67*, 4821–4827.
 108. V. J. Olsson, K. J. Szabó, *J. Org. Chem.* **2009**, *74*, 7715–7723.
 109. H. P. Deng, L. Eriksson, K. J. Szabó, *Chem. Commun.* **2014**, *50*, 9207–9210.
 110. Z.-L. Tao, X.-H. Li, Z.-Y. Han, L.-Z. Gong, *J. Am. Chem. Soc.* **2015**, *137*, 4054–4057.
 111. A. J. Catino, R. E. Forslund, M. P. Doyle, *J. Am. Chem. Soc.* **2004**, *126*, 13622–13623.
 112. T. K. M. Shing, P. L. Su, *Org. Lett.* **2006**, *8*, 3149–3151.
 113. W. G. Salmond, M. A. Barta, J. L. Havens, *J. Org. Chem.*, **1978**, *43*, 2057–2059.
 114. M. A. Umbreit, K. B. Sharpless, *J. Am. Chem. Soc.* **1977**, *99*, 5526–5528.
 115. M. F. Lipton, R. H. Shapiro, *J. Org. Chem.*, **1978**, *43*, 1409–1413.
 116. R.-A. F. Rarig, M. Scheideman, E. Vedejs, *J. Am. Chem. Soc.* **2008**, *130*, 9182–9183.
 117. A. G. Myers, M. Movassaghi Highly Efficient Methodology for the Reductive Coupling of Aldehyde Tosylhydrazones with Alkylolithium Reagents *J. Am. Chem. Soc.* **1998**, *120*, 8891–8892.
 118. D. A. Evans, A. H. Hoveyda, *J. Org. Chem.* **1990**, *55*, 5190–5192.
 119. S. Sebelius, O. A. Wallner, K. J. Szabó, *Org. Lett.* **2003**, *5*, 3065–3068

120. T. Sakamoto, T. Takahashi, T. Yamazaki, T. Kitazume, *J. Org. Chem.* **1999**, *64*, 9467–9474.
121. M. Kimura, M. Shimizu, S. Tanaka, Y. Tamaru, *Tetrahedron* **2005**, *61*, 3709–3718.
122. O. Jacquet, T. Bergholz, C. Magnier-Bouvier, M. Mellah, R. Guillot, J.-C. Fiaud, *Tetrahedron* **2010**, *66*, 222–226.
123. H. Ito, S. Kunii, M. Sawamura, *Nat. Chem.* **2010**, *2*, 972–976.
124. H. Ito, T. Miya, M. Sawamura, *Tetrahedron* **2012**, *68*, 3423–3427.
125. J. W. J. Kennedy, D. G. Hall, *J. Am. Chem. Soc.* **2002**, *124*, 11586–11587.
126. H. Ito, T. Taguchi, Y. Hanzawa, *Tetrahedron Lett.* **1992**, *33*, 1295–1298.
127. M. Coffinet, F. Jaroschik, J.-L. Vasse, *Eur. J. Org. Chem.* **2016**, *13*, 2319–2327.
128. E.-I. Negishi, N. Okukado, A. O. King, D. E. Van Horn, B. I. Spiegel, *J. Am. Chem. Soc.* **1978**, *100*, 2254–2256.
129. E.-I. Negishi, T. Takahashi, S. Baba, D. E. Van Horn, N. Okukado, *J. Am. Chem. Soc.* **1987**, *109*, 2393–2401.
130. Wipf P., J. H. Smitrovich, *J. Org. Chem.*, **1991**, *56*, 6494–6496.
131. Corresponding alcohol was isolated as mixture of diastereomers after 3 hours of reaction as a sole product.
132. Isomers could be separated; however, it was not necessary as all of them converge into one triketone **1.158**.
133. J. D. More, N. S. Finney, *Org. Lett.* **2002**, *4*, 3001–3003.
134. X. Chen, Y. Zhou, M. Hong, Y. Ling, D. Yin, S. Wang, X. Zhang, W. Rao, *Adv. Synth. Catal.* **2018**, *360*, 3700–3708.
135. R. Yunoki, A. Yajima, T. Taniguchi, H. Ishibashi, *Tetrahedron Lett.* **2013**, *54*, 4102–4105.
136. B. Domínguez, B. Iglesias, A. R. de Lera, *J. Org. Chem.* **1998**, *63*, 4135–4139.
137. C. P. Ting, T. J. Maimone Total Synthesis of Hyperforin *J. Am. Chem. Soc.* **2015**, *137*, 10516–10519.
138. D. T. Hong, F. M. E. Huber, G. Jiménez-Osés, P. Mayer, K. N. Houk, D. Trauner, *Chem. Eur. J.* **2015**, *21*, 13646–13665.
139. Y. Mi, J. V. Schreiber, E. J. Corey, *J. Am. Chem. Soc.* **2002**, *124*, 11290–11291.
140. E. V. Boltukhina, A. E. Sheshenev, I. M. Lyapkalo, *Synthesis* **2011**, *21*, 3507–3515.

141. R. E. Mewshaw, *Tetrahedron Lett.* **1989**, 30, 3753–3756.
142. L. F. Tietze, C. A. Vock, I. K. Krimmelbein, L. Nacke, *Synthesis* **2009**, 12, 2040–2060.
143. T. D. Michels, J. U. Rhee, C. D. Vanderwal, *Org. Lett.* **2008**, 10, 4787–4790.
144. J. Wang, V. Boyarskikh, J. D. Rainier, *Org. Lett.* **2011**, 13, 700–702.
145. A. F. Barrero, J. E. Oltra, M. M. Herrador, E. Cabrera, J. F. Sanchez, J. F. Quilez, F. J. Rojas, J. F. Reyes, *Tetrahedron* **1993**, 49, 141–150.
146. P. Valenta, N. A. Drucker, J. W. Bode, P. J. Walsh, *Org. Lett.* **2009**, 11, 2117–2119.
147. D. M. Hodgson, L. T. Boulton, G. N. Maw, *Tetrahedron* **1995**, 51, 3713–3724.
148. D. S. Matteson, R. J. Moody, P. K. Jesthi, *J. Am. Chem. Soc.* **1975**, 97, 5608–5609.
149. D. S. Matteson, R. J. Moody, *Organometallics* **1982**, 1, 20–28.
150. S. Namirembe, C. Gao, R. P. Wexler, J. P. Morken, *Org. Lett.* **2019**, 21, 4392–4394.
151. J. R. Coombs, L. Zhang, J. P. Morken, *Org. Lett.* **2015**, 17, 1708–1711.
152. B. Domínguez, B. Iglesias, A. R. de Lera, *J. Org. Chem.* **1998**, 63, 4135–4139.
153. V. Farina, B. Krishman, *J. Am. Chem. Soc.* **1991**, 113, 9585–9595.
154. K. C. Nicolaou, A. A. Estrada, M. Zak, S. H. Lee, B. S. Safina, *Angew. Chem., Int. Ed.* **2005**, 44, 1378–1382.
155. J. Y. Su, Y. H. Meng, L. M. Zen, X. Fu, F. J. Schmitz, *J. Nat. Prod.* **1994**, 57, 1450–1451.
156. T. McCabe, J. Clardy, L. Minale, C. Pizza, F. Zollo, R. Riccio, *Tetrahedron Lett.* **1982**, 23, 3307–3310.
157. C. P. Delaney, V. M. Kassel, S. E. Denmark, *ACS Catal.* **2020**, 10, 73–80.
158. T. C. McKee, H. R. Bokesch, J. L. McCormick, M. A. Rashid, D. Spielvogel, K. R. Gustafson, M. M. Alavanja, J. H. Cardellina II, M. R. Boyd, *J. Nat. Prod.* **1997**, 60, 431–438.
159. S.-A. Tang, Q. Zhou, W.-Z. Guo, Y. Qiu, R. Wang, M. Jin, W. Zhang, K. Li, T. Yamori, S. Dan, D. Kong, *Mar. Drugs* **2014**, 12, 4200–4213.
160. R. Wang, Q. Zhang, X. Peng, C. Zhou, Y. Zhong, X. Chen, Y. Qiu, M. Jin, M. Gong, D. Kong, *Sci. Rep.* **2016**, 6, 27071.
161. J. Guo, J. Zhou, Y. Zhang, R. Deng, J. Liu, G. Feng, Z. Liu, D. Xiao, S. Deng, X. Zhu, *Cell Biol. Int.* **2008**, 32, 48–54.

CHAPTER 2. GENERAL BLUEPRINT TOWARDS TERPENOID ARCHITECTURES

2.1 Introduction

Natural product research is vital for drug development. It has been informing the pharmaceutical industry for decades and has led to the development of a plethora of essential small-molecule therapeutics increasing the quality of our lives.¹ Humanity is capable of combating an ever-growing spectrum of various infectious diseases taking inspiration from natural mechanisms of defense. Complexity of naturally-occurring biologically active compounds, minute isolation yields, and non-ideal pharmacokinetic profiles prevent their immediate inclusion into the existent pharmacopeia. However, initial studies directed towards identification of an active pharmacophore and molecular target, structure-activity relationship, and mechanism of action ultimately brings new chemical leads into realm of medicinal chemistry.

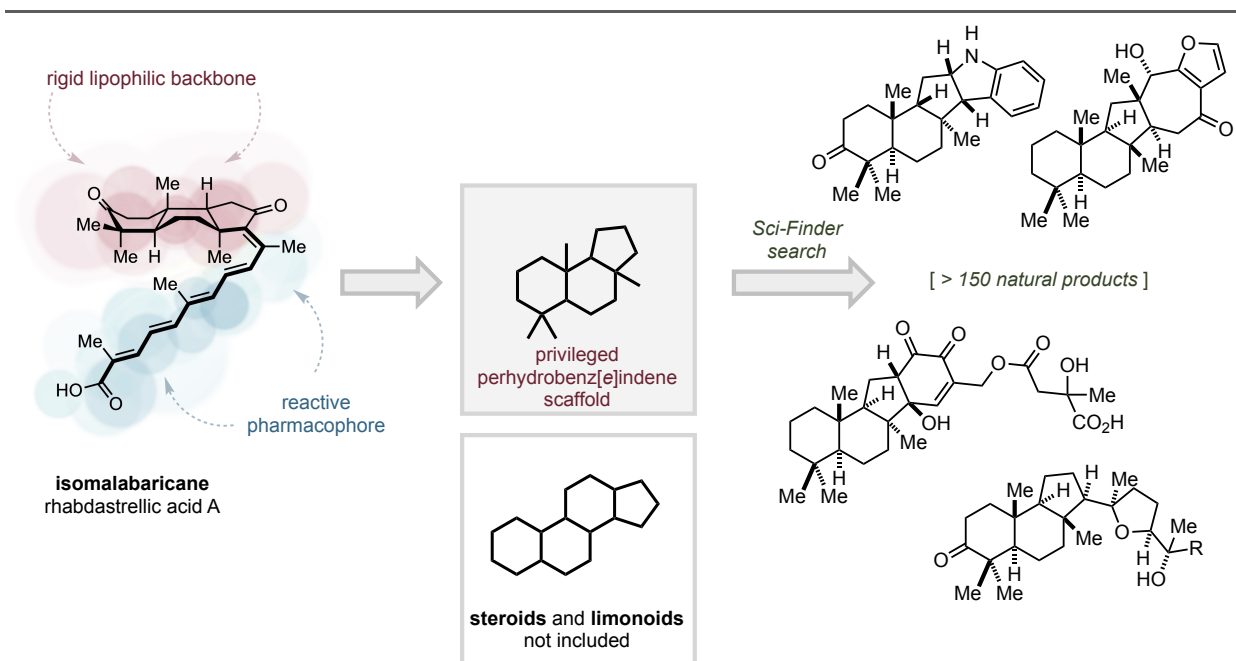


Figure 2.1 Perhydrobenz[e]indene as a privileged scaffold in natural products.

Conceptually, families of natural products are differentiated based on a unified biosynthetic pathway. The result of such a mechanistically close relationship among various members of each family is that they share the same pharmacophore as the most vivid structural feature. Notably, the isolation source and biological activity still may vary significantly for those compounds. Recent total synthesis efforts strive for scalable and practical routes that would allow for diversification

at various stages. This approach enables expedient access to numerous members of a family as well as artificial analogues crucial for further biological investigation and optimization of a potential drug candidate. Thus, developed strategies, albeit flexible in some regard, are usually constrained to a certain class of natural products as they are centered around a key construct, the pharmacophore. However, some structural motifs are highly conserved within naturally occurring compounds more broadly, which at first glance do not bear reactive centers and therefore likely are not involved in key interactions with a target.² Perhaps, the role of such motifs is to provide a rigid backbone which could bring an active pharmacophore into proximity with key amino acid residues within the binding pocket and thereby secure desired interactions. Moreover, these privileged structures are utilized by nature in a broad spectrum of bioactive compounds and therefore their use is neither inherently limited to a certain activity nor to a single class of natural products.

Let us consider isomalabaricane triterpenoids as an example (Figure 2.1). Although detailed studies have yet to be carried out, we surmise that the highly conjugated polyenic structure is a primary pharmacophore. In parallel, the perhydrobenz[*e*]indene tricyclic core is deficient in polar functional groups, and yet bears significant stereochemical information. One might speculate that role of this framework is to offer conformational rigidity to the overall structure and modulate lipophilicity, indirectly increasing its potency *in vivo*. Importantly, search of this substructure in a natural product database returned astonishing results. The perhydrobenz[*e*]indene motif is conserved in more than 150 bioactive terpenoids. Examples of di-, tri-, sesqui- and meroterpenoids all contain this fragment. As expected, analysis of biological activity and isolation source did not reveal any consistent patterns. It is important to also note that this tricyclic system can be encountered in other important natural products such as steroids and limonoids as a part of larger framework. Again, the conveyed principle is observed: various biological activities correlate with polar groups, i.e. primary pharmacophores, whereas the lipophilic core remains conserved throughout the series.

Based on aforementioned observations we formulated a concept of privileged molecular recognition moiety; a structural backbone that is commonly encountered in diverse natural products, the role of which is to induce favorable interactions between pharmacophore and targeting enzyme. A synthetic strategy centered around such a backbone with proper functional handles would enable the synthesis of natural products from different families under unified

approach. From a medicinal chemistry standpoint, mixing and matching of these privileged scaffolds with known pharmacophores might enable the discovery of new chemical leads for drug development programs. To the best of our knowledge this design of retrosynthesis has not been explicitly formulated previously, however its core principle is extensively used in library generation approaches such as “complexity to diversity”.³

With this concept in mind, and a synthetic scheme for isomalabaricanes in hand, we set out to develop general blueprint for the syntheses of diverse natural products, containing the privileged molecular recognition perhydrobenz[*e*]indene core.

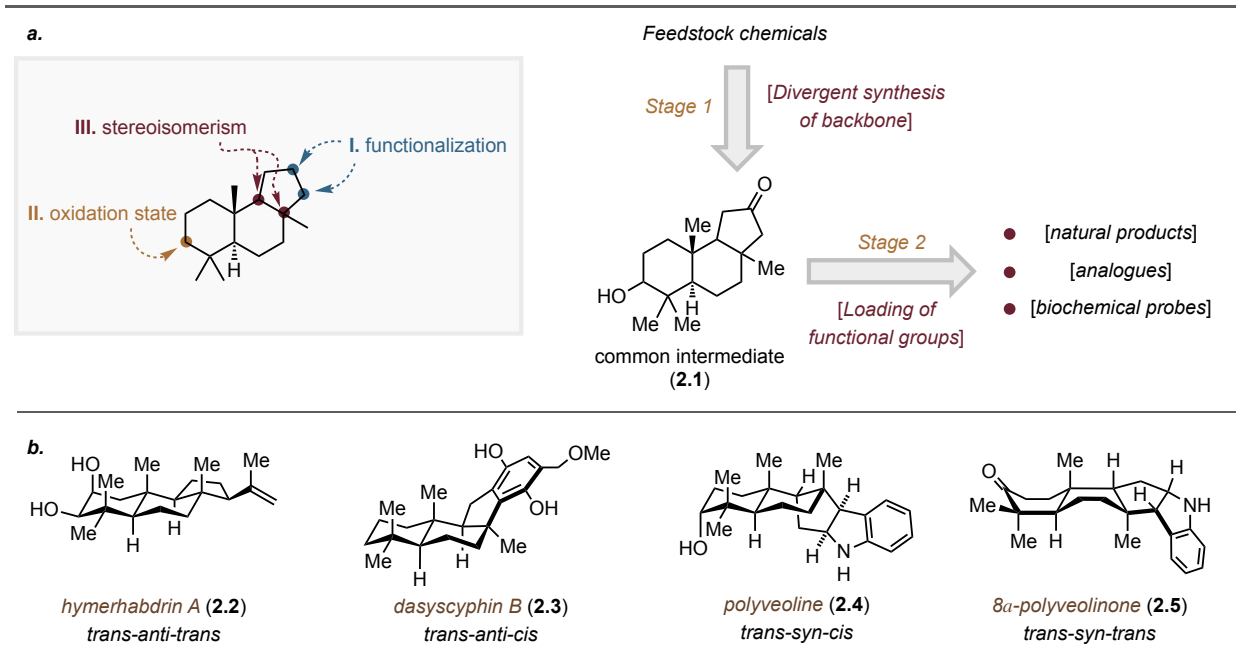


Figure 2.2.a Backbone skeleton oriented approach towards medicinally relevant compounds; **b** Targeted terpenoids.

Structural analysis of terpenoids shown on Figure 2.2.a reveals several points of diversification. The most noticeable feature is decoration of the C-ring of the tricyclic core with various cyclic and alicyclic structural motifs. The oxidation state at C3 can alternate: natural products with ketone, alcohol, and completely reduced methylene are found in nature. Finally, this subset of terpenoids possesses not only structural, but also stereochemical diversity. Four stereocenters embedded into perhydrobenz[*e*]indene core give rise to eight possible diastereomeric structures. The *trans* relationship between A and B rings is conserved across the members as a manifestation of the likely polyene cyclization involved in the biosynthesis of these terpenoids. All four remaining isomeric structures are found in nature. To accomplish the envisioned goal of

a general blueprint, our synthetic strategy must address described points of diversification in programmable fashion, and we decided on a two-stage approach.

First, robust and scalable access to a common intermediate has to be developed. In order to address stereochemical diversity, the synthesis is required to be stereodivergent. Striving for the most practical solution, we aimed to perform stereodetermining steps as late in the synthesis as possible to increase overall efficiency of the route. The second stage includes adjustment of the C3 oxidation state and loading of the active pharmacophore onto the backbone structure. Tricyclic ketone **2.1** was envisioned as a common intermediate as it bears requisite functional handles to rapidly elaborate its core framework into final products. This approach has several benefits from a medicinal chemistry standpoint. Late-stage loading of biologically active warheads simplifies the syntheses of analogues. This in turn enables rapid interrogation of the system, identification of mode of action, and optimization of the structure for further drug development if a promising hit is identified. Use of a common intermediate eliminates the need to redesign initial steps of the synthesis for this purpose. Finally, the stereodivergence of the route unlocks stereoisomers typically inaccessible using conventional tactics. This tool might help to elucidate the importance of configuration for the backbone structure and its overall role. To demonstrate the power and versatility of the route we targeted four different terpenoids (Figure 2.2.b): diterpenoid hymerhabdrin A (**2.2**, *trans-anti-trans* junction), meroterpenoid dasyscyphin B (**2.3**, *trans-anti-cis* junction), indolosesquiterpene polyveoline (**2.4**, *trans-syn-cis* junction) and its congener 8 α -polyveolinone (**2.5**, *trans-syn-trans* junction).⁴⁻⁷ Such selection was made based on structural diversity considerations: this set encompasses all three oxidation states at C3, all four diastereomeric core scaffolds, and different types of C-ring decoration. Moreover, these molecules possess important biological activities and three out of four have not been previously synthesized.⁸

2.2 Background

Since our blueprint will cover the space of perhydrobenz[*e*]indene natural products, it is important to discuss previous approaches to these targets. The main focus will be on techniques that were utilized in the literature to establish the key stereocenters of the tricyclic motif and their inherent constraints.

The *trans-anti-trans* configured tricyclic core is perhaps the most prevalent isomer among perhydrobenz[*e*]indene natural products (Chart 2.1). This observation, however, has a plausible explanation. Such a stereochemical relationship is produced by polyene cyclization ubiquities in

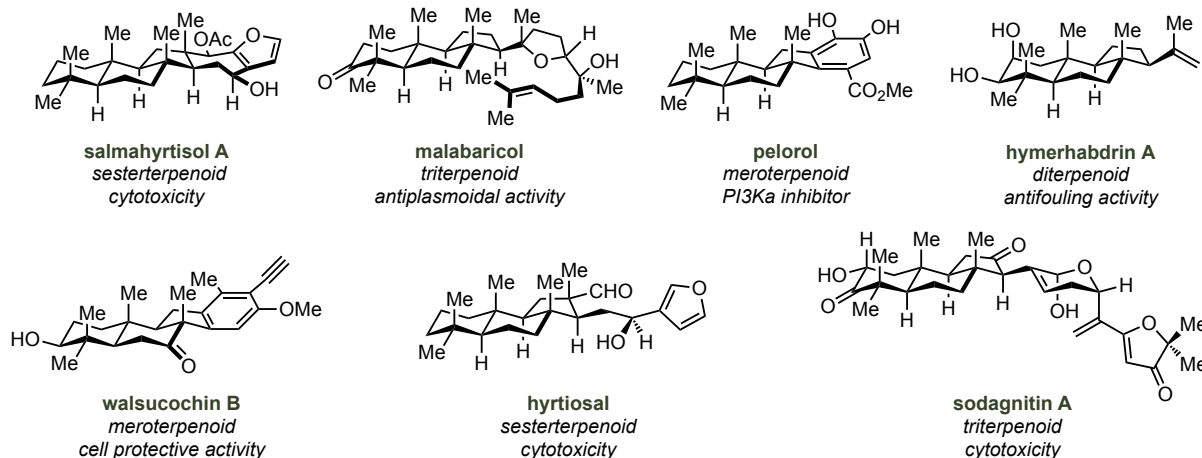
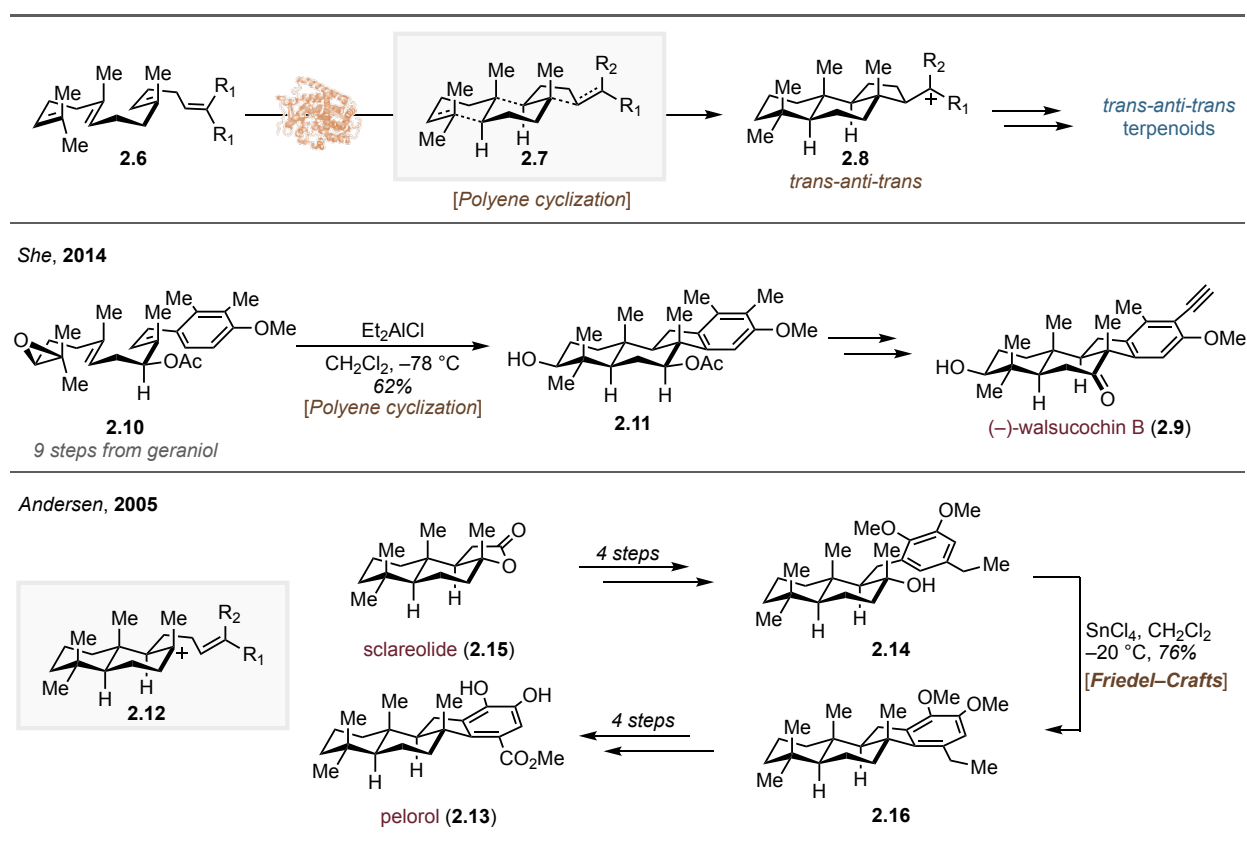


Chart 2.1 Perhydrobenz[*e*]indene natural products with *trans-anti-trans* configuration.

terpenoid biogenesis (Scheme 2.1). It has been long established that the cyclization typically favors chair-chair transition state **2.7**, albeit with some exceptions such as lanosterol synthase (see p. 3). Biosynthetic origins of these natural products correspondingly pave the path for their total synthesis. Indeed, polyene cyclization is among the most efficient ways to access *trans-anti-trans* fused tricycles due to the expedient generation of complexity that can be reproduced in the flask without use of elaborate enzymes.^{9,10} For example (–)-walsucochin B (**2.9**), a meroterpenoid with cell protective properties, was synthesized through this powerful disconnection.¹⁰ Linear precursor **2.10**, containing an epoxide as an initiating motif, was subjected to Lewis acid mediated cyclization. Three C–C bonds and four stereocenters were formed in a single step, affording product **2.11** in 62% yield. Compound **2.11** was readily elaborated to the natural product **2.9**.

Generation of the carbocation **2.12** can be considered as a descendant of the biomimetic approach (Scheme 2.1). While **2.12** is not a true intermediate in the polyene cyclization, its chemical behavior is expected to be similar. Indeed, this strategy was proven to be viable by Andersen and co-workers in a total synthesis of sponge meroterpenoid pelorol (**2.13**).¹¹ First, carbocation precursor, tertiary alcohol **2.14**, was synthesized. The authors chose a semisynthetic approach using (+)-sclareolide (**2.15**) as starting material over *de novo* synthesis. Upon treatment of **2.14** with strong Lewis acid, intramolecular Fridel–Crafts cyclization occurred. Notably, *trans-anti-trans* product **2.16** was obtained with exclusive diastereoselectivity. At this point only few

chemical manipulations were required to complete the total synthesis of pelorol (**2.13**). Overall, these discussed tactics point out the ease with which the *trans-anti-trans* core can be assembled. Thus, elaboration and decoration of the tricyclic architecture, rather than its construction, is efficiency-limiting, which has led to quite lengthy linear sequences of steps in some cases.⁸ Moreover, it is worthwhile to mention that the devised strategies are not amenable to production of any other diastereomers, and therefore could not be used as a backbone of the general blueprint for synthesis of perhydrobenz[*e*]indene terpenoids.



Scheme 2.1 Previous studies on *trans-anti-trans* configured perhydrobenz[*e*]indene natural products.

The *trans-anti-cis* configuration of the perhydrobenz[*e*]indene core is not as prevalent in nature as *trans-anti-trans* diastereomer. This motif has been found only in cytotoxic merosquiterpenoids isolated from *Dasyscyphus niveus* (Chart 2.2).⁵ The *Cis*-junction of the five-membered ring within the tricycle renders a standard chemical toolbox pertinent for its construction from substituted bicyclic drimane-like scaffolds (Scheme 2.2). For example, Alvarez-Manzaneda and co-workers completed a semisynthesis of akaol (**2.17**) employing trivial intramolecular aldol condensation to establish the *trans-anti-cis* configuration.¹² First, aldehyde **2.18** was synthesized from (–)-sclareol (**2.19**) in seven steps. Then **2.18** was converted into enone

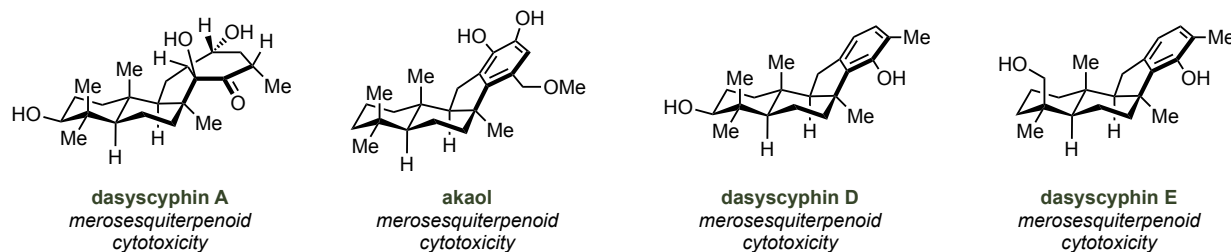
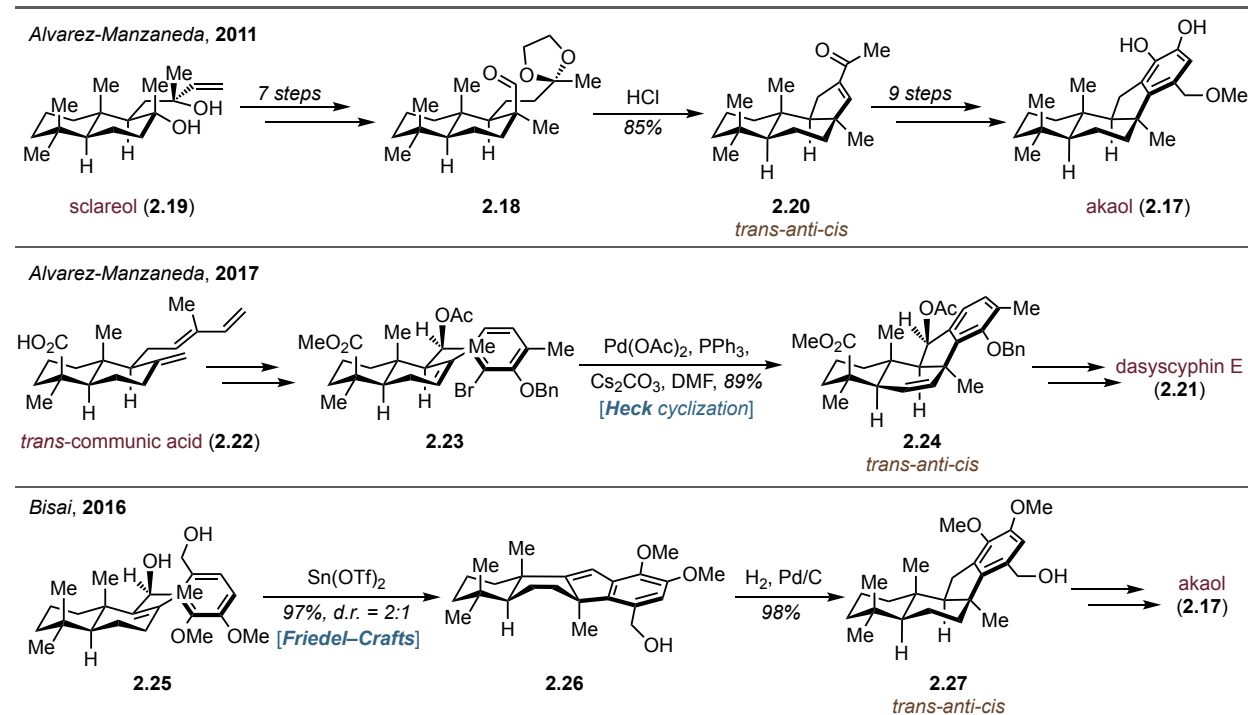


Chart 2.2 Perhydrobenz[*e*]indene natural products with *trans-anti-cis* configuration.

2.20 under acidic conditions in excellent yield. Unfortunately, numerous manipulations were further needed to complete the synthesis, which is attributed to the required arduous benzannulation and subsequent adjustment of oxidation states. Later, the same group disclosed an alternative strategy for the semisynthesis of dasyscyphin E (**2.21**), where a critical *trans-anti-cis* configuration was set through intramolecular Heck cyclization.¹³ Towards this goal, *trans*-communic acid (**2.22**) was converted into advanced intermediate **2.23** in a 14-step linear sequence.



Scheme 2.2 Previous studies on *trans-anti-trans* configured perhydrobenz[*e*]indene natural products.

A Pd-catalyzed Heck reaction proceeded smoothly to install the requisite quaternary stereocenter in **2.24** with excellent diastereoselectivity. Finally, reduction of several functional groups delivered the natural product. Another example of synthesis of a *trans-anti-cis* perhydrobenz[*e*]indene natural product was disclosed by Bisai and co-workers.¹⁴ The advanced intermediate **2.25** was

subjected to intramolecular Friedel–Crafts reaction, reminiscent of one that was used for the synthesis of pelorol (**2.13**, Scheme 2.1). Notably, due to additional sp^2 hybridized atoms within the linker between reaction centers and corresponding conformational change, diastereoselectivity is significantly diminished. A mixture of isomers was produced in 2:1 ratio. Resulting styrene **2.26** was simply hydrogenated to set the final tertiary stereocenter. This precedent reveals greater steric accessibility of the α -face of **2.26**. Three additional steps were required to complete the total synthesis of akaol (**2.17**). Overall, discussed examples demonstrate that assembly of this diastereomeric version of the tricycle is not associated with significant kinetic or thermodynamic penalties and thus does not require the overhead of deliberate synthetic planning for that step.

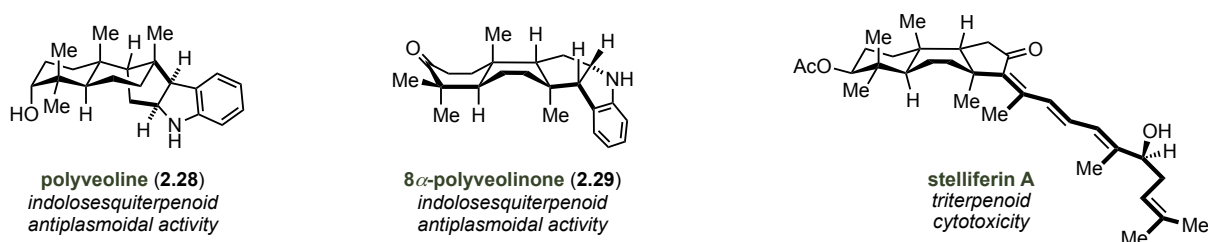
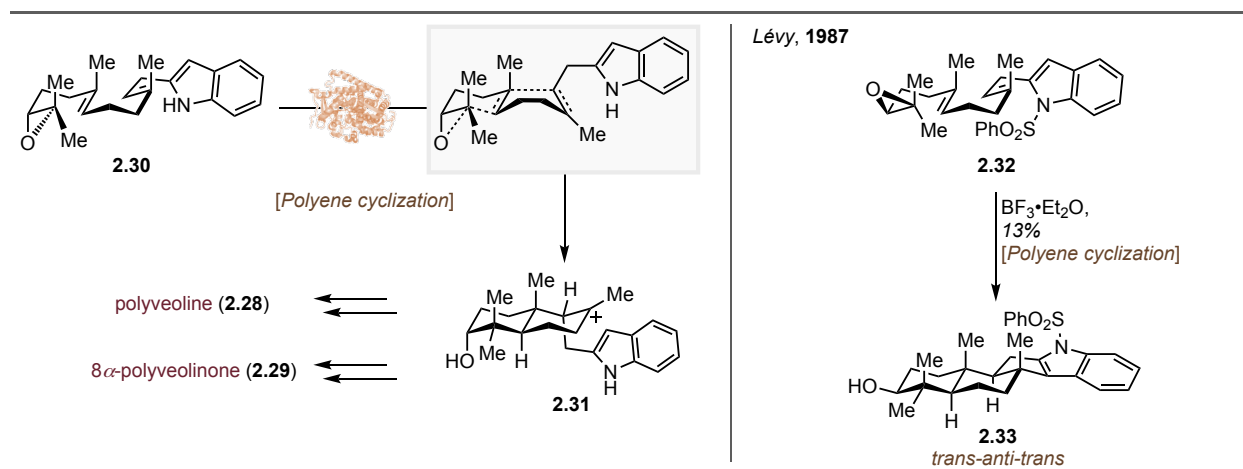


Chart 2.3 Perhydrobenz[*e*]indene natural products with *trans-syn-cis* and *trans-syn-trans* configurations.

The *Trans-syn-cis* configured perhydrobenz[*e*]indene core is solely represented by indolosesquiterpene polyveoline (**2.28**, Chart 2.3).⁶ After 33 years since its original isolation another congener **2.29** from the same producing organism was identified.⁷ Indolosesquiterpene 8 α -polyveolinone (**2.29**) in contrast to previous examples, possesses a *trans-syn-trans* junction. Aside from **2.29**, the *trans-syn-trans* configured core is highly characteristic for a large family of triterpenoid with four subclasses, the isomalabaricanes (see Chapter I). Given the close relationship between **2.28** and **2.29**, a divergent biogenesis was proposed (Scheme 2.3). Enzymatic polyene cyclization of the linear precursor **2.30** furnishes carbocation **2.31**, which represents a point of bifurcation, as the final cyclization event would lead to two different products. Most likely, a cyclase enzyme guides the formation of all stereocenters simultaneously through preorganization of the substrate in its binding pocket rendering hypothetical carbocation **2.31** not an actual intermediate along the reaction coordinate. Biomimetic cyclization was attempted by Lévy and co-workers in 1987.¹⁵ Perhaps unsurprising in retrospect, only the undesired *trans-anti-trans* isomer **2.33** was obtained, which corroborates previous studies shown on the Scheme 2.2. Thus, no synthesis of a terpenoid with *trans-syn-cis* has been completed to date. The only existing strategy

towards any of the *trans-syn-trans* perhydrobenz[*e*]indene natural products, in turn, was reported by us as exemplified by the total synthesis of isomalabaricane triterpenoids (see Chapter I).

Overall these two categories of terpenoids, namely *trans-syn-cis* and *trans-syn-trans*, are drastically different from previously discussed *trans-anti-trans* and *trans-anti-cis*. These stereochemical variations are much harder to acquire through synthesis, and retrosynthetic planning should be centered around construction of the corresponding backbones, rather than the appendage of functional groups.



Scheme 2.3 Previous studies on *trans-syn-cis* configured perhydrobenz[*e*]indene natural products.

2.3 Results and Discussion

2.3.1 Computational investigation of perhydrobenz[*e*]indene strain energies

With the concept of the general blueprint in mind, we decided to rank all desired isomeric forms of perhydrobenz[*e*]indene in order of their relative *I*-strain. This assessment might provide a meaningful comparison of their thermodynamic stability. Moreover, predicted preferred geometries for each isomer can also illuminate the steric interactions within the core. Overall, this computational tool would assist in predicting the stereoselectivities of envisioned transformations on a thermodynamic and kinetic basis with high confidence and thus guide our synthetic planning. For better representation, all eight existing isomers of the tricycle **2.1** were computed, including ones that share *cis* junction of A/B ring and have yet to be found in nature. All calculations were performed in release version of ORCA 4.0.1.¹⁶ The following work-flow was executed: first, a set of conformers was generated manually with all structures being fully optimized. Lowest energy structures were then selected for all diastereomers. Geometries were optimized using PBEh-3c method.¹⁷ Analytical frequency calculation was used to confirm that geometries are true stationary

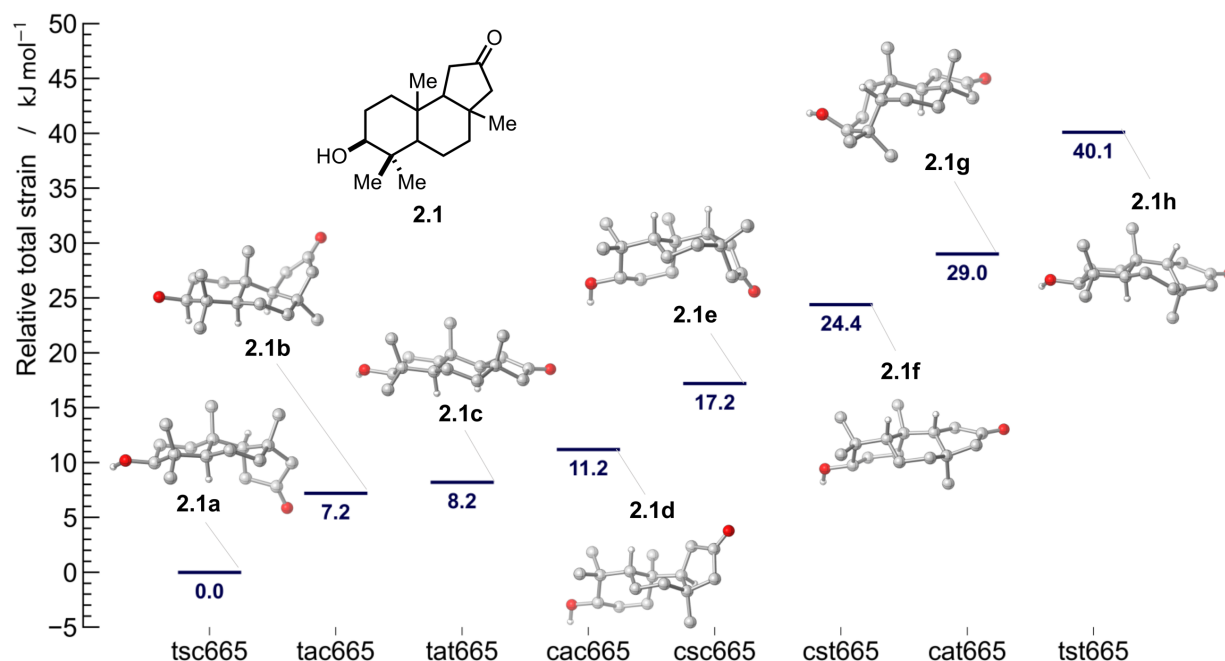


Figure 2.3 Comparison of the relative I-strain energies of tricyclic ring systems containing natural product-like oxidation. DLPNO-CCSD(T) / *def2-TZVPP* // PBEh-3c; c – *cis*; t – *trans*; s – *syn*; a – *anti*.

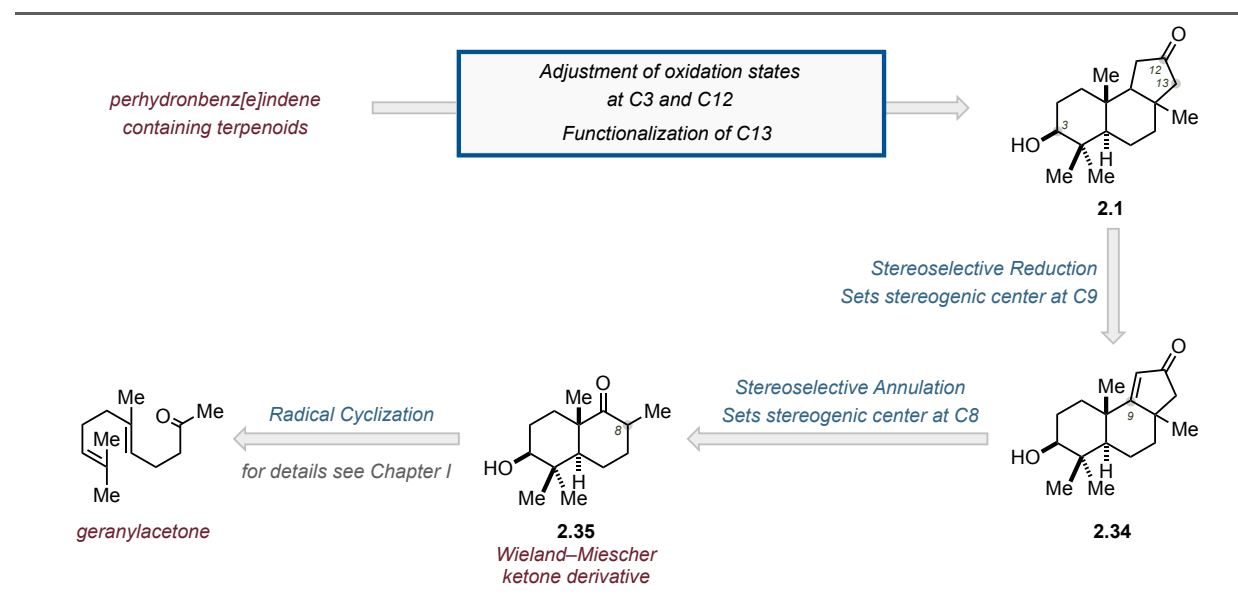
points by absence of imaginary frequencies. High level single point energies were then calculated using DFT geometries. Standard enthalpies of formation refer to *ideal gas* state and were calculated using a modified approach by E. Paulechka and A. Kazakov.¹⁸ Relative I-strain was then determined as the difference between the enthalpies of formation between a given model and the reference model. Obtained data is plotted in Figure 2.3 along with optimized geometries for each diastereomer. *Trans-syn-cis* fused ketone **2.1a** was determined to be the lowest energy isomer and was used as a reference model. It's worthwhile to mention that even though *trans-syn-cis* core is considered to be a relative minimum in the current study, it still has severe 1,3-diaxial repulsions between methyl groups at the quaternary stereocenters. Thus, it is important to bear in mind that Figure 2.3 is a representation of only *relative* strain energies and does not provide information on their absolute values. Interestingly, *trans-anti-trans* isomer **2.1c** is higher in energy by 8.2 kJ mol⁻¹ than the reference. Therefore, polyene cyclization depicted in Scheme 2.3 is an illustrative example of kinetic versus thermodynamic control over the reaction, where the less thermodynamically favorable products can only be formed due to kinetic preference. In accordance with our suspicions, *trans-syn-trans* isomer **2.1h** significantly outcompeted any other structures in its embedded strain. This result is also indirectly supported by the encountered challenges that this core posed to us during the total synthesis campaign towards isomalabaricanes (see Chapter I).

Any transformation that could potentially yield either *trans-syn-trans* or *trans-antic-cis* product would selectively deliver the latter (**2.1b**) as it lies 32.9 kJ mol^{-1} lower in energy (thermodynamic factor was additionally empowered by the kinetic preference)!

According to the computational results, the strategy designed for isomalabaricane triterpenoids total synthesis (Chapter I) is capable of providing *the most challenging* isomer with exceptional stereoselectivity. It gave us a premise to speculate that our originally tailored approach can be expanded for broader use. All four desired diastereomers of the perhydrobenz[*e*]indene core (**2.1a**, **2.1b**, **2.1c**, **2.1h**, Figure 2.3) can be synthesized following the general outline, if appropriate modifications can be made to render stereodivergence.

2.3.2 Design of the divergent strategy

Fusing our results from total synthesis of isomalabaricanes and new insight into energetic features of the system, the following conceptual retrosynthesis was devised (Scheme 2.4). All perhydrobenz[*e*]indene containing natural products can be traced back to the tricyclic ketone **2.1** with ambiguous configuration, which is dictated by the desired target. This retrosynthetic simplification was accomplished through adjustment of C3 oxidation state and functionalization of the C-ring employing the preexisting carbonyl group as a handle. Here, the first point of bifurcation is approached, where four ketones **2.1** can be synthesized from only two diastereomeric



Scheme 2.4 Retrosynthesis for stereodivergent synthesis of perhydrobenz[*e*]indene natural products.

enones **2.34** via stereoselective reduction. Stereoselective annulation of the bicyclic ketone **2.35** was envisaged as a second point of bifurcation. Thus, if successful, all four ketones **2.1** can be derived from the single compound **2.35** or an even more advanced intermediate *en route* towards **2.34**.

From our experience with *trans-syn-trans* versus *trans-anti-cis* selectivity of the enone reduction, it became apparent that accessing the latter will be exceptionally easy using our approach (for details see p. 25). Moreover, all transformations towards both ketones **2.1b** and **2.1h** were already optimized and realized in enantioselective fashion. However, a crucial question was awaiting its answer: can the Rautenstrauch cycloisomerization be turned into a stereodivergent process.

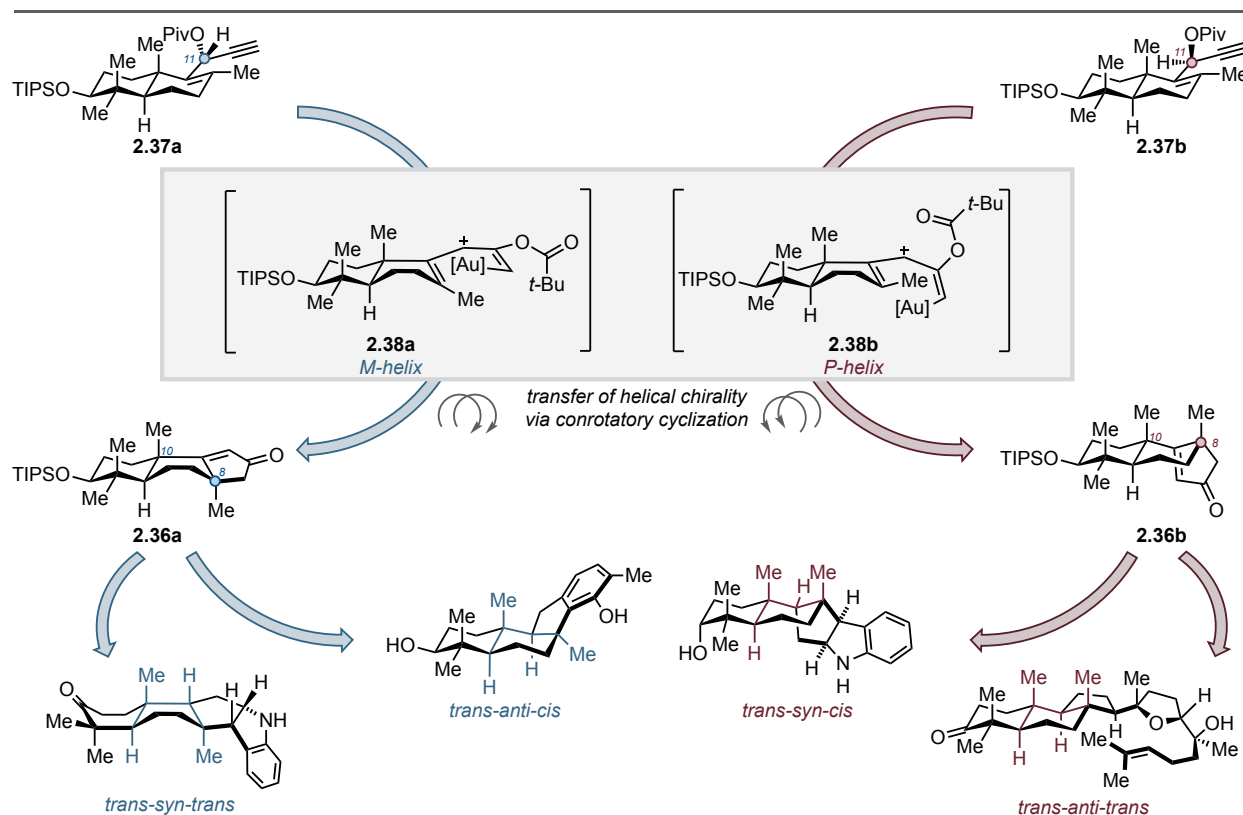


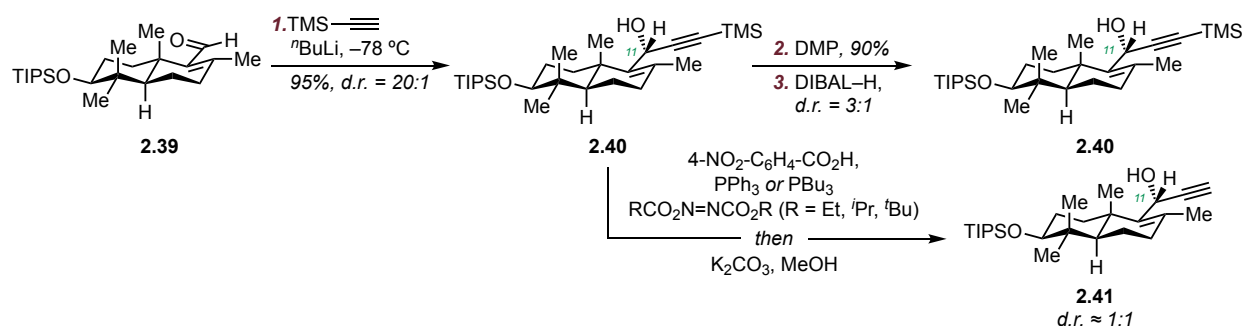
Figure 2.4 Transfer of stereogenicity in the Rautenstrauch cycloisomerization.

2.3.3 Divergence based on transfer of stereogenicity

It was postulated that quaternary stereocenter at C8 in **2.36a** is set through transfer of stereogenicity from the C11 stereocenter of the enyne **2.37a** in the interim of cycloisomerization (Figure 2.4). High steric encumbrance of the intermediary carbocation **2.38a** prevents free rotation, thus preserving the conformation of the helix, which further translates into stereoselective

formation of the new C–C bond. Accordingly, we hypothesized that use of the C11-epimer would divert the stereochemical outcome and unlock the envisioned first bifurcation point. Thus, the synthesis of **2.37b** was undertaken.

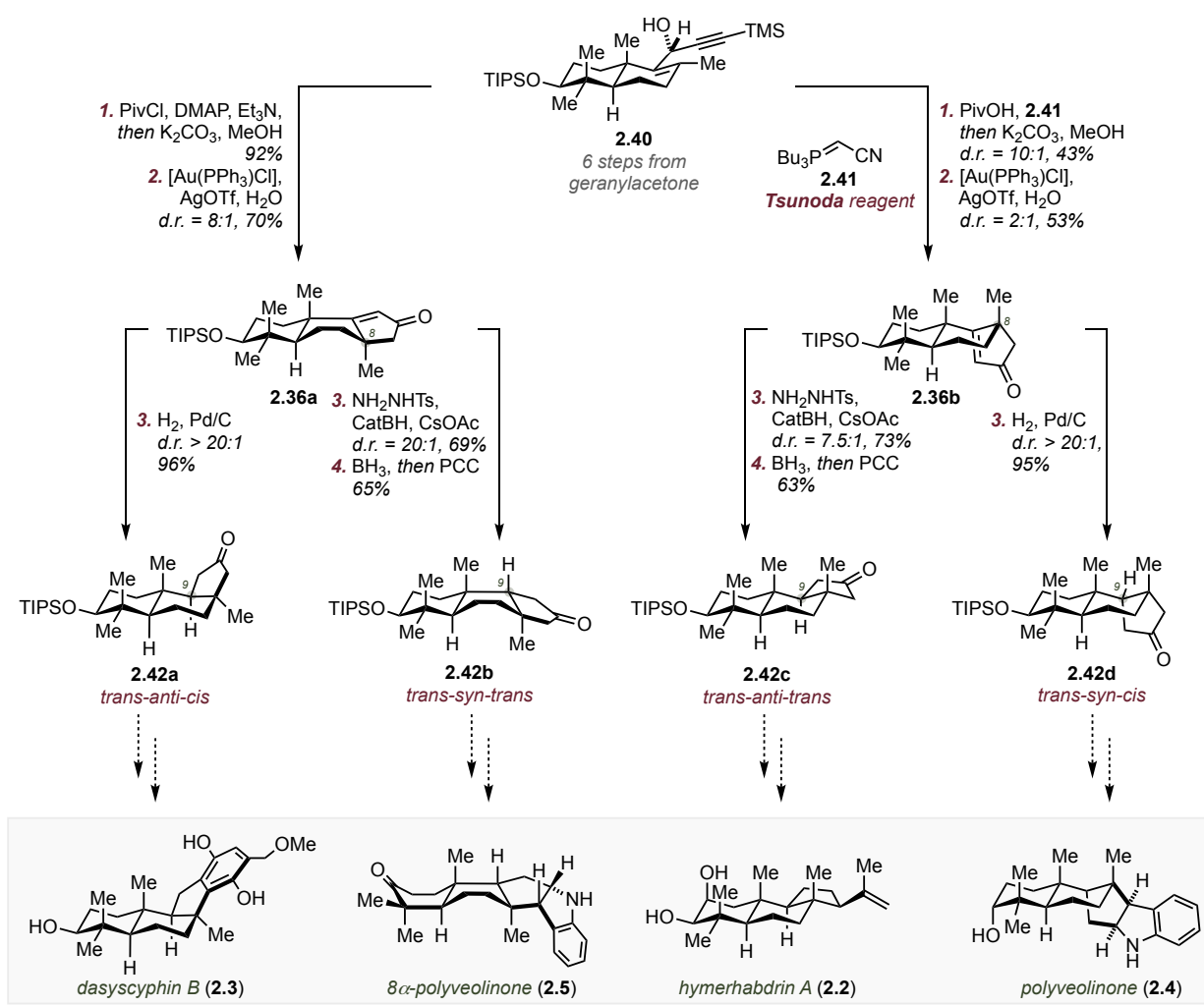
Essential C11-stereocenter was formed by substrate-controlled addition of acetylide to the corresponding aldehyde **2.39** (Scheme 2.5). The process possesses exquisite selectivity, therefore modulation of conditions for the addition did not seem as a viable route to epimer **2.37b**. Thus, an oxidation/reduction sequence was explored. The premise of success was an assumption that a suitable hydride source might approach the electrophile from the same face as the organometallic specie in the preceding step, thus selectively yielding an opposite diastereomer. A silyl-protecting group was placed on the alkyne terminus to increase stability of the substrate towards purification. Oxidation of **2.40** smoothly proceeded employing Dess–Martin periodinane. Reduction of the ynone was affected by DIBAL–H, and the product was obtained as a mixture of diastereomers in 3:1 ratio in favor of the original configuration (**2.40**). Numerous other hydride sources were examined; however, no promising lead was identified.



Scheme 2.5 Attempts towards epimerization at C11.

A Mitsunobu reaction was investigated next as a plausible solution to the problem. Use of pivalic acid would directly afford the desired precursor for the Rautenstrauch cycloisomerization in a single step (the silyl group can be easily removed in the same pot). However, due to its low nucleophilicity, no conversion of the alcohol **2.40** was observed under standard conditions. A more conventional nucleophile for inversion purposes, *p*-nitrobenzoic acid, was exploited next. To facilitate analysis, *in situ* TMS-removal and ester hydrolysis was executed. Numerous conditions including various permutations of different phosphines, diazocarboxylates and solvents led to a similar outcome: a near equimolar mixture of diastereomers was obtained. The highly activated nature of the substrate **2.40** accounts for S_N1 type reactivity, rather than desired S_N2. Additionally,

troublesome purification of the labile product substantially hampered further studies. Therefore, milder conditions with use of pivalic acid as a nucleophile were sought. Fortuitously, reagent **2.41** developed by Tsunoda and co-workers fit this purpose (Scheme 2.6, top-right corner).¹⁹ The pivalate **2.37b** was obtained after *in situ* deprotection in great diastereoselectivity. Even though the yield was only moderate, this discovery enabled further progression of the project.



Scheme 2.6 General blueprint towards perhydrobenz[e]indene natural products.

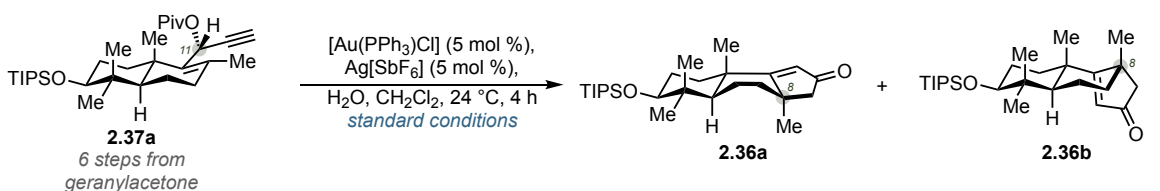
Subjecting substrate **2.37b** (not shown in Scheme 2.6) to the previously utilized conditions for the Rautenstrauch cycloisomerization, to our delight, delivered desired enone **2.36b** as a major product. Thus, transfer of stereogenicity was verified, and the first point of bifurcation for the synthesis of all isomers of perhydrobenz[e]indene natural products was achieved. The diminished diastereoselectivity and yield compared with diastereomeric system **2.36a**, however, are noticeable. We speculate that this is manifestation of the mismatching case between the helix and

preexisting stereocenters within the bicycle. The second bifurcation point, stereoselective reduction, was tackled next. Conditions for the synthesis of *trans-anti-cis* and *trans-syn-trans* isomers of the ketone from enone **2.36a** were previously discovered *en route* towards isomalabaricanes. Heterogeneous hydrogenation of **2.36a** delivered **2.42a** with excellent selectivity. In contrast, a Caglioti reaction yielded an olefin with *trans-syn-trans* configuration, which was further converted into **2.42b** by a hydroboration / oxidation sequence. The same set of conditions were then applied to the enone **2.36b**. Heterogeneous hydrogenation yielded thermodynamically and kinetically preferred product **2.42d** in excellent yield and diastereoselectivity. Strategic use of the substrate control to produce less favorable *trans-anti-trans* product was executed via the same Caglioti reaction, which following hydroboration and oxidation furnished ketone **2.42c** in good yield and diastereoselectivity. Thus, all four requisite diastereomers were produced from the corresponding enones with excellent control and the second point of bifurcation was set. These results conclude the development of a general blueprint as further elaborations of the substrates must be dictated by the specific target. However, before proceeding with the syntheses of representative perhydrobenz[e]indene terpenoids (**2.2-2.5**) we opted to address the low efficiency of the stereodivergent annulation.

2.3.4 Stereodivergent catalysis of Rautenstrauch cycloisomerization

Despite preliminary success of our design, certain aspects required further addressing. Namely, low throughput of material from the enyne **2.40** to the enone **2.36b** was a significant drawback. Moreover, Mitsunobu inversion under Tsunoda's conditions was not amenable to scale increase and delivered products with poor purity profile. Finally, any attempts to improve the yield and distereoselectivity of the Rautenstrauch reaction also failed. Thus, we decided to explore the possibility of stereodivergent cycloisomerization. If successful, the divergence would be enabled by a different mode of catalysis rather than differential substrates. Moreover, the low-yielding Mitsunobu inversion would be completely avoided and the overall step count to the enone **2.36b** would be reduced.

Pivalate **2.37a**, an intermediate in our synthesis of stelletin A and other isomalabaricanes, was used as a common precursor. Previously described conditions employing gold-catalysis in the presence of PPh₃ as a ligand led to the product **2.36a** in 8:1 diastereoselectivity and 70% yield (entry 1, Table 2.1). A number of reaction parameters were modified and an interesting observation was made. Change of PPh₃ to any other phosphine in the majority of cases drastically

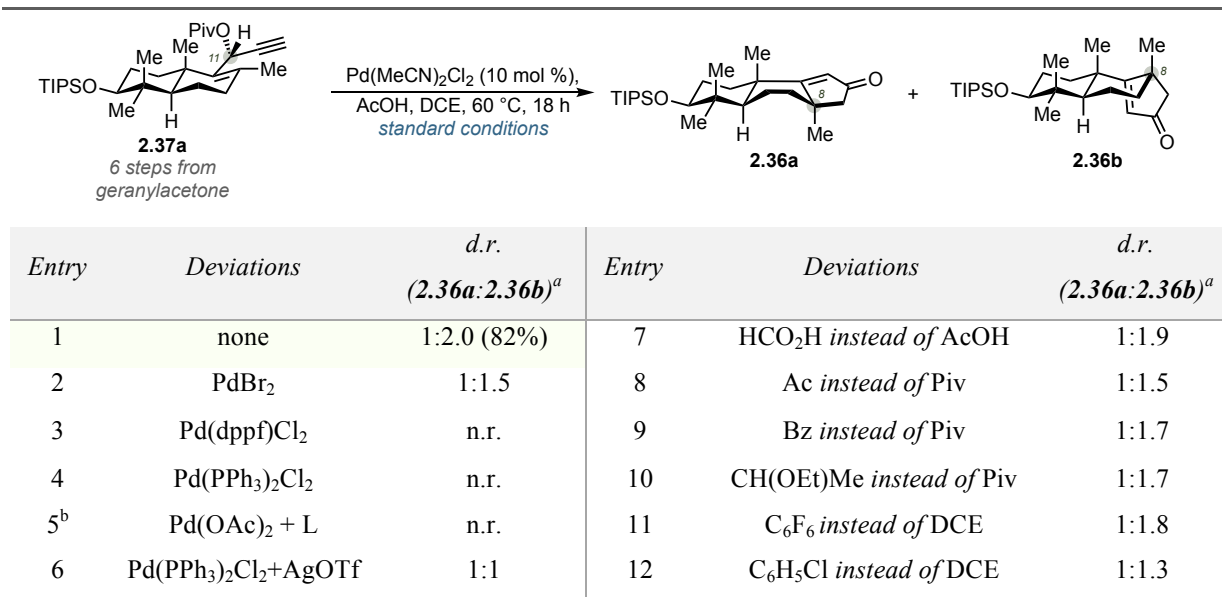
					
Entry	Deviations	<i>d.r.</i> (2.36a : 2.36b) ^a	Entry	Deviations	<i>d.r.</i> (2.36a : 2.36b) ^a
1	none	8:1 (80%)	7	IPr	1.9:1
2	QPhos	n.r.	8 ^b	(<i>S,S</i>)-Me,Me-Duphos	1.4:1
3	RuPhos	n.r.	9 ^b	(<i>R</i>)-DTBM-Segphos	2.3:1
4 ^c	SPhos	11:1	10 ^b	(<i>S,S</i>)-DIPAPM	9:1
5	PCy ₃	3:1.	11	JohnPhos for C11 epimer	1:1.2
6	JohnPhos	1.1:1 (78%)	12	IPr for C11 epimer	1.2:1

^a measured by NMR. ^b Au : L = 2:1. ^c ~30% conversion

Table 2.1 Diastereoselectivity in gold-catalyzed cycloisomerization.

decreased *d.r.* Of note JohnPhos as a supporting ligand (entry 6) afforded an equimolar mixture of isomers in 78% yield.²⁰ While these conditions are lacking selectivity, it was an optimal solution for simultaneous synthesis of several isomeric tricycles to facilitate downstream studies. Several chiral ligands were tested on *racemic* material as well, since diverse backbone structures could lead to new catalyst-substrate interactions (entries 8-10). In any case, none of the examined conditions delivered **2.36b** as a major product. Screening of silver salts showed a negligible effect on the reaction diastereoselectivity. Further screening of solvents and protic additives revealed their importance for the reaction efficiency, but not for diastereoselectivity (not shown, for discussion see p. 21). Several control experiments were carried out on the C11-epimer (entries 11-12). Interestingly, similar ratios of products were obtained, indicating a potential switch of mechanism. At this point, the incompatibility of gold-catalysis with desired stereodivergence became evident. Thus, Pd(II)-catalysis, a system originally developed by Rautenstrauch himself, was interrogated next (Table 2.2).²¹ To our delight, the reaction proceeded smoothly in presence of catalytic amount of Pd(MeCN)₂Cl₂ in 1,2-dichloroethane in the presence of acetic acid (entry 1). Conversion was exceptionally clean, albeit slower than for gold-catalysis. The most notable feature of the transformation is the diastereoselectivity. For the first time enone **2.36b** was obtained as the major product in a 2:1 ratio and 82% overall yield. Encouraged by these results, further optimization was attempted. At the outset of our studies, very little was known about this

transformation. Despite being disclosed over 36 years ago, there was not a single use of Pd-catalyzed Rautenstrauch cycloisomerization in synthesis. Moreover, no detailed mechanistic



^a measured by NMR. ^b Pd : L = 1:1

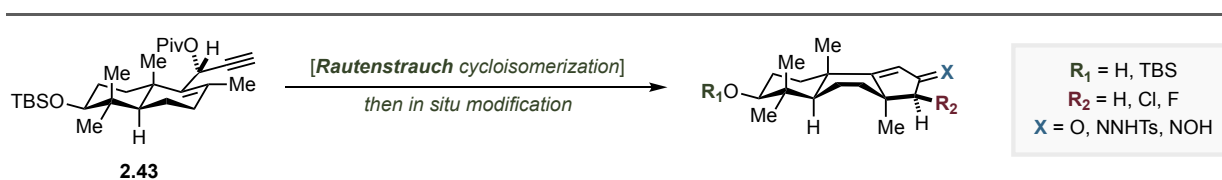
Table 2.2 Diastereoselectivity in palladium-catalyzed cycloisomerization.

studies have been reported either.²² First, it became apparent that any phosphine ligand totally shuts down the reactivity, indicating the necessity of 14-electron palladium complex and at least two vacant sites for the substrate to bind (entries 3, 4). Attempts to substitute halogens with less coordinating counter-ions in presence of the phosphine ligand turned out to be fruitless (entry 5, L = 15 diverse phosphine ligands). Importantly, the catalytic activity was regained in the presence of a silver salt to sequester chloride anions and generate a cationic complex in similar fashion to gold-catalysis (entry 6). The current speculative interpretation of the acquired results is offered as follows: change of stereoelectronic properties of the ligand as well as a switch to the palladium yields a less rigid intermediate and therefore disables the chirality transfer mechanism through sturdy helical configuration. The reaction proceeds via open carbocation, which delivers the final product in slight preference for isomer **2.36b**. Notably, a similar ratio of the products was observed for the intramolecular Friedel–Crafts cyclization reported by Bisai (Scheme 2.2), which proceeds through an analogous cationic intermediate. Accordingly, both epimers of the enyne **2.37** yield nearly identical ratios. Next, the effect of the protic additive was examined by testing compounds with various acidity. Only acetic and formic acids affected transformation, albeit with identical *d.r.* (entry 7). In contrast to gold-catalysis, various esters (entries 8, 9) and even acetal (entry 10)

were susceptible towards cycloisomerization, however no change in diastereoselectivity was observed. Finally, a thorough solvent screen was conducted. Twenty different solvents were tested, including ones known to affect the coordination sphere of the catalyst such as tetrachloroethylene. DCE and some halogenated aromatic solvents were suitable for the reaction, however only minor changes in diastereoselectivity were observed (entries 11, 12). Thus, despite our efforts the initial lead could not be improved upon. Given the success in entry 6, however, further efforts will be directed towards identification of a suitable ligand (perhaps chiral) to enforce the diastereoselectivity. Nevertheless, significant advancement of our divergent design was achieved in the grand scheme. The synthesis of enone **2.36b** was shortened by one step, and the efficiency of its synthesis was increased more than three-fold in spite of the moderate stereoselectivity. Importantly, the rest of material mostly accounts for the second diastereomer **2.36a**, which is valuable for future studies towards *trans-anti-cis* and *trans-syn-trans* isomeric natural products.

2.3.5 Efforts towards *trans-anti-cis* configured dasyscyphin B

Once the first phase of the general blueprint was successfully completed, we initiated our second phase of studies: loading hypothetical pharmacophores onto lipophilic scaffolds. The main objectives pursued in this study were (1) presentation of full power of our design by *expeditious* total synthesis of perhydrobenz[*e*]indene natural products with various backbone configurations and (2) development of a toolbox for diverse functionalizations of the tricyclic core for further use in synthesis of medicinally relevant structures. In this regard, it is worthwhile mentioning the versatility of the Rautenstrauch cycloisomerization. In the course of our investigations several sets of conditions were developed in order to halogenate the C13 carbon, transform the carbonyl group, and cleave silyl ether at C3 in a single pot (Scheme 2.7). Thus, an entire range of compounds derived from **2.43** became available to us as a starting point for further explorations.



Scheme 2.7 Flexibility of Rautenstrauch cycloisomerization.

First, *trans-anti-cis* fused terpenoid dasyscyphin B (**2.3**) was tackled. Considering that step count is of high importance, this target posed a daunting challenge as it calls for unusual benzannulation around the cyclopentanone motif. Of note, a similar exercise was performed by

Alvarez-Manzaneda and co-workers in their synthesis of akaol, where 9 steps for the assembly of the phenol ring were required (Scheme 2.2).¹² According to our divergent blueprint (Scheme 2.6) the desired configuration can be accessed through simple heterogeneous hydrogenation. In

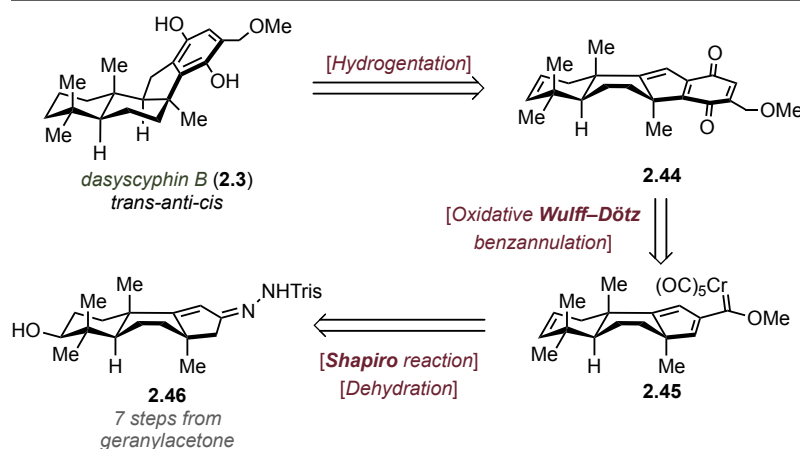
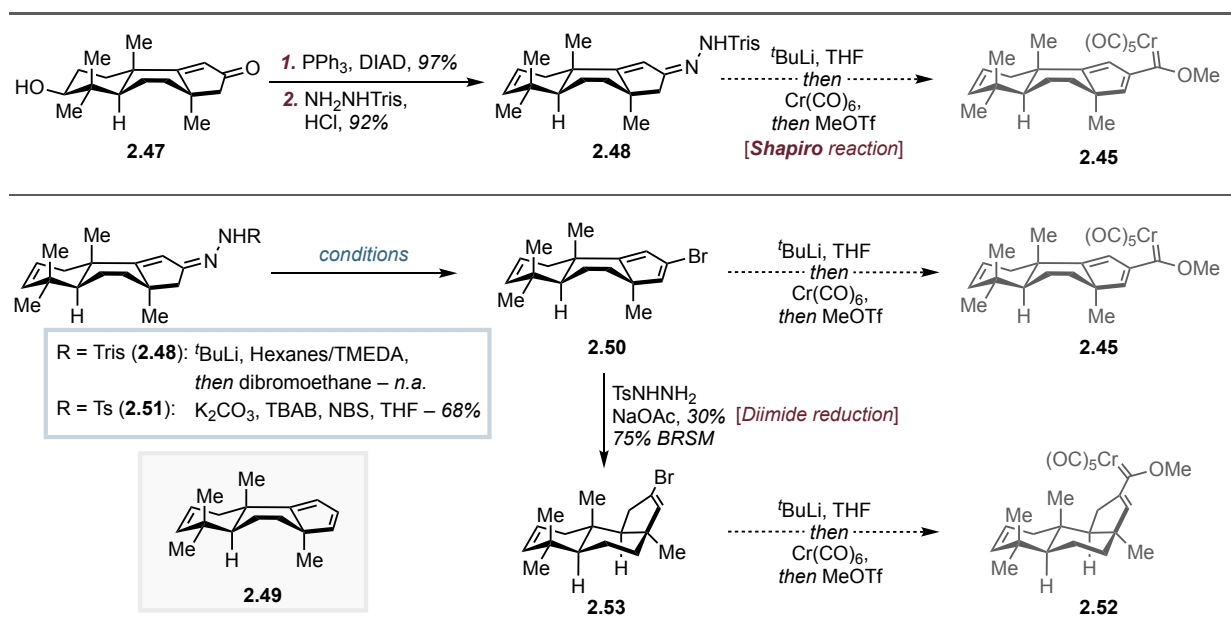


Figure 2.5 Retrosynthesis of dasyscyphin B (**2.3**).

order to maximize redox efficiency of the synthesis this step can be coupled with additional reduction events, thus **2.3** ultimately was traced back to the **2.44** (Figure 2.5). Analysis of the substitution and oxidation pattern of the quinone motif within the structure revealed Wolff–Dötz benzannulation as a powerful transform. Accordingly, **2.44** was traced back to the intricate Fischer carbene **2.45**, which in turn can be synthesized from the hydrazone **2.46** employing a Shapiro transform. Fischer carbenes as complex as **2.45** have rarely been deployed in the literature.²³ Nevertheless, this disconnection was pursued despite high risk, since the overall synthetic sequence was projected to consist of only 4 steps.

Alcohol **2.47** was subjected to dehydration followed by condensation with hydrazide, affording hydrazone **2.48** in 90% yield (Scheme 2.8). We were able to identify only two examples of a Shapiro / Wolff–Dötz combination in the literature.^{23,24} To our dismay, application of the reported conditions did not provide any of the desired product **2.45**. Control experiments allowed us to pinpoint the problem: the dianion of hydrazone **2.48** does not readily collapse into the corresponding vinyl lithium species at cryogenic temperatures. At warmer conditions, however, this strong nucleophile deactivates upon generation via facile quenching by the solvent, yielding diene **2.49**. The classical solution to this issue would be use of hexanes / TMEDA as a solvent mixture.²⁵ Unfortunately, these conditions are incompatible with our particular transformation as use of a strong electrophile (MeOTf) is required in the same pot. Thus, an alternative bypass was sought. The intermediacy of vinyl bromide **2.50** as a precursor for vinyl lithium species was considered. Its synthesis was attempted using the same Shapiro reaction from hydrazone **2.48**. As previously noted, the reaction proceeded at a slower rate than competitive decomposition of the

reactive intermediates, therefore no product was obtained. In order to circumvent the Shapiro reaction, a synthesis of **2.50** was attempted using recently described conditions by Prabhu and co-workers.²⁶ Simultaneous presence of bromine as nucleophile and electrophile in presence of base converts hydrazone **2.51** into gem-dibromide, which further undergoes elimination furnishing desired product in 68% yield. With key precursor in hand Wolff–Dötz benzannulation was further explored.²⁷ After numerous attempts only degradation was noted, which was attributed to the instability of the corresponding carbene **2.45**.²⁸ It was hypothesized that the reduced analogue **2.52** could have improved stability. In order to selectively reduce dienyl bromide to **2.53** diimide was exploited following precedent reported by Fukuyama and co-workers.²⁹ While conversion was slow, only a single alkene was reduced. Surprisingly, even the *cis*-disubstituted olefin in the A-ring remained untouched. With sufficient amounts of bromide **2.53** Wolff–Dötz benzannulation was conducted. Despite our hopes, only carbene decomposition was observed again. Consequentially, the further research of this disconnection was ceased.



Scheme 2.8 Efforts towards dasyscyphin B applying Wolff–Dötz benzannulation approach.

In a separate retrosynthetic analysis dasyscyphin B was traced back to hydroquinone **2.54** (Figure 2.6). Diels–Alder cycloaddition between Michel acceptor **2.55** and substituted furan **2.56** was recognized as a viable disconnection.³⁰ Functionalization of the carbonyl at C12 was envisaged for synthesis of the appropriate dienophile **2.55**. Notably, the electron-withdrawing group also will serve as a leaving group to deliver aromatized product **2.54**. A method for

formation of *trans-anti-cis* fusion and deoxygenation at C3 was adopted from previous retrosynthetic planning.

Nitroalkene **2.57** was identified as a primary target due to expected high reactivity for the Diels–Alder cycloaddition and the well-known ability of the nitro-substituent to function as a leaving group (Scheme 2.9). Oxime **2.58** and α -chloro oxime **2.59** were used as a starting point.

All efforts to carry out oxidation/elimination or oxidation/halogenation/elimination sequences were fruitless. Occasional α -functionalization was detected, but no oxidation of the oxime moiety into the nitro-group was ever attained. Subsequently, sulfone **2.60** was considered as an appropriate alternative. For its synthesis ketone **2.61** was converted into triflate, which was further coupled with sodium sulfinate under palladium catalysis.³¹ We found the intermediary triflate to

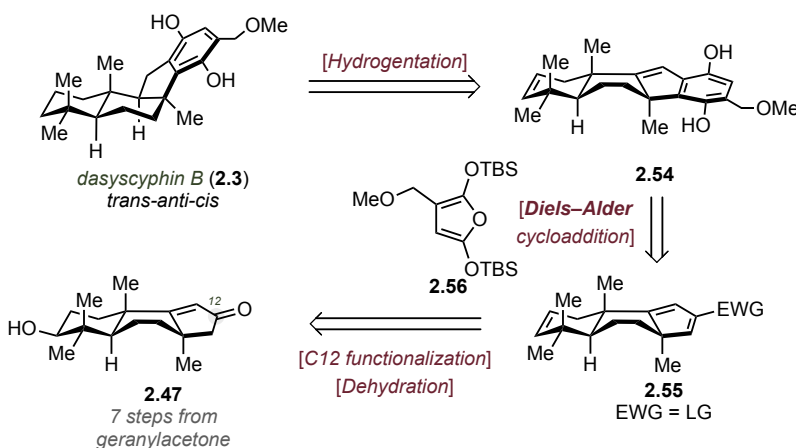
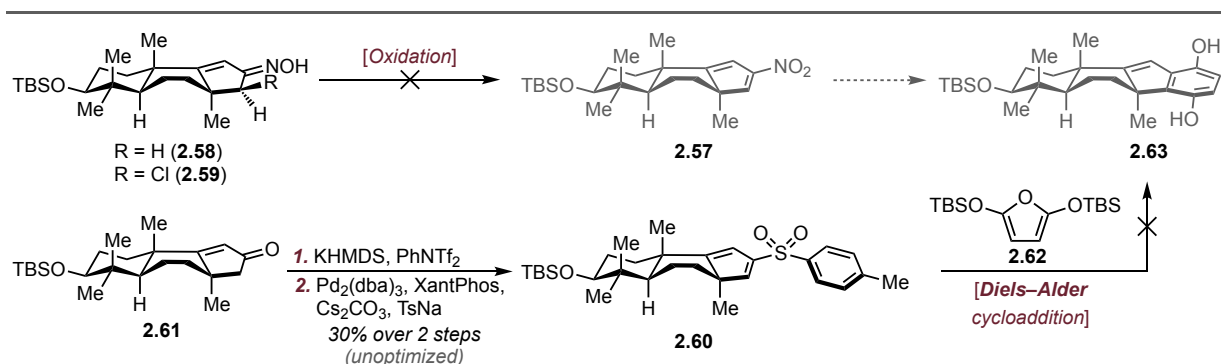


Figure 2.6 Revised retrosynthesis of dasyscyphin B (**2.3**).

be highly unstable and the organic stream after extraction should be used directly for the coupling to avoid rapid decomposition. Sulfone **2.60** was subjected to the cycloaddition with model furan **2.62** under thermal conditions. Our preliminary results indicate poor reactivity of the dienophile, perhaps, due to steric encumbrance. However, more experimental data is needed to verify such a conclusion. Several additional strategies are currently being explored in parallel and their results will be reported in due course.



Scheme 2.9 Efforts towards dasyscyphin B applying Diels–Alder approach.

2.3.6 Efforts towards *trans-syn-cis* configured polyveoline

Studies towards total synthesis of polyveoline (**2.4**) we initiated concurrently. Despite the lowest strain energy enclosed in the characteristic *trans-syn-cis* core, synthesis of such a perhydrobenz[*e*]indene isomer has never been reported to the best of our knowledge (Figure 2.3).

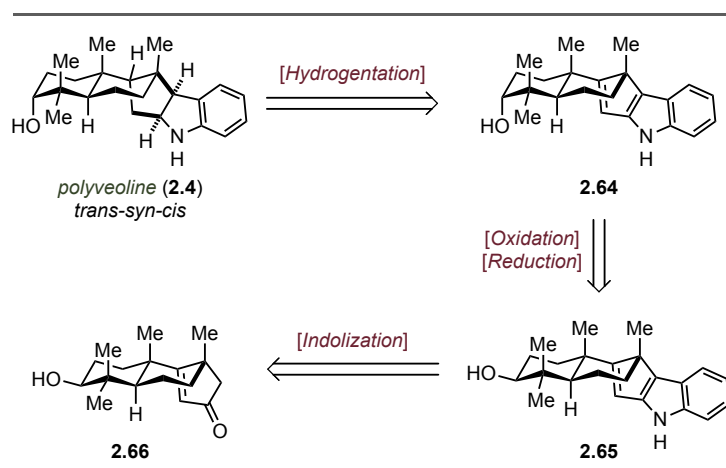
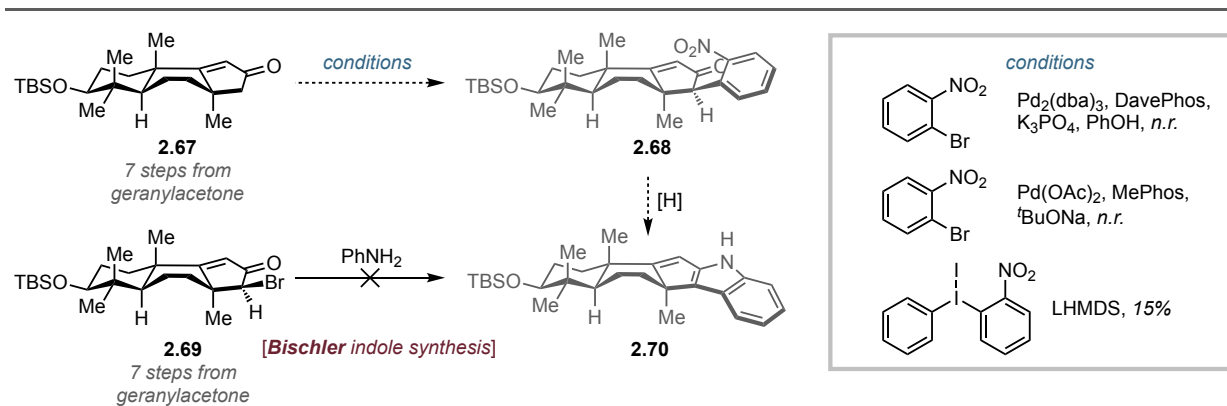


Figure 2.7 Retrosynthesis of polyveoline (**2.4**).

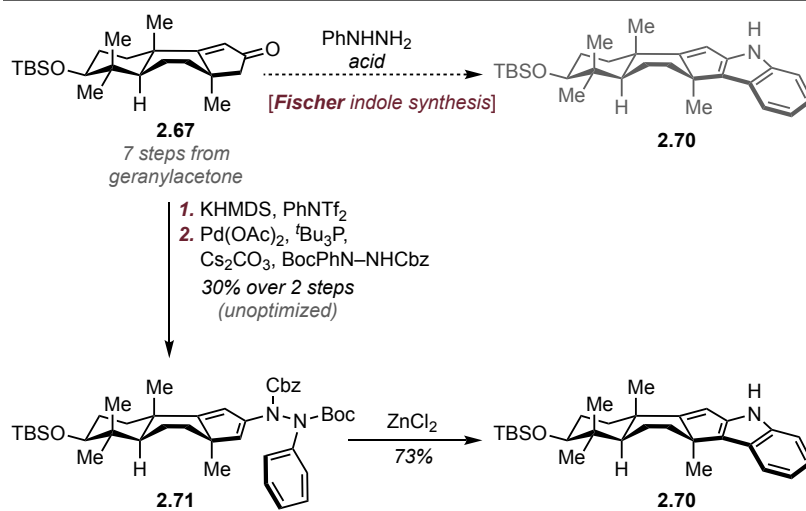
Nevertheless, development of a divergent approach (Scheme 2.6) suggests that hydrogenation or any other simple reduction conditions of the indole **2.64** should deliver the desired product with exclusive diastereoselectivity for all three newly forming stereocenters (Figure 2.7). Axial alcohol at C3 was sought to be synthesized through an oxidation/reduction sequence from **2.65**.³² Finally, pentacyclic compound **2.65** was traced back to the simple enone **2.66** via classical indolization.

Since appropriate conditions for the indole synthesis needed to be identified first, we decided to exploit a diastereomer of the enone **2.66** as a model system, as it was more readily available at the time (Scheme 2.10). One of the most ubiquitous way to perform indolization of a ketone in complex settings is Pd-catalyzed α -arylation using ortho-halonitrobenzene, followed by chemoselective reduction of the nitro-group and spontaneous intramolecular condensation.³³ This approach was examined first. Unlike reported literature examples, the substrate **2.67** possesses a quaternary center in vicinal position from the hypothetical enolate. Therefore, α -arylation was expected to be extremely challenging due to this steric factor. Indeed, neither of the established conditions for the desired transformation delivered even traces of the product (**2.68**) as was judged by NMR and LCMS.^{34,35} We acknowledge the fact that thorough screening of the conditions could yield satisfactory result. However, considering the myriad of techniques available to perform the desired indolization, screening efforts were reserved for later. In contrast to palladium, use of hypervalent iodine for α -arylation allowed for isolation of the desired product **2.68**, albeit in low yield.³⁶ Several known modifications were applied, but conversion was not improved.^{37,38} As a result, the hunt for an effective indolization method was continued. Bishler indole synthesis from



Scheme 2.10 Efforts towards polyveoline.

α -bromo enone **2.69** gave no conversion of the starting material.³⁹ Finally, the venerable Fischer method was investigated (Scheme 2.11). While this transformation is perhaps the most common for the synthesis of indoles, to our wonder we found very little precedent for use of cyclopentanones as substrates. In agreement with observation, a broad range of typical conditions employing Brønsted or Lewis acid catalysis yielded only intermediary hydrazone, and no signs of further [3,3]-rearrangement were noticed. Based on this result along with other evidence, such as instability of the triflate, inability to form the enamine from ketone, *etc.* we postulated that tautomerization of the hydrazone does not occur under reaction conditions. To prove this hypothesis,



Scheme 2.11 Use of Fischer indole synthesis towards *epi*-polyveoline.

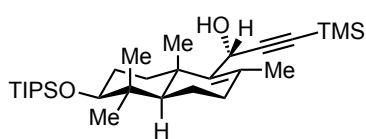
interception of the tautomer was attempted following a protocol developed by Cho and co-workers.⁴⁰ Towards this goal, the ketone was coupled with hydrazine via triflate under Pd-catalyzed conditions. Ene-hydrazine **2.71** was isolated in 30% yield over 2 steps. Subjection of the **2.71** to zinc (II) chloride in refluxing toluene induces deprotection unleashing the [3,3]-sigmatropic rearrangement. To our delight, desired indole **2.70** was isolated in 73% yield. At

the moment, the process is being studied in greater detail to apprehend whether effectiveness of this approach can be improved upon.

2.4 Conclusions and Outlook

In the present study, the perhydrobenz[*e*]indene tricyclic core was identified as a privileged molecular recognition moiety. A database search revealed over 150 natural products unrelated through biogenesis that feature this backbone. Three points of diversification among the structures were recognized, and based on that analysis a unified retrosynthesis was proposed. The designed strategy is amenable to profound modification of the structure, thus delivering a general blueprint to perhydrobenz[*e*]indene containing natural products. Computational techniques were utilized to facilitate the development of the approach. The overall project was nominally segregated into two phases: stereodivergent synthesis of the backbone and loading of the active pharmacophores / syntheses of natural products using provided structures from the first phase. Building on results obtained from our total synthesis of the isomalabaricanes, phase one was completed using stereodivergent Rautenstrauch cycloisomerization followed by selective reduction. Overall, the key building blocks for further elaboration towards medicinally relevant compounds can be accessed enantioselectively in only 8-9 steps from geranylacetone. Studies on phase two were initiated and several promising leads were obtained for further optimization.

2.5 Experimental Section

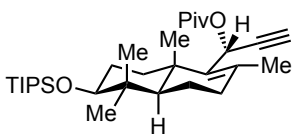


Synthesis of compound 2.40:

Trimethylsilylacetylene (0.57 mL, 4.07 mmol, 1.6 equiv.) was dissolved in dry THF (20 mL) and cooled to $-78\text{ }^{\circ}\text{C}$ under inert atmosphere. $n\text{-BuLi}$ (2.4 mL, 1.6 M, 3.82 mmol, 1.5 equiv.) was added slowly to this mixture. The solution was stirred for 30 min at $-78\text{ }^{\circ}\text{C}$ followed by the addition of a solution of aldehyde (1.00 g, 2.55 mmol, 1.0 equiv.) in THF (2 mL, 0.1 M overall). After 3 hours at this temperature, full conversion was observed by TLC. The reaction was quenched at $-78\text{ }^{\circ}\text{C}$ with NH_4Cl (aq. sat. 20 mL), and the mixture was partitioned between Et_2O (50 mL) and water (50 mL). The organic layer was separated and the aqueous phase was washed with Et_2O ($2 \times 30\text{ mL}$). The combined organic fractions were washed with brine (50 mL), dried over MgSO_4 , filtered, and concentrated.

Product **2.40** (1.20 g, 2.44 mmol, 94%, *d.r.* = 20:1) was isolated as yellow oil and used without additional purification.

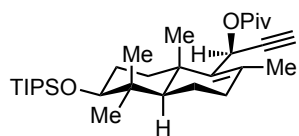
R_f: 0.29 (SiO₂, hexanes : EtOAc = 25:1); **¹H NMR**: (500 MHz, CDCl₃): δ 5.02 (dd, *J* = 3.6 Hz, 1H), 3.40 (m, 1H), 2.08 (m, 2H), 1.91 (s, 3H), 1.88 (dt, *J* = 13.1, 3.6 Hz, 1H), 1.73 – 1.68 (m, 3H), 1.68 – 1.65 (m, 1H), 1.46 (m, 1H), 1.38 (m, 1H), 1.09 (m, 1H), 1.06 (s, 21H), 1.00 (s, 3H), 0.98 (s, 3H), 0.79 (s, 3H), 0.15 (s, 9H); **¹³C NMR**: (126 MHz, CDCl₃): δ 140.4, 134.4, 107.6, 89.0, 79.8, 59.4, 51.3, 39.9, 38.6, 35.1, 34.7, 28.6, 28.2, 21.1, 20.7, 18.8, 18.52, 18.45, 16.0, 13.2, 0.0; **HRMS**: (ES⁺, *m/z*) [*M*+H]⁺ calcd. for C₂₉H₅₅O₂Si₂, 491.3741; found, 491.3736; **IR**: (ATR, neat, cm⁻¹): 2943 (br), 2893 (m), 2866 (s), 1249 (m), 1112 (s), 1067 (m), 882 (m), 843 (s), 677 (w)



Synthesis of compound 2.37a:

A solution of the alcohol **2.40** (270 mg, 0.550 mmol, 1.0 equiv.) in CH₂Cl₂ (1 mL, 0.5 M) was sequentially treated with Et₃N (92 μL, 0.660 mmol, 1.2 equiv.), DMAP (13 mg, 0.110 mmol, 0.2 equiv.) and pivaloyl chloride (81 μL, 0.660 mmol, 1.2 equiv.) under inert atmosphere and at ambient temperature. The reaction was stirred for 12 hours. Upon complete conversion, as judged by TLC, MeOH (4.5 mL, 0.1 M) was added followed by K₂CO₃ (228 mg, 1.65 mmol, 3.0 equiv.). The reaction was stirred for 1 hour and quenched with NH₄Cl (aq. sat., 5.0 mL). The mixture was poured in CH₂Cl₂ : H₂O (1:1, 80 mL). The organic layer was separated and the aqueous phase was washed with CH₂Cl₂ (2 × 20 mL). The combined organic fractions were washed with brine (40 mL), dried over MgSO₄, filtered and concentrated. The crude material was purified by flash chromatography (C₁₈ reverse phase SiO₂, gradient 90% → 100% MeCN in H₂O), which afforded **2.37a** as white crystalline material (252 mg, 0.500 mmol, 92%).

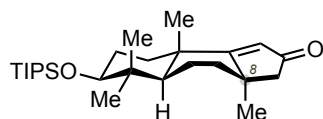
R_f: 0.68 (SiO₂, hexanes : EtOAc = 20:1); **T_{melt.}**: 97.4 – 98.9 °C; **¹H NMR**: (500 MHz, CDCl₃): δ 6.01 (d, *J* = 2.4 Hz, 1H), 3.38 (m, 1H), 2.44 (d, *J* = 2.4 Hz, 1H), 2.12–2.09 (m, 2H), 1.89 (s, 3H), 1.83 (dt, *J* = 13.0, 3.6 Hz, 1H), 1.71–1.64 (m, 3H), 1.46 (tdd, *J* = 13.0, 10.2, 7.7 Hz, 1H), 1.21 (s, 9H), 1.15 (dd, *J* = 11.2, 5.2 Hz, 1H), 1.08–1.04 (m, 1H), 1.06 (s, 21H), 1.03 (s, 3H), 1.00 (s, 3H), 0.79 (s, 3H); **¹³C NMR**: (126 MHz, CDCl₃): δ 177.3, 136.7, 136.4, 82.5, 79.8, 72.7, 60.1, 51.4, 40.0, 38.9, 38.8, 35.2, 34.4, 28.7, 28.2, 27.2, 21.1, 20.7, 18.8, 18.52, 18.46, 16.2, 13.2; **HRMS**: (EI⁺, *m/z*) [*M*]⁺ calcd. for C₃₁H₅₄O₃Si, 502.3842; found, 502.3855. **IR**: (ATR, neat, cm⁻¹): 3311 (w), 2942 (m), 2866 (m), 1736 (s), 1141 (s), 1113 (s), 1067 (w), 882 (m)



Synthesis of compound 2.37b:

Alcohol **2.40** (56 mg, 0.11 mmol, 1.0 equiv.) was dissolved in dry benzene (8 mL, 0.1 M) under inert atmosphere. Pivalic acid (40 μ L, 0.34 mmol, 3.0 equiv.) and (cyanomethylene)tributylphosphorane (90 μ L, 0.34 mmol, 3.0 equiv.) were added, and the reaction vessel was sealed and heated to 50 $^{\circ}$ C. After 48 hours, the reaction was cooled down to ambient temperature, MeOH (3.0 mL) and K_2CO_3 (158 mg, 1.14 mmol, 10 equiv.) were added. The suspension was stirred for 5 hours at 24 $^{\circ}$ C and quenched with NH_4Cl (aq. sat. 8 mL). The mixture was poured in CH_2Cl_2 : H_2O (1:1, 30 mL). The organic layer was separated and the aqueous phase was washed with CH_2Cl_2 (2×10 mL). The combined organic fractions were washed with brine (20 mL), dried over $MgSO_4$, filtered and concentrated. This crude material was subjected to flash chromatography (SiO_2 , 200:1 Hexanes/ Et_2O) that allowed for isolation of the desired product **2.37b** (38 mg, 65% purity by NMR, 0.49 mmol, 43%, *d.r.* = 10:1) as colorless oil.

R_f: 0.66 (SiO_2 , hexanes : $EtOAc$ = 20:1); **1H NMR**: (500 MHz, $CDCl_3$): δ 5.99 (d, J = 2.4 Hz, 1H), 3.42 (dd, J = 10.7, 5.4 Hz, 1H), 2.46 (d, J = 2.4 Hz, 1H), 2.11 – 2.09 (m, 2H), 1.89 (s, 3H), 1.87 (m, 1H), 1.71 – 1.66 (m, 3H), 1.44 – 1.39 (m, 1H), 1.35 (dd, J = 12.3, 5.5 Hz, 1H) 1.21 (s, 9H), 1.12 (dd, J = 12.7, 1.8 Hz, 1H), 1.06 (m, 21H), 1.00 (s, 3H), 0.93 (s, 3H), 0.78 (s, 3H).; **^{13}C NMR**: (126 MHz, $CDCl_3$): δ 177.2, 137.1, 135.6, 82.2, 79.7, 72.9, 59.8, 51.1, 39.9, 39.0, 38.6, 35.0, 34.8, 28.6, 28.1, 27.3, 21.0, 19.4, 18.7, 18.53, 18.45, 16.1, 13.2.; **HRMS**: (ES⁺, *m/z*) [$M+Na$]⁺ calcd. for $C_{31}H_{54}O_3NaSi$, 525.3740; found, 525.3738.; **IR**: (ATR, neat, cm^{-1}): 3312 (w), 2942 (m), 2866 (m), 1732 (s), 1143 (s), 1113 (s), 1067 (w), 882 (m)

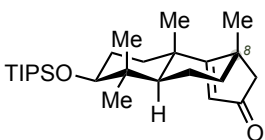


Synthesis of compound 2.36a:

Enyne **2.37a** (450 mg, 0.895 mmol, 1.0 equiv.) was dissolved in CH_2Cl_2 (4.5 mL, 0.2 M) and H_2O (32 μ L, 1.79 mmol, 2.0 equiv.) was added. A separate 4 mL vial was charged with $[Au(PPh_3)Cl]$ (11 mg, 0.022 mmol, 2.5 mol %) and $AgOTf$ (5.7 mg, 0.022 mmol, 2.5 mol%) inside of a nitrogen-filled glovebox. Dry CH_2Cl_2 (0.3 mL) was added under inert atmosphere and stirred at room temperature with protection from light. After 10 minutes, precipitated $AgCl$ was visible and the suspension was transferred into the reaction mixture. Conversion was monitored by TLC. Once full conversion was achieved (about 1 – 2 h),

the reaction was quenched with NH_4OH (aq., 2 M, 2 mL). The resulting biphasic solution was partitioned between CH_2Cl_2 (10 mL) and water (10 mL). The organic layer was separated and the aqueous layer was washed with CH_2Cl_2 (3×5 mL). Combined organic phases were dried over MgSO_4 , filtered, and concentrated *in vacuo*. Flash chromatography (SiO_2 , hexanes : EtOAc = 20:1) allowed for isolation of isomeric enones **2.36a** and **2.36b** as a colorless oil (261 mg, 0.623 mmol, 70%, *d.r.* = 8:1). The diastereomers were separated by reverse phase preparative HPLC (Kinetex[®] 5 μm EVO C18 100 Å LC Column 150 \times 21.2 mm, 25 mL/min, 100% MeCN, detection at $\lambda=230$ nm, t_R = 5.11 min).

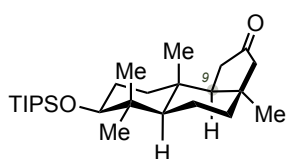
R_f: 0.16 (SiO_2 , hexanes : EtOAc = 10:1); **¹H NMR**: (500 MHz, CDCl_3): δ 5.78 (s, 1H), 3.42 (dd, J = 10.7, 5.0 Hz, 1H), 2.28 (d, J = 16.7 Hz, 1H), 2.23 (d, J = 16.7 Hz, 1H), 1.97 – 1.86 (m, 3H), 1.83 – 1.73 (m, 3H), 1.72 – 1.63 (m, 2H), 1.45 (td, J = 13.1, 4.6 Hz, 1H), 1.37 (s, 3H), 1.17 (s, 3H), 1.08 (s, 21H), 1.01 (s, 3H), 0.91 (s, 3H); **¹³C NMR**: (126 MHz, CDCl_3): δ 208.6, 200.0, 124.4, 80.0, 56.1, 44.4, 42.8, 40.4, 39.4, 36.6, 30.9, 29.9, 28.7, 28.3, 25.7, 18.52, 18.46, 17.2, 16.0, 13.2; **HRMS**: (ES⁺, m/z) [$\text{M}+\text{H}$]⁺ calcd. for $\text{C}_{26}\text{H}_{47}\text{O}_2\text{Si}$, 419.3345; found, 419.3355.; **IR**: (ATR, neat, cm^{-1}): 2942 (br), 2865 (s), 1705 (s), 1461 (w), 1107 (m), 881 (m)



Synthesis of compound 2.36b:

Enyne **2.37b** (80 mg, 65% purity, 0.10 mmol, 1.0 equiv.) was dissolved in CH_2Cl_2 (0.5 mL, 0.2 M) and H_2O (4 μL , 0.21 mmol, 2.0 equiv.) was added. A separate 4 mL vial stock solution of the catalyst was prepared by combining in equimolar proportions $[\text{Au}(\text{PPh}_3)\text{Cl}]$ and AgOTf inside of a nitrogen-filled glovebox, dissolving in dry CH_2Cl_2 , and stirring for 10 min with protection from ambient light. The catalyst (0.0026 mmol, 2.5 mol %) was then quickly transferred into reaction mixture in a single portion at ambient temperature. Conversion was monitored by TLC. Once full conversion was achieved (about 1 – 2 h) reaction was quenched with NH_4OH (aq. 2 M, 1 mL). Biphasic solution was partitioned between CH_2Cl_2 (5 mL) and water (5 mL). The organic layer was separated and the aqueous layer was washed with CH_2Cl_2 (3×3 mL). Combined organic phases were dried over MgSO_4 , filtered, and concentrated *in vacuo*. Flash chromatography (SiO_2 , hexanes : EtOAc = 20:1) allowed for isolation of **2.36b** (30 mg, 0.071 mmol, 69%, *d.r.* = 2:1) as colorless oil. Diastereomers were separated by reverse phase preparative HPLC (Kinetex[®] 5 μm EVO C18 LC Column 150 \times 21.2 mm, 25 mL/min, 100% MeCN, detection at $\lambda=230$ nm, t_R = 5.72 min).

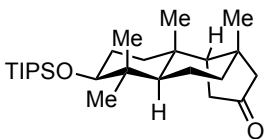
R_f: 0.12 (SiO₂, hexanes : EtOAc = 20:1); **¹H NMR**: (500 MHz, CDCl₃): δ 5.67 (s, 1H), 3.42 (m, 1H), 2.30 (d, *J* = 18.1 Hz, 1H), 2.26 (d, *J* = 18.1 Hz, 1H), 2.04 (dt, *J* = 12.9, 3.2 Hz, 1H), 1.80 – 1.64 (m, 5H), 1.52 (m, 1H), 1.41 (m, 1H), 1.35 (s, 3H), 1.22 (s, 3H), 1.07 (s, 21H), 1.01 (s, 3H), 0.96 (m, 1H), 0.88 (s, 3H); **¹³C NMR**: (126 MHz, CDCl₃): δ 208.6, 196.2, 123.7, 79.5, 54.7, 54.1, 44.3, 42.0, 41.0, 40.1, 36.6, 28.6, 28.4, 27.8, 19.9, 19.1, 18.53, 18.46, 16.1, 13.2; **HRMS**: (ES⁺, *m/z*) [M+H]⁺ calcd. for C₂₆H₄₇O₂Si, 419.3345; found, 419.3336.; **IR**: (ATR, neat, cm⁻¹): 2943 (br), 2865 (s), 1704 (s), 1464 (w), 1108 (m), 882 (m)



Synthesis of compound 2.42a:

The enone **2.36a** (15 mg, 0.036 mmol) was dissolved in EtOAc (0.36 mL, 0.1 M). Pd/C (4 mg, 10% w/w) was added and the suspension was subjected hydrogenation (150 psi, 24 °C, 24 hours) in stainless steel autoclave. The resulting mixture was filtered through celite and concentrated *in vacuo*. Analytically pure ketone **2.42a** (14 mg, 0.033 mmol, 93%) was isolated as a white solid without additional purification.

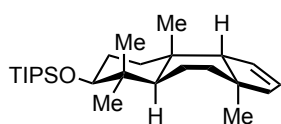
R_f: 0.27 (SiO₂, hexanes : EtOAc = 20:1); **T_{melt.}**: 88.7 – 89.2 °C; **¹H NMR**: (500 MHz, CDCl₃): δ 3.42 (dd, *J* = 10.7, 4.9 Hz, 1H), 2.42 (dd, *J* = 19.2, 8.5 Hz, 1H), 2.34 (d, *J* = 18.7 Hz, 1H), 2.19 (d, *J* = 19.2 Hz, 1H), 1.89 (m, 1H), 1.73 (d, *J* = 18.7 Hz, 1H), 1.63 – 1.53 (m, 5H), 1.46 – 1.37 (m, 2H), 1.07 (s, 21H), 1.03 (s, 6H), 0.94 (m, 1H), 0.85 (m, 1H), 0.79 (s, 3H), 0.77 (s, 3H); **¹³C NMR**: (126 MHz, CDCl₃): δ 221.2, 80.2, 56.7, 53.3, 49.0, 40.5, 39.9, 39.2, 39.1, 37.5, 36.9, 33.3, 29.0, 27.5, 18.9, 18.53, 18.47, 16.4, 15.2, 13.2; **HRMS**: (ES⁺, *m/z*) [M+H]⁺ calcd. for C₂₆H₄₉O₂Si, 421.3502; found, 421.3495.; **IR**: (ATR, neat, cm⁻¹): 2942 (br), 2865 (s), 1743 (s), 1462 (w), 1111 (m), 882 (m).



Synthesis of compound 2.42d:

The enone **2.36b** (7.6 mg, 0.018 mmol, 1.0 equiv.) was dissolved in EtOAc (0.36 mL, 0.05 M). Pd/C (2 mg, 10% w/w) was added and the suspension was subjected hydrogenation (150 psi, 24 °C, 24 hours) stainless steel autoclave. The resulting mixture was filtered through celite and concentrated *in vacuo*. Analytically pure ketone **2.42d** (7.3 mg, 0.018 mmol, 96%) was obtained as a colorless oil without additional purification.

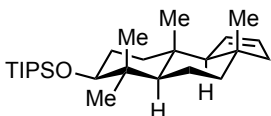
R_f: 0.18 (SiO₂, hexanes/EtOAc = 20:1); **¹H NMR**: (500 MHz, CDCl₃): δ 3.33 (dd, *J* = 11.4, 4.5 Hz, 1H), 2.32 (dd, *J* = 19.1, 12.1 Hz, 1H), 2.24 (dd, *J* = 19.1, 9.0 Hz, 1H), 2.16 (d, *J* = 18.0 Hz, 1H), 2.04 (d, *J* = 18.0 Hz, 1H), 1.81 (dd, *J* = 12.1, 9.0 Hz, 1H), 1.71 (qd, *J* = 13.1, 4.1 Hz, 1H), 1.59 (m, 1H), 1.56 – 1.45 (m, 3H), 1.28 (s, 3H), 1.25 – 1.19 (m, 3H), 1.17 (s, 3H), 1.07 (s, 21H), 1.04 (dd, *J* = 11.2, 2.6 Hz, 1H), 1.00 (s, 3H), 0.80 (s, 3H); **¹³C NMR**: (126 MHz, CDCl₃): δ 218.4, 80.3, 57.2, 56.6, 45.6, 40.8, 39.8, 38.9, 36.4, 36.2, 35.6, 28.8, 27.8, 27.7, 23.8, 18.9, 18.54, 18.47, 16.1, 13.2; **HRMS**: (ES⁺, *m/z*) [M+H]⁺ calcd. for C₂₆H₄₉O₂Si, 421.3502; found, 421.3493.; **IR**: (ATR, neat, cm⁻¹): 2942 (br), 2924 (m), 2865 (m), 1743 (m), 1115 (w), 1042 (w)



Synthesis of compound S2.1:

Enone **2.36a** (405 mg, 0.967 mmol, 1.0 equiv.) was mixed with *p*-toluenesulfonyl hydrazide (360 mg, 1.93 mmol, 2.0 equiv.) in EtOH (8.0 mL, 0.1 M). The solution was heated to 80 °C for 8 hours. Once full conversion was achieved, as judged by TLC, the solution was cooled down, all volatiles were removed *in vacuo*, and the residue was azeotropically distilled with toluene (2 × 0.5 mL). The white foam was redissolved in degassed CHCl₃ (8.0 mL, 0.1 M) under inert atmosphere. The solution was cooled to 0 °C and treated with catecholborane (0.207 mL, 1.93 mmol, 2.0 equiv.). The ice-bath was removed and the reaction was stirred for 1.5 hours. Then NaOAc•3H₂O (395 mg, 2.90 mmol, 3.0 equiv.) was added in one portion and the pale-yellow suspension was heated to 65 °C for an additional 1.5 hours. The resulting thick suspension was cooled down and filtered through celite, and the residual oil was purified by flash chromatography (SiO₂, 100% hexanes). The desired olefin **S2.1** (268 mg, 0.662 mmol, 69%, *d.r.* = 20:1) was isolated as a colorless oil.

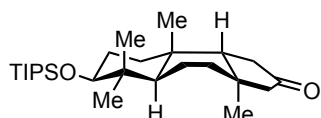
R_f: 0.79 (SiO₂, 100% hexanes); **¹H NMR**: (500 MHz, CDCl₃): δ 5.84 – 5.79 (m, 2H), 3.43 (dd, *J* = 10.5, 6.0 Hz, 1H), 2.34 (m, 1H), 1.97 (dd, *J* = 14.4, 2.9 Hz, 1H), 1.86 (d, *J* = 14.4 Hz, 1H), 1.82 (dd, *J* = 12.4, 9.1 Hz, 1H), 1.78 – 1.72 (m, 2H), 1.66 – 1.60 (m, 2H), 1.58 (dd, *J* = 8.9, 4.3 Hz, 1H), 1.54 (dt, *J* = 13.6, 3.6 Hz, 1H), 1.47 – 1.36 (m, 2H), 1.11 (s, 3H), 1.08 (s, 21H), 1.03 (s, 3H), 1.00 (s, 3H), 0.80 (s, 3H); **¹³C NMR**: (126 MHz, CDCl₃): δ 131.8, 130.4, 80.8, 61.6, 51.0, 45.9, 45.5, 40.3, 35.2, 34.9, 33.7, 29.9, 29.8, 26.3, 24.1, 18.6, 18.58, 18.53, 16.6, 13.3; **HRMS**: (ES⁺, *m/z*) [M-H]⁺ calcd. for C₂₆H₄₇O₂Si, 419.3345; found, 419.3338.; **IR**: (ATR, neat, cm⁻¹): 2941 (br), 2865 (s), 1462 (w), 1105 (s), 1056 (s), 882 (m), 676 (m)



Synthesis of compound S2.2:

The enone **2.36b** (110 mg, 0.263 mmol, 1.0 equiv.) was mixed with *p*-toluenesulfonyl hydrazide (98 mg, 0.525 mmol, 2.0 equiv.) in EtOH (2.5 mL, 0.1 M). The solution was heated to 80 °C for 8 hours. Once full conversion was achieved, as judged by TLC, the solution was cooled down, all volatiles were removed *in vacuo* and the residue was azeotropically distilled with toluene (2 × 0.5 mL). The white foam was redissolved in degassed CHCl₃ (2.5 mL, 0.1 M) under inert atmosphere. The solution was cooled to 0 °C and treated with catecholborane (55 μL, 0.511 mmol, 2.0 equiv.). The ice-bath was removed and the reaction was stirred for 1.5 hours. Then NaOAc•3H₂O (104 mg, 0.767 mmol, 3.0 equiv.) was added in one portion and the pale-yellow suspension was heated to 65 °C for an additional 1.5 hours. The resulting thick suspension was cooled down and filtered through celite, and the residual oil was purified by flash chromatography (SiO₂, 100% hexanes). The desired olefin **S2.2** (76 mg, 0.190 mmol, 73%, *d.r.* = 7:1) was isolated as a colorless oil, which was inseparable from the minor diastereomer.

R_f: 0.80 (SiO₂, 100% hexanes); **¹H NMR**: (500 MHz, CDCl₃, *Major isomer*): δ 5.86 – 5.80 (m, 2H), 3.40 (dd, *J* = 11.3, 4.5 Hz, 1H), 1.92 (m, 2H), 1.88 (d, *J* = 14.2 Hz, 1H), 1.78 (dd, *J* = 8.9, 3.2 Hz, 1H), 1.72 (m, 1H), 1.67 – 1.61 (m, 3H), 1.54 – 1.45 (m, 2H), 1.08 (s, 22H), 0.98 (s, 3H), 0.95 (s, 3H), 0.90 (s, 3H), 0.83 (dd, *J* = 11.7, 2.7 Hz, 1H), 0.79 (s, 3H); (500 MHz, CDCl₃, *Minor isomer, only distinguishable peaks are listed*): δ 5.60 (dq, *J* = 5.6, 2.6 Hz, 1H), 3.37 (dd, *J* = 11.3, 4.2 Hz, 1H), 2.15 (ddt, *J* = 15.7, 4.3, 2.3 Hz, 1H), 2.04 (dt, *J* = 3.5, 1.7 Hz, 1H), 1.23 (s, 3H), 0.96 (s, 3H), 0.78 (s, 3H); **¹³C NMR**: (126 MHz, CDCl₃, *Major isomer S2.2*): δ 131.8, 131.2, 80.5, 67.8, 55.8, 49.2, 47.6, 40.0, 39.1, 39.0, 36.1, 28.6, 27.8, 22.1, 19.7, 18.6, 18.5, 18.2, 15.5, 13.3; (126 MHz, CDCl₃, *Minor isomer S2.2', only distinguishable peaks are listed*): δ 131.1, 129.3, 80.6, 65.7, 49.9, 47.7, 42.5, 39.9, 36.6, 36.3, 36.1, 28.5, 27.9, 22.8, 19.0, 16.0; **HRMS**: (ES⁺, *m/z*) [M–H]⁺ calcd. for C₂₆H₄₇O₂Si, 419.3345; found, 419.3329.; **IR**: (ATR, neat, cm^{–1}): 2941 (br), 2865 (s), 1463 (w), 1111 (s), 1091 (m), 1067 (w), 1052 (w), 882 (m), 676 (w), 658 (m).



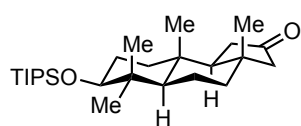
Synthesis of compound 2.42b:

PCC oxidation protocol: Olefin **S2.1** (79 mg, 0.20 mmol, 1.0 equiv.) was dissolved in dry THF (2.0 mL, 0.1 M) under inert atmosphere, cooled down to 0 °C, and treated with BH₃•THF (0.290 mL, 1.0 M, 0.29 mmol, 1.5 equiv.). The

ice bath was removed and the reaction was allowed to stir for 4 hours at ambient temperature. The unreacted borane was quenched with water at 0 °C and the mixture was poured into Et₂O/H₂O (10 mL, 1:1). The organic layer was separated and the aqueous layer was washed with Et₂O (3 × 5 mL). Combined organic phases were dried over MgSO₄, filtered, and concentrated *in vacuo*. Water was azeotropically removed by distillation with benzene (1 mL) and dried for 2 hours *in vacuo*. The resulting clear oil was redissolved in CH₂Cl₂ (2.0 mL, 0.1 M), and 4Å mol. sieves (10 mg) and PCC (290 mg, 1.4 mmol, 7.0 equiv.) were added under inert atmosphere. The reaction was heated to 45 °C and stirred for 3 hours. The resulting solution was cooled down and partitioned between CH₂Cl₂ (10 mL) and water (10 mL). The organic layer was separated and the aqueous layer was washed with CH₂Cl₂ (2 × 5 mL). Combined organic phases were dried over MgSO₄, filtered, concentrated *in vacuo*, and purified by flash chromatography (SiO₂, 1% Et₂O in hexanes). Desired ketone **2.42b** (53 mg, 0.130 mmol, 65%) was isolated as a colorless oil.

One-pot protocol: Olefin **S2.1** (50 mg, 0.120 mmol, 1.0 equiv.) was dissolved in dry THF (0.60 mL, 0.2 M) under inert atmosphere, cooled down to 0 °C and treated with BH₃•THF (0.190 mL, 1.0 M, 1.5 equiv.). The ice-bath was removed and the reaction was allowed to stir for 4 hours at ambient temperature. In a separate vial, a solution of pyridine (0.5 mL, 6.2 mmol, 50 equiv.) in CH₂Cl₂ (3.1 mL, 2.0 M) was treated with CrO₃ (310 mg, 3.1 mmol, 25 equiv.) in portions over the course of 10 min at 0 °C, warmed up to 24 °C, and stirred for additional 30 min. The resulting suspension of CrO₃•2py was slowly added to the reaction mixture over the course of 10 min. Stirring was continued for another 20 min. The suspension was passed through a celite plug, washed with HCl (1.0 M, 10 mL), concentrated *in vacuo*, and purified by flash chromatography (SiO₂, 1% Et₂O in hexanes). Desired ketone **2.42b** (25 mg, 0.059 mmol, 48%) was isolated as a colorless oil.

R_f: 0.23 (SiO₂, hexanes : EtOAc = 20:1); **¹H NMR**: (500 MHz, CDCl₃): δ 3.43 (m, 1H), 2.18 – 2.07 (m, 3H), 1.94 (d, *J* = 16.9 Hz, 1H), 1.90 (dd, *J* = 13.4, 8.6 Hz, 1H), 1.80 – 1.70 (m, 4H), 1.67 (dd, *J* = 12.9, 8.4 Hz, 1H), 1.61 (dd, *J* = 12.3, 1.4 Hz, 1H), 1.52 – 1.45 (m, 1H), 1.44 – 1.39 (m, 1H), 1.32 (dt, *J* = 12.7, 3.7 Hz, 1H), 1.15 (s, 3H), 1.07 (s, 21H), 1.02 (s, 3H), 1.01 (s, 3H), 0.81 (s, 3H); **¹³C NMR**: (126 MHz, CDCl₃): δ 218.7, 80.5, 60.2, 52.8, 47.1, 40.4, 38.8, 37.0, 35.9, 35.3, 33.7, 29.62, 29.55, 25.9, 23.3, 18.5, 18.6, 17.9, 16.6, 13.2; **HRMS**: (ES⁺, *m/z*) [M+H]⁺ calcd. for C₂₆H₄₉O₂Si, 421.3502; found, 421.3487.; **IR**: (ATR, neat, cm⁻¹): 2943 (m), 2865 (w), 1744 (s), 1114 (w), 1098 (w), 1060 (w), 733 (s)



Synthesis of compound 2.42c:

PCC oxidation protocol: Olefin **S2.2** (76 mg, 0.19 mmol, 1.0 equiv.) was dissolved in dry THF (1.9 mL, 0.1 M) under inert atmosphere, cooled down to 0 °C, and treated with $\text{BH}_3 \cdot \text{THF}$ (0.290 mL, 1.0 M, 0.29 mmol 1.5 equiv.). The ice bath was removed and the reaction was allowed to stir for 4 hours at ambient temperature. The unreacted borane was quenched with water at 0 °C and the mixture was poured into $\text{Et}_2\text{O}/\text{H}_2\text{O}$ (10 mL, 1:1). The organic layer was separated and the aqueous layer was washed with Et_2O (3 \times 5 mL). Combined organic phases were dried over MgSO_4 , filtered, and concentrated *in vacuo*. Water was azeotropically removed by distillation with benzene (1 mL) and dried *in vacuo* for 2 hours. The resulting clear oil was redissolved in CH_2Cl_2 (1.9 mL, 0.1 M), and 4Å mol. sieves (10 mg) and PCC (280 mg, 1.3 mmol, 7.0 equiv.) were added under inert atmosphere. The reaction was heated to 45 °C and stirred for 3 hours. The resulting solution was cooled down and partitioned between CH_2Cl_2 (10 mL) and water (10 mL). The organic layer was separated and the aqueous layer was washed with CH_2Cl_2 (2 \times 5 mL). Combined organic phases were dried over MgSO_4 , filtered, and concentrated *in vacuo*, and purified by flash chromatography (SiO_2 , 1% Et_2O in hexanes). Desired ketone **2.42c** (50 mg, 0.12 mmol, 63%) was isolated as a colorless oil that solidifies upon storage.

R_f: 0.21 (SiO_2 , hexanes : EtOAc = 20:1); **T_{melt.}:** 64.1 – 64.9 °C; **¹H NMR:** (500 MHz, CDCl_3): δ 3.41 (dd, J = 11.2, 4.8 Hz, 1H), 2.12 – 2.02 (m, 2H), 2.02 (d, J = 16.9 Hz, 1H), 1.96 (d, J = 16.9 Hz, 1H), 1.90 (dt, J = 12.6, 3.2 Hz, 1H), 1.73 – 1.67 (m, 2H), 1.66 – 1.60 (m, 1H), 1.59 (m, 1H), 1.56 – 1.50 (m, 2H), 1.43 – 1.34 (m, 2H), 1.07 (s, 21H), 1.00 (s, 3H), 0.97 (s, 3H), 0.94 (dd, J = 12.2, 2.5 Hz, 1H), 0.90 (s, 3H), 0.81 (s, 3H); **¹³C NMR:** (126 MHz, CDCl_3): δ 218.7, 80.5, 58.6, 58.4, 56.2, 40.6, 40.3, 40.1, 38.7, 36.2, 35.9, 28.5, 27.6, 21.2, 19.2, 18.54, 18.47, 15.8, 15.4, 13.2; **HRMS:** (ES+, m/z) [$\text{M}+\text{H}$]⁺ calcd. for $\text{C}_{26}\text{H}_{49}\text{O}_2\text{Si}$, 421.3502; found, 421.3490.; **IR:** (ATR, neat, cm^{-1}): 2941 (br), 2865 (m), 1744 (s), 1463 (w), 1110 (s), 1062 (m), 882 (w), 677 (w)

2.6 Acknowledgment of Contributions

Y. D. Boyko formulated concept of the general blueprint and designed overall strategy. S. A. Shved performed computational analysis, optimized geometries and computed *I*-strain for the isomeric structures of perhydrobenz[*e*]nindene core. Y. D. Boyko, Z. Yi and S. Ning explored

stereodivergency of Rautenstrauch cycloisomerization. S. Ning conducted experiments and analyzed results *en route* towards polyveoline. The rest of synthetic work, experimental design and analysis was carried out by Y. D. Boyko.

2.7 References

1. M. S. Butler, *J. Nat. Prod.* **2004**, *67*, 2141–2153.
2. The statement has exceptions and is, perhaps, oversimplification that was used for more lucid narrative. For example, stelletin E is proposed to target oxy-sterol binding protein with its lipophilic core as a competitive inhibitor. A. W. G. Burgett, T. B. Poulsen, K. Wangkanont, D. R. Anderson, C. Kikuchi, K. Shimada, S. Okubo, K. C. Fortner, Y. Mimaki, M. Kuroda, J. P. Murphy, D. J. Schwalb, E. C. Petrella, I. Cornella-Taracido, M. Schrire, J. A. Tallarico, M. D. Shair, *Nat. Chem. Biol.* **2011**, *7*, 639–647.
3. R. W. I. I. Huigens, K. C. Morrison, R. W. Hicklin, T. A. Flood, M. F. Richter, P. J. Hergenrother, *Nat. Chem.* **2013**, *5*, 195–202.
4. S.-T. Fang, B.-F. Yan, C.-Y. Yang, F.-P. Miao, N.-Y. Ji, *J. Antibiot.* **2017**, *70*, 1043–1046.
5. V. R. de la Parra, V. Mierau, T. Anke, O. Sterner, *Tetrahedron* **2006**, *62*, 1828–1832.
6. R. Hocquemiller, G. Dubois, M. Leboeuf, A. Cavé, N. Kunesch, C. Riche, A. Chiaroni, *Tetrahedron Lett.* **1981**, *22*, 5057–5060.
7. S. F. Kouam, A. W. Ngouonpe, M. Lamshöft, F. M. Talontsi, J. O. Bauer, C. Strohmman, B. T. Ngadjui, H. Laatsch, M. Spiteller, *Phytochemistry* **2014**, *105*, 52–59.
8. A. Akhaouzan, A. Fernández, A. I. Mansour, E. Alvarez, A. Haidöur, R. Alvarez-Manzaneda, R. Chahboun, E. Alvarez-Manzaneda, *Org. Biomol. Chem.* **2013**, *11*, 6176–6185.
9. X. Chen, D. Zhang, D. Xu, H. Zhou, G. Xu, *Org. Lett.* **2020**, *22*, 6993–6997.
10. S. Xu, J. Gu, H. Li, D. Ma, X. Xie, X. She, *Org. Lett.* **2014**, *16*, 1996–1999.
11. L. Yang, D. E. Williams, A. Mui, C. Ong, G. Krystal, R. van Soest, R. J. Andersen, *Org. Lett.* **2005**, *7*, 1073–1076.
12. E. Alvarez-Manzeneda, R. Chahboun, E. Alvaerz, A. Fernández, R. Alvarez-Manzeneda, A. Haidöur, J. M. Ramos, A. Akhaouzan, *Chem. Comm.* **2012**, *48*, 606–608.

13. F. Jimenez, A. Fernández, E. Boulifa, A. I. Mansour, R. Alvarez-Manzeneda, R. Chahboun, E. Alvarez-Manzeneda, *J. Org. Chem.* **2017**, *82*, 9550–9559.
14. B. N. Kakde, N. Kumar, P. K. Mondal, A. Bisai, *Org. Lett.* **2016**, *18*, 1752–1755.
15. C. Mirand, M. D. de Maindreville, D. Cartier, J. Lévy, *Tetrahedron Lett.* **1987**, *28*, 3565–3568.
16. F. Neese, *Wiley Interdiscip. Rev. Comput. Mol. Sci.* **2012**, *2*, 73–78.
17. S. Grimme, J. G. Brandenburg, C. Bannwarth, A. Hansen, *J. Chem. Phys.* **2015**, *143*, 054107.
18. E. Paulechka, A. Kazakov, *J. Phys. Chem. A* **2017**, *121*, 4379–4387.
19. T. Tsunoda, F. Ozaki, S. Itô, *Tetrahedron Lett.* **1994**, *35*, 5081–5082.
20. C. Nieto-Oberhuber, S. López, A. M. Echavarren, *J. Am. Chem. Soc.* **2005**, *127*, 6178–6179.
21. V. Rautenstrauch, *J. Org. Chem.* **1984**, *49*, 950–952.
22. P. A. Caruana, A. J. Frontier, *Tetrahedron*, **2007**, *63*, 10646–10656.
23. J. King, P. Quayle, J. F. Malone, *Tetrahedron Lett.* **1990**, *31*, 5221–5224.
24. W. D. Wulff, P.-C. Tang, K.-S. Chan, J. S. McCallum, D. C. Yang, S. R. Gilbertson *Tetrahedron*, **1985**, *41*, 5813–5832.
25. A. R. Chamberlin, S. H. Bloom, *Org. React.* **1990**, *39*, 1–83.
26. D. P. Ojha, K. R. Prabhu, *Org. Lett.* **2015**, *17*, 18–21.
27. C. A. Merlic, C. C. Aldrich, J. Albaneze-Walker, A. Saghatelian, *J. Am. Chem. Soc.* **2000**, *122*, 3224–3225.
28. W. D. Wulff, K. S. Chan, P. C. Tang, *J. Org. Chem.* **1984**, *49*, 2293–2295.
29. T. Nishimura, A. K. Unni, S. Yokoshima, T. Fukuyama, *J. Am. Chem. Soc.* **2013**, *135*, 3243–3247.
30. P. Brownbridge, T.-H. Chan, *Tetrahedron Lett.* **1980**, *21*, 3423–3426.
31. S. Cacchi, G. Fabrizi, A. Goggiamani, L. M. Parisi, R. Bernini, *J. Org. Chem.* **2004**, *69*, 5608–5614.
32. C. He, J. Hu, Yu. Wu, H. Ding, *J. Am. Chem. Soc.* **2017**, *139*, 6098–6101.
33. N. A. Godfrey, D. J. Schatz, S. V. Pronin, *J. Am. Chem. Soc.* **2018**, *140*, 12770–12774.
34. J. M. Fox, X. Huang, A. Chieffi, S. L. Buchwald, *J. Am. Chem. Soc.* **2000**, *122*, 1360–1370.

35. J. L. Rutherford, M. P. Rainka, S. L. Buchwald, *J. Am. Chem. Soc.* **2002**, *124*, 15168–15169.
36. P. Gao, P. S. Portoghese, *J. Org. Chem.* **1995**, *60*, 2276–2278.
37. K. Chen, G. F. Koser *J. Org. Chem.* **1991**, *56*, 5764–5767.
38. S. A. Kozmin, V. H. Rawal, *J. Am. Chem. Soc.* **1998**, *120*, 13523–13524.
39. A. D. Napper, J. Hixon, T. McDonagh, K. Keavey, J.-F. Pons, J. Barker, W. T. Yau, P. Amouzegh, A. Flegg, E. Hamelin, R. J. Thomas, M. Kates, S. Jones, M. A. Navia, J. O. Daunders, P. S. DiStefano, R. Curtis, *J. Med. Chem.* **2005**, *48*, 8045–8054.
40. B.-Y. Lim, B.-E. Jung, C.-G. Cho, *Org. Lett.* **2014**, *16*, 4492–4495.

CHAPTER 3. TOTAL SYNTHESIS OF NORCEMBRANOID DITERPENOIDS

3.1 Introduction

Marine sponges and corals along the course of evolution have developed mechanisms of self-defense in their native competitive environments. One of these mechanisms is chemical defense with toxic secondary metabolites that allow producing species to grow and prosper. Once appreciated, marine flora and fauna became rich sources of bioactive molecules for researchers, with potential applications in drug development such as cancer treatment. In many cases these secondary metabolites demonstrate not only high cytotoxicity, but also remarkable selectivity, which allow them to become viable drug leads with wide therapeutic window. FDA-approved drugs or advanced candidates in clinical trials such as Yondelis[®] (3.1), Zalypsis[®] (3.2), Vira-A[®] (3.3), Halaven[®] (3.4), Bryostatin 1 (3.5), etc. showcase the ultimate success of this strategy for the pharmaceutical industry (Chart 3.1).¹

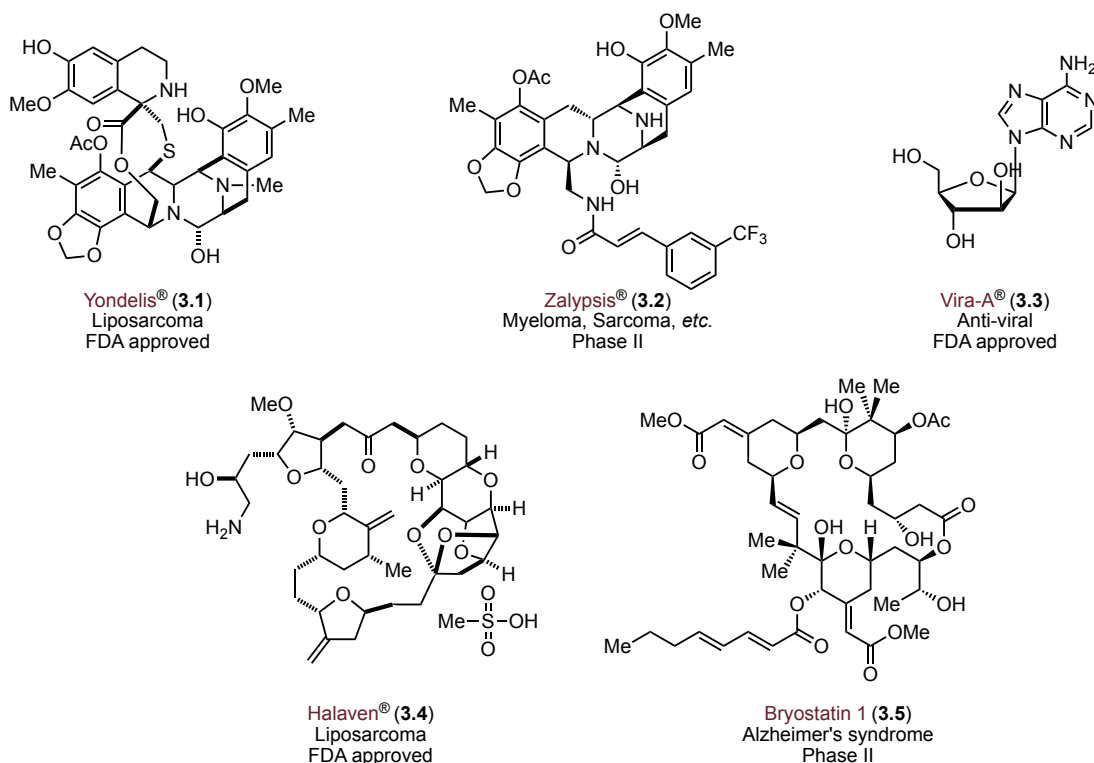


Chart 3.1 Marine natural products in modern pharmacopeia.

Since the late 90's, *Sinularia* genus (*Alcyoniidae* family) of soft coral, globally occurring in temperate and tropical seas, has been established as a unique source of polycyclic

furanobutenolide-derived norcembranoids (Figure 3.2, **3.6**).²⁻⁹ These natural products have demonstrated moderate cytotoxicity and anti-inflammatory activity; however, no detailed studies have been conducted, primarily due to low isolation yields. Specificity, generality of chemotype, and most importantly mechanism of action is yet to be determined. Structurally, furanobutenolide-derived norcembranoids are characterized by a highly oxygenated polycyclic architecture with a conserved [5,5]-bicyclic lactone, cyclohexa- or cycloheptanone central ring with additional attached cycle on the periphery. Some of the norcembranoids (e.g., ineleganolide (**3.7**), sinulochmodin C (**3.8**), Chart 3.2) are further decorated with overarching dihydrofuran, bringing

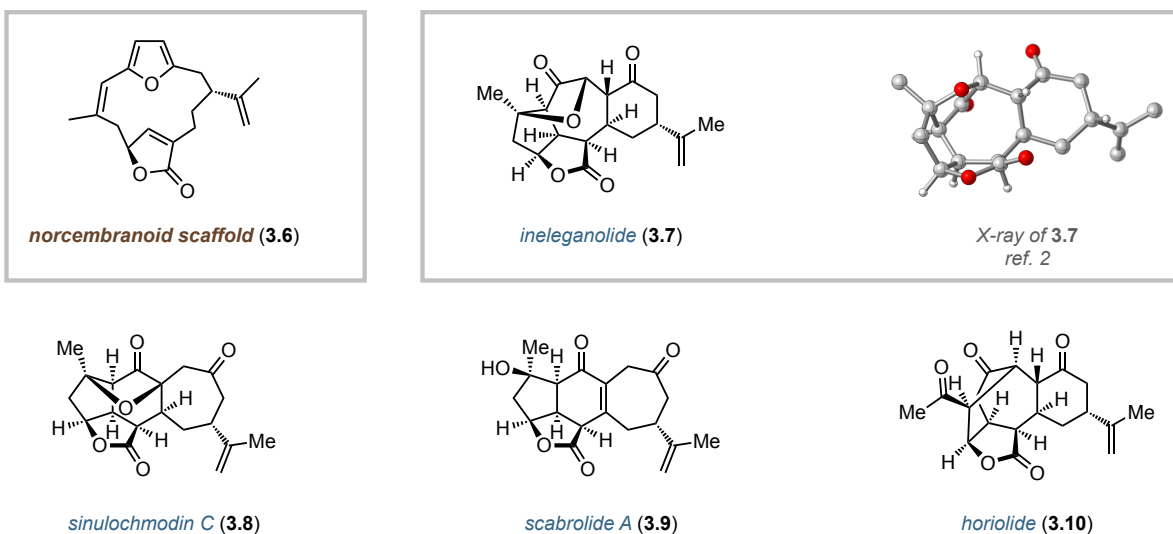


Chart 3.2 Furanobutenolide-derived norcembranoid natural products.

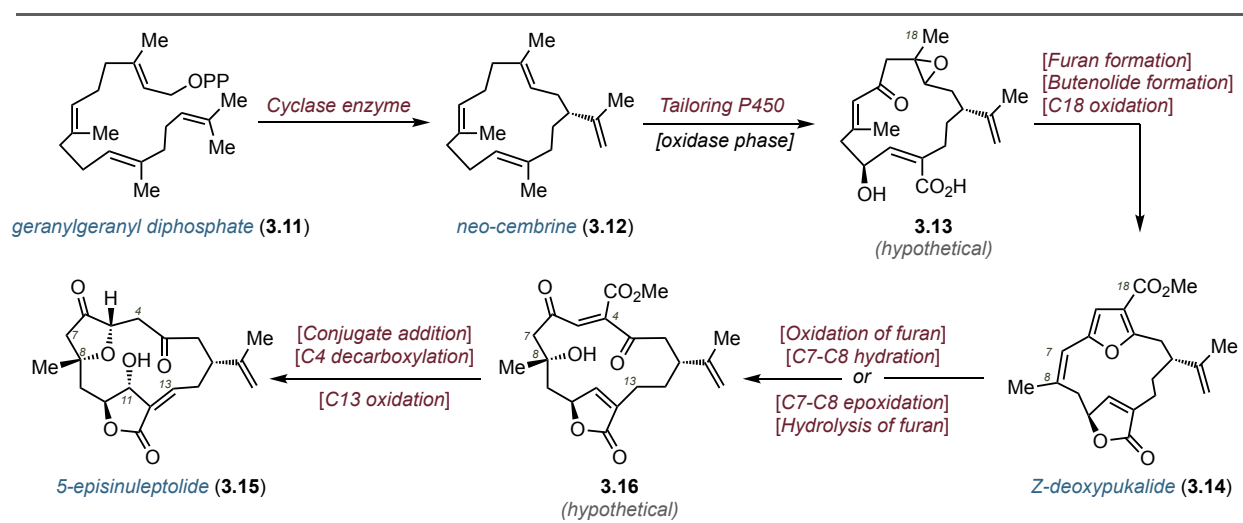
an additional level of complexity. Given the intricate structure and potential utility of the scaffold for further biological investigations, this family of natural products has drawn lots of attention from the synthetic community. Rightfully, ineleganolide (**3.7**) was recognized as a flagship member of the family with a challenging cupped pentacyclic skeleton containing nine stereocenters, eight of which are contiguous, and a highly decorated central seven-membered ring. Historically, most of the reported synthetic studies were directed towards ineleganolide, albeit none of them led to ultimate success. Notably, **3.7** was synthesized by Pattenden in 2011 via biomimetic semisynthesis (for details see Scheme 3.3).¹⁰ Admiring and challenged by structural complexity of ineleganolide, we embarked on its total synthesis. It is worthwhile to mention that at the moment of initiation of this project in our laboratory, none of the furanobutenolide-derived norcembranoid had been synthesized de novo, despite their original isolation and structural

characterization nearly two decades ago. Only recently, in 2020, has the Stoltz group reported on first total synthesis of (–)-scabrolide A (**3.9**) (for discussion see p. 143).¹¹

3.2 Background

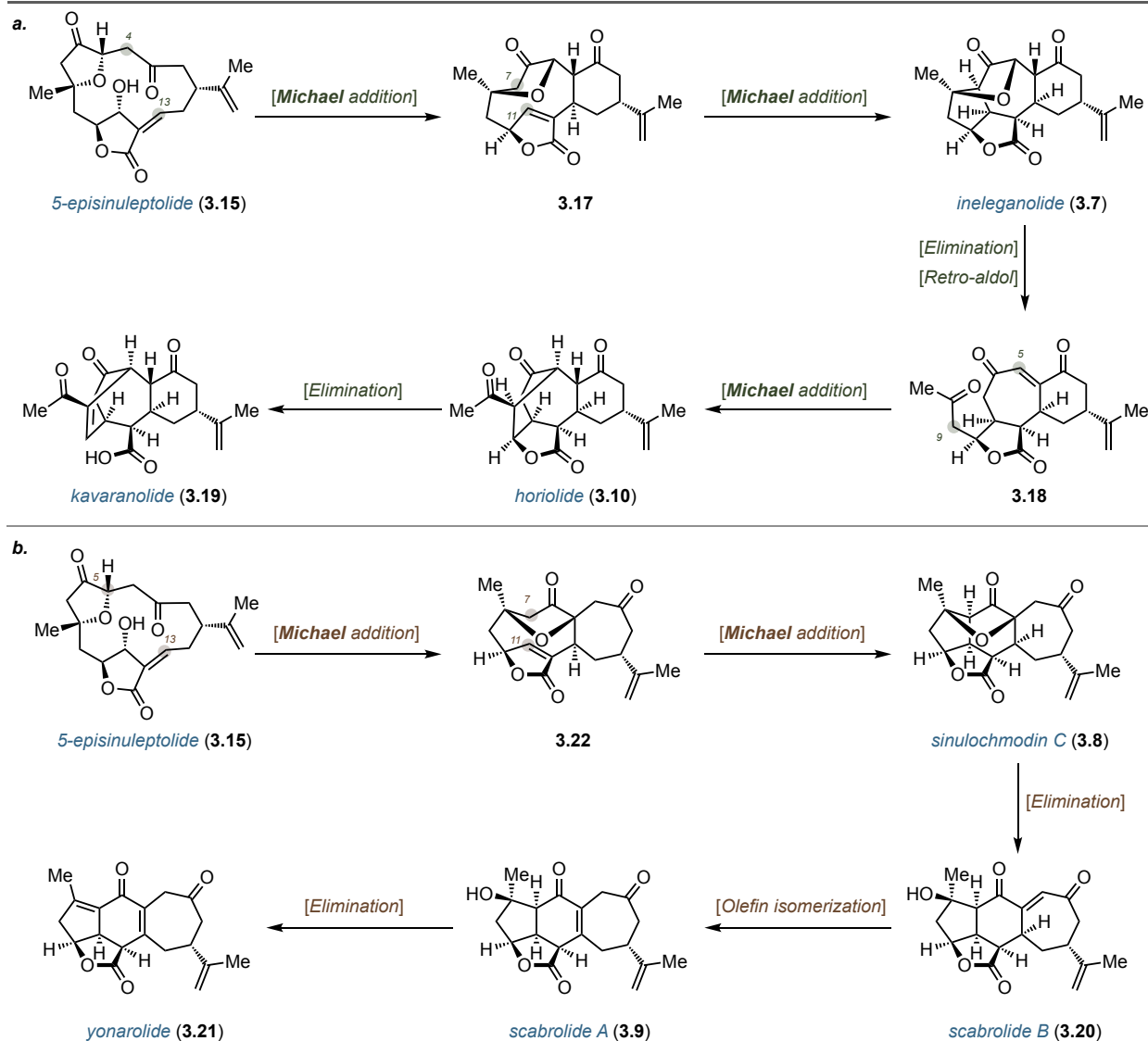
3.2.1 Biosynthesis

Extensive biosynthetic studies of norcembranoids (C_{19}) along with their close relatives, cembranoid diterpenoids (C_{20}), were carried out by Pattenden,¹² Trauner¹³ and others. Important to note as an outset that there is little known on which genes and enzymes are involved in the biosynthesis of these marine natural products. The relationship between metabolites and their potential interconversion was proposed based on the structures of co-occurring congeners, chemical behavior in vitro and general understanding of available repertoire of transformations in vivo.



Scheme 3.1 Biosynthesis of macrocyclic norcembranoid **3.15**.

As postulated, geranylgeranyl diphosphate (**3.11**) undergoes venerable polyene cyclization to render 14-membered macrocycle, neo-cembrene (**3.12**, Scheme 3.1). Then, tailoring P450 enzymes catalyze multiple oxidation events of the carbon skeleton to afford hypothetical intermediate **3.13**. Following lactonization and furan formation via cyclodehydration along with C18 oxidation leads to **Z-deoxypukalide (3.14)**, the common biosynthetic precursor for both cembranoid and norcembranoid diterpenoids. In order to link **3.14** with 5-episinuleptolide (**3.15**), the established progenitor of norcembranoids, the following sequence of events was proposed:



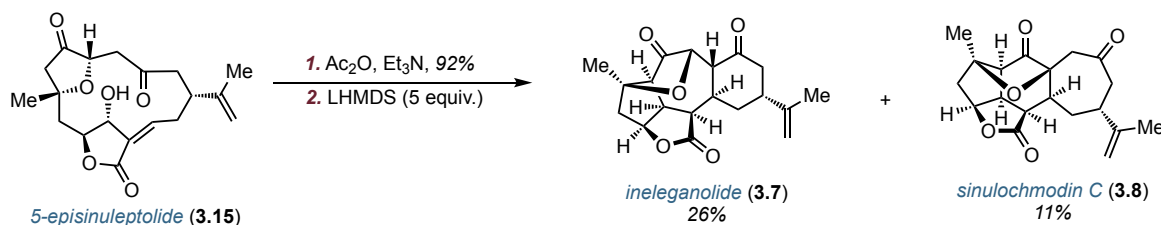
Scheme 3.2.a Proposed biosynthesis of ineleganolide and related norcembranoids; **b** Proposed biosynthesis of scabrolide B and related norcembranoids.

oxidative opening of the furan, hydration of C8-C7 olefin followed by putative transannular conjugate addition. Alternatively, the precursor for the cyclization reaction **3.16** can be formed via C8-C7 epoxidation / hydrolytic cleavage of the furan. At this point, the envisioned intermediate is susceptible towards decarboxylation at C4, presumably by a decarboxylase enzyme. Final oxidative tailoring of C13 furnishes *macrocylic* norcembranoid **3.15**, which co-occurs with more elaborate *polycyclic* norcembranoids in *Sinularia*. Ineleganolide (**3.7**), as well as other related norcembranoids that share central seven-membered rings could be formed by *6-exo-trig* cyclization within 5-episinuleptolide framework followed by transannular Michael addition from

the C7 center (Scheme 3.2.a). In turn, ineleganolide can undergo retro-conjugate addition and retro-aldol reaction to yield ketone **3.18**. Given that **3.18** has not been isolated from natural sources, it is postulated that subsequent intramolecular Michael reaction occurs spontaneously yielding horiolide (**3.10**). Simple dehydration would furnish kavaranolide (**3.19**) respectively.

5-Episinuleptolide (**3.15**) also provides a viable biosynthetic route towards sinulochmodin C (**3.8**), scabrolide B (**3.20**), scabrolide A (**3.9**) and yonarolide (**3.21**). These compounds are characterized by the central six-membered ring whereas the seven-membered cycle is located at the periphery (Scheme 3.2b). First, Michael addition at C4 is envisioned that yields cycloheptanone within the framework of **3.22**. Next, another Michael addition at C7 can furnish sinulochmodin C (**3.7**), while additional elimination delivers scabrolide B (**3.20**). Olefin isomerization to the more substituted position leads to scabrolide A (**3.9**). Finally, dehydration yields yonarolide (**3.21**). Notably, while the olefin isomerization within scabrolide B seems to be thermodynamically unfavorable due to loss of additional conjugation with cycloheptanone, experimental evidence indirectly suggests the viability of this process.

To support their biosynthetic speculations, Pattenden and co-workers attempted a biomimetic semisynthesis of ineleganolide (**3.7**) (Scheme 3.3).¹⁰ Treatment of 5-episinuleptolide, (**3.15**) obtained from the natural isolate, with acetic anhydride to convert C11 alcohol into appropriate nucleofuge followed by excess of LHMDS indeed delivered ineleganolide (**3.7**) as the major product. Notably, sinulochmodin C (**3.8**) was also obtained as a minor component of the reaction. The latter can be attributed to partial equilibration of enolates from C4 to more acidic C5 position under reaction conditions. Importantly, these results provide additional support for the proposed biosynthetic routes and offer avenue for biomimetic total synthesis of norcembranoid diterpenoids.



Scheme 3.3 Semisynthesis of ineleganolide.

3.2.2 Synthetic studies towards ineleganolide and other norcembranoids

Within the span of the last ten years many research groups disclosed their attempts towards norcembranoid diterpenoids. Nicolaou, Frontier, Romo and Moeller designed distinct approaches towards ineleganolide (Figure 3.1).¹⁴⁻¹⁷ Accordingly, Nicolaou and Pratt attempted a biomimetic approach and constructed the macrocycle first.¹⁴ No success has been achieved as desired lactone **3.23** could not be obtained from synthesized intermediate **3.24**. Romo and Liu, in turn, attempted transannular C–H-insertion to forge [5,5]-bicycle, however this strategy failed while studying the model system.¹⁶ Finally, Moeller and Tang attempted to construct medium-size ring (**3.28**) employing an electrochemical oxidation.¹⁷ This manifold did not deliver expected results due to spatial separation of coupling terminals within the substrate **3.27**.

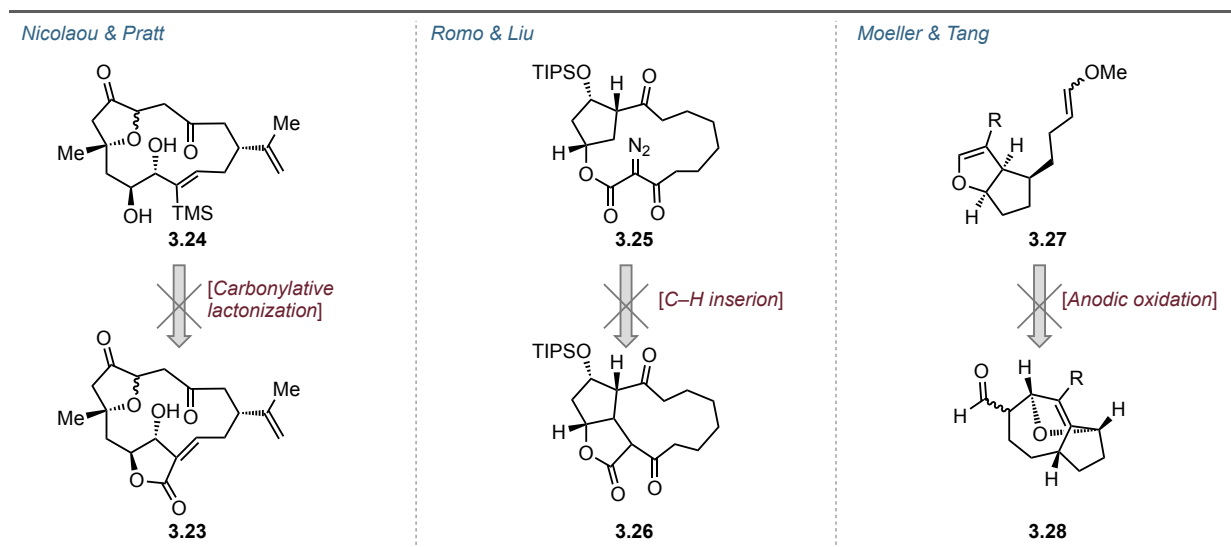
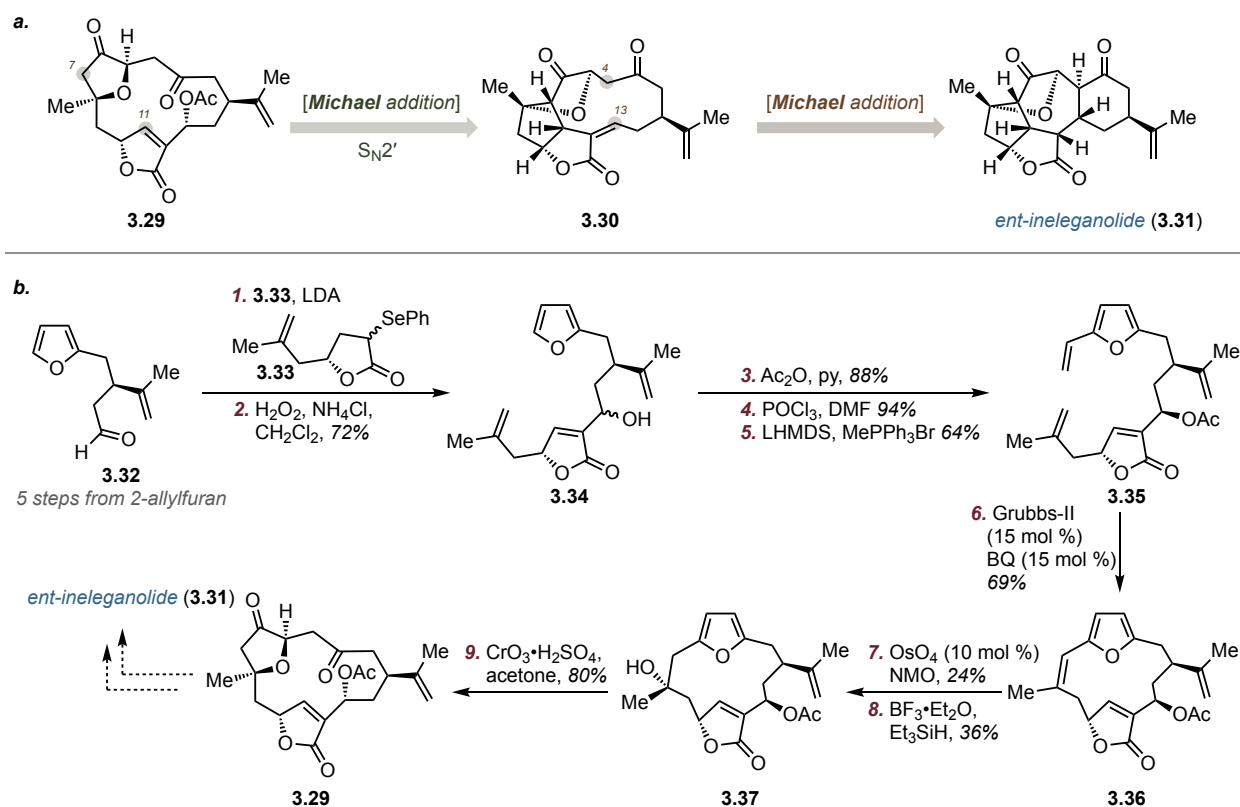


Figure 3.1 Previous synthetic studies towards ineleganolide.

Recently Gaich and Breunig reported a biomimetic approach towards ineleganolide.¹⁸ The central goal was to synthesize constitutional isomer of 5-episinuleptolide **3.29**, which would allow for interception of the pathway reported by Pattenden (Scheme 3.4). It was hypothesized that inverse order of carbon bond forming events can be executed with identical outcome. Namely, C7-C11 bond construction was envisioned first via addition / elimination mechanism, followed by second cyclization establishing C4-C13 connectivity. In a forward sense, two elaborate fragments **3.32** and **3.33** were coupled through aldol reaction followed by installation of the C11-C12 olefin in 72% yield. The mixture of diastereomeric alcohols **3.34** was acetylated. Formylation of the furan moiety was carried out followed by Wittig olefination. The basic conditions of the latter step also allowed for convergence of diastereomers at C13 position delivering compound **3.35** in 53% over

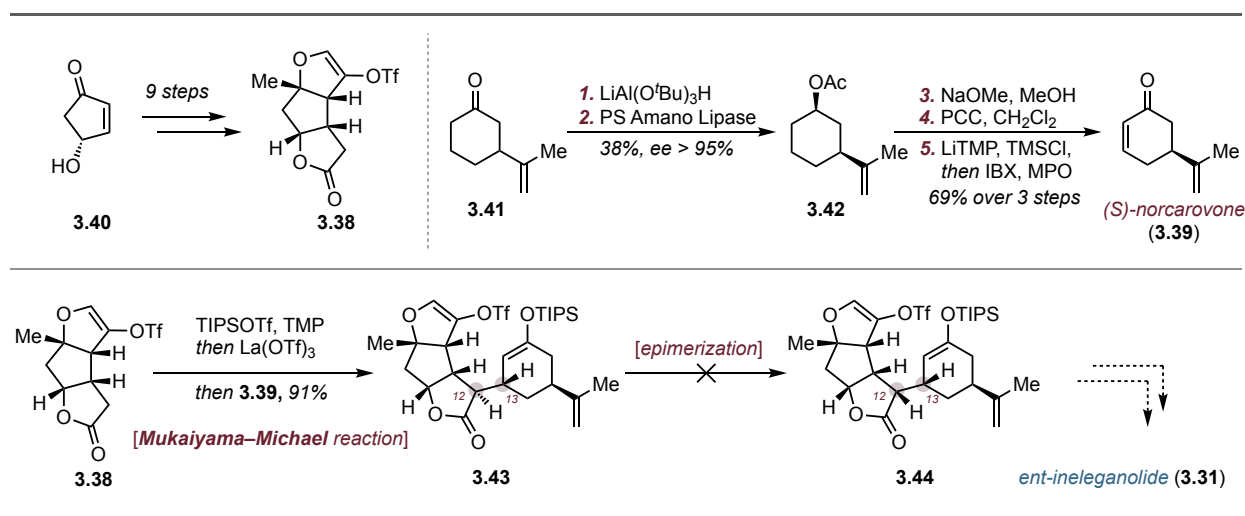
3 steps. Macrocycle **3.36** was formed employing standard RCM in 69% yield. Dihydroxylation of the more electron-rich olefin and subsequent chemoselective ionic reduction of benzylic alcohol furnished compound **3.37**, albeit in low yield. Mimicking the biosynthetic proposal, furan was oxidatively opened under Jones condition affording key intermediate **3.29** in 80% yield. As was noted, further explorations were halted due to initially observed undesired reactivity of **3.29** coupled with low throughput of material, which hampered required more in-depth studies.



Scheme 3.4 Synthetic studies towards ineleganolide by Gaich and Breunig. **a** central hypothesis; **b** synthetic sequence towards key intermediate **3.29**.

Another convergent approach towards ineleganolide was reported by Vanderwal and co-workers (Scheme 3.5).^{19,20} *Ent*-ineleganolide (**3.31**) was retrosynthetically traced back to two chiral building blocks: **3.38** and **3.39**, through intermolecular Mukaiyama-Michael and oxocarbenium cyclization transforms. Tricyclic all-*cis* configured building block **3.38** was synthesized from readily available hydroxycyclopentenone **3.40** in 9 steps using conventional transformations. In turn, norcarvone (**3.39**), frequently employed in synthetic attempts towards norcembranoids, was obtained in 5 steps. Ketone **3.41** was diastereoselectively reduced with bulky hydride reagent, followed by enzymatic kinetic resolution with lipase. The acetate **3.42** with

required configuration was subsequently hydrolyzed and oxidized. Unsaturation was installed under Nicolaou oxidation conditions. The first key transformation proceeded smoothly: coupling between **3.38** and **3.39** delivered **3.43** in 91% yield with exquisite diastereoselectivity. Guided by the bowl-like shape of the **3.38**, addition occurred from convex face. Notably, configuration at C13 corresponded to one in the natural product and was dictated by the isopropenyl unit that adopted pseudo-equatorial orientation. The obtained undesired configuration at C12 was anticipated by the authors and subsequent epimerization to **3.44** was planned to correct that stereocenter. However, neither direct epimerization nor more elaborate multi-step strategies were successful. Thus, ineleganolide remained unconquered once again.



Scheme 3.5 Synthetic studies towards ineleganolide by Vanderwal and co-workers.

A series of four publications details the significant progress in the area of the synthesis of norcembranoids made by the Stoltz group.²¹⁻²⁵ Divinylcyclopropane rearrangement was recognized as the key transform en route towards **3.31** to construct central seven-membered ring and serves as the main theme of their research program. While this crucial transformation enabled construction of the complete core of the natural product, downstream functional group interconversion turned out to be challenging. Various perturbations of the original retrosynthetic analysis were examined to bypass observed undesired reactivities. Thus, only one of such modifications will be discussed herein, which delivered the most advanced intermediate and also illuminated the important features that guided our synthetic endeavor.²⁴

Ent-ineleganolide was sought to be accessed through intermediacy of **3.45** via double olefin isomerization into conjugation with both carbonyl groups followed by conjugate addition to form

dihydrofuran motif (Figure 3.2). Ketone **3.45** was traced back to the cyclopropane **3.46** through oxidative manipulation of the olefin within **3.47** and the preceding central transform: Cope rearrangement. Compound **3.46** in turn was further disconnected to the acid **3.49** and alcohol **3.50** through intramolecular cyclopropanation and esterification.

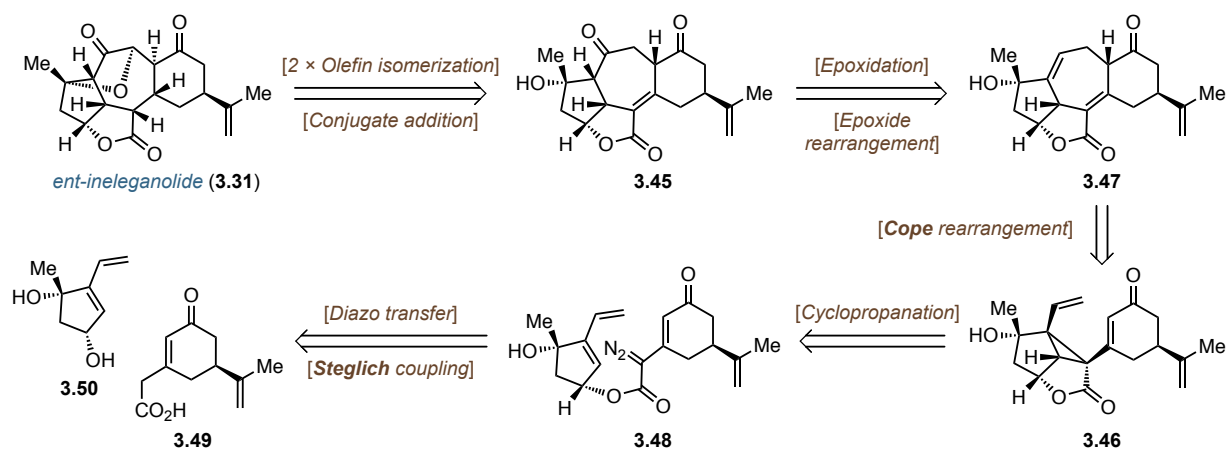
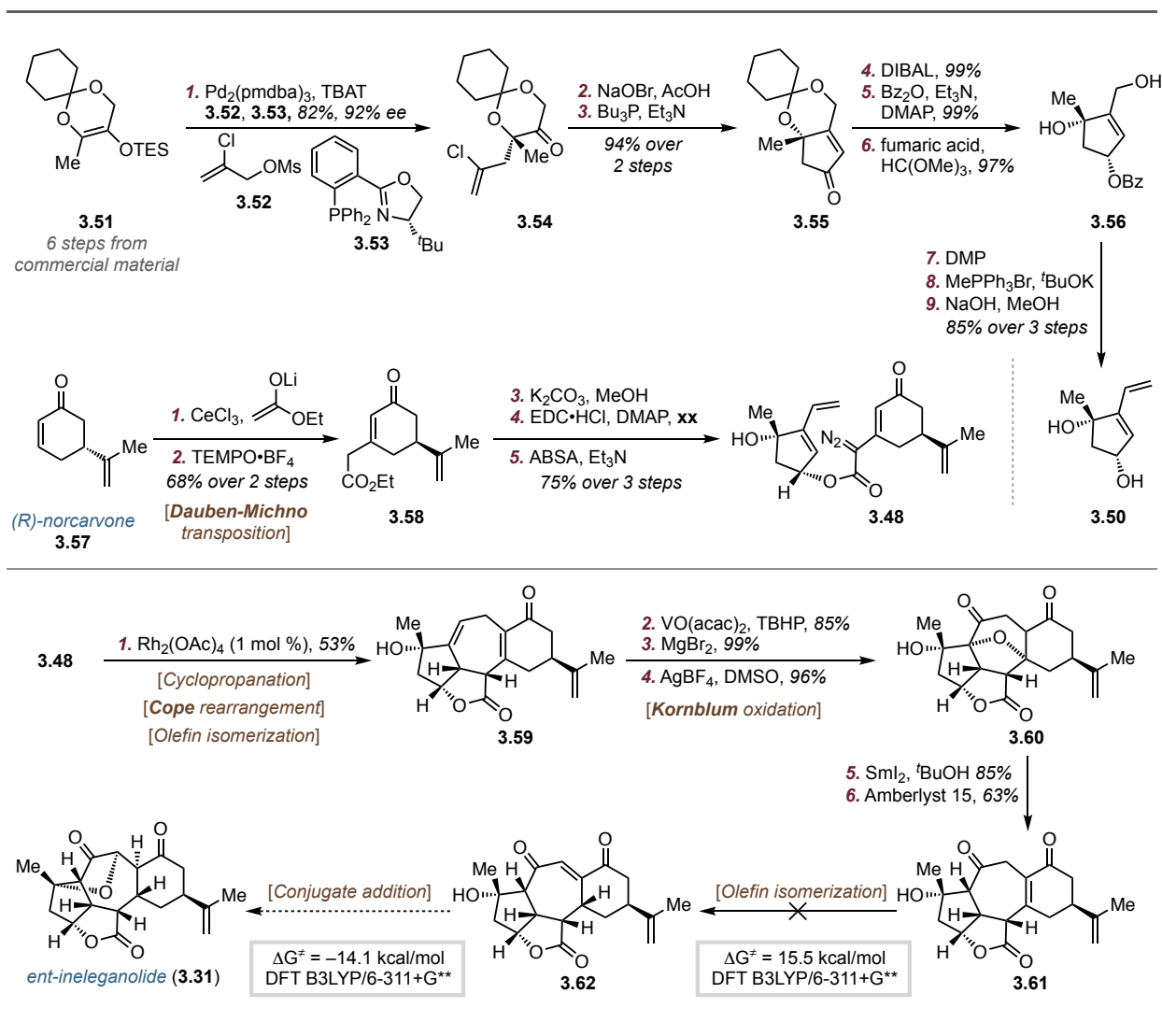


Figure 3.2 Retrosynthesis devised by Stoltz and co-workers towards *ent*-ineleganolide.

In the forward direction, silyl enol ether **3.51**, synthesized in 6 steps from commercial material, was subjected to asymmetric allylation, delivering product **3.54** in 82% with good enantioselectivity (Scheme 3.6). Vinyl chloride **3.54** was transformed into bromo-ketone, which was further subjected to intramolecular Horner–Wittig olefination in 94% yield over two steps. Resulting enone **3.55** underwent 1,2-reduction with DIBAL, followed by benzylation and diol deprotection under acidic conditions, affording **3.56** in 96% yield over three steps. Finally, the coupling partner **3.50** was prepared in 85% yield through a three-step sequence consisting of Dess–Martin oxidation, Wittig methylenation and benzoyl hydrolysis. The acid coupling partner **3.49** was prepared from (*R*)-norcarvone (**3.57**), which was subjected to 1,2-addition of lithium enolate of ethyl acetate. TEMPO-derived nitrosonium-mediated oxidative transposition of the adduct furnished enone **3.58** in 68% over two steps. The acid **3.49** obtained via hydrolysis of the ethyl ester was subjected to the Steglich coupling with alcohol **3.50** followed by diazo transfer using ABSA. Thus, the precursor for the key cyclopropanation / rearrangement sequence **3.48** was obtained in 75% based on alcohol **3.50**. Treatment of **3.48** with 1 mol % of rhodium acetate smoothly catalyzed the designed cascade process, which was accompanied by olefin migration, furnishing product **3.59** in 53% yield. At this point the entire carbon framework of ineleganolide was assembled in 18 steps with all requisite C–C bonds, and only adjustment of oxidation states

remained to be accomplished. However, it turned out to be a rather arduous task, where various explored approaches have failed. Ultimately, after many trials the following sequence was



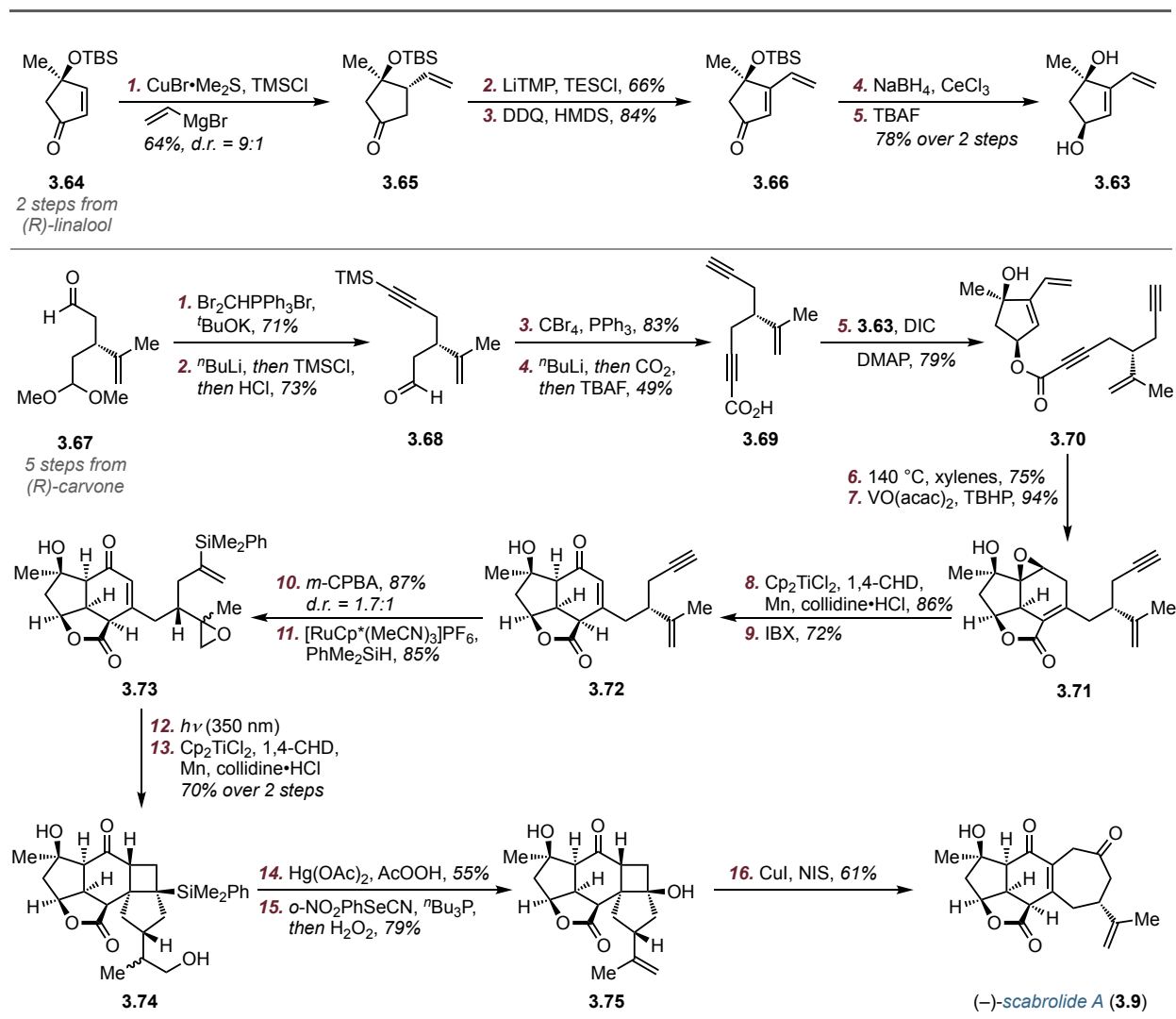
Scheme 3.6 Synthetic efforts of Stoltz and co-workers towards *ent*-ineganolide.

discovered: directed Sharpless epoxidation followed by nucleophilic opening at the more sterically accessible site and Kornblum oxidation afforded ketone **3.60** in 81% yield. Samarium(II)-mediated α -deoxygenation and acid-catalyzed dehydration delivered penultimate intermediate **3.61**. Only single olefin migration with presumably spontaneous conjugate addition stood between **3.61** and target compound **3.31**. Despite seemingly favorable conjugation with both carbonyl groups the olefin was reluctant towards desired isomerization. All attempts to move unsaturation away from ring fusion led to decomposition. To understand the observed behavior, DFT calculations of

geometry and corresponding relative energies for **3.61** and **3.62** were carried out. While reported data does not provide insight into kinetic profile, the process (**3.61** \rightarrow **3.62**) is highly endergonic ($\Delta G^\ddagger = 15.5 \pm 0.23$ kcal/mol), therefore side-reactions dominate over olefin isomerization. Notably, the analogous preference for olefin position was proposed in the biosynthesis of other norcembranoids (scabrolide B (**3.20**) \rightarrow scabrolide A (**3.9**), Scheme 3.2.b) despite different polycyclic arrangement. Importantly, similar calculations were carried out for the supposed conjugate addition (**3.62** \rightarrow **3.31**), predicting an exergonic process with $\Delta G^\ddagger = -14.1 \pm 0.23$ kcal/mol and thus highly favorable (at least from thermodynamic standpoint). Alternative functional group manipulations within the core of **3.60** were also unsuccessful, and the Stoltz group was unable to complete total synthesis of ineleganolide so far.

A milestone in the research of norcembranoids was set by the Stoltz group in 2020, who reported the first total synthesis of (–)-scabrolide A (Scheme 3.7).¹¹ Use of chiral pool material rendered the synthesis asymmetric. Several features of the approach sharply resonate with previous strategies that were applied towards ineleganolide. First, the same building block **3.63** for the construction of western hemisphere was utilized. However, its assembly was significantly streamlined (enantiomer of **3.50**, 7 steps instead of 15, Scheme 3.6). Thus, enone **3.64** derived from (*R*)-linalool was treated with vinyl cuprate, followed by regeneration of unsaturation through DDQ-mediated oxidation of the corresponding silyl enol ether. Enone **3.66** was reduced in a 1,2-fashion and tertiary alcohol was revealed with TBAF delivering **3.63** in 28% yield over five steps. The second building block **3.67** was accessed from (*R*)-carvone in five synthetic operations according to literature procedure. Both aldehyde entities within **3.67** were converted into alkynes using two sequential Corey–Fuchs reactions. Hence compound **3.69** was synthesized in four steps and 21% yield. Union of alcohol **3.63** and acid **3.69** under Steglich conditions delivered precursor **3.70** for the first key ring-forming event, a Diels–Alder reaction. The transformation proceeded smoothly under thermal condition and furnished diene in 75% yield and excellent diastereoselectivity, which was governed by well-defined geometry of the [5,5]-bicycle. Notably, analogously decorated intermediate (in terms of oxidation state of the central ring) was pursued in attempts towards ineleganolide, where six-membered ring is exchanged to seven-membered (**3.47**, Figure 3.2). Sharpless directed epoxidation followed by reductive epoxide opening mediated by Ti(III) and oxidation of the resulting secondary alcohol with IBX accompanied by olefin migration furnished enone **3.72** in 58% over three steps.

Consonantly with synthetic efforts towards ineleganolide, seven-membered carbocycle formation was envisioned through ring expansion strategy, namely [2+2]-photocycloaddition /



Scheme 3.7 Total synthesis of (-)-scabrolide A by Stoltz and co-workers.

fragmentation sequence was contemplated. To prepare the appropriate substrate, the terminal olefin was protected as an epoxide, which was formed with low but inconsequential, diastereoselectivity. Afterwards, the alkyne was subjected Ru-catalyzed hydrosilylation. Compound **3.73** was irradiated with UV-light leading to cyclobutane formation, which was further treated with Ti(III) in the presence of 1,4-cyclohexadiene to convert the epoxide into a primary alcohol. Thus, product **3.74** was obtained in 70% over two steps and great diastereoselectivity. In order to exchange the silane group into suitable handle for designed fragmentation, Fleming–Tamao oxidation was executed. Perhaps, due to the severe steric hindrance of the substrate only

Hg(II)-mediated conditions were productive. Terminal olefin was regenerated using Grieco dehydration, yielding **3.75** in 43% over two steps. Finally, treatment of tertiary alcohol **3.75** with NIS in presence of Cu(I) generated oxygen-centered radical, which underwent fragmentation, recombination with I• and in situ elimination through E1_{cB} mechanism, furnishing (–)-scabrolide A (**3.9**) in 61% yield. Overall, the presented synthesis consists of 21 steps in the longest linear sequence and is the first and only total synthesis of norcembranoid diterpenoid to date.

3.3 Results and Discussion

3.3.1 Retrosynthesis

Given the numerous failed synthetic attempts that were inspired by Pattenden's semisynthetic studies, we sought to approach the construction of ineleganolide through a novel series of disconnections.^{14,18} Retrosynthetically, construction of dihydrofuran moiety of ineleganolide (**3.7**) could be envisioned through intramolecular conjugate addition of tertiary alcohol to the spatially proximal Michael acceptor (Figure 3.3). DFT studies performed by Stoltz and co-workers displayed the significant thermodynamic driving force for this process and provided additional confidence in this transform.²⁴ Striving for convergent synthesis, the central seven-membered ring of intermediate **3.76** with four contiguous stereocenters was sought to be formed at the final stage of the synthesis. However, given relative flexibility of this medium-sized ring, we anticipated challenges with diastereoselectivity. To mitigate these concerns, late-stage ring expansion of 1,3-diketone **3.77** was envisioned. Due to the contracted nature of the cyclohexane in the polycyclic system in **3.77**, any stereochemical deviations from what is desired would lead to substantial steric and energetic penalties, ensuring correct assembly of the core. Compound **3.77** was further traced back to the enone **3.78** through intramolecular Michael reaction transform and adjustment of the oxidation states of the resulting tetracyclic product. Similar transformation was performed by Vanderwal and co-workers in an intermolecular fashion.^{19,20} Due to the cupped shape of the western hemisphere, aldol reaction yielded the undesired diastereomer at C12 exclusively (Scheme 3.5). To obviate this outcome, an intramolecular process was envisioned instead, since approach from the convex face under such regime is impossible due to geometrical constraints. Notably, the C13 stereocenter was formed with high selectivity in favor of desired configuration in Vanderwal's case. The stereoselection was rationalized by the

conformation of the cyclohexenone unit, where the isopropenyl substituent adopts a pseudoequatorial position. In accordance the hypothesis, preference for the pseudoequatorial position of that fragment was noted in DFT calculations performed by the Stoltz group and supported by acquired X-ray structures of synthetic intermediates.²³⁻²⁵ We reasoned that the same effects would govern selectivity of the intramolecular process. Thus, our synthetic design was expected to deliver compound **3.77** with high diastereoselectivity for both C12 and C13. Enone **3.78** was disconnected to two fragments of similar size, (*R*)-norcarvone (**3.57**) and aldehyde **3.79**, via a Morita–Baylis–Hillman (MBH) transform.

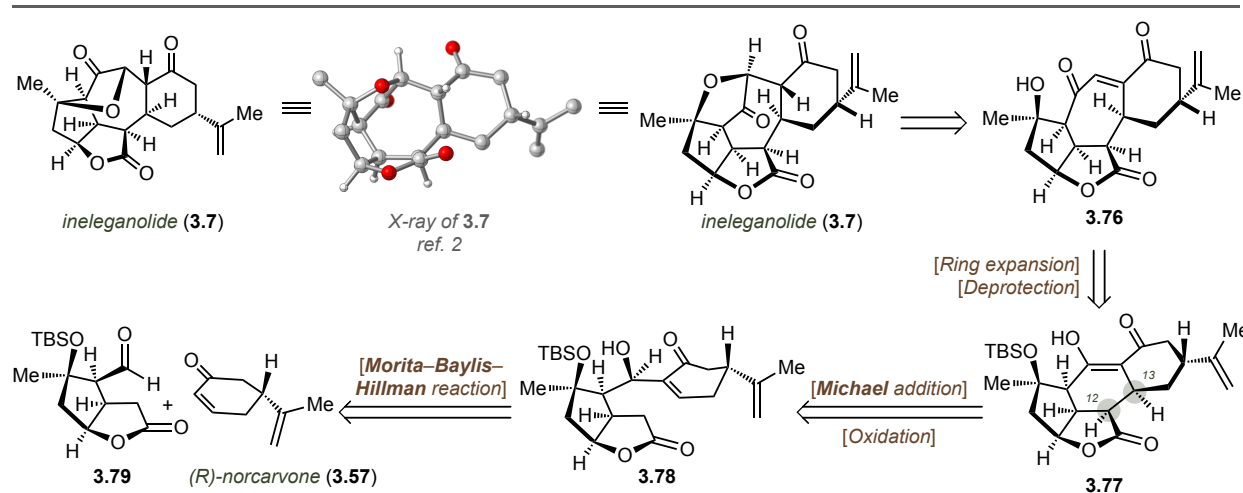
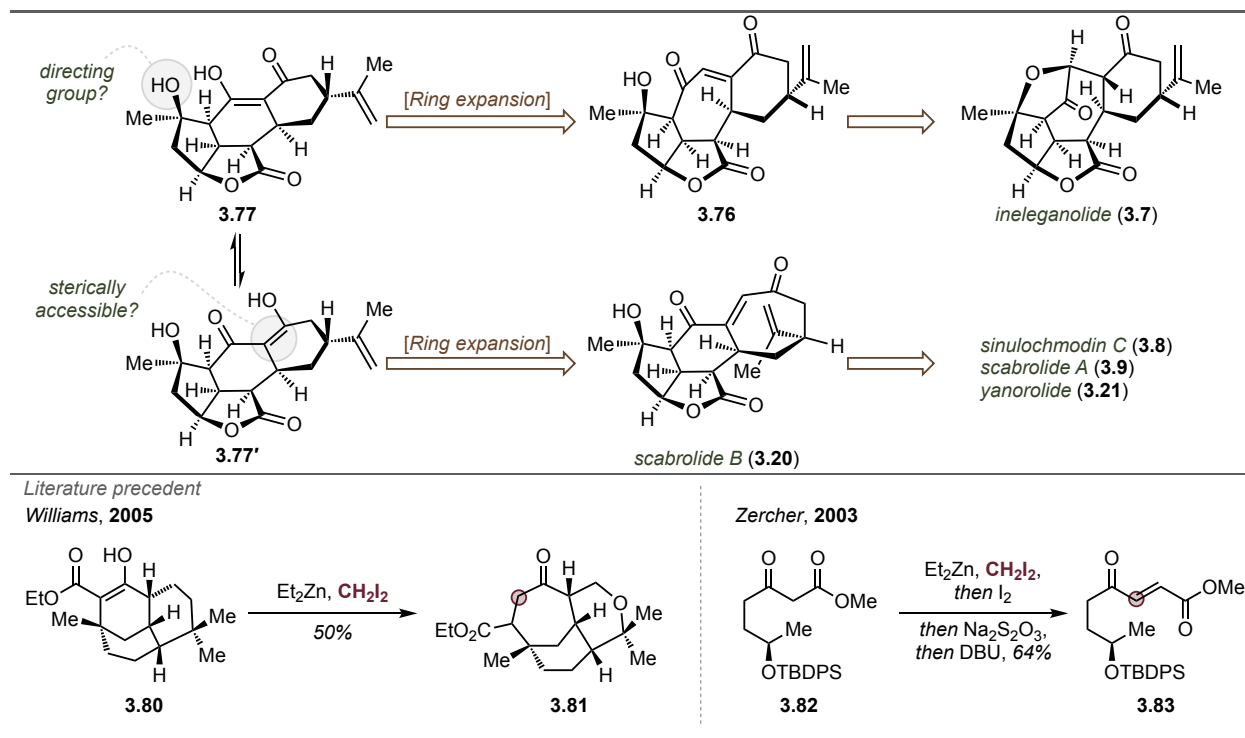


Figure 3.3 Retrosynthesis of ineleganolide.

During our retrosynthetic analysis, we realized an additional benefit of the ring expansion strategy (Scheme 3.8). Compound **3.77** is an unsymmetrical 1,3-diketone and therefore can exist in two tautomeric forms. While expansion of **3.77** would yield desired compound **3.78**, the reaction on the second tautomer **3.77'** would deliver scabrolide B (**3.20**) directly. Scabrolide B can be advanced further to other norcembranoids (e.g., sinulochmodin C (**3.8**), scabrolide A (**3.9**), yonarolide (**3.21**)) according to their biosynthetic relationship. Thus, intermediacy of the [5,5,6,6]-tetracycle renders the overall approach divergent. Moreover, we speculate that some level of regiocontrol can be exerted for selective functionalization of one tautomer over another (assuming their interconversion under reaction conditions). Arguably, enol motif within **3.77'** is more sterically accessible, while enol in **3.77** possesses a neighboring alcohol, which is located in close proximity and therefore can serve as a directing group. Importantly, relevant literature precedent for the proposed ring expansion was identified. Williams and co-workers applied

Simmons–Smith cyclopropanation conditions to convert six-membered 1,3-dicarbonyl **3.80** into seven-membered 1,4-dicarbonyl **3.81** within caged substrate with similar steric hindrance to our

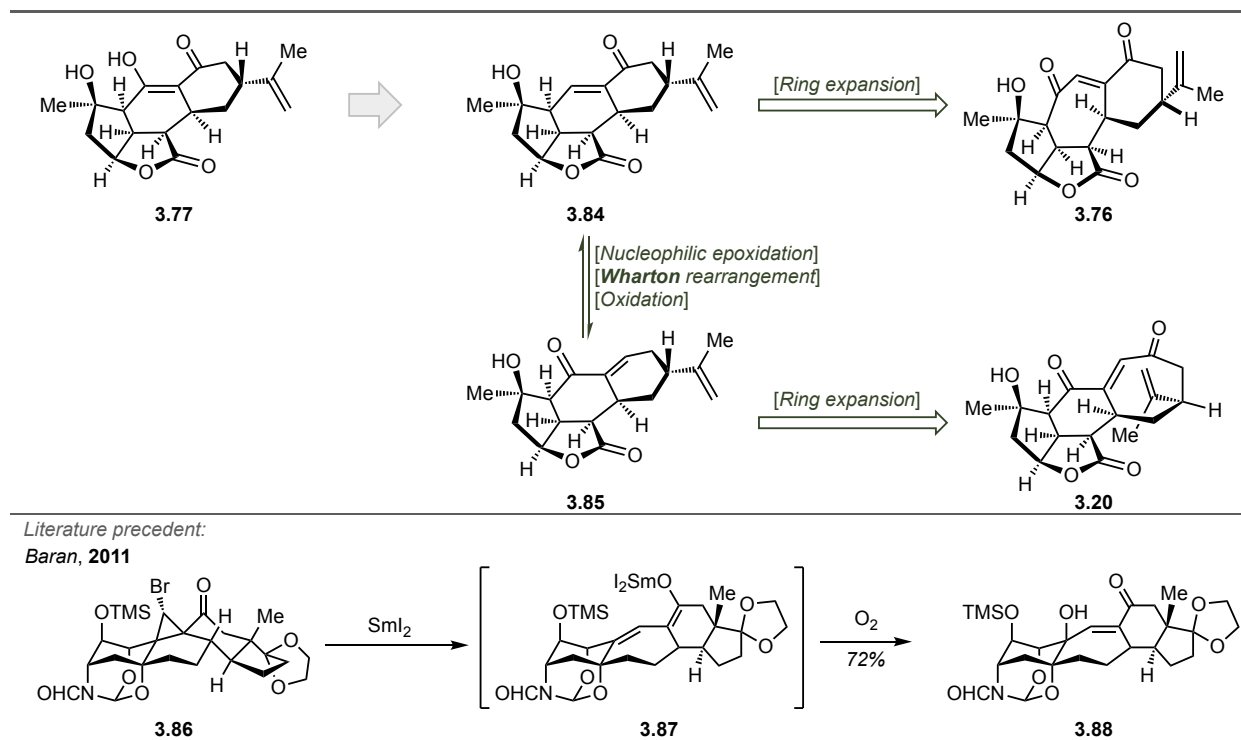


Scheme 3.8 Divergent access to various norcembranoids.

hypothetical intermediate **3.77**.²⁶ Additionally, Zercher and co-workers reported a method for homologation of 1,3-dicarbonyl substrates and installation of unsaturation in a single pot (**3.82**→**3.83**). Fortuitously, this exact transformation is needed to obtain **3.76** from **3.77** directly.²⁷

The proposed design is ambitious and we anticipate unforeseen challenges, and therefore a backup plan was prepared in advance (Scheme 3.9). Intermediate **3.77** was reimagined as an enone **3.84**. Such shift would eliminate potential regioselectivity problems. Nevertheless, this modified strategy still can be rendered divergent. To achieve that, a three-step sequence for oxidation states manipulation was projected. Enone **3.84** can undergo nucleophilic epoxidation. Condensation with hydrazine would trigger Wharton rearrangement and constitutional isomer **3.85** can be obtained after oxidation of the secondary alcohol. The same sequence can be applied in the opposite direction to convert **3.85** into **3.84**. Of note, this approach would require increase in oxidation state of employed C1-synthon during ring expansion to achieve desired outcome. The relevant precedent was found in the synthetic studies towards cortistatin reported by Baran and co-workers (Scheme 3.9).²⁸ Bromocyclopropane **3.86** was transformed into vinylogous samarium

enolate **3.87** under reductive conditions followed by further oxidation at the γ -position to deliver **3.88** in 72% yield. As a result of our retrosynthetic exercise, the three intermediates **3.77**, **3.84** and **3.85** were identified as viable and were pursued simultaneously.

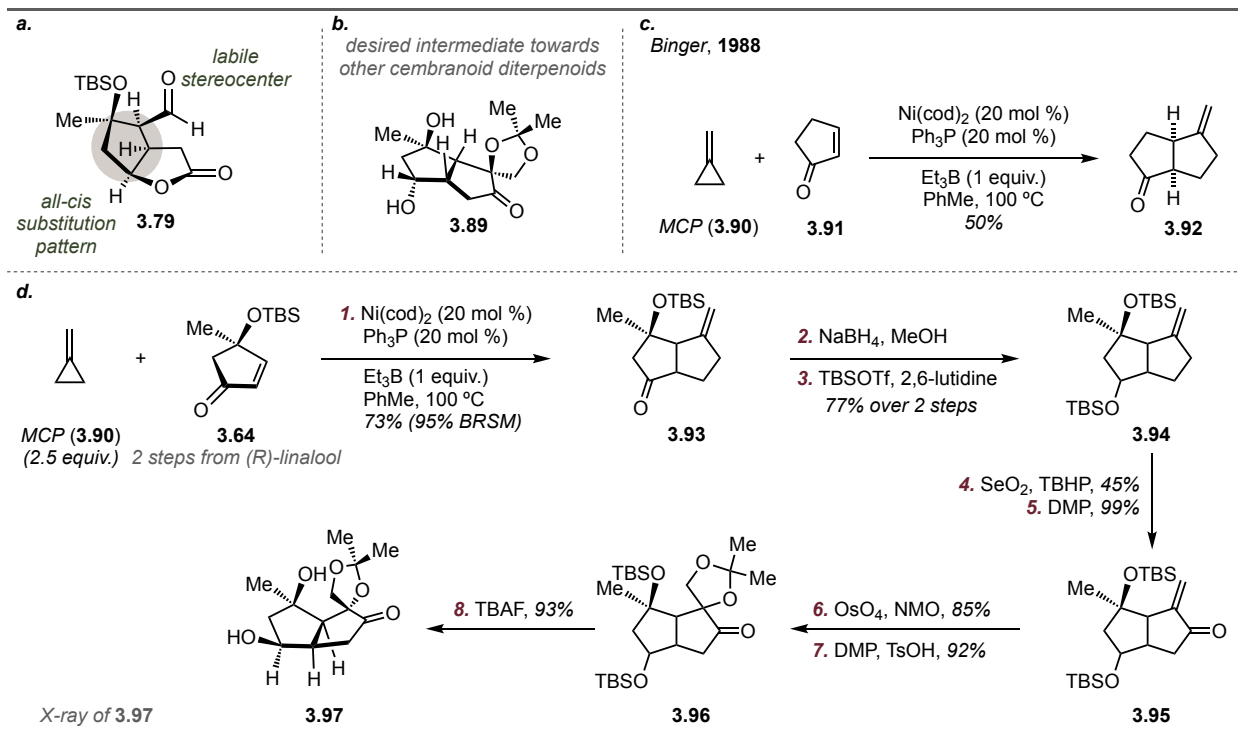


Scheme 3.9 Alternative route to key precursors **3.76** and **3.20**.

3.3.2 Synthesis of the coupling partners for MBH reaction

Despite its relatively small size, aldehyde **3.79** presented a significant synthetic challenge. It contains all-*cis* pentasubstituted cyclopentane core with a quaternary stereocenter (Scheme 3.10.a). In addition, the aldehyde functionality could be sensitive to epimerization and therefore would require delicate conditions for its synthesis and further use. This problem was solved serendipitously. The bicycle **3.89** was originally targeted for another cembranoid diterpene natural product synthesis (Scheme 3.10.b). Derived from chiral pool, enone **3.64** was exploited as a starting material due to its availability, cost and presence critical quaternary stereocenter (Scheme 3.10.d).²⁹ Seeking a method to perform annulation and form [5,5]-bicyclic system in one step, we unearthed an old report from Binger and co-workers (Scheme 3.10.c).^{30,31} Methylcyclopropane (MCP, **3.90**) was utilized as a three-carbon synthon for pentannulation of Michael acceptors under Ni-catalysis in the presence of stoichiometric amounts of Et_3B . This reaction is reminiscent of Pd-catalyzed TMM-cycloaddition developed by Trost, however opposite

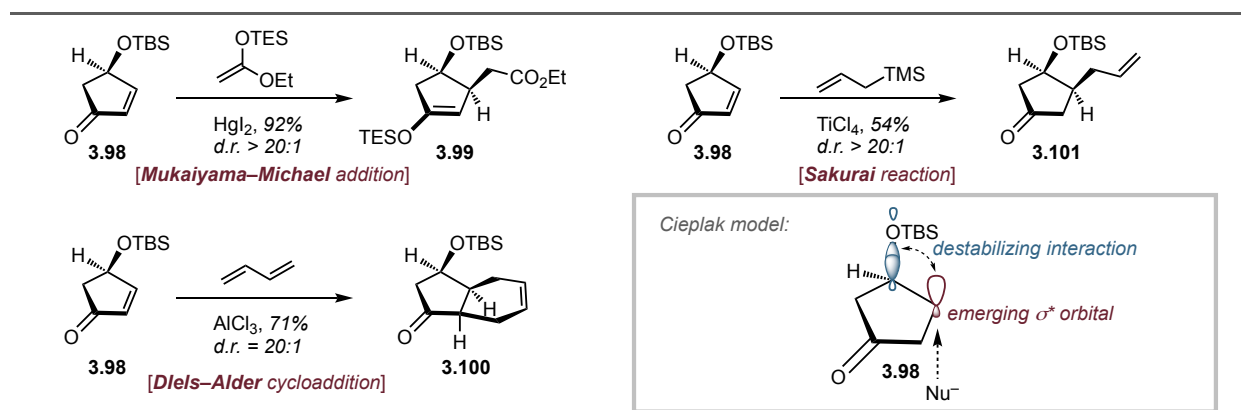
regioselectivity is acquired.³² Notably, this unique annulation reaction has never been used in synthetic context, as opposed to its TMM counterpart that found wide application in synthesis.



Scheme 3.10.a Desired synthetic intermediate; **b** Targeted bicycle *en route* towards another cembranoid; **c** Previous report on Ni-catalyzed pentannulation using MCP; **d** Attempted synthesis of **3.89** and observation of unexpected diastereoselectivity.

Despite limited exploration of the scope, we were delighted to find enone **3.64** smoothly transformed into bicycle **3.93** in 73% yield and excellent diastereoselectivity. Based on the steric argument and literature precedent for the diastereoselective cuprate addition^{11,29} to this substrate, we assumed that the reaction proceeded from convex face. Ketone **3.93** was further reduced and protected to yield silyl ether **3.94**. Allylic oxidation followed by DMP oxidation delivered enone **3.95** in 44% yield. Dihydroxylation, diol protection and cleavage of both silyl groups yielded compound **3.97** that was crystalized and subjected to single crystal X-ray diffraction analysis. Surprisingly, the crystal structure revealed that the annulation in fact occurred from the concave face. Puzzled by this unexpected outcome, we later found a series of examples with similar observations (Scheme 3.11).³³⁻³⁶ It has been reported that desmethlyated **3.64**,—venerable protected 4-hydroxycyclopentenone (**3.98**)—as well as 4-hydroxycyclohexenone (*not shown*), offer the same stereochemical outcome in presence of Lewis acids for numerous transformations such as Diels–Alder cycloaddition, Michael addition, etc. While this phenomenon was observed

on multiple occasions, Danishefsky was the first one who studied this aspect in greater details.³⁶ Cieplak's model was utilized to explain the stereoselection of the process.³⁷ It was postulated that, when a nucleophile approaches *anti* to the electron-withdrawing substituent, emerging σ^* -orbital experiences destabilizing interactions with σ -orbital of the C–O bond. In the opposite case, this repercussion is mitigated. Therefore, electronic effects guide approach of the nucleophile from the *syn* face of –OTBS substituent, contradictory to the steric argument. Interestingly, the stereochemical outcome reverses once Lewis acid is removed from the equation. This model applies to the pentannulation reaction of the enone **3.64**, where Et₃B is used as a Lewis acid. Of note, whereas omission of Lewis acid might potentially change stereoselectivity of the process, it is absolutely necessary for activation of the Michael acceptor.

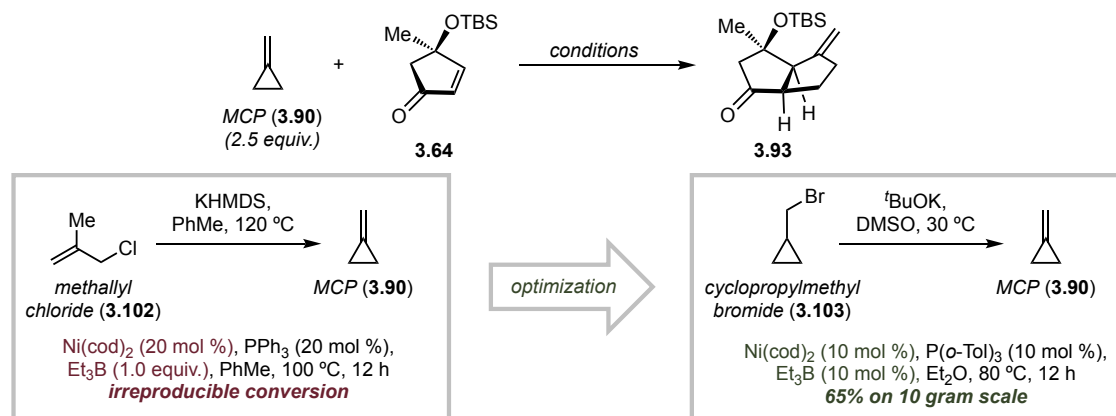


Scheme 3.11 Previously observed unusual diastereoselectivity of addition to protected 4-hydroxycyclopentenone (**3.98**) and corresponding rationale.

While the outcome was initially undesired as obtained stereochemistry did not map on targeted cembranoid, it was recognized that the obtained intermediates (**3.93**, **3.94**) open new opportunity for the total synthesis of ineleganolide and related diterpenoids. In particular configuration of the stereogenic centers of cyclopentanone moiety within compound **3.93** matches the ones present in aldehyde **3.79**. However, before progressing forward towards ineleganolide, the key annulation reaction required optimization. While initial results were high yielding, the reaction became irreproducible and yield suffered accordingly. Full conversion of the enone **3.64** was never achieved due to catalyst instability. Further complicating the matter, the starting material and product **3.93** are not separable by liquid flash chromatography. Regardless, overall conditions were far from optimal for early-stage total synthesis: high loadings of an expensive catalyst and stoichiometric use of Et₃B, which is both pyrophoric and had to be used neat. Finally, the synthesis

and handling of methylenecyclopropane (b.p. = 9 °C) had to be redesigned to increase practicality.³⁸

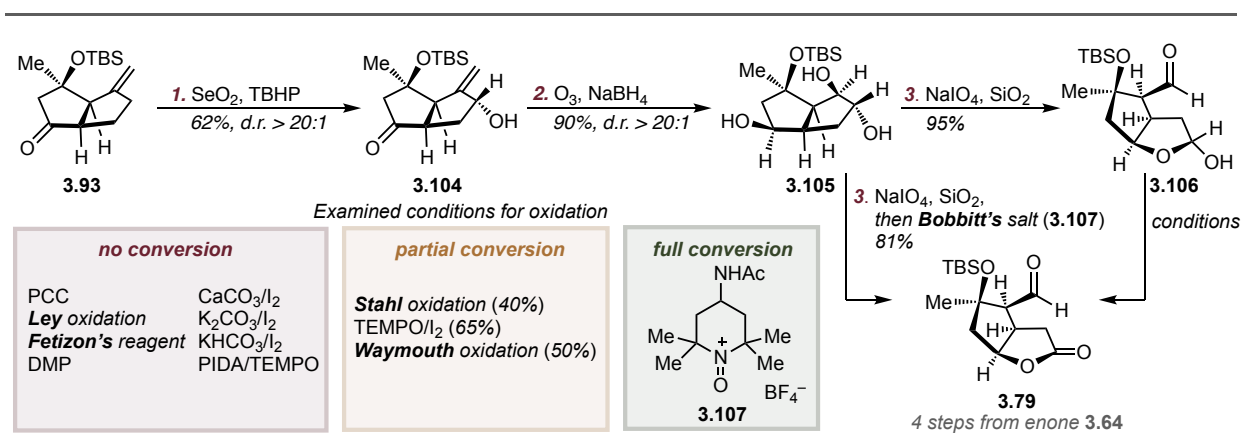
After significant efforts were invested, the set aim was achieved (Scheme 3.12).³⁹ (1) Catalyst loading was reduced by half and P(*o*-Tol)₃ stabilized the active catalytic species, without detrimental effect on the rate of reaction. Thus, full conversion became attainable. (2) The loading of hazardous Lewis acid was reduced tenfold. (3) A new process for synthesis of methylenecyclopropane was developed, decreasing cost and improving reproducibility, purity and ease of handling. With this optimized protocol in hand, the annulation could be routinely performed at multigram scales with an average of 65% yield, excellent diastereoselectivity and remarkable reproducibility. Thus, ample amount of the bicycle **3.93** was secured, enabling further synthetic explorations.



Scheme 3.12 Optimization of Ni-catalyzed pentannulation using MCP as three-carbon synthon.

Conversion of the bicycle **3.93** into desired aldehyde **3.79** seemed rather straightforward (Scheme 3.13). Indeed, allylic oxidation using Sharpless conditions yielded alcohol **3.104** in 62%. Of note, other SeO₂-mediated conditions led to overoxidation, while alternative methods returned starting material. Alcohol **3.104** was subjected to reductive ozonolysis affording triol **3.105** in 90% yield and high diastereoselectivity. Diol oxidative cleavage went smoothly using sodium periodate impregnated onto SiO₂, albeit conversion was slow due to *trans*-configuration of the diol.⁴⁰ The resulting hemiacetal **3.106** was unstable towards purification and was used crude. At this stage only oxidation of the acetal to the corresponding lactone in presence of the aldehyde moiety remained to complete the synthesis of **3.79**. Surprisingly, this seemingly trivial transformation posed a challenge. Most standard conditions returned starting material. Copper-catalyzed aerobic

oxidation developed by Stahl,⁴¹ palladium-catalyzed oxidation developed by Waymouth⁴² and TEMPO/I₂ system⁴³ afforded partial conversion. Regardless of stoichiometry and reaction time, full consumption of acetal **3.106** was never attained. These results were unsatisfactory as the product **3.79** was also unstable towards purification. A screen of various absorbents (Figure 3.4) revealed that aldehyde **3.79** can tolerate only activated carbon, while other options would lead to significant decrease of mass balance or apparent decomposition. Therefore, only clean and complete conversion would suffice without room for compromise.



Scheme 3.13 Synthesis of aldehyde **3.79**.

In order to optimize this troublesome oxidation, nitrosonium-mediated oxidants were investigated following our initial lead employing TEMPO / I₂ conditions. Bobbitt's salt **3.107**, a bench stable oxidant, caught our attention due to the ease of preparation, mild conditions, broad spectrum of application and minimal operations to remove by-products after reaction.⁴⁴ To our delight, oxidation went smoothly using 1.5 equivalents of the reagent and SiO₂ as an acidic additive. In situ NMR studies revealed the origin for sluggish oxidation and unique ability of

Bobbitt's salt to mediate the transformation. Due to the bowl-like shape of the hemiacetal, the proton required for abstraction is buried in the concavity of the molecule. However, under the reaction conditions, the hemiacetal can partially epimerize and expose the proton for abstraction to the oxidant and thus drive the reaction to completion. Moreover, diol cleavage and hemiacetal oxidation can be combined in a single step, as both reactions can be performed in the same solvent

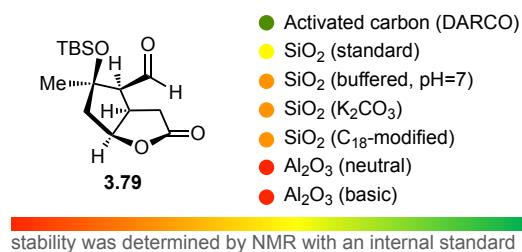
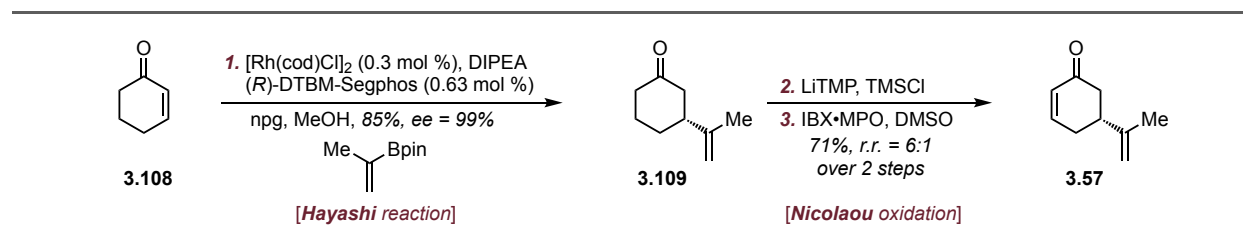


Figure 3.4 Stability studies of aldehyde **3.79**.

in presence of SiO₂. Thus, triol **3.105** can be converted into crucial aldehyde **3.79** in a single step and 81% yield with no need for purification.

With the first coupling partner for conceived Morita–Baylis–Hillman reaction in hand, we moved our focus to the (*R*)-norcarovone **3.57**. Several approaches have been developed towards this ubiquitous building block. However, they suffer either from lengthy linear sequences or from inefficiency due to a kinetic resolution step to render synthesis enantioselective.^{45,20} Hence, more expedient route towards **3.57** was sought (Scheme 3.14). Fortuitously, recently Bristol Myers SquibbTM reported on their achievements in the research program targeting BTK inhibitor.⁴⁶ Enantiomer of the substituted cyclohexanone **3.109** was one of the early-stage intermediates, and kilogram quantities of it were required for further development. The task was elegantly solved through mechanism-guided optimization of an enantioselective Hayashi addition based on the pioneering work of Corey and Lalic.^{47,48} Adopting this highly scalable and practical protocol, synthesis of (*R*)-norcarvone was achieved in only three steps. Cyclohexenone **3.108** was subjected to optimized Hayashi addition conditions. Product was obtained in 85% in our hands after purification by distillation. Regioselective formation of silyl enol ether from **3.109** followed by Nicolaou oxidation furnished the desired material in 61% yield over two steps.

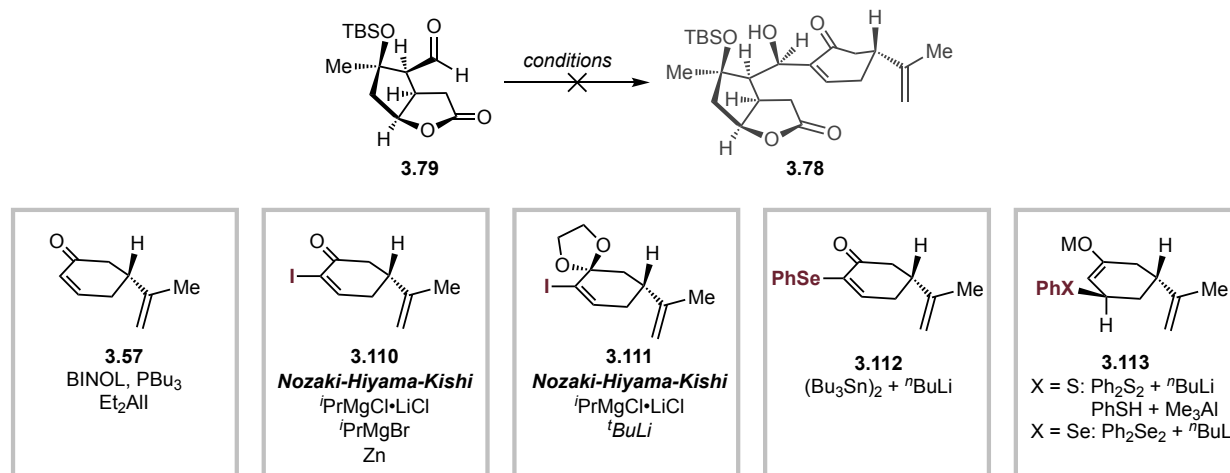


Scheme 3.14 Enantioselective three-step synthesis of norcarvone.

3.3.3 Strategy I: Morita–Baylis–Hillman reaction

The stage was set for the first C–C bond construction between two fragments. First, direct coupling of aldehyde **3.79** and enone **3.57** was attempted under classical Morita–Baylis–Hillman (MBH) conditions (Scheme 3.15).⁴⁹ Perhaps unsurprisingly, no product was observed and complete decomposition of the aldehyde **3.79** occurred. A number of prefunctionalized substrates were synthesized to ease the coupling process and add additional options for the desired transformation. For example, vinyl iodide **110** was sought to undergo Nozaki–Hiayama–Kishi reaction with aldehyde⁵⁰, or serve as a precursor for organomagnesium⁵¹ or zinc reagents. As no promising results were obtained, ketone was converted to the ketal **3.111** for more direct

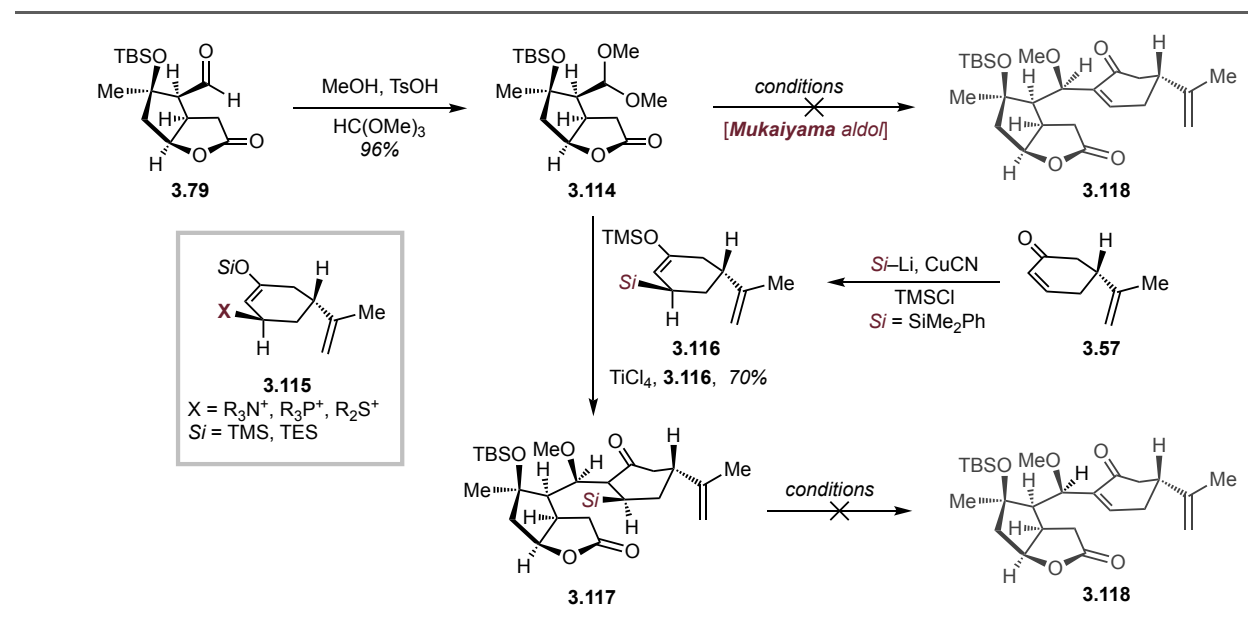
metalation. However, this substrate also turned out to be reluctant towards coupling. Selenide **3.112** was briefly explored as well.⁵² Even though coupling product in this case was detected by LCMS, it never was isolated or observed in crude NMR. Finally, MBH process was reimaged as a stepwise transformation: enolate of norcarvone **3.113** can be generated first stoichiometrically followed by addition of aldehyde and in situ β -elimination of the original nucleophilic species.



Scheme 3.15 Examined conditions for coupling between aldehyde **3.79** and (*R*)-norcarvone.

Since sulfides or selenides are typically used for this purpose, oxidative workup is performed to facilitate elimination of S(IV) or Se(IV) species.⁵³⁻⁵⁵ No product was obtained employing this approach either. Notably, complete consumption of aldehyde **3.79** observed in each case led us to suspect its exceptional instability towards basic conditions. Thus, attention was shifted towards acidic conditions and the Mukaiyama reaction appeared to be a viable strategy (Scheme 3.16). Aldehyde **3.79** was transformed into acetal **3.114** in excellent yield. Silyl enol ether **3.115** was generated in situ in the presence of an appropriate nucleophile and silyl trapping reagent. Numerous conditions were examined, but regardless of reagent combinations, all attempts were to no avail.^{49,56,57} Only a single set of conditions gave a positive outcome.⁵⁸ Using silyl-anion as a nucleophile for generation of silyl enol ether **3.116**, Mukaiyama reaction occurred in presence of TiCl_4 in good yield. It was a very encouraging result, as for the first time we were able to unite the two fragments with appreciable efficiency. Nevertheless, that particular transformation turned out to be a stalemate. Halogenative desilylation of **3.117** for the subsequent elimination did not tolerate the presence of another olefin. Thus, the pursuit for effective MBH-type coupling conditions was continued.

It was hypothesized that the use of milder and less basic conditions could mitigate decomposition of **3.79** and deliver the desired product. After an extensive literature search, an intriguing report by Livinghouse on bifunctional reagent **3.119** caught our attention (Scheme 3.17).⁵⁹ It was shown that **3.119** readily reacts with enones, leading to a boron enolate that can undergo aldol reaction in the same pot. Oxidative workup with hydrogen peroxide regenerates

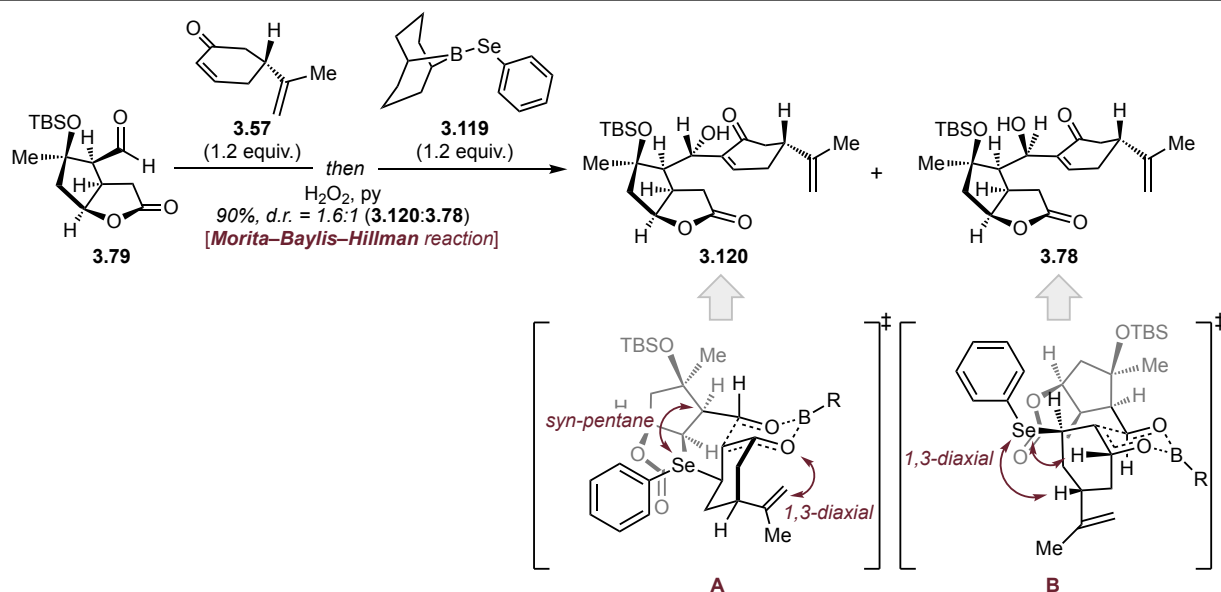


Scheme 3.16 Attempted conditions for Mukaiyama reaction to couple **3.79** and (*R*)-norcarvone.

Unsaturation, leading to the formal MBH-product. Since boron enolates are significantly less basic than previously examined lithium counterparts, this reagent could satisfy the requirements. While use of **3.119** posed certain shortcomings—namely short shelf life and high sensitivity towards oxygen and light—the desired product was obtained in 90% and 1.6:1 diastereoselectivity. Slight excess of norcarvone is required to achieve this remarkable outcome. Of note, despite its mild conditions and outstanding performance, bifunctional reagent **3.119** has not found application in synthesis to date. Negligible diastereoselectivity can be attributed to the interplay of the steric factors in the transition states **A** and **B** en route towards products **3.120** and **3.78** respectively (Scheme 3.17). Phenyl selenide adds in conjugate fashion to the olefin from the opposite side of the isopropenyl substituent. The resulting boron enolate undergoes aldol reaction via a Zimmerman–Traxler transition state. In the case of **A**, unfavorable *syn*-pentane interactions between phenyl selenide and aldehyde moiety are present as well as a 1,3-diaxial interaction of the isopropenyl motif. The alternative approach is characterized by alleviated *syn*-pentane repulsions

that are exchanged, however, for two additional 1,3-diaxial interactions. Thus, neither transition state represents a definitive energetic preference (at least by simple models and intuition). Moreover, the additional steric factor of the remote lactone ring is present, complicating matters due to its rotational freedom in respect to the cyclohexane ring.

With access to the MBH-products, we began investigations of the key *6-endo-trig* cyclization to construct the ineleganolide core and set all the requisite stereocenters.



Scheme 3.17 Successful MBH-type coupling using Se-B bifunctional reagent.

First, conversion of the hydroxyl group at C6 into an appropriate leaving group was attempted (Figure 3.5). Due to the severe steric hindrance of the reactive center, the conversion was sluggish. However, upon application of forcing conditions, diene **3.122** was the observed major product. Next, direct cyclization of the substrate in presence of excess of base was explored (Scheme 3.18). The MBH-product (**3.78** or **3.120**) has a number of acidic positions for the deprotonation (besides –OH), namely α - to the ketone, α - to the lactone and γ - to the ketone (shown in red). Moreover six-membered enones typically have lower pKa values than γ -lactones. Thus, execution of the direct cyclization without prior tailoring of the substrate for better regioselectivity was an ambitious aim. Nevertheless, the brevity of such transformation and expeditious access to the desired tetracycle in case of success gave us enthusiasm to explore this option in depth. At the outset, it is important to note that a substantial difference in reactivity between diastereomers **3.78** and **3.120** was noticed, hence they were studied separately. To our delight, an excess of LDA

triggered 1,2-cyclization of **3.120** (major diastereomer from MBH). After optimization of the reaction parameters, the major product **3.123** was obtained in 40% yield. Additional isomers were formed in course of the reaction as well, but their quantities were insufficient for structural elucidation. Deprotection of the tertiary alcohol afforded crystalline product **3.124**, for which single crystal X-ray diffraction measurement was conducted. Configurations of C6 and C13 stereocenters were unambiguously determined. Interestingly, if the counterion was changed from

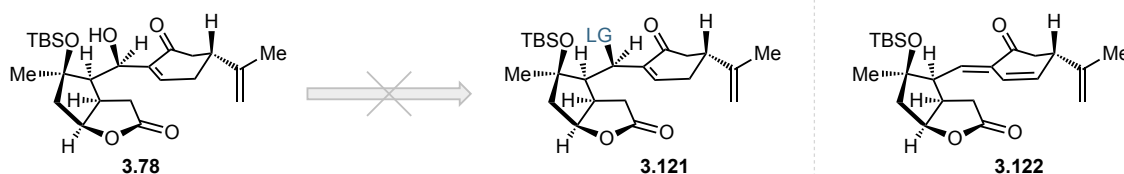
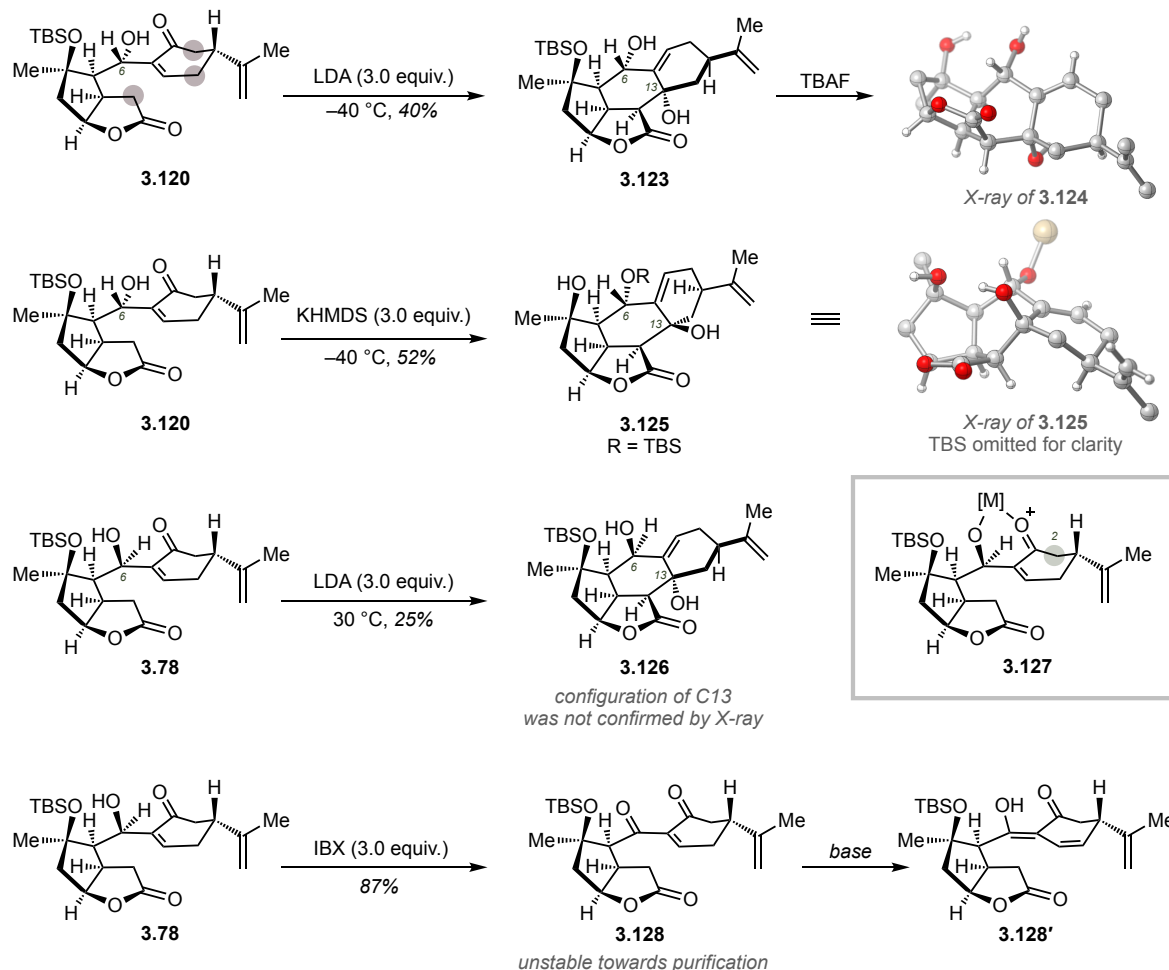


Figure 3.5 Failed functionalization of secondary alcohol **3.78**.

lithium to the less coordinating potassium, cyclization takes different pathway. Treatment of **3.120** with an excess of KHMDS delivered **3.125** as a single product in 52% yield. Compound **3.125** has opposite configuration at C13 and the silyl protecting group migrated from tertiary to secondary alcohol. Structure of **3.125** was confirmed by X-ray analysis. The diastereomer **3.78** (minor diastereomer from MBH) also could undergo cyclization, however inverse addition at warmer temperatures was required. The yield of **3.126** was significantly lower and less reproducible. While these results were rather encouraging as they demonstrate the feasibility of cyclization, 1,4-cyclization was not achieved. The following reasons are proposed to account for primarily 1,2-addition: (1) after first deprotonation of the secondary alcohol the ketone moiety can rotate towards lactone, due to electrostatic interactions between alkoxide and lone pair of carbonyl; (2) 1,4-addition would place the negatively charged enolate in close proximity to negatively charged alkoxide that would lead to significant destabilization of the product; (3) *6-exo-trig* cyclization can outcompete *6-endo-trig* cyclization kinetically. To override the intrinsic selectivity in favor of desired conjugate addition, use of chelating additives was explored. We postulated that formation of chelate **3.127** would obviate adverse electrostatic interactions and lock substrate in the favorable conformation for the conjugate addition. Unfortunately, 1,2-addition was not observed in this case, nor any reactivity at all. Regardless of the additive (over 20 salts of coordinating metals were examined), pure unreacted starting material was recovered. This can be ascribed to drastically decreased pKa of C2 position upon chelation, which prevented formation of the enolate from

lactone. Finally, MBH-product **3.78** was converted to the diketone **3.128** in order to increase electrophilicity of the Michael acceptor and empower 1,4-conjugate addition. Unfortunately, that maneuver also was not effective as compound **3.128** readily tautomerizes to its enol form **128'**, discharging its β -position.

Overall, after exploration of the originally proposed strategy, promising results were obtained: key tetracyclic intermediate **3.123** was formed in a short synthetic sequence from readily available enone **3.64** (Figure 3.6). However, only the undesired regioselectivity was



Scheme 3.18 Outcome of direct cyclization under basic conditions.

observed regardless of conditions applied. While oxidation states could be easily adjusted within the ring fusion, further studies were halted, as the product has the incorrect configuration of the stereocenter at C1 (comparing with **3.129**). Therefore, slight modifications of the strategy were required to enable desired mode of cyclization.

3.3.4 Strategy II: C12 prefuntionalization

Prefunctionalization at C12 position was explored in order to access a more mild and selective Michael addition (Scheme 3.19). Given the success of the intermolecular Mukaiyama–Michael reaction

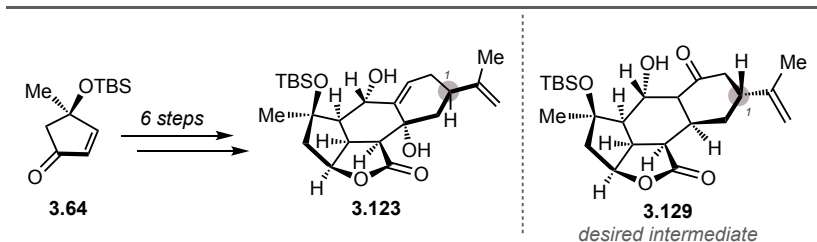


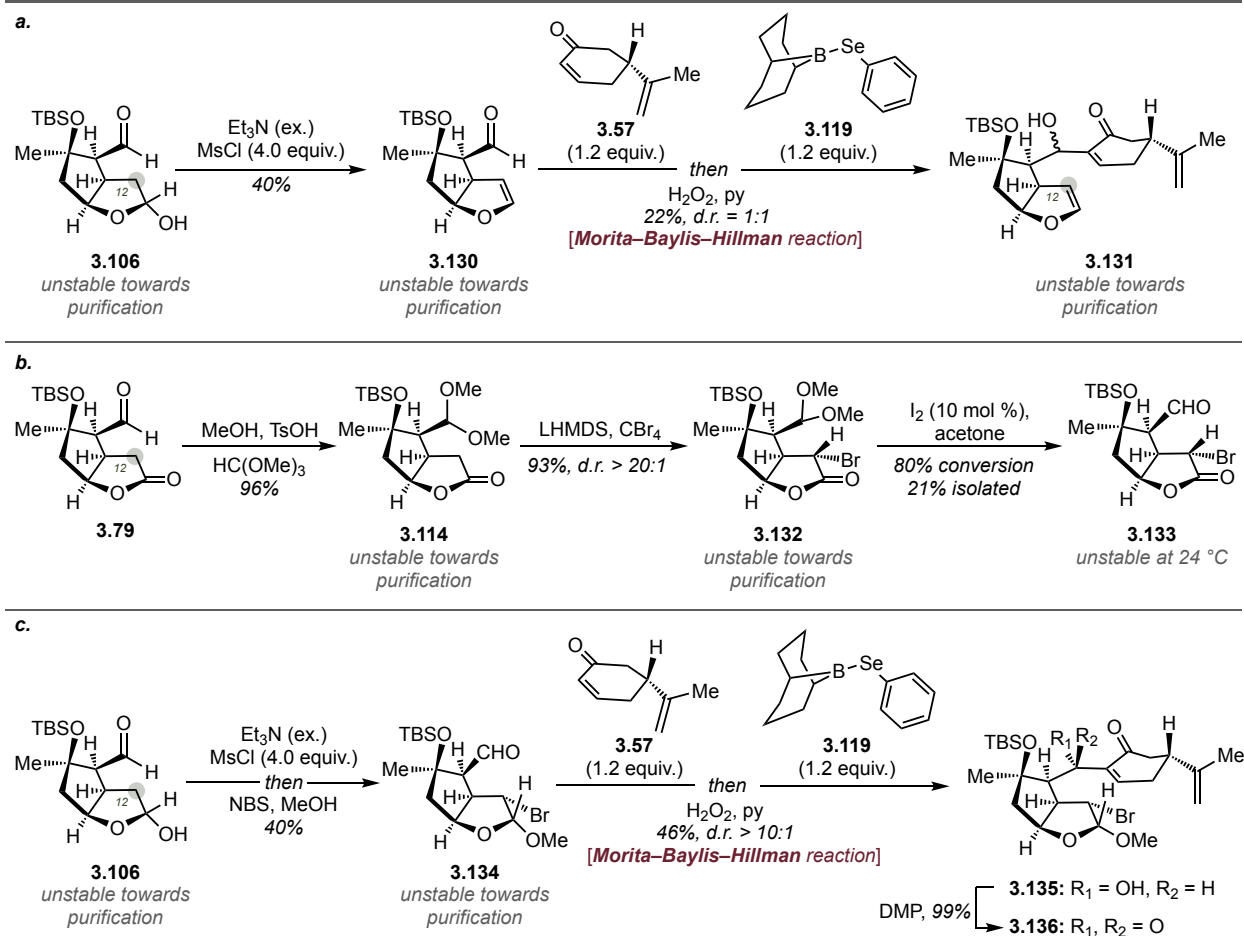
Figure 3.6 Intermediary results using the original approach.

demonstrated by Vanderwal and co-workers,²⁰ vinyl ether of the lactone was pursued. Direct formation of silyl enol ether from the lactone **3.79** was not possible due to free alcohol and issues associated with its protection / capping. Thus, generation of alkyl vinyl ether was planned prior MBH-coupling.⁶⁰ Towards this goal, dehydration of the hemiacetal **3.106** was conducted, furnishing vinyl ether **3.130**. Compound **3.130** was unstable and isolated yields were modest, despite clean and complete conversion by crude NMR. Inherent sensitivity of the vinyl ether translated to the MBH reaction, leading to low yield of the coupling product. Further investigations of substrate **3.131** were ceased due to low throughput, inconsistent results and difficult access to clean material.

Next, bromine substituent at C12 was sought, as it would open two possible paths: selective enolization via Reformatsky reaction (Scheme 3.19.b) and a radical approach through intramolecular Giese-type addition (Scheme 3.19.c).^{61,62} Direct bromination of aldehyde **3.79** under basic conditions turned out to be troublesome. Rapid equilibration of the kinetically-formed enolate of the lactone with the aldehyde motif led to unselective functionalization. To circumvent this obstacle, aldehyde **3.79** was first protected as an acetal, to yield **3.114**, which was brominated to deliver **3.132** in 93% yield. Surprisingly, sluggish cleavage of the dimethoxyacetal was faced. Only use of catalytic iodine in presence of acetone for transacetalization allowed for isolation of the desired product. However, bromolactone **3.133** was highly unstable as well, which manifested itself in low isolation yields and an inability to handle the compound neat due to spontaneous decomposition. Thus, intermediate **3.133** was also abandoned.

We speculated that decrease in the oxidation state of the bromolactone could diminish sensitivity of the intermediate. To test the hypothesis hemiacetal **3.106** was converted into bromoacetal **3.134** through dehydration / bromination sequence in 40% yield. Compound **3.134**,

while more amenable for handling than bromolactone **3.133**, was still unstable to purification. To our delight, MBH-coupling proceeded with acceptable efficiency delivering product **3.135** in 46%. Perhaps, the actual yield of this transformation is higher, however purification was required at this stage that led to partial decomposition. Notably, only a single diastereomer was obtained showcasing close steric interaction between lactone ring and boron-enolate in the transition state (configuration was determined based on analogy of ^1H NMR). Alcohol **3.135** could

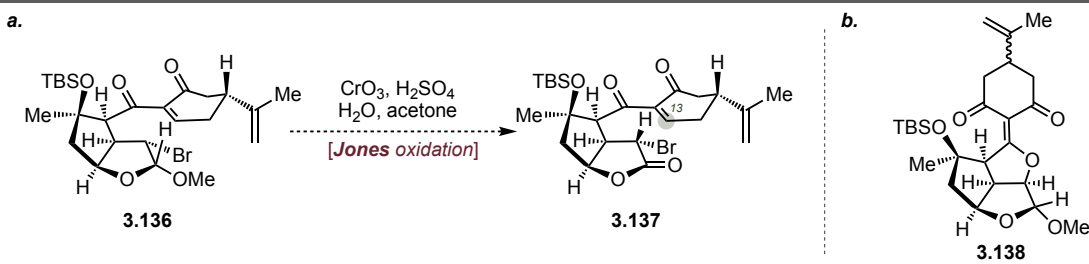


Scheme 3.19 Attempts to synthesize precursors for intramolecular Mukaiyama reaction (**a**), Reformatsky reaction (**b**), and Giese addition (**c**).

be quantitatively oxidized into diketone **3.136** upon treatment with DMP. Thus, two substrates (**3.135** & **3.136**) were obtained for further investigations of cyclization.

Initially diketone **3.136** was explored as we thought that extremely reactive Michael acceptor would be more susceptible to the desired cyclization. Propensity towards enolization, however, was kept in mind and basic conditions were avoided. First, Jones oxidation conditions were applied to convert acetal **3.136** into the lactone **3.137** that would serve as a direct precursor

for envisioned Reformatsky–Michael reaction (Scheme 3.20). Transformation proceeded in nearly quantitative yield within 30 minutes and afforded compound **3.138** as a sole product. Based on the resulting structure we speculate that water adds to the activated enone at C13; the resulting enolate acts as a *O*-nucleophile to substitute the bromide in S_N2 fashion. This *5-exo-tet* cyclization is especially facile, since substituents are located in near perfect alignment for the back-side attack. Finally, secondary alcohol undergoes oxidation delivering the final product. Of note, acetal was

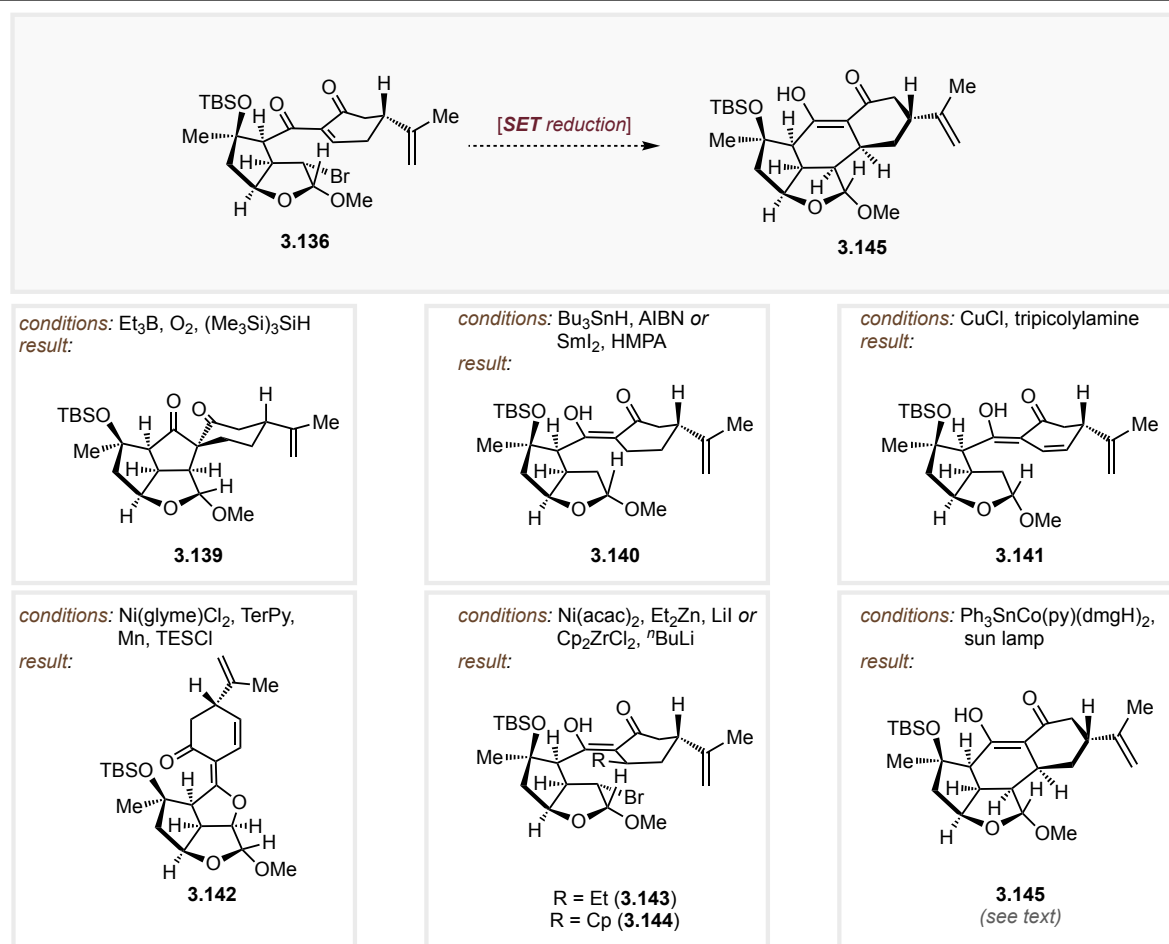


Scheme 3.20.a Attempts to synthesize precursors for intramolecular Reformatsky reaction; **b** Jones oxidation product.

not cleaved under reaction conditions. The possible bypass would be use of alternative alkyl group for acetal with a specific trigger for deprotection. Nevertheless, focus was shifted to single electron processes, which would allow for direct use of the **3.136** (Scheme 3.21). Unexpectedly, use of Et_3B in presence of supersilane gave cyclization product **3.139**! Reaction exhibited strong preference for kinetically more facile *5-exo-trig* cyclization over *6-endo-trig* despite overwhelming electronic bias. Other singlet electron reduction conditions such as Bu_3SnH / AINB or SmI_2 afforded rapid conjugate addition followed by slow reduction of the bromide (**3.140**).^{63,64} Using copper-mediated reduction in presence of amine ligands only led to tautomerization, perhaps expectedly as copper(I) species generally cannot access the reduction potentials required to participate in the desired reaction.⁶⁵ Reductive coupling conditions developed by Weix and co-workers similarly induced tautomerization, which was followed by intramolecular substitution by the enol form, yielding tricycle **3.142**.⁶⁶ Low-valent nickel and zirconium species were shown to generate radicals from activated bromides through electron transfer mechanism.^{67,68} However, in the case of **3.136**, nucleophilic species present in the reaction mixture simply added to the reactive electrophile (**3.143**, **3.144**) without the desired reduction. Finally, low-valent cobalt complexes were examined for the Heck-type reactivity in presence of visible light irradiation. Using the conditions from Carreira's total synthesis of daphanidin E, we were able to isolate desired product **3.145**.⁶⁹ Unfortunately, this result was highly irreproducible as the starting material was prompt

towards spontaneous enolization, which prevents further reactivity. Recognizing uncontrollable behavior of the Michael acceptor within the substrate **3.136**, reduced analogue **3.135** with attenuated reactivity was explored next (Scheme 3.22).

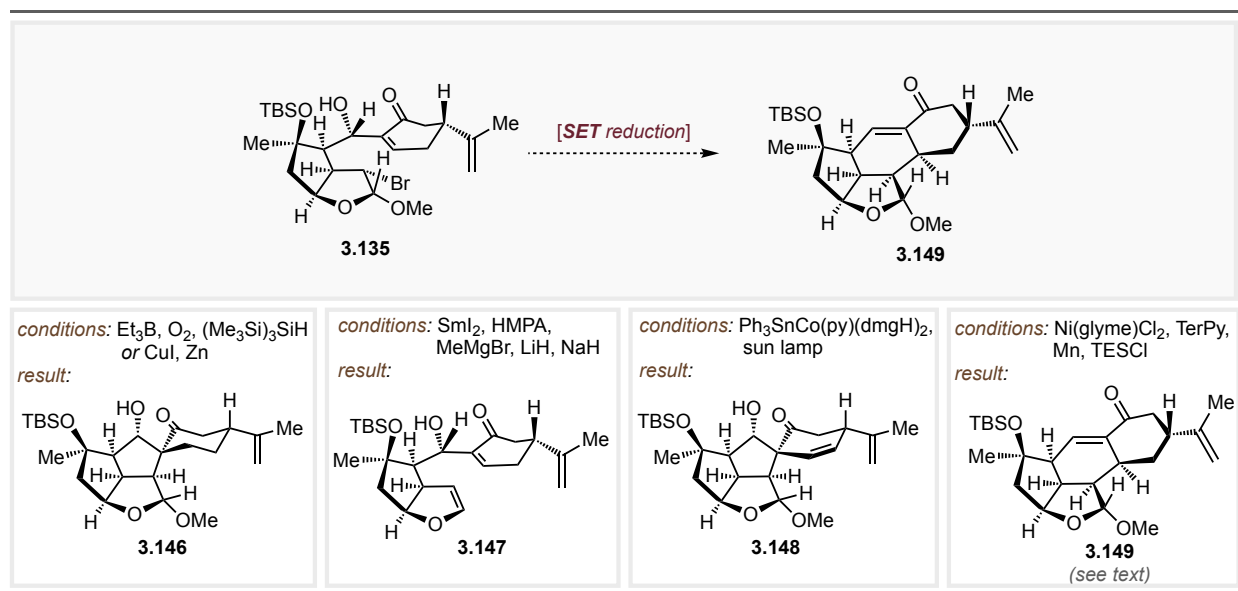
Classical conditions for radical generation delivered *5-exo-trig* cyclization product **3.146** with exquisite selectivity as in previous cases. Using SmI₂ in presence of various bases for alcohol deprotonation led to the formation of vinyl ether **3.147** via double electron transfer to the bromide,



Scheme 3.21 Single electron reduction of bromide **3.136** for intramolecular Giese addition.

followed by elimination. Of note, use of other additives and co-solvents to modulate the reduction potential of samarium did not significantly change the outcome of transformation. Employing low-valent cobalt complex, which provided a promising lead for diketone **3.136**, new product **3.148** was obtained. Heck cyclization occurred, however *5-exo-trig* selectivity outweighed the electronic bias of the substrate. Finally, after numerous attempts, appropriate conditions were identified. Ni-catalyzed reductive coupling conditions reported by Weix delivered the desired product **3.149**

in 35% yield as a major component. The hydroxyl group was eliminated, presumably as a silanol, to provide key intermediate en route towards ineleganolide. To optimize the process, significant amount of material was needed. Upon increasing the scale of the reaction (**3.106** → **3.134**) irreproducibility and propensity of the bromide **3.134** towards spontaneous and rapid decomposition was noted. Therefore, despite encouraging results on the frontline, further progress stalled as a reliable pipeline of the material could not be established. Later, additional



Scheme 3.22 Single electron reduction of bromide **3.135** for intramolecular Giese addition.

details became available that shed light onto origin of this sensitivity. As noted before, the functional group at C6 is in close proximity to C12 and situated perfectly for the back-side attack if substituent is present. We hypothesized that the carbonyl group is capable of acting as a nucleophile to generate oxocarbenium ion **3.150**, which further undergoes rapid decomposition (Figure 3.7). Indirect evidence was obtained through in situ NMR studies. Considering that the problem is intrinsic to the substrate and does not correlate with reaction conditions or isolation techniques, we saw no way for its mitigation, and thus the strategy was abandoned.

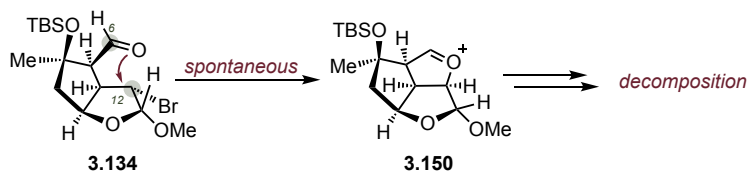
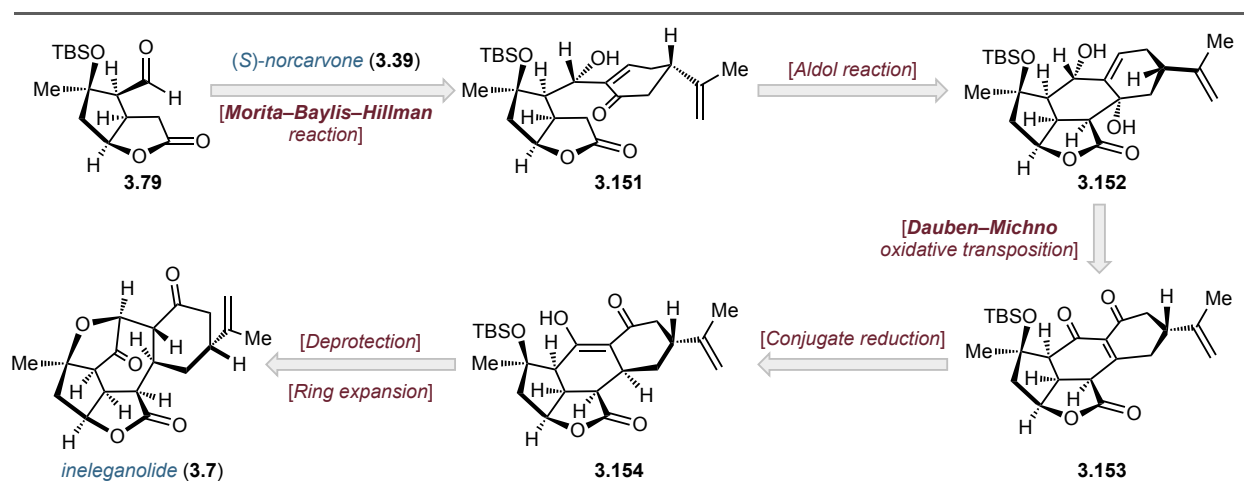


Figure 3.7 Origin of instability of **3.134** and related intermediates.

3.3.5 Strategy III: use of (*S*)-norcarvone

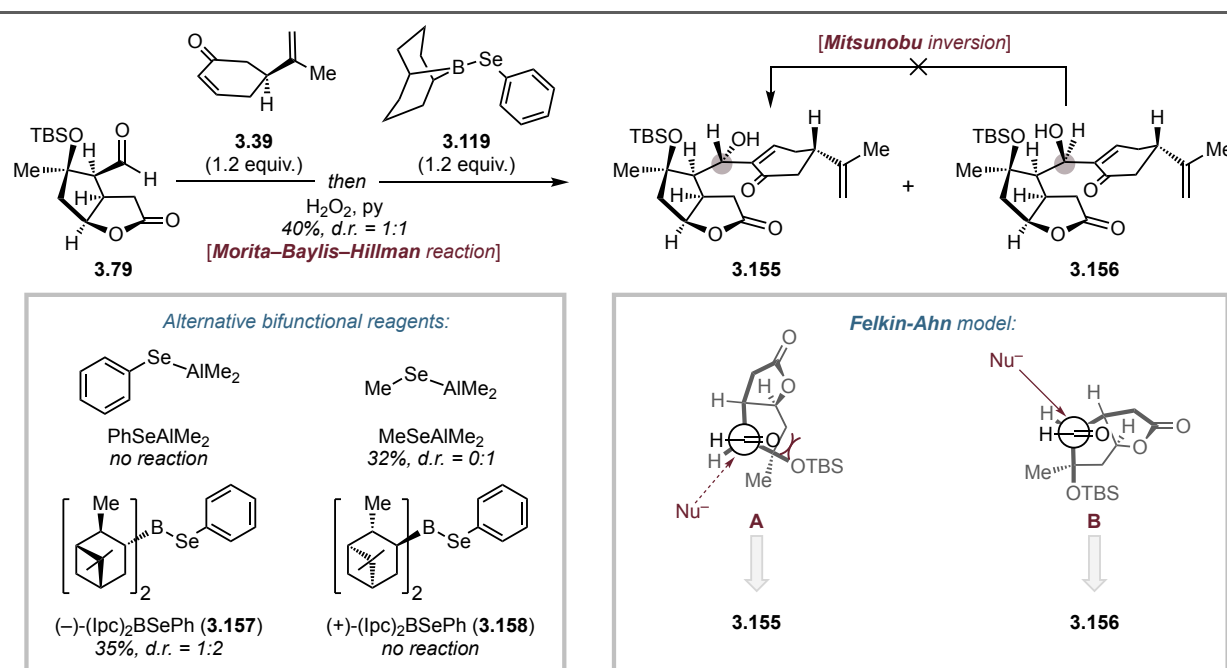
Since conjugate mode of addition was out of reach, an alternative approach was proposed based on previously established 1,2-cyclization. In order to accommodate undesired connectivity resulting from 1,2-addition, manipulation of oxidation states at the core were envisaged (Scheme 3.23). In the forward sense, aldehyde **3.79** would be merged with norcarvone as previously developed. Use of (*S*)-enantiomer would deliver the correct stereocenter at C1 after intramolecular aldol cyclization. Oxidation of the diol **3.152** with concomitant transposition would deliver diketone **3.153**. Conjugate reduction of **3.153** should be facile due to electronic activation despite high steric hindrance and readily furnish key precursor **3.154** en route towards ineleganolide.²⁵ Potential use of (*S*)-norcarvone, however, raises the concerns regarding translation of previously obtained results to the diastereomeric system.



Scheme 3.23 Revised approach towards ineleganolide.

Applying previously developed conditions for MBH-coupling, an equimolar mixture of products **3.155** and **3.156** was obtained in 40% yield (Scheme 3.24). Perhaps, lower productivity and selectivity in this case is a manifestation of the distinct interactions between the lactone ring and the diastereomeric phenyl selenide residue due to use of enantiomeric norcarvone (see p. 155). From prior studies, lower reactivity of **3.156** during cyclization was anticipated (as was proven later). Thus, an increase in the diastereoselectivity of the coupling towards **3.155** was desired. First, similar bifunctional reagents derived from Me_3Al were examined.⁵⁵ Not only lower yields were observed, but also exclusive selectivity towards undesired alcohol **3.156**. Presumably, use of more reactive and basic aluminum enolate facilitates the decomposition pathway in larger extent. Different diastereoselectivity, in turn, was ascribed to a change in the mode of

addition. The transformation proceeds through open transition state rather than closed one. Hence, exclusive formation of the **3.156** can be attributed to the stereoselection under Felkin–Ahn control. Transition state **A** is significantly disfavored by steric repulsions between the carbonyl lone pair and the bulky silyl protecting group (Scheme 3.30). These interactions are alleviated, however, in **B**, which ultimately leads to the observed product **3.156**. Lack of selectivity under standard conditions hinted at the possibility to bias the ratio by applying a chiral reagent. Use of **3.157**, prepared from (–)-pinene and benzeneselenol, afforded products **3.155** and **3.157** in similar yield

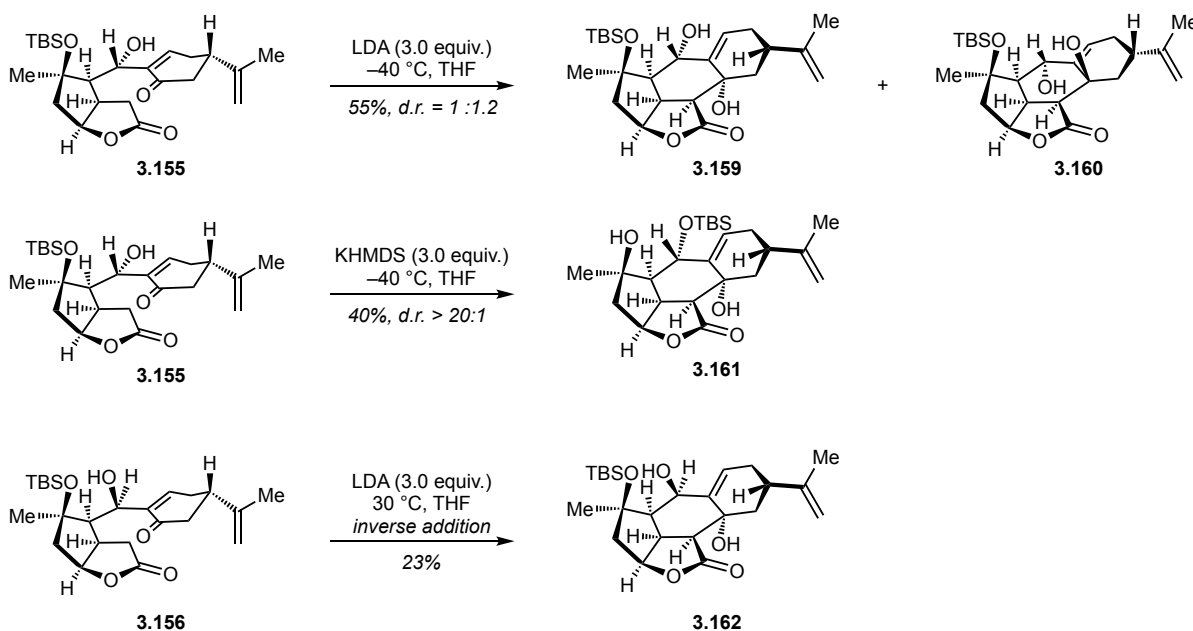


Scheme 3.24 MBH-coupling of aldehyde **3.79** with (*S*)-norcarvone.

and 1:2 diastereoselectivity. Notwithstanding, switch to enantiomeric (+)-pinene led only to the decomposition instead of favoring **3.155** in MBH-coupling, thus depicting mismatching case between chiral reagent **3.158** and the starting material. Attempts to convert **3.156** into **3.155** via Mitsunobu-type inversion also were fruitless. Due to severe steric hindrance of the substrate, it remained unchanged under most of the explored reaction conditions. Only use of Tsunoda's protocol⁷⁰ in presence of 4-methoxybenzoic acid allowed for appreciable conversion, however, only in undesired $\text{S}_{\text{N}}2'$ fashion (not shown). We recognized that the potential solution for the stereocontrolled MBH-coupling might dwell in exploiting chelation control, favoring transition state **A**. As such an approach would require different protecting groups for the tertiary alcohol and

probable reoptimization of the coupling conditions and as prior steps, it was not pursued for the time being.

Cyclization process was not significantly affected by the reversed stereocenter of the isopropenyl unit (Scheme 3.25). Similar results were obtained, with prevailing 1,2-aldol reaction over intramolecular Michael addition. A range of compounds (**3.159**, **3.160**, **3.161**, **3.162**) was obtained under various conditions in moderate yields. The structures were assigned by analogy with the previous system (see p. 157) and their convergence after chemical manipulations such as deprotection and/or oxidation (see later). Notably, both points of diversity—the configuration of the secondary and tertiary alcohols—are not present in the aforementioned intermediates. Thus, there was an expectation that the low stereoselectivity of the certain steps discussed so far could be inconsequential if appropriate conditions for their parallel reactivity were identified.

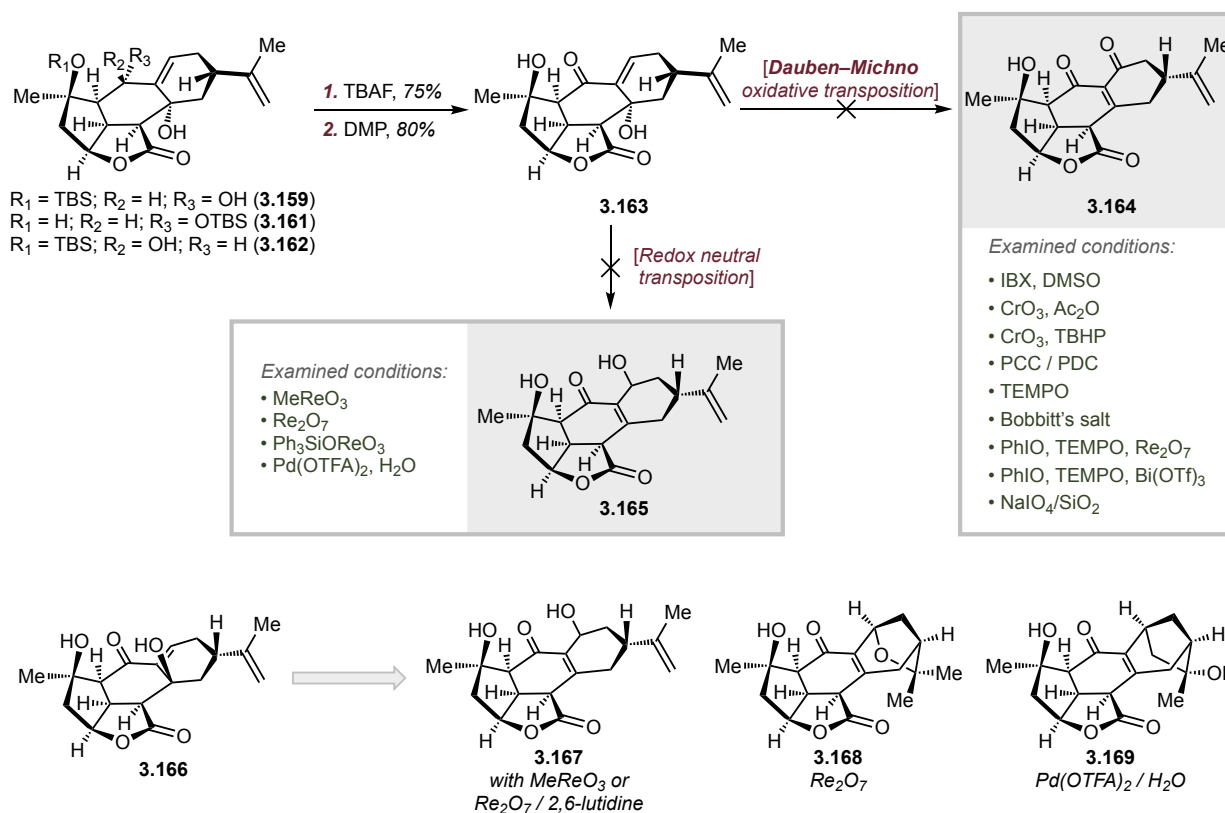


Scheme 3.25 Intramolecular cyclization of MBH-coupling products from (*S*)-norcarvone.

Towards this goal, compounds **3.159**, **3.161** and **3.162** converged upon TBAF-deprotection and oxidation (Scheme 3.26). The substrate **3.163** was explored for either oxidative or redox neutral transposition. Unfortunately, only starting material was recovered under numerous tested conditions. In contrast, diastereomer **3.166** derived from **3.160** turned out to be more reactive. Use of either MTO⁷¹ or rhenium(VII) oxide,⁷² buffered with 2,6-lutidine, delivered desired transposed allylic alcohol **3.166** with excellent conversion as a single diastereomer (configuration was not determined). Notably, Lewis acidic rhenium(VII) oxide in the absence of buffer or Pd(II)⁷³

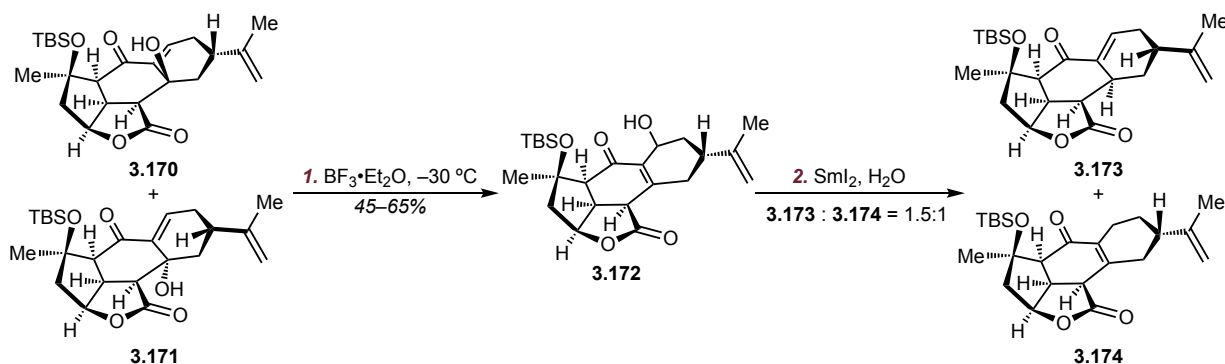
furnished bridged products **3.168** and **3.169** respectively, revealing propensity of the tertiary alcohol towards ionization.

After significant experimentation, it was discovered that strong Lewis and Bronsted acids are competent mediators for the desired redox neutral transposition on both substrates **3.170** and **3.171** (Scheme 3.27). Thus, compound **3.172** can be obtained in moderate yield employing $\text{BF}_3 \cdot \text{Et}_2\text{O}$ (unoptimized). Preliminary studies demonstrated feasibility of the conjugate reduction, which can provide divergent access to the key precursors enone **3.173** or diketone **3.154**, but further optimization is required.



Scheme 3.26 Investigation of transposition of diastereomeric allylic alcohols.

While this strategy is capable of providing key elaborate intermediates for the final contemplated ring expansion, it did not fully adhere to our standards. Multiple redox manipulations as well as the necessity to carry numerous diastereomers through the sequence rendered it rather impractical. Thus, an alternative approach was explored simultaneously with further investigations of the strategy discussed above.



Scheme 3.27 Successful allylic transposition.

3.3.6 Strategy IV: acyl-Stille transform

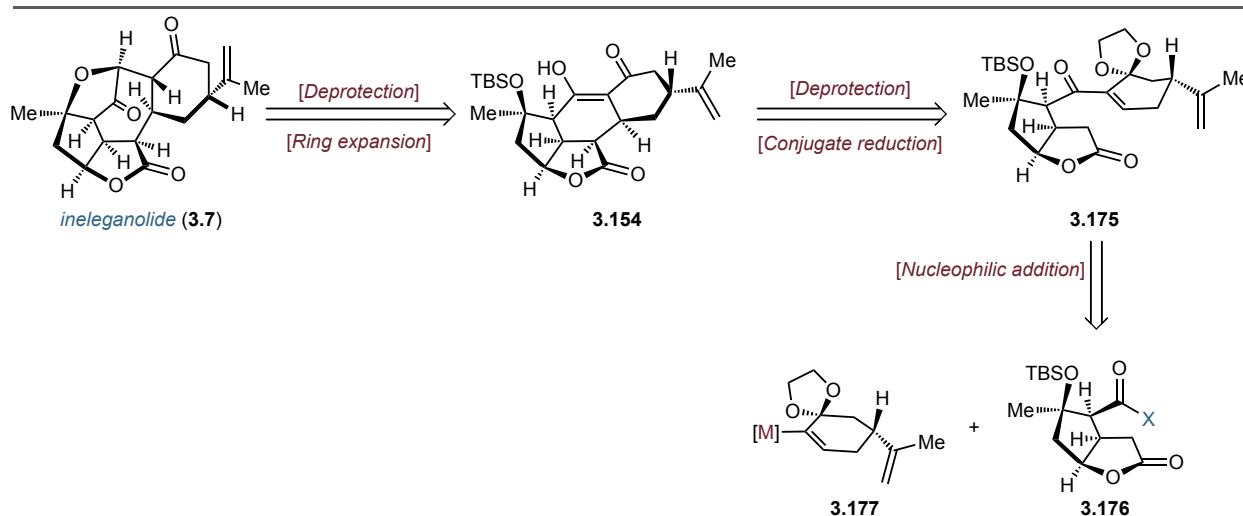
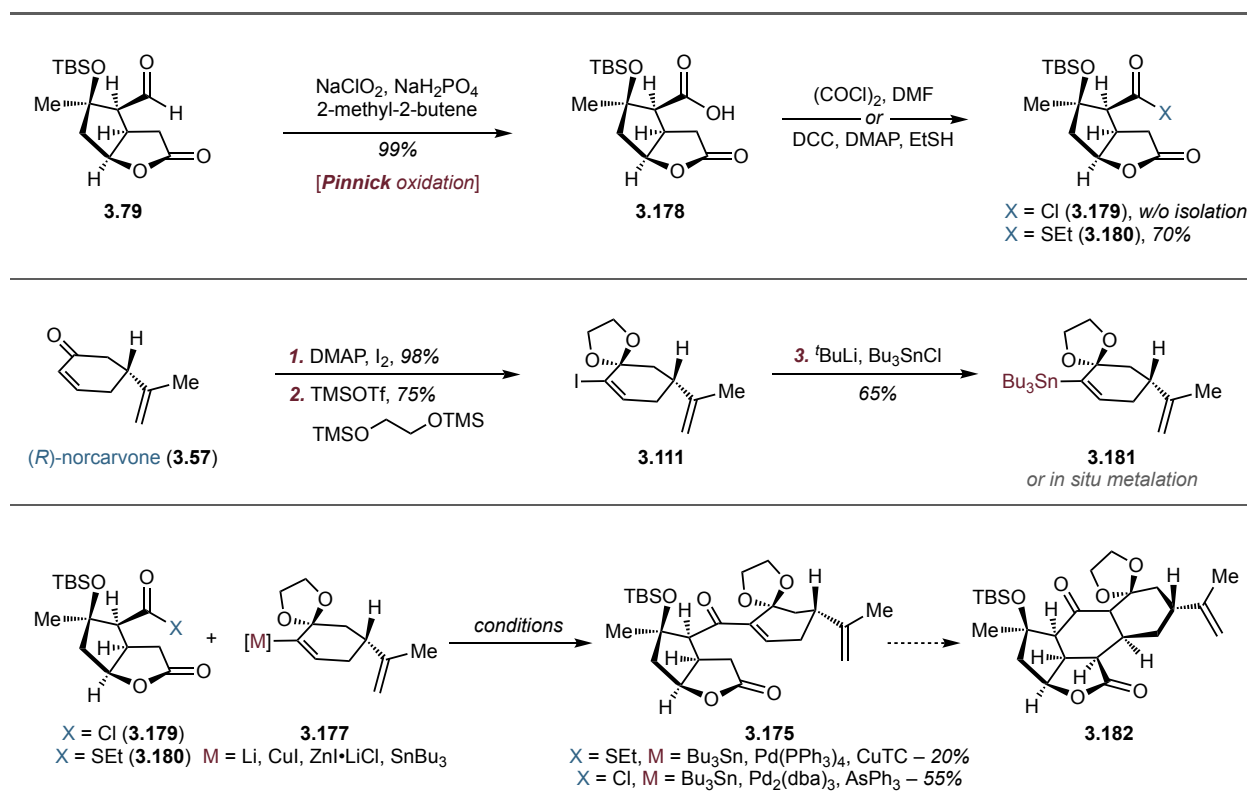


Figure 3.8 Redesigned retrosynthesis towards ineleganolide.

Cognizant of the pitfalls in the previous strategy, **3.175** was explored as masked diketone **3.128**, an alternative precursor for the cyclization event (Figure 3.8). We hypothesized that intermediacy of **3.175** would provide several advantages. First, this substrate has fewer kinetically accessible positions for deprotonation, thus a potentially higher yield for the cyclization could be anticipated. Second, substrate **3.175** has no possible competition between 1,2- and 1,4-addition. Hence, originally planned Michael addition would obviate additional manipulations previously required for oxidation state adjustments. Third, contrasting to MBH-reaction, coupling between two partners (**3.176** and **3.177**) does not generate a diastereomeric mixture, enhancing the practicality of the approach. Merging the two fragments was envisioned through simple nucleophilic addition of norcarvone-derived nucleophile to the appropriate electrophile.

Towards this goal, aldehyde was oxidized to the acid under Pinnick conditions in quantitative yield (Scheme 3.28). Acid **3.178** in turn was converted either to the hydrolytically unstable acyl chloride **3.179** or isolable thioester **3.180**. Access to the pronucleophile was secured through α' -iodination followed by glycol protection under Noyori conditions. Vinyl iodide **3.111** was directly transformed into a nucleophilic species either in situ via direct metalation or as stable vinyl stannane **3.181**. Various conditions were explored in order to bring both fragments together. ⁷⁴ Seemingly straightforward addition of the vinyl lithium (**3.177**, M = Li) to acyl chloride **3.179** failed to deliver the desired product **3.175**. Only exclusive lactone opening was observed. The preferential reactivity was ascribed to steric inaccessibility of the acyl chloride located in the

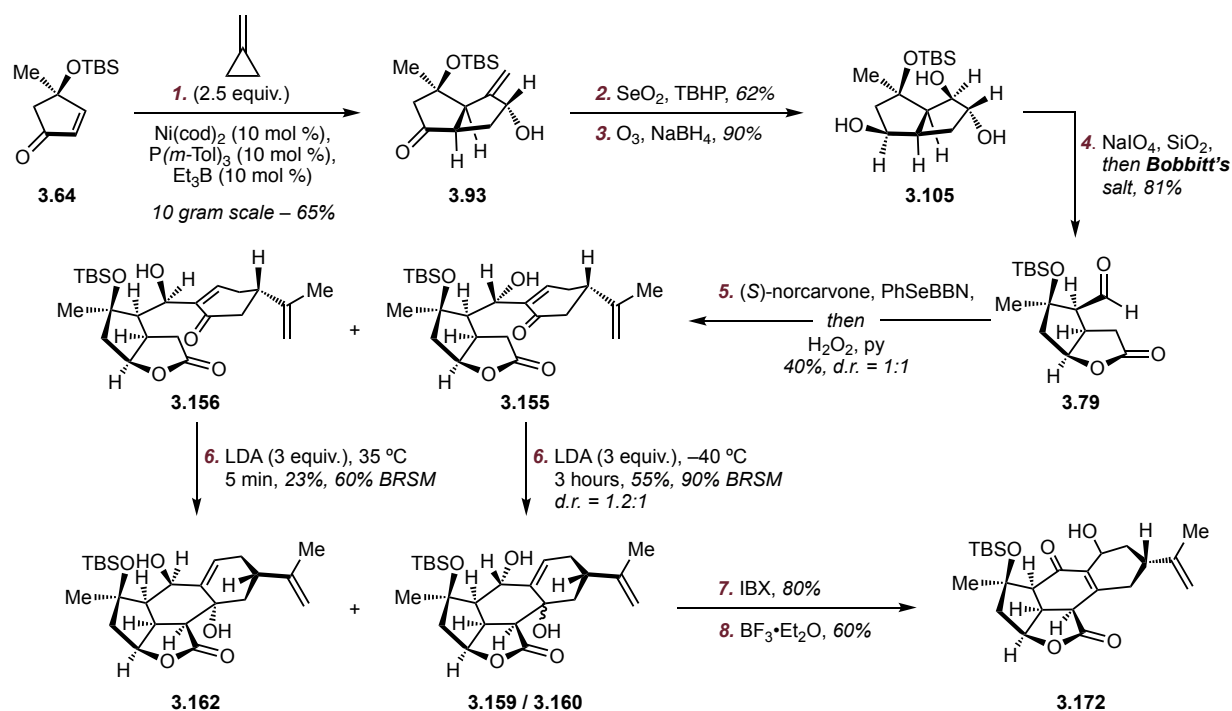


Scheme 3.28 Alternative coupling of two fragments: aldehyde **3.79** and (R)-norcarvone.

concavity of the molecule. Less reactive vinyl metal species such as cuprates or manganates returned starting material unchanged.⁷⁵ Subsequently, transition-metal-catalyzed processes were explored. Neither acyl-Negishi⁷⁶ (**3.177**, M = Zn; **3.179** X = Cl) nor acyl-Kumada (**3.177**, M = Mg; **3.179** X = Cl) couplings afforded any of the desired product. Use vinyl tin reagent (**3.177**, M = SnBu₃), however, proved to be more efficient. To our delight, coupling of **3.181** with thioester **3.180** under Liebeskind–Srogl conditions furnished desired product **3.175** in 20% yield

(unoptimized). Better results were obtained utilizing acyl-Stille cross-coupling (55%, unoptimized).⁷⁷ Thus, the stage was set for investigations of the Michael addition, which is currently ongoing in our laboratory.

3.4 Conclusion and Outlook



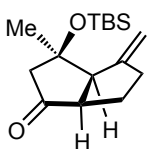
Scheme 3.29 Developed route towards ineleganolide.

To summarize, a novel divergent strategy towards norcembranoid diterpenoids was designed. In order to access advanced intermediates, unorthodox transformations have been employed. For example, a unique Ni-catalyzed pentannulation enabled rapid assembly of all-*cis* bicyclic intermediate in excellent diastereoselectivity. An underutilized boron-selenium bifunctional reagent, in turn, empowered MBH-type coupling inaccessible under any other examined conditions. Despite unexpected reactivity and challenging stereochemical puzzles, elaborated intermediates were attained in rather expedient fashion. The current approach is summarized in the Scheme 3.29. The route to the last key precursor consists of only eight steps, emphasizing the efficiency of the synthetic sequence and executed retrosynthetic disconnections. The final ring expansion reaction is needed to conclude the first total synthesis of ineleganolide.

Moreover, a more practical alternative route is being explored in parallel to ensure the positive outcome of this research project.

3.5 Experimental Section

Synthesis of compound 3.93:



Preparation of methylenecyclopropane stock solution: Methylenecyclopropane (**3.90**) was prepared by modification of the literature protocol for its isotopolog.

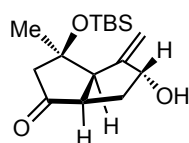
The scale of the protocol should be $3 \times$ that of the planned annulation to ensure enough methylenecyclopropane is prepared. The reaction was performed under a stream of nitrogen to ensure full collection of the methylenecyclopropane in the cold trap. In an oven-dried 3-neck round bottom flask equipped with a stir bar, reflux condenser, and a connecting line to a 2-neck flask attached to a cold finger at $-78\text{ }^{\circ}\text{C}$ was added potassium *tert*-butoxide (10.77 g, 96.0 mmol, 1.20 equiv.) and dry DMSO (108 mL) and the suspension was heated to $45\text{ }^{\circ}\text{C}$ whereupon the solution became clear. (Bromomethyl)cyclopropane (7.76 mL, 80.0 mmol, 1.0 equiv.) was added dropwise over 10 min. and the reaction was stirred a further 30 min. A tared Schlenk tube filled with 13.4 mL Et₂O was then cooled to $-78\text{ }^{\circ}\text{C}$ under nitrogen atmosphere and the methylenecyclopropane was transferred to this solution via cannula, ensuring the end of the cannula was below the level of the Et₂O. The solution of methylenecyclopropane was then weighed to determine the yield (3.39 g, 62.7 mmol, 78%) and concentration 4.70 M.

Nickel-catalyzed methylenecyclopropane annulation: The reaction was performed in 6 parallel microwave vials and was combined at the end for purification. In a nitrogen filled glove box, an oven-dried microwave vial equipped with stir bar was charged with Ni(cod)₂ (121 mg, 0.442 mmol, 10 mol %) and P(*m*-tol)₃ (134 mg, 0.442 mmol, 10 mol%) and the vial was sealed. Enone **3.64** (1.00 g, 4.42 mmol, 1.0 equiv.) was then added under nitrogen and the solution was stirred 5 min. before the addition of neat Et₃B (64.0 μL , 0.442 mmol, 10 mol%) and stirring an additional 5 min. The dark red solution was then cooled to $-78\text{ }^{\circ}\text{C}$ and the methylenecyclopropane solution (1.88 mL, 8.83 mmol, 4.70 M, 2.0 equiv.) was added. The vial was detached from nitrogen and was heated to $75\text{ }^{\circ}\text{C}$ overnight whereupon a black precipitate was observed. The 6 vials were combined, concentrated over Celite, and purified by flash chromatography (SiO₂, hexanes : EtOAc

= 30:1 → 15:1) to give the desired compound as a yellow oil (5.58 g, 19.9 mmol, 75%). NMR analysis of the final product showed >95% conversion.

¹H NMR: (500 MHz, CDCl₃) δ 5.03 – 4.99 (m, 1H), 4.99 – 4.96 (m, 1H), 2.99 (dq, *J* = 9.6, 1.6 Hz, 1H), 2.94 – 2.83 (m, 1H), 2.51 – 2.39 (m, 3H), 2.32 (dt, *J* = 16.4, 7.3, 2.0 Hz, 1H), 1.92 (q, *J* = 8.1 Hz, 2H), 1.49 (s, 3H), 0.81 (s, 9H), 0.06 (s, 3H), 0.03 (s, 3H).; **¹³C NMR:** (126 MHz, CDCl₃) δ 218.6, 151.7, 108.5, 79.6, 58.9, 55.8, 53.3, 34.8, 27.9, 27.8, 25.9, 18.2, –2.21, –2.25.

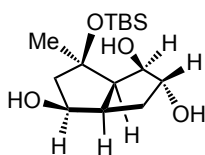
Synthesis of compound 3.104:



To a stirred suspension of SeO₂ (156 mg, 1.40 mmol, 0.50 equiv.) in CH₂Cl₂ (28.1 mL) at ambient temperature in a water bath was added 70% aqueous TBHP (770 μL, 5.62 mmol, 2.0 equiv.). The reaction was stirred for 30 min. at the same temperature before the addition of bicycle **3.93** (788 mg, 2.81 mmol, 1.0 equiv.) in CH₂Cl₂ (14.0 mL) and the reaction was allowed to stir until complete by TLC (*ca.* 3.5 h). Upon completion, the reaction was quenched with 3:1 10% aq. Na₂HPO₄:10% aq. Na₂S₂O₃ (20 mL) and diluted with EtOAc (50 mL). The two phases were shaken vigorously and separated, and the aqueous phase was extracted with EtOAc (3 × 20 mL). The organic phase was washed with 10% aq. Na₂HPO₄:10% aq. Na₂S₂O₃ (3:1, 20 mL), brine (20 mL), dried over MgSO₄, filtered and concentrated. The crude residue was purified by flash chromatography (SiO₂, hexanes:EtOAc = 4:1 → 1:1) to give the desired compound as an off white solid (668 mg, 2.25 mmol, 80%).

R_f: 0.18 (SiO₂, hexanes : EtOAc = 2:1); **T_{melt.}:** 80.2 – 80.6 °C; **¹H NMR:** (500 MHz, CDCl₃) δ 5.34 – 5.27 (m, 1H), 5.22 – 5.13 (m, 1H), 4.53 (t, *J* = 6.6 Hz, 1H), 3.17 (dd, *J* = 10.4, 1.7 Hz, 1H), 2.99 (td, *J* = 10.4, 5.9 Hz, 1H), 2.49 (d, *J* = 16.4 Hz, 1H), 2.43 (d, *J* = 16.4 Hz, 1H), 2.28 (dt, *J* = 13.4, 6.6 Hz, 1H), 1.82 (ddd, *J* = 13.4, 10.4, 5.9 Hz, 1H), 1.52 (s, 4H), 0.80 (s, 9H), 0.07 (s, 3H), 0.04 (s, 3H).; **¹³C NMR:** (126 MHz, CDCl₃) δ 217.5, 154.3, 110.5, 79.2, 75.8, 57.4, 55.5, 49.0, 36.8, 27.5, 25.9, 18.3, –2.2, –2.3.; **HRMS:** (EI+, *m/z*) [*M*]⁺ calcd. for C₁₆H₂₈O₃Si, 296.1808; found, 296.1812; **IR:** (ATR, neat, cm^{–1}): 3317 (br), 2929 (m), 1738 (s), 1253 (s), 1051 (m), 1018 (w); **[α]_D:** –141.1 ° (*c* = 1.0, CHCl₃, 21 °C)

Synthesis of compound 3.105:

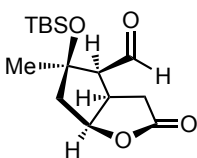


Allyl alcohol **3.104** (3.39 g, 11.4 mmol, 1.0 equiv.) was dissolved in CH₂Cl₂ (114 mL) and cooled to –78 °C. The reaction was sparged with ozone until a blue color persisted. After 1 min. of excess ozone, the reaction was then sparged

with nitrogen. MeOH (57.2 mL) was then added followed by the portionwise addition of NaBH₄ (2.16 g, 57.2 mmol, 5.0 equiv.). The cold bath was removed and the reaction was allowed to warm to ambient temperature and stirred 3 hr. The reaction was then concentrated over silica gel and purified by flash chromatography (SiO₂, 4% → 8% MeOH in CH₂Cl₂) to give the desired compound as a white solid [3.09 g, 10.2 mmol, 89%].

R_f: 0.24 (SiO₂, EtOAc); **T_{melt.}**: 112.5 – 113.7 °C; **¹H NMR** (500 MHz, CDCl₃) δ 4.34 (d, *J* = 4.3 Hz, 1H), 4.21 (q, *J* = 4.3 Hz, 1H), 4.13 – 4.00 (m, 2H), 2.84 (d, *J* = 8.9 Hz, 1H), 2.73 (tdd, *J* = 9.9, 7.2, 5.1 Hz, 1H), 2.51 (dd, *J* = 9.9, 6.1 Hz, 1H), 2.33 (dt, *J* = 14.2, 5.5 Hz, 1H), 2.13 – 1.97 (m, 3H), 1.56 (ddd, *J* = 14.0, 9.9, 4.1 Hz, 1H), 1.45 (s, 3H), 0.89 (s, 9H), 0.18 (s, 6H).; **¹³C NMR**: (126 MHz, CDCl₃) δ 83.9, 80.4, 79.0, 72.3, 56.6, 51.9, 44.5, 32.3, 30.7, 26.0, 18.1, –1.7, –2.2.; **HRMS**: (ES⁺, *m/z*) [M+Na]⁺ calcd. for C₁₅H₃₀O₄SiNa, 325.1811; found, 325.1806; **IR**: (ATR, neat, cm^{–1}): 3390 (br), 2931 (m), 1257 (m), 1155 (m), 1039 (s), 1010 (s).

Synthesis of lactone **3.79**:

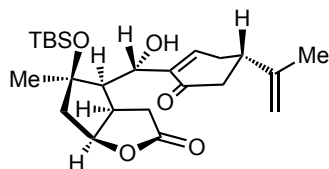


To a vigorously stirred suspension of NaIO₄ supported on SiO₂ (2.0 g / 1 mmol substrate) in CH₂Cl₂ (135 mL) under nitrogen atmosphere in a water bath, was added triol **3.105** (3.50 g, 9.26 mmol, 1.0 equiv.) in CH₂Cl₂ (50 mL) dropwise via addition funnel over 10 min. The reaction was stirred until complete by ¹H NMR (aliquot, *ca.* 24 h). On complete conversion, Bobbitt's salt (**3.107**, 3.06 g, 10.2 mmol, 1.1 equiv.) was added and the reaction was stirred until complete by ¹H NMR (aliquot, *ca.* 24 h). On completion, the reaction was filtered over Celite and washed with CH₂Cl₂ : MeOH = 20:1 (300 mL). The filtrate was concentrated and the crude residue was taken up in EtOAc (200 mL). The organic phase was washed with 10% aq. Na₂S₂O₃ (100 mL), brine (100 mL), dried over MgSO₄, filtered, and concentrated. The residue was purified by flash chromatography (C₁₈ SiO₂, 5% → 95% MeCN in H₂O) to give the desired compound as a colorless oil [2.38 g, 7.97 mmol, 86%].

R_f: 0.06 (SiO₂, hexanes : EtOAc = 3:1); **¹H NMR** (500 MHz, CDCl₃) δ 9.88 (s, 1H), 5.02 (t, *J* = 7.8 Hz, 1H), 3.29 (dtd, *J* = 11.5, 8.6, 6.1 Hz, 1H), 2.84 (dd, *J* = 18.9, 6.1 Hz, 1H), 2.69 (dd, *J* = 18.9, 11.5 Hz, 1H), 2.55 (d, *J* = 8.6 Hz, 1H), 2.30 (d, *J* = 15.5 Hz, 1H), 2.01 (dd, *J* = 15.5, 7.8 Hz, 1H), 1.60 (s, 3H), 0.78 (s, 10H), 0.09 (s, 3H), 0.08 (s, 3H).; **¹³C NMR**: (126 MHz, CDCl₃) δ 201.2, 177.4, 83.7, 83.0, 64.1, 48.2, 39.0, 31.8, 27.6, 25.8, 18.2, –1.9, –2.5.; **HRMS**: (ES⁺, *m/z*) [M+H]⁺ calcd. for C₁₅H₂₇O₄Si, 299.1679; found, 299.1672; **IR**: (ATR, neat, cm^{–1}): 3317 (br), 2929 (m),

1738 (s), 1253 (s), 1051 (m), 1018 (w); $[\alpha]_D$: +35.1 ° (c = 1.0, CHCl₃, 23 °C)

Synthesis of compound 3.155:



(*S*)-norcarvone (297 mg, 2.18 mmol, 1.3 equiv.) was slowly added to the solution of PhSeBBN (**3.119**) in PhMe (3.63 mL, 2.18 mmol, 0.6 M, 1.3 equiv.) at 24 °C under inert atmosphere in a foil-wrapped vessel. After being stirred for 3 h solution was treated with aldehyde

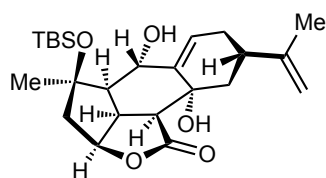
3.79 in PhMe (500 mg, 1.68 mmol, 1.0 equiv., 1.0 M). Reaction was aged for 10 h. Finally, reaction mixture was diluted with CH₂Cl₂ (5 mL) and cooled to 0 °C. Pyridine (1.4 mL, 21.8 mmol, 10.0 equiv.) and H₂O₂ (aq. 30 w/w %, 1.7 mL, 21.8 mmol, 10.0 equiv.) were carefully added sequentially. Ice-bath was removed and reaction was kept for another 3 h with vigorous stirring. EtOAc was added (30 mL) and solution was transferred into separatory funnel. Organic phase was washed with NaHCO₃ (aq. sat., 30 mL), water (30 mL), CuSO₄ (10 w/w %, 30 mL), water (30 mL), brine (30 mL), dried over Na₂SO₄, filtered and concentrated. The crude residue was purified by flash chromatography (SiO₂, hexanes : EtOAc = 5:1 → 3:1) to give compound **3.155** (140 mg, 0.32 mmol, 19%) and **3.156** (151 mg, 0.35 mmol, 21%) as colorless viscous oil.

R_f: 0.23 (SiO₂, hexanes : EtOAc = 2:1); **¹H NMR** (500 MHz, CDCl₃) δ 6.93 (dd, *J* = 5.8, 2.6 Hz, 1H), 4.93 (t, *J* = 7.8 Hz, 1H), 4.85 (s, 1H), 4.78 (s, 1H), 4.55 (d, *J* = 8.7 Hz, 1H), 3.13 (br, 1H), 2.88–2.79 (m, 2H), 2.62–2.52 (m, 3H), 2.43–2.25 (m, 6H), 1.94 (dd, *J* = 15.5, 7.8 Hz, 1H), 1.76 (s, 3H), 1.56 (s, 3H), 0.91 (s, 9H), 0.18 (s, 3H), 0.15 (s, 3H); **¹³C NMR**: (126 MHz, CDCl₃) δ 201.0, 177.7, 147.9, 145.8, 139.3, 111.4, 83.9, 83.1, 72.5, 56.0, 49.1, 43.8, 42.0, 41.2, 31.5, 31.2, 28.7, 26.2, 20.6, 18.6, –1.6, –2.2; **HRMS**: (ES⁺, *m/z*) [M+H]⁺ calcd. for C₂₄H₃₉O₅Si, 435.2567; found, 435.2558; **IR**: (ATR, neat, cm^{–1}): 2930 (m), 1765 (s), 1667 (s), 1376 (m), 1193 (s); $[\alpha]_D$: +1.7 ° (c = 1.0, CHCl₃, 23 °C)

Synthesis of compounds 3.159 & 3.160:

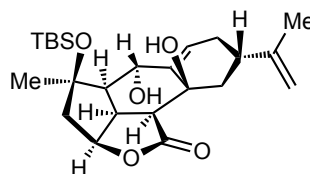
Enone **3.155** (125 mg, 0.29 mmol, 1.0 equiv.) was dissolved in THF (14 mL, 0.02 M) and cooled to –35 °C. Solution of LDA in THF (0.88 mmol, 3.0 equiv., 1.0 M) was added dropwise under inert atmosphere. The reaction mixture was maintained at the above temperature for 1 h and quenched with NH₄Cl (aq., sat., 5 mL). EtOAc was added and the mixture was transferred into separatory funnel. The two phases were shaken vigorously and separated, and the aqueous phase

was extracted with EtOAc (3×10 mL). The organic phase was washed with brine (30 mL), dried over MgSO_4 , filtered and concentrated. The crude residue was purified by flash chromatography (SiO_2 , hexanes : EtOAc = 5:1 \rightarrow 1:1) to give compound **3.159** (31 mg, 71 μmol , 25%) and **3.160** (37 mg, 85 μmol , 30%) as colorless viscous oil.



Compound 3.159:

R_f: 0.45 (SiO_2 , hexanes : EtOAc = 2:1); **¹H NMR** (500 MHz, CDCl_3) δ 6.00 (dd, J = 5.4, 2.5 Hz, 1H), 4.79 (s, 1H), 4.76 (s, 1H), 4.74 (s, 1H), 4.66 (d, J = 9.1 Hz, 1H), 3.98 (s, 1H), 3.02 (tdd, J = 10.5, 7.5, 2.6 Hz, 1H), 2.91 (s, 1H), 2.87 (dd, J = 11.2, 2.4 Hz, 1H), 2.59 (m, 1H), 2.34–2.23 (m, 3H), 2.08 (m, 1H), 1.98–1.88 (m, 2H), 1.76 (s, 3H), 1.61 (dd, J = 12.8, 11.6 Hz, 1H), 1.43 (s, 3H), 0.9 (s, 9H), 0.19 (s, 3H), 0.17 (s, 3H); **¹³C NMR**: (126 MHz, CDCl_3) δ 177.9, 148.8, 139.0, 121.9, 109.4, 82.8, 82.4, 69.1, 66.7, 57.7, 49.7, 46.2, 45.2, 39.5, 36.7, 30.7, 30.3, 26.0, 21.1, 18.3, –1.8, –2.2; **HRMS**: (ES+, m/z) [$\text{M}+\text{Na}$]⁺ calcd. for $\text{C}_{24}\text{H}_{38}\text{O}_5\text{SiNa}$, 457.2386; found, 457.2379;



IR: (ATR, neat, cm^{-1}): 2929 (m), 1747 (s), 1257 (m), 1162 (s), 1043 (m) 1001 (s); **[α]_D**: –11.4 ° (c = 1.0, CHCl_3 , 22 °C)

Compound 3.160:

R_f: 0.10 (SiO_2 , hexanes : EtOAc = 2:1); **¹H NMR** (500 MHz, CDCl_3) δ 6.24 (dd, J = 4.8, 2.4 Hz, 1H), 4.94 (s, 1H), 4.89 (s, 1H), 4.73 (td, J = 7.4, 3.6 Hz, 1H), 4.41 (s, 1H), 4.37 (d, J = 10.1 Hz, 1H), 3.25 (s, 1H), 3.21 (dt, J = 9.9, 7.9 Hz, 1H), 2.97 (dd, J = 14.0, 5.2 Hz, 1H), 2.91 (d, J = 10.0 Hz, 1H), 2.59 (s, 1H), 2.48 (ddt, J = 18.4, 4.9, 2.0 Hz, 1H), 2.41 (dt, J = 6.5, 3.3 Hz, 1H), 2.38–2.33 (m, 2H), 2.18 (dd, J = 14.5, 3.7 Hz, 1H), 2.08 (ddd, J = 14.0, 3.7, 1.4 Hz, 1H), 1.90 (s, 3H), 1.39 (s, 3H), 0.90 (s, 9H), 0.17 (s, 3H), 0.15 (s, 3H); **¹³C NMR**: (126 MHz, CDCl_3) δ 174.8, 151.1, 135.9, 127.5, 111.4, 85.1, 80.0, 70.8, 67.9, 52.2, 47.8, 45.8, 39.7, 36.9, 35.8, 30.5, 29.3, 26.0, 22.7, 18.1, –2.0, –2.1; **HRMS**: (ES+, m/z) [$\text{M}+\text{H}$]⁺ calcd. for $\text{C}_{24}\text{H}_{39}\text{O}_5\text{Si}$, 435.2567; found, 435.2580; **IR**: (ATR, neat, cm^{-1}): 2930 (m), 1764 (s), 1254 (m), 1159 (m), 1099 (s), 1010 (s); **[α]_D**: +1.7 ° (c = 1.0, CHCl_3 , 23 °C)

3.6 Acknowledgment of Contributions

Y. D. Boyko designed retrosynthesis and carried out initial experiments of Ni-catalyzed pentannulation. Dr. L. W. Hernandez optimized MCP annulation and designed protocol amenable

for large scale. Dr. L. W. Hernandez established enantioselective route to norcarvone. Y. D. Boyko carried out the rest synthetic investigations and evaluations of strategies described herein.

3.7 References

1. M. A. Ghareeb, M. A. Tammam, A. El-Demerdash, A. G. Atanasov, *Curr. Biotechnol.* **2020**, 2, 88–102.
2. C.-Y. Duh, S.-K. Wang, M.-C. Chia, M. Y. Chiang, *Tetrahedron Lett.* **1999**, 40, 6033–6035.
3. J.-H. Sheu, A. F. Ahmed, R.-T. Shiue, C.-F. Dai, Y.-H. Kuo, *J. Nat. Prod.* **2002**, 65, 1904–1908.
4. Y.-J. Tseng, A. F. Ahmed, C.-F. Dai, M. Y. Chiang, J.-H. Sheu, *Org. Lett.* **2005**, 7, 3813–3816.
5. P. Radhika, P. V. Subba Rao, V. Anjaneyulu, R. N. Asolkar, H. Laatsch, *J. Nat. Prod.* **2002**, 65, 737–739.
6. K.-E. Lillsunde, C. Festa, H. Adel, S. de Marino, V. Lombardi, S. Tilvi, D. Nawrot, A. Zampella, L. D'Souza, M. D'Auria, P. Tammela, *Mar. Drugs* **2014**, 12, 4045–4068.
7. M. Kobayashi, K. M. C. A. Rao, M. M. Krishna, V. Anjaneyulu, *J. Chem. Res. (S)* **1995**, 188–189.
8. K. Iguchi, K. Kajiya, Y. Yamada, *Tetrahedron Lett.* **1995**, 36, 8807–8808.
9. R. A. Craig II, B. M. Stoltz, *Chem. Rev.* **2017**, 117, 7878–7909.
10. Y. Li, G. Pattenden, *Tetrahedron* **2011**, 67, 10045–10052.
11. N. J. Hafeman, S. A. Loskot, C. E. Reiman, B. P. Pritchett, S. C. Virgil, B. M. Stoltz, *J. Am. Chem. Soc.* **2020**, 142, 8585–8590.
12. Y. Li, G. Pattenden, *Nat. Prod. Rep.* **2011**, 28, 12691310.
13. P. A. Roethle, D. Trauner, *Nat. Prod. Rep.* **2008**, 25, 298–317
14. B. A. Pratt, Ph.D. Thesis, Scripps Research Institute, La Jolla, California, 2008.
15. C. O'Connell, Ph.D. Thesis, Queen's University of Belfast, Belfast, Northern Ireland, U.K., 2006
16. G. Liu, Ph.D. Thesis, Texas A&M University, College Station, Texas, 2011
17. F. Tang, Ph.D. Thesis, Washington University in St. Louis, St. Louis, Missouri, 2009.

18. M. Breunig, Ph.D. Thesis, University of Konstanz, Konstanz, 2019.
19. E. J. Horn, Ph.D. Thesis, University of California at Irvine, Irvine, CA, 2014.
20. E. J. Horn, J. S. Silverston, C. D. Vanderwal, *J. Org. Chem.* **2016**, *81*, 1819–1838.
21. J. L. Roizen, Ph.D. Thesis, California Institute of Technology, Pasadena, CA, 2009
22. R. A. Craig II, J. L. Roizen, R. C. Smith, A. C. Jones, S. C. Virgil, B. M. Stoltz, *Chem. Sci.* **2017**, *8*, 507.
23. J. L. Roizen, A. C. Jones, R. C. Smith, S. C. Virgil, B. M. Stoltz, *J. Org. Chem.* **2017**, *82*, 13051–13067.
24. R. A. Craig II, R. C. Smith, J. L. Roizen, A. C. Jones, S. C. Virgil, B. M. Stoltz, *J. Org. Chem.* **2018**, *83*, 3467–3485.
25. R. A. Craig II, R. C. Smith, J. L. Roizen, A. C. Jones, S. C. Virgil, B. M. Stoltz, *J. Org. Chem.* **2019**, *84*, 7722–7746.
26. R. Heim, S. Wiedemann, C. M. Williams, P. V. Bernhardt, *Org. Lett.* **2005**, *7*, 1327–1329.
27. M. D. Ronsheim, C. K. Zercher, *J. Org. Chem.* **2003**, *68*, 4535–4538.
28. J. Shi, G. Manolikakes, C.-H. Yeh, C. A. Guerro, R. A. Shenvi, H. Shigehisa, P. S. Baran, *J. Am. Chem. Soc.* **2011**, *133*, 8014–8027.
29. Z. G. Brill, H. K. Grover, T. J. Maimone, *Science* **2016**, *352*, 1078–1082.
30. R. Noyori, T. Odagi, H. Takaya, *J. Am. Chem. Soc.* **1970**, *92*, 5780–5781.
31. P. Binger, B. Schäfer, *Tetrahedron Lett.* **1988**, *29*, 4539–4542.
32. B. M. Trost, G. Mata, *Acc. Chem. Res.* **2020**, *53*, 1293–1305.
33. S. J. Danishefsky, M. P. Cabal, K. Chow, *J. Am. Chem. Soc.* **1989**, *111*, 3456–3457.
34. R. E. Donaldson, J. C. Saddler, S. Byrn, A. T. McKenzie, P. L. Fuchs, *J. Org. Chem.* **1983**, *48*, 2167–2188.
35. K. Michalak, J. Wicha, *Tetrahedron*, **2014**, *70*, 5073–5081.
36. L. O. Jeroncic, M. P. Cabal, S. J. Danishefsky, G. M. Shulte, *J. Org. Chem.* **1991**, *56*, 387–395.
37. A. S. Cieplak, *J. Am. Chem. Soc.* **1981**, *103*, 4540–4552.
38. P. Binger, A. Brinkmann, P. Wedemann, *Synthesis* **2002**, *10*, 1344–1346.
39. L. W. Hernandez, Ph.D. Thesis, University of Illinois at Urbana-Champaign, Champaign, IL, 2020.
40. Y.-L. Zhong, T. K. M. Shing, *J. Org. Chem.* **1997**, *62*, 2622–2624.

41. S. Prévost, K. Thai, N. Schützenmeister, G. Coulthard, W. Erb, V. K. Aggarwal, *Org. Lett.* **2015**, *17*, 504–507.
42. K. Chung, S. M. Banik, A. G. De Crisci, D. M. Pearson, T. R. Blake, J. V. Olsson, A. J. Ingram, R. N. Zare, R. M. Waymouth, *J. Am. Chem. Soc.* **2013**, *135*, 7593–7602.
43. R. A. Miller, R. S. Hoerrner, *Org. Lett.* **2003**, *5*, 285–287.
44. M. A. Mercadante, C. B. Kelly, J. M. Bobbitt, L. J. Tilley, N. E. Leadbeater, *Nat. Prot.* **2013**, *8*, 666–676.
45. M. A. González, S. Ghosh, F. Rivas, D. Fisher, E. A. Theodorakis, *Tetrahedron Lett.* **2004**, *45*, 5039–5041.
46. G. Beutner, R. Carrasquillo, P. Geng, Y. Hsiao, E. C. Huang, J. Janey, K. Katipally, S. Kolotuchin, T. La Porte, A. Lee, P. Lobben, F. Lora-Gonzalez, B. Mack, B. Mudryk, Y. Qiu, X. Qian, A. Ramirez, T. M. Razler, T. Rosner, Z. Shi, E. Simmons, J. Stevens, J. Wang, C. Wei, S. R. Wisniewski, Y. Zhu, *Org. Lett.* **2018**, *20*, 3736–3740.
47. E. M. Simmons, B. Mudryk, A. G. Lee, Y. Qiu, T. M. Razler, Y. Hsiao, *Org. Process Res. Dev.* **2017**, *21*, 1659–1667.
48. G. Lalic, E. J. Corey, *Tetrahedron Lett.* **2008**, *49*, 4894.
49. D. Basavaiah, A. J. Rao, T. Satyanarayana, *Chem. Rev.* **2003**, *103*, 811–892.
50. D. L. Comins, A.-C. Hiebel, S. Huang, *Org. Lett.* **2001**, *3*, 769–771.
51. A. Cernijenko, R. Risgaard, P. S. Baran, *J. Am. Chem. Soc.* **2016**, *138*, 9425–9428.
52. L. Song, H. Yao, L. Zhu, R. Tang, *Org. Lett.* **2013**, *15*, 6–9.
53. K. Shinya, U. Yoshio, T. Takeshi, *Bull. Chem. Soc. Jpn.* **1993**, *66*, 2720–2724.
54. J. Jauch, *J. Org. Chem.* **2001**, *66*, 609–611.
55. A. Itoh, S. Ozawa, K. Oshima, H. Nozaki, *Bull. Chem. Soc. Jpn.* **1981**, *54*, 274–278.
56. J. E. Kitulagoda, A. Palmelund, V. K. Aggarwal, *Tetrahedron*, **2010**, *66*, 6293–6299.
57. A. N. Flyer, C. Si, A. G. Myers, *Nat. Chem.* **2010**, *2*, 886–892.
58. D. J. Ager, I. Fleming, S. K. Patel, *J. Chem. Soc., Perkin Trans. I*, **1981**, 2520–2526.
59. W. R. Leonard, T. Livinghouse, *J. Org. Chem.* **1985**, *50*, 730–732.
60. P. Duhamel, L. Hennequin, N. Poirier, J.-M. Poirier, *Tetrahedron Lett.* **1985**, *26*, 6201–6204.
61. D. Chapdelaine, J. Belzile, P. A. Deslongchamps, *J. Org. Chem.* **2002**, *67*, 5669–5672.

62. K. Mukai, D. Urabe, S. Kasuya, N. Aoki, M. A. Inoue, M. *Angew. Chem. Int. Ed.* **2013**, *52*, 5300–5304.
63. Y. Sun, R. Li, W. Zhang, A. Li, *Angew. Chem. Int. Ed.* **2013**, *52*, 9201–9204.
64. G. A. Molander, D. J. St. Jean, *J. Org. Chem.* **2002**, *67*, 3861–3865.
65. F. Ghelfi, F. Roncaglia, M. Pattarozzi, V. Giangiordano, G. Petrillo, F. Sancassan, A. F. Parsons, *Tetrahedron*, **2009**, *65*, 10323–10333.
66. R. Shrestha, D. J. Weix, *Org. Lett.* **2011**, *13*, 2766–2769.
67. A. Vaupel, P. Knochel, *J. Org. Chem.* **1996**, *61*, 5743–5753.
68. K. Fujita, H. Yorimitsu, K. Oshima, *Synlett*, **2002**, 337–339.
69. M. E. Weiss, E. M. Carreira, *Angew. Chem. Int. Ed.* **2011**, *50*, 11501–11505.
70. T. Tsunoda, Y. Yamamiya, Y. Kawamura, S. Itô, *Tetrahedron Lett.* **1995**, *36*, 2529–2530.
71. J. Jacob, J. H. Espenson, J. H. Jensen, M. S. Gordon, *Organometallics* **1998**, *17*, 1835–1840.
72. A. T. Herrman, T. Saito, C. E. Stivala, J. Tom, A. Zakarian, *J. Am. Chem. Soc.* **2010**, *132*, 5962–5963.
73. J. Li, C. Tan, J. Gong, Z. Yang, *Org. Lett.* **2014**, *16*, 5370–5373.
74. R. K. Dieter, *Tetrahedron* **1999**, *55*, 4177–4236.
75. A. Krasovskiy, V. Malakhaov, A. Gavryushin, P. Knochel, *Angew. Chem. Int. Ed.* **2006**, *45*, 6040–6044.
76. Y. Hu, M. Bai, Y. Yang, J. Tian, Q. Zhou, *Org. Lett.* **2020**, *22*, 6308–6312.
77. V. Farina, B. Krishnan, *J. Am. Chem. Soc.* **1991**, *113*, 9585–9595.